

Application of Quantitative MRI Techniques in Ischemic and Congenital Heart Disease

image-guided therapy

Matthijs van Kranenburg

Layout and printing: Optima Communicatie, Rotterdam, the Netherlands.

Layout by: Lisa Keijzer en Erwin Timmerman

Cover art is produced by M. Verdoes, all rights reserved.

Proof reading is performed by <http://www.proof-reading-service.com/>

ISBN: 978-94-92683-63-2

Copyright, 2017, M. van Kranenburg, Rotterdam, the Netherlands, all rights reserved. No part of this publication may be reproduced, stored in a retrieval system of any nature, or transmitted in any form by any means, electronic, mechanical, photocopying, recording, or otherwise, without the written permission of the author.

Note: medical knowledge and circumstances are constantly changing. As new information becomes available, changes in treatment and drugs become necessary. The author has taken care to ensure that the information given is accurate. However, readers, investigators and medical practitioners are strongly advised to verify that the information, especially with regard to drug usage, MRI protocols and contrast agents, complies with the standards of practice. Readers are advised to check the most current information provided by the manufacturer of the product to be administered, to confirm the recommended dose or formula, the method and duration of administration, and contra-indications. It is the responsibility of each individual practitioner, relying on his or her own experience and knowledge of the patient, to make diagnoses with MRI, and to translate results of this thesis into individual patient care and further research, and to take all appropriate safety precautions during MRI examination especially with respect to patients with ICD's and pacemakers, ferromagnetic, electrically conductive or radiofrequency - reactive components. Nor the author, nor the editors accept any legal liability for any injury and/or damage to persons or property arising from this publication (related to any use of the material, misuse or misapplication).

**Application of Quantitative MRI Techniques
in Ischemic and Congenital Heart Disease
image-guided therapy**

Toepassing van kwantitatieve MRI technieken
in ischemische en aangeboren hartziekten
beeld-gestuurde therapie

Proefschrift

ter verkrijging van de graad van doctor aan de
Erasmus Universiteit Rotterdam
op gezag van de
rector magnificus

prof.dr. H.A.P. Pols

en volgens besluit van het College voor Promoties.
De openbare verdediging zal plaatsvinden op

Vrijdag 10 november 2017 om 11:30 uur

Matthijs van Kranenburg
geboren te Rhoon, gemeente Albrandswaard

Erasmus University Rotterdam



PROMOTIECOMMISSIE:

Promotoren: Prof.dr. R.J.M. van Geuns
Prof.dr. G.P. Krestin

Overige leden: Prof.dr.ir. H. Reiber
Prof.dr. J.W. Roos-Hesselink
Prof.dr. W.A. Helbing

Copromotor: dr. O.C. Manintveld

Voor mijn familie

Financial support for publishing this thesis was generously provided by :

Stichting DIRA

Sanofi

Medis

Pfizer

Servier Nederland Farma B.V.

Chipsoft

Pie medical imaging

MRI centrum

Department of Radiology and Nuclear Medicine, Erasmus MC, Rotterdam,
the Netherlands

Department of Cardiology, Erasmus MC, Rotterdam, the Netherlands

Financial support by the Dutch Heart Foundation for the publication of this thesis is gratefully acknowledged



*Funded by
the dutch heart foundation*

Hartstichting



CONTENTS

Part 1 PREFACE

Chapter 1	General introduction and outline of the thesis	13
-----------	--	----

Part 2 VALIDATION OF MAGNETIC RESONANCE ANGIOGRAPHY AND CMR 4D FLOW IN PATIENTS WITH RESISTENT HYPERTENSION AND CONGENITAL HEART DISEASE

Chapter 2	Validation of renal artery dimensions measured by magnetic resonance angiography in patients referred for renal sympathetic denervation.	29
-----------	--	----

Van Kranenburg M, Karanasos A, Chelu RG, van der Heide E, Ouhlous M, Nieman K, van Mieghem N, Krestin G.P, Niessen W, Zijlstra F, van Geuns RJM, Daemen J. Acad Radiol. 2015 Sep;22(9):1106-14.

Chapter 3	Serial quantitative magnetic resonance angiography follow-up of renal artery dimensions following treatment by four different renal denervation systems.	47
-----------	--	----

van Zandvoort L, **van Kranenburg M**, Karanasos A, van Mieghem N, Ouhlous M, van geuns RJM, van Domburg R. Daemen J. EuroIntervention. 2017 Jan 3; 12(13).

Chapter 4	Qualitative grading of aortic regurgitation: a pilot study comparing CMR 4D flow and echocardiography.	61
-----------	--	----

Chelu RG, van den Bosch AE, **van Kranenburg M**, Hsiao A, van den Hoven AT, Ouhlous M, Budde RPJ, Beniest, KM, Swart LE, Coenen A, Lubbers MM, Wielopolski PA, Vasanawala SS, Roos-Hesselink JW, Nieman K. Int J Cardiovasc Imaging. 2016 Feb;32(2):301-7.

Part 3 CARDIAC MAGNETIC RESONANCE IMAGING IN ISCHEMIC HEART DISEASE TRIALS

Part 3.1 ANIMAL STUDIES

Chapter 5	VEGF165A microsphere therapy for myocardial infarction suppresses acute cytokine release and increases microvascular density but does not improve cardiac function.	77
-----------	---	----

Uitterdijk A, Springeling T, **van Kranenburg M**, van Duin RWB, Krabbendam-Peters I, Gorsse-Bakker C, Sneep S, van Haeren R, Verrijck R, van Geuns RJM, van der Giessen WJ, Markkula T, Duncker DJ, van Beusekom HMM. Am J Physiol Heart Circ Physiol. 2015 Aug 309(3):H396-406.

- Chapter 6 Multiple common co-morbidities produce left ventricular diastolic dysfunction associated with coronary microvascular dysfunction, cardiac oxidative stress and myocardial stiffening. 103

O. Sorop, I. Heinonen, **M. van Kranenburg**, V.J. de Beer, Y. Octavia, R.W.B. van Duin, K. Stam, R.J. van Geuns, A.H. van den Meiracker, A.H. Danser, W.J. Paulus, J. van der Velden, D. Merkus and D.J. Duncker, submitted to Journal of Molecular and Cellular Cardiology.

Part 3.2 HUMAN STUDIES

- Chapter 7 Prognostic value of microvascular obstruction and infarct size, as measured by CMR in STEMI patients. 129

van Kranenburg M, Magro M, Thiele H, de Waha S, Eitel I, Cochet A, Cottin Y, Atar D, Buser P, Wu E, Lee D, Bodi V, Klug G, Metzler B, Delewi R, Bernhardt P, Rottbauer W, Boersma E, Zijlstra F, van Geuns RJM. JACC Cardiovasc Imaging. 2014 Sep;7(9):930–9.

- Chapter 8 Prognostic significance of microvascular obstruction and infarct size measured by cardiovascular magnetic resonance for the prediction of adverse left ventricular remodelling in patients with ST-segment elevation myocardial infarction: insight from a pooled analysis of individual patient data. 147

M. van Kranenburg, O.C. Manintveld, T. Yetgin, V. Bodi, D. Atar, P. Buser, E. Wu, D. Lee, P. Bernhardt, W. Rottbauer, A.C. van Rossum, E. Boersma, G. Krestin, F. Zijlstra, R.J.M. van Geuns. Submitted

- Chapter 9 Ischemic postconditioning after routine thrombus aspiration during primary percutaneous coronary intervention: rationale and design of the POstconditioning Rotterdam Trial. 167

Yetgin T, **van Kranenburg M**, ten Cate T, Duncker DJ, de Boer MJ, Diletti R, van Geuns RJM, Zijlstra F, Manintveld OC. Catheter Cardiovasc Interv. 2016 Oct;88(4):508–514.

Part 4 OUTCOME STUDIES IN CONGENITAL HEART DISEASE

- Chapter 10 Atrial-based pacing has no benefit over ventricular pacing in preventing atrial arrhythmias in adults with congenital heart disease. 185

Opic P, Yap S-C, **Van Kranenburg M**, Van Dijk AP, Budts W, Vliegen HW, van Erven L, Can A, Sahin G, de Groot NMS, Witsenburg M, Roos-Hesselink JW. Europace. 2013 Dec;15(12):1757–62.

Chapter 11	Complications of pacemaker therapy in adults with congenital heart disease: A multicenter study.	199
	Opić P, van Kranenburg M , Yap S-C, van Dijk AP, Budts W, Vliegen HW, van Erven L, Can A, Sahin G, Theuns DAMJ, Witsenburg M, Roos-Hesselink JW.	
	Int J Cardiol. 2013.	

Part 5 SUMMARY, GENERAL DISCUSSION AND FUTURE PERSPECTIVES

Chapter 12	Summary, general discussion and future perspectives	217
Chapter 13	Samenvatting en discussie	231
Appendix	ACKNOWLEDGEMENTS / DANKWOORD	241
	PHD PORTFOLIO SUMMARY	247
	LIST OF PUBLICATIONS / ABSTRACTS	249
	CURRICULUM VITAE	253
	ABBREVIATIONS	255

PART 1

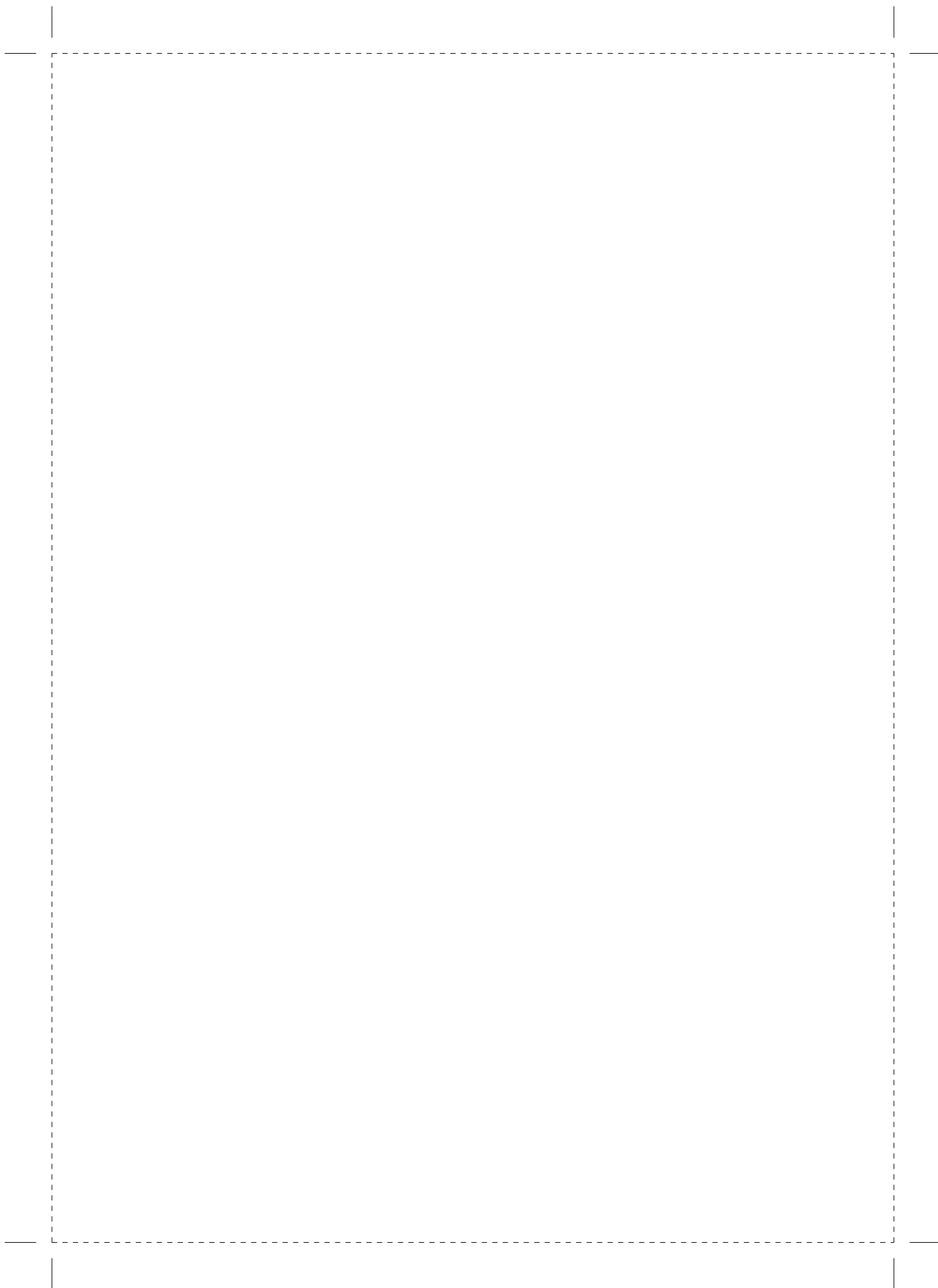
PREFACE



Chapter 1

General introduction
and outline of the thesis

M. van Kranenburg



INTRODUCTION

The management and, consequently, the outcome of acute coronary syndromes (ACS) due to coronary heart disease have improved impressively over the last decades (1), but ACS or myocardial infarction or heart attack in mother tongue, a different condition than cardiac arrest, still remains the most important cause of re-hospitalisation, repeat interventions, heart failure and death worldwide (1-3). It is estimated that each year, 30,000 people in the Netherlands suffer from myocardial infarction, and is in fact a major public health care burden. Next to ischaemic heart disease (IHD), thanks to modern medicine, more and more patients with congenital heart disease (CHD) reach adulthood, but nonetheless require lifelong professional care (4, 5). Imaging techniques are essential in these two groups of patients for establishing diagnosis, guiding therapy and predicting outcomes. While echocardiography remains the first line diagnostic imaging test, with improved functional assessment in evaluating ischaemic and congenital heart disease, cardiac magnetic resonance (CMR) and computed tomography (CT) provide valuable information.

Early reperfusion of the ischaemic myocardium caused by an occluded coronary artery, in patients with atherosclerosis, is the cornerstone in the treatment of patients with ST-segment elevation myocardial infarction (STEMI). A primary percutaneous coronary intervention (pPCI) – defined as an emergent percutaneous catheter intervention in the setting of STEMI, without previous fibrinolytic treatment - is the preferred reperfusion therapy (6). However a large proportion of patients experience a “no-reflow” phenomenon, caused by distal atherothrombotic embolisation, reperfusion injury, ischaemic injury or patient characteristics (7). Despite the opening of an infarct related artery, microvascular obstruction (MO) could persist (8). Although prompt myocardial reperfusion with a pPCI has reduced mortality and morbidity, the benefits of pPCI are blunted by MO, which prevents full recovery of distal flow (9). No-reflow can be assessed with angiography and ST-segment resolution, and since the 1980’s also with contrast-enhanced magnetic resonance imaging (MRI) (10). Magnetic resonance imaging reveals the presence and extent of MO, location of the infarction, the size of the infarction (IS%LV), oedema and its consequences on regional and global left ventricular (LV) function. The reproducibility of these measurements are excellent (11). The technique has become an established imaging tool in investigating ischaemic and congenital heart disease. Due to end-user driven, technical developments over the past twenty years, it is possible to image the beating heart (12). In Figures 1 and 2, an example of the heart visualised with MRI is depicted. If used properly with the right sequence protocols, it provides excellent spatial and temporal resolution to investigate cardiac diseases. Moreover, due to developments in electrocardiogram (ECG) gating and the introduction of breath-hold sequences, disturbing motion artefacts are less likely to occur. As IHD is a consequence

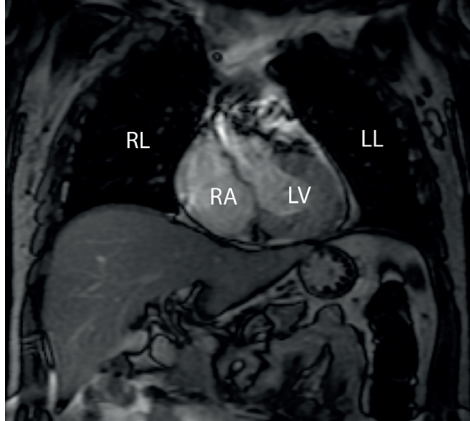


Figure 1. An MRI image of a patient with acute myocardial infarction. The compartments of a human heart are depicted. Abbreviations: RL: right lung, LL: left lung, RA: right atrium, LV: left ventricle

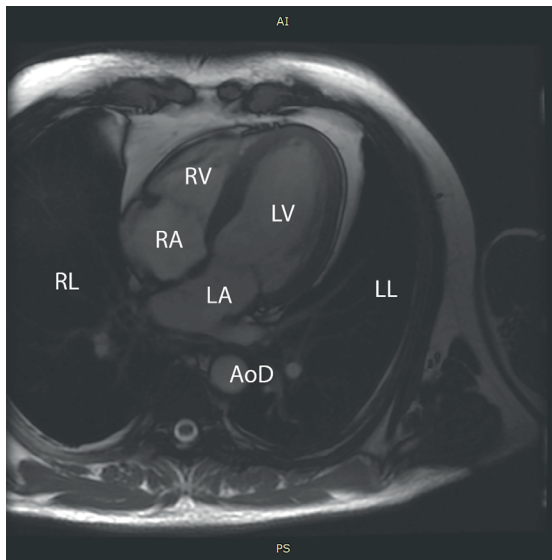


Figure 2. An MRI image of a patient with acute myocardial infarction. The compartments of a human heart are depicted. Abbreviations: RL: right lung, LL: left lung, RV: right ventricle, LV: left ventricle, RA: right atrium, LA: left atrium, AoD: descending aorta.

of coronary artery disease (CAD) which by itself is importantly triggered by hypertension, and the prevalence of congenital heart disease (CHD), and the adult population with CHD (GUCH) is expected to rise, the contribution of dedicated imaging techniques to reduce the impact on these disease on the populations is essential and needs further improvement. Many of the quantification techniques investigated in this thesis, can be both applied in IHD and CHD.

Late gadolinium enhancement imaging is an important part of infarct size determination, and in the evaluation of prognosis in patients with STEMI. This T1-weighted technique (T1 relaxation describes the recovery of the z-component (M_z) of the magnetisation following an RF pulse) is the cornerstone of myocardial tissue characterisation. It is able to dem-

onstrate the presence and extent of myocardial scarring. In brief, a gadolinium-chelate contrast agent is administered into an antebrachial vein and diffuses into the extracellular myocardial compartment. The gadolinium-chelate accumulates in myocardial scar tissue. With T1-weighted imaging the accumulated gadolinium is depicted as a hyperintense signal (bright) (13). The normal myocardium has a hypointense signal or appears as black. In STEMI, a disease due to an occluded coronary artery, the non-vascularised myocardium is in a region of ischaemia, lacks oxygen and becomes necrotic. During this process, starting from the endocardial border where the oxygen supply is first compromised, myocardial muscle cells become necrotic over time. With T1-weighted sequences, end-users are able to depict necrotic myocardial tissue. In this necrotic tissue, a dark rim is frequently seen and is associated with obstruction of the small arteries, the so-called MO. Figure 3 depicts MRI images of a patient with myocardial necrosis.

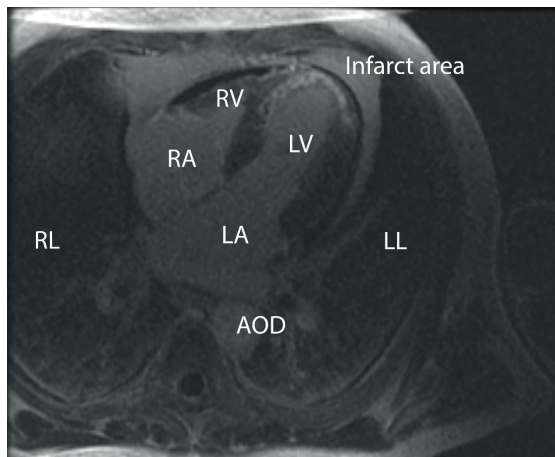


Figure 3. An MRI (late gadolinium enhancement) image of a patient with acute myocardial infarction. Notice the hyperenhanced, bright signal of the left ventricular muscle. The black areas are associated with obstruction of the small vessels. Abbreviations: RL: right lung, LL: left lung, RV: right ventricle, LV: left ventricle, RA: right atrium, LA: left atrium, Aod: descending aorta.

Moreover MRI techniques may be applied in resistant hypertension. Hypertension is a known risk factor for IHD. There are numerous classes of anti-hypertensive drugs. In case of therapy resistant hypertension renal denervation is being used as an experimental therapy to lower blood pressure. However, the long term safety of the first generation radiofrequency devices used in renal denervation are unknown. MRI can be used to assess vessel patency over time.

Furthermore, MRI may be applied in patients with CHD. The quantification of left and right ventricular function is equally important in patients with CHD as in those with IHD. Perhaps, especially in the field of CHD, focus on the right side of the heart is of eminent importance. Congenital heart disease is a common type of birth defect with a prevalence of 8.0 per 1000 births (14). The most common heart defects are ventricular septal defect (VSD, 34%), atrial septal defect (ASD, 13%), persistent ductus arteriosus (10%), pulmonary stenosis (8%), tetralogy of Fallot (ToF, 5%), coarctation of the aorta



Figure 4. An MRI (late gadolinium enhancement) image of a Yorkshire pig with a posterolateral myocardial infarction due to occlusion of the left circumflex artery. Notice the white area, with a dark rim.

(CoA, 5%), transposition of the great arteries (TGA, 5%), aortic stenosis (4%) (15). The incidence of Wolff-Parkinson-White Syndrome is estimated around 1-3 per 1000 births. The population of adult patients with CHD is rapidly expanding due to advances in paediatric cardiology and cardiothoracic surgery over the past decades. This results in a growing number of adults with CHD with an estimation of 35,000 in the Netherlands (16). Although survival has improved, morbidity is substantial. The most common complications in adults with CHD are arrhythmias and heart failure. The risks differ amongst the various congenital lesions. While echocardiography remains the first line imaging modality with improved functional assessment and emerging techniques to visualise the right ventricle (17), CMR is also able to image the right side of the heart and subtle changes can be depicted. With emerging sequences, MRI provides excellent possibili-

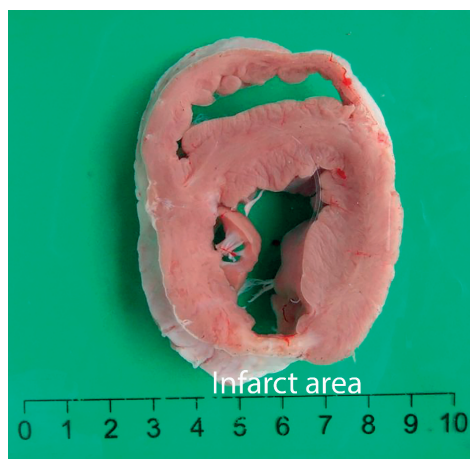


Figure 5. An example of the heart ex-vivo. Notice the white fibrotic area.

ties to image the beating heart. For example, cine gradient echo (GRE) sequences are applied to evaluate LV and RV function and dimensions, to measure velocities and flow, and to evaluate valvular stenosis or regurgitation. Furthermore, the sequence is useful in detection of the Qp/Qs ratio in intracardiac shunting lesions to decide whether there will be an indication for therapy, and to visualise conduits in patients with transposition of the great arteries (TGA). A four dimensional (4D) flow sequence, to quantify myocardial blood flow, is a new kid on the block and is recently introduced.

In this thesis, we apply several MRI techniques in patients with IHD and CHD.

The specific aims of this thesis were to:

- Reduce infarct size and obstruction of the small vessels with bivalirudine and post-conditioning in patients with STEMI. LV function, infarct size and MO will be measured with CMR as surrogate endpoints.
- Evaluate the hypothesis that MO and infarct size as expressed as a percentage of the LV are independent predictors of major adverse cardiovascular events and death in patients with STEMI undergoing pPCI. Moreover we evaluate the hypothesis that MO and infarct size are predictors for adverse LV remodeling.
- Validate magnetic resonance angiography (MRA) against invasive ultrasound techniques (IVUS), to measure the renal arteries in patients with high blood pressure. MRA will be used to evaluate safety of renal denervation, an experimental treatment to lower blood pressure.
- Describe the effects of VEGF165A microsphere therapy, an experimental therapy in an animal model with a reperfused myocardial infarction. In a second experimental study, our aim was to induce diastolic dysfunction in a swine model. We evaluate the impact of induction of hypertension, DM and hypercholesterolemia in animal experiment, using quantitative MRI techniques.
- Validate a four dimensional (4D) flow sequence to quantify myocardial blood flow against echocardiography and 2D phase contrast MRI sequences in patients with CHD.
- Count complications in patients with CHD, and describe the complications of pacemaker therapy in a challenging group of patients with CHD.

Part 2: VALIDATION OF NOVEL MRI SEQUENCES AND ITS APPLICATION

Resistant hypertension, or high blood pressure not controlled by medication, is a condition that is associated with the occurrence of IHD (18) and diastolic heart failure. In **chapter 2**, renal artery measurements are validated against intravascular ultrasound to select patients for renal denervation out of patients with resistant hypertension. The cause of resistant hypertension is multifactorial. Chronic activation of the sympathetic nervous system plays a central role in blood pressure elevation. Reduction of renal

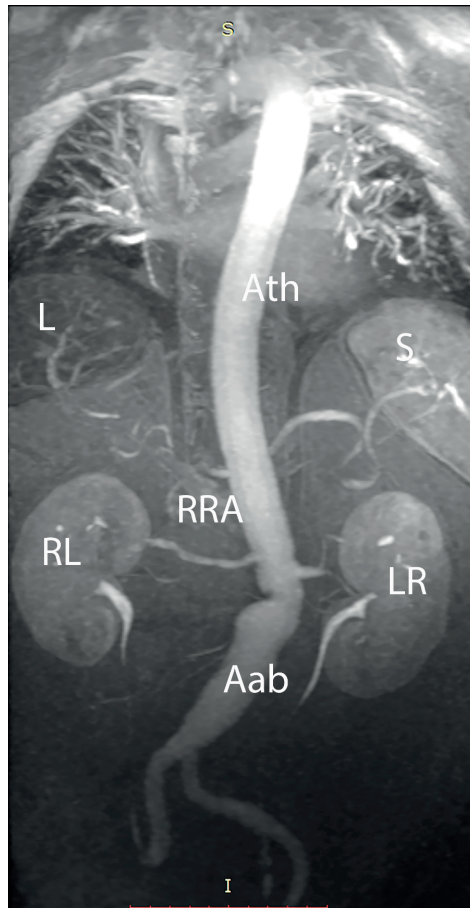


Figure 6. A magnetic resonance angiography image of a patient referred for renal denervation. Abbreviations: L: liver, S: spleen, Ath: aorta thoracalis, RRA: right renal artery, RL: right kidney, LR: left kidney, Aab: aorta abdominalis.

sympathetic afferent and efferent activity by catheter-based denervation might lower blood pressure. In this thesis, MRA is used to select eligible patients with appropriate renal artery anatomy for renal denervation (RDN), a novel experimental procedure to disrupt renal artery nerves, in cases of uncontrolled hypertension (19). Figure 6 depicts an example of a renal artery as measured by MRI. In chapter 2, intra observer and inter observer reproducibility of renal artery dimensions are studied. In **chapter 3**, short term safety of RDN procedures is evaluated with MRA. With emerging sequences, MRI is an excellent and unique tool for the diagnosis and follow-up of CHD. **Chapter 4** describe the research performed in visualisation of blood velocities through the heart and the large vessels (Figure 7), the so-called four dimensional flow (4D flow). Four dimensional flow MRI refers to phase contrast MR sequence with flow-encoding in all three spatial directions, and to the dimension of time along the cardiac cycle. It is a straightforward acquisition, and it enables retrospective calculation of blood flow through any plane. Four-dimensional flow MRI has enabled more comprehensive access to intra- and extra-

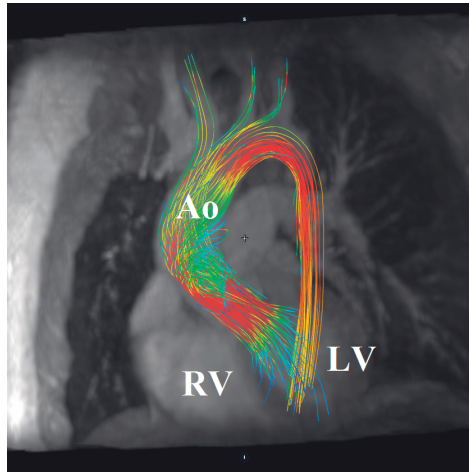


Figure 7. Published with permission from colleague Saru; an 4D flow crosssection image of the heart. Abbreviations: Ao = aorta ascendens, LV = Left ventricle, RV = right ventricle.

cardiac blood flow, with typical spatial resolution of $1.5 \times 1.5 \times 1.5$ to $3 \times 3 \times 3$ mm³, typical temporal resolution of 30–40 ms, and acquisition times of 5 to 25 min (20). We evaluated 4D flow data, and assessed its accuracy for the detection and grading of aortic and pulmonary valve regurgitation using transthoracic echocardiography as a reference.

Part 3: CARDIAC MAGNETIC RESONANCE IMAGING IN ISCHAEMIC HEART DISEASE TRIALS

The MRI characteristics of an experimental therapy in an animal model with a reperfused myocardial infarction are studied. In **chapter 5** we describe the effects of VEGF165A microsphere therapy. Magnetic resonance imaging is used as an endpoint in this study (Figures 4 and 5). **Chapter 6** covers the application of MRI in diastolic heart disease, a condition is known as impaired relaxation of the heart chambers. Predicting the risk of heart failure and death after myocardial infarction with use of MRI, and its use in cardiovascular trials, has recently become a subject of great interest. In **chapter 7 to 8**, in an international meta-analysis of individual patient data, we describe a study that evaluated the predictive value of infarct size, MO and LVEF in patients with STEMI on the medium term occurrence of cardiac death and major adverse cardiovascular events (MACE). In studies of myocardial reperfusion, both in experimental models and in patients, the realisation that reperfusion injury could exacerbate the effects of myocardial infarction also came to the fore early on, and the role of MO consequent to reperfusion injury has been extensively recognised (21). In **chapter 9**, we describe in detail how to setup a study to investigate the effect of postconditioning, an experimental treatment of acute myocardial infarction in humans (Figure 8) (22).

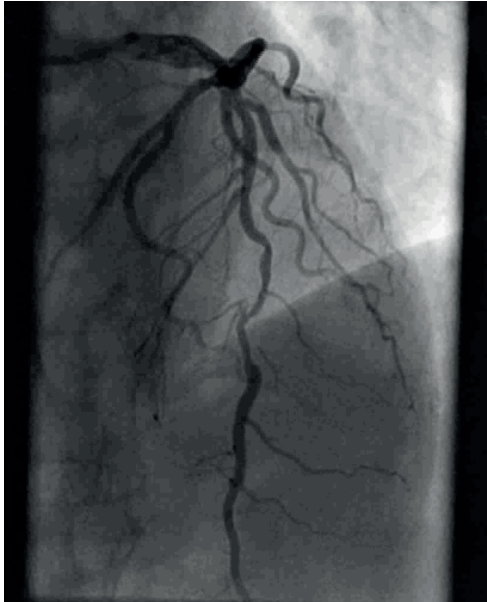


Figure 8. example of coronary angiography image in a patient with atherosclerosis, landmark during primary PCI or stent treatment (a stent could be placed in the occluded artery) during myocardial infarction to limit infarct size, the left coronary artery is depicted

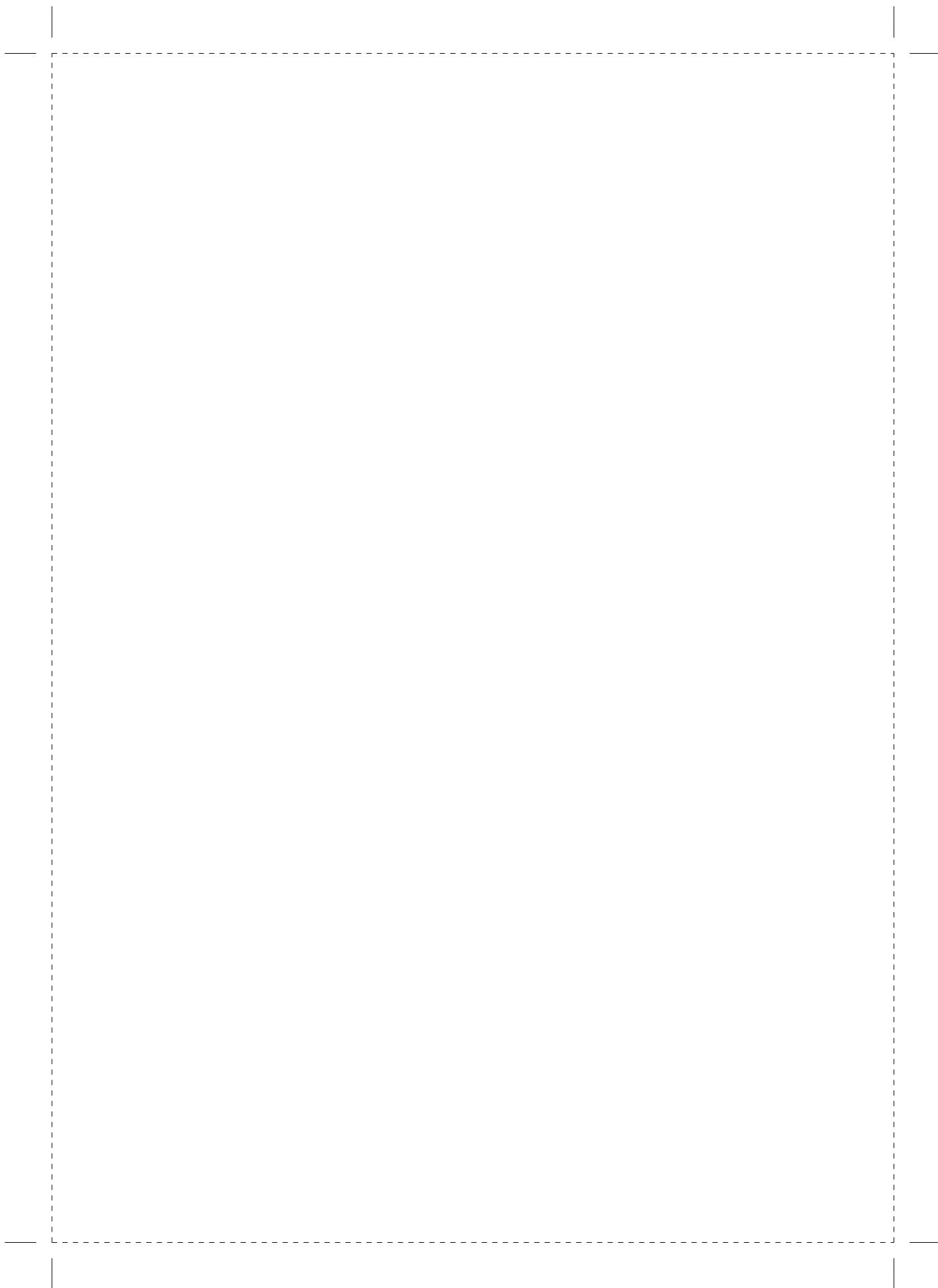
Part 4: OUTCOME STUDIES IN CONGENITAL HEART DISEASE

The improved survival in patients with CHD is hampered in the long term in a substantial number of patients by sinus node dysfunction, atrial arrhythmias such as atrial fibrillation and atrioventricular blocks. Many require pacemaker therapy and are subject to lifelong need for re-interventions and follow-up (23). In **chapters 10 and 11**, we investigated pacemaker therapy in adults with congenital heart disease. In a large cohort, peri procedural and late pacemaker complications were studied. Knowledge regarding pacemaker therapy is lacking in patients with CHD due to its small population. Therefore we set up a multicentre study.

REFERENCES

1. Luscher TF. Acute coronary syndromes: mechanisms, reperfusion injury, antithrombotic therapy, and current outcomes. *European heart journal*. 2016;37(16):1257-9.
2. Nichols M, Townsend N, Scarborough P, Rayner M. Cardiovascular disease in Europe 2014: epidemiological update. *European heart journal*. 2014;35(42):2929.
3. Writing Group M, Mozaffarian D, Benjamin EJ, Go AS, Arnett DK, Blaha MJ, et al. Heart Disease and Stroke Statistics-2016 Update: A Report From the American Heart Association. *Circulation*. 2016;133(4):e38-60.
4. Luscher TF. Imaging as a basis of clinical decision-making in congenital and coronary disease and heart failure. *European heart journal*. 2016;37(15):1171-3.
5. Verheugt CL, Uiterwaal CS, van der Velde ET, Meijboom FJ, Pieper PG, van Dijk AP, et al. Mortality in adult congenital heart disease. *European heart journal*. 2010;31(10):1220-9.
6. Task Force on the management of ST-segment elevation myocardial infarction, Steg PG, James SK, Atar D, Badano LP, Blomstrom-Lundqvist C, et al. ESC Guidelines for the management of acute myocardial infarction in patients presenting with ST-segment elevation. *European heart journal*. 2012;33(20):2569-619.
7. Niccoli G, Burzotta F, Galiuto L, Crea F. Myocardial no-reflow in humans. *Journal of the American College of Cardiology*. 2009;54(4):281-92.
8. Kloner RA, Ganote CE, Jennings RB. The "no-reflow" phenomenon after temporary coronary occlusion in the dog. *The Journal of clinical investigation*. 1974;54(6):1496-508.
9. Ambrosio G, Savino K. CMR assessment of microvascular obstruction in STEMI: ready for prime time? *Journal of the American College of Cardiology*. 2014;64(12):1227-30.
10. van Kranenburg M, Magro M, Thiele H, de Waha S, Eitel I, Cochet A, et al. Prognostic value of microvascular obstruction and infarct size, as measured by CMR in STEMI patients. *JACC Cardiovascular imaging*. 2014;7(9):930-9.
11. Thiele H, Kappl MJ, Conradi S, Niebauer J, Hambrecht R, Schuler G. Reproducibility of chronic and acute infarct size measurement by delayed enhancement-magnetic resonance imaging. *Journal of the American College of Cardiology*. 2006;47(8):1641-5.
12. Guttman MA, Dick AJ, Raman VK, Arai AE, Lederman RJ, McVeigh ER. Imaging of myocardial infarction for diagnosis and intervention using real-time interactive MRI without ECG-gating or breath-holding. *Magnetic resonance in medicine*. 2004;52(2):354-61.
13. Dastidar AG, Rodrigues JC, Baritussio A, Bucciarelli-Ducci C. MRI in the assessment of ischaemic heart disease. *Heart*. 2016;102(3):239-52.
14. Dolk H, Loane M, Garne E, European Surveillance of Congenital Anomalies Working G. Congenital heart defects in Europe: prevalence and perinatal mortality, 2000 to 2005. *Circulation*. 2011;123(8):841-9.
15. van der Linde D, Konings EE, Slager MA, Witsenburg M, Helbing WA, Takkenberg JJ, et al. Birth prevalence of congenital heart disease worldwide: a systematic review and meta-analysis. *Journal of the American College of Cardiology*. 2011;58(21):2241-7.
16. van der Bom T, Bouma BJ, Meijboom FJ, Zwinderman AH, Mulder BJ. The prevalence of adult congenital heart disease, results from a systematic review and evidence based calculation. *American heart journal*. 2012;164(4):568-75.
17. McGhie JS, Menting ME, Vletter WB, Frowijn R, Roos-Hesselink JW, Soliman OI, et al. A Novel 13-Segment Standardized Model for Assessment of Right Ventricular Function Using Two-Dimensional iRotate Echocardiography. *Echocardiography*. 2016;33(3):353-61.

18. Levy D, Larson MG, Vasan RS, Kannel WB, Ho KK. The progression from hypertension to congestive heart failure. *Jama*. 1996;275(20):1557-62.
19. Krum H, Schlaich M, Whitbourn R, Sobotka PA, Sadowski J, Bartus K, et al. Catheter-based renal sympathetic denervation for resistant hypertension: a multicentre safety and proof-of-principle cohort study. *Lancet*. 2009;373(9671):1275-81.
20. Dyverfeldt P, Bissell M, Barker AJ, Bolger AF, Carlhall CJ, Ebbers T, et al. 4D flow cardiovascular magnetic resonance consensus statement. *Journal of cardiovascular magnetic resonance : official journal of the Society for Cardiovascular Magnetic Resonance*. 2015;17(1):72.
21. Reichek N. Meta-analysis of MACE in MI: what's the MO? *JACC Cardiovascular imaging*. 2014;7(9):953-5.
22. Yetgin T, van Kranenburg M, Ten Cate T, Duncker DJ, de Boer MJ, Diletti R, et al. Ischemic postconditioning after routine thrombus aspiration during primary percutaneous coronary intervention: Rationale and design of the POSTconditioning Rotterdam trial. *Catheterization and cardiovascular interventions : official journal of the Society for Cardiac Angiography & Interventions*. 2015.
23. Yap SC, Harris L, Chauhan VS, Oechslin EN, Silversides CK. Identifying high risk in adults with congenital heart disease and atrial arrhythmias. *The American journal of cardiology*. 2011;108(5):723-8.



PART 2

VALIDATION OF MAGNETIC
RESONANCE ANGIOGRAPHY AND
CMR 4D FLOW IN PATIENTS WITH
RESISTENT HYPERTENSION AND
CONGENITAL HEART DISEASE



Chapter 2

Validation of Renal Artery Dimensions
Measured by Magnetic Resonance
Angiography in Patients Referred for Renal
Sympathetic Denervation.

Matthijs van Kranenburg, MD, Antonis Karanasos, MD, Raluca Gabriela Chelu, MD, Elco van der Heide, Mohamed Ouhlous, MD, PhD, Koen Nieman, MD, PhD, Nicolas van Mieghem, MD, Gabriel Krestin, MD, PhD, Wiro Niessen, PhD, Felix Zijlstra, MD, PhD, Robert-Jan van Geuns, MD, PhD, Joost Daemen, MD, PhD

Acad Radiol 2015; 22:1106–1114

ABSTRACT

Rationale and Objectives - Magnetic resonance angiography (MRA) is a well-established modality for the assessment of renal artery stenosis. Using dedicated quantitative analyses, MRA can become a useful tool for assessing renal artery dimensions in patients referred for renal sympathetic denervation (RDN) and for providing accurate measurements of vascular response after RDN. The purpose of this study was to test the reproducibility of a novel MRA quantitative imaging tool and to validate these measurements against intravascular ultra- sound (IVUS).

Materials and Methods - In nine patients referred for renal denervation, renal artery dimensions were measured. Bland–Altman analysis was used to assess the intraobserver and interobserver reproducibility.

Results - Mean lumen diameter was 5.8 ± 0.7 mm, with a very good intraobserver and interobserver variability of 0.7% (reproducibility: bias, 0 mm; standard deviation [SD], 0.1 mm) and 1.2% (bias, 0 mm; SD, 0.1 mm), respectively. Mean total lumen volume was 1035.3 ± 403.6 mm³ with good intraobserver and interobserver variability of 2.9% (bias, 9.7 mm³; SD, 34.0 mm³) and 2.8% (bias, 11.4 mm³; SD, 42.4 mm³). The correlation (Pearson R) between mean lumen diameter measured with MRA and IVUS was 0.750 ($P = .002$).

Conclusions - Using a novel MRA quantitative imaging tool, renal artery dimensions can be measured with good reproducibility and accuracy. MRA-derived diameters and volumes correlated well with IVUS measurements.

Keywords: Renal artery; percutaneous renal sympathetic denervation; magnetic resonance angiography; intravascular ultrasound.

INTRODUCTION

Percutaneous renal sympathetic denervation (RDN) is currently being studied as a potential treatment to lower sympathetic nerve activity in a broad spectrum of diseases (1, 2). At present, more than 53 devices are available to disrupt renal afferent and efferent nerves traveling along the renal arterial wall. Besides the fact that initial promising, but noncontrolled studies on clinical efficacy in patients with therapy-resistant hypertension were recently challenged by a negative randomized controlled trial, data on long-term safety are mainly limited to the use of the first-generation radiofrequency devices (3-5). The currently available data on the incidence of renal artery stenosis, mostly derived from duplex ultrasound findings, are showing a low rate of adverse events, both at short and longer term follow-up (4-6). Published data from computed angiography (CTA) or magnetic resonance angiography (MRA) report only binary outcomes (7), precluding firm conclusion on the true vascular response to RDN itself. As new renal denervation systems are being introduced, there is a need for dedicated volumetric noninvasive imaging tools to accurately assess renal artery integrity at the medium to long term (8). Furthermore, balloon-based RDN devices require accurate sizing to avoid complications due to oversizing (9). The aim of the present study was to evaluate a new software tool allowing automated vessel segmentation for quantitative renal artery lumen dimension assessment. Intraobserver and interobserver reproducibility were studied, and MRA-derived measurements were validated with intravascular ultrasound (IVUS).

MATERIALS AND METHODS

Patient Selection

Nine consecutive patients underwent both MRA and preprocedural IVUS at the time of the renal denervation procedure. Because of an early trifurcation in the vessel in one patient, automated segmentation with MRA was not successful in one artery. For the MRA analyses, 17 vessels were used. For the correlation analyses between MRA and IVUS, MRA vessel length was determined and manually adjusted on the basis of the length of the IVUS pullback with either the ostium or bifurcation as landmark. Because of a lack of IVUS measurement in 1 vessel and a lack of visualization of either bifurcation or ostium, a total of 16 arteries in which both MRA and IVUS data were available were used for validation of MRA against IVUS measurements. The study was approved by the hospital ethics committee and conforms to the declaration of Helsinki. All patients provided written informed consent before inclusion.

Magnetic Resonance Angiography Acquisition

MRA was performed on a 1.5T MRI scanner (Discovery MR450; GE Medical systems, Milwaukee, WI). Patients were positioned in supine position, and an eight-channel cardiac coil was placed on the thorax and upper abdomen. A dedicated RDN-MRI protocol was used. As part of this MRI protocol, a three-dimensional (3D) Vasc Fast time of flight (TOF) spoiled gradient-echo sequence was used to acquire images of the renal vasculature, after a test bolus procedure. Images were acquired during a breath-hold. The following parameters were used: field of view, 46 cm 41.4 cm; matrix, 320 x 192, upsampled to 512 x 512; number of excitations, 0.75; pixel size, 0.89 x 0.89 mm; flip angle, 17°; slice thickness, 1.6 mm; location per slab, 28 upsampled to 56 with ZIP2; repetition time, 3.2 milliseconds; echo time, 1.2 milliseconds; band- width, 83.33 Hz. Approximately, 20 seconds was the duration of the breath-hold, depending on the locations per slab. A power injector (Medrad Spectris, Warrendale, PA) was used to inject gadobutrol (Gadovist 1.0 mmol/mL; Bayer, Mijdrecht, The Netherlands). Gadovist was injected, around 18 seconds before acquisition, with a dose of 0.1 mmol/kg into an antecubital vein followed by 15 mL of saline at a rate of 2.5 mL/s to visualize the renal arteries.

MRA Analysis

Renal arteries were analyzed with CAAS MRA version 1.0 (Pie Medical Imaging B.V, Maastricht, The Netherlands). The segmentation was initialized by placing four delimiter points on the volumetric rendered contrast-enhanced MRA view; root delimiter point at the thoracic aorta, abdominal aorta, and finally two points distal of the bifurcation of the renal artery (Supplementary Figure 1). Ray tracing was used to extract the 3D position of the user-defined delimiter points within the rendered volume. The acquired position was centralized within the lumen by image processing techniques. The 3D segmentation used a deformable model algorithm (10) that iteratively optimized the location of the surface to- ward the luminal border based on image gradients while simultaneously maintaining local smoothness of the 3D segmented surface. After segmentation, the center lines of the 3D segmentation were extracted as the minimum path of maximal inscribed spheres from the root delimiter point to the distal delimiter points (11). Within this process, the diameter of the spheres resembled the minimum diameter along the center line of the 3D segmentation (Supplementary Figure 2). The ostium and bifurcation of the renal arteries were automatically detected, by generation of a polygon of confluence (POC) (12). The center line splits in the POC from the proximal main vessel splits in the renal artery and the bifurcation of the renal artery. Outside the POC, the cross-sectional area was defined perpendicular to the lumen wall along each position of the center line. Based on the cross-sectional area, the lumen diameter was defined as the equivalent diameter on the basis of the assumption of circularity. For analysis, the arteria renal was selected, which is the single vessel segment between the ostial

POC and the bifurcation POC. In case of failure of this method, only the bifurcation of the renal artery was selected manually. The automatically segmented arteries were inspected, and borders were manually corrected if necessary in the stretched multi-planar rendering and perpendicular view. Vessel length of the renal arteries was defined as the distance between the automatically defined ostium and bifurcation of the renal artery (Fig 1). Minimal lumen diameter, mean lumen diameter, and total lumen volume were based on semiautomatic segmentation. To compare and validate MRA with IVUS, images were matched and MRA dimensions were measured again with use of IVUS references. IVUS-derived borders were used as a reference. To be able to validate the MRA volumetric measurements with IVUS, the segment of interest was matched by using either the ostium or bifurcation of the renal artery as a landmark. MRA borders were adjusted according to the vessel length measured with IVUS. In this way, we were able to validate the volume measurements of the renal artery segment between MRA and IVUS.

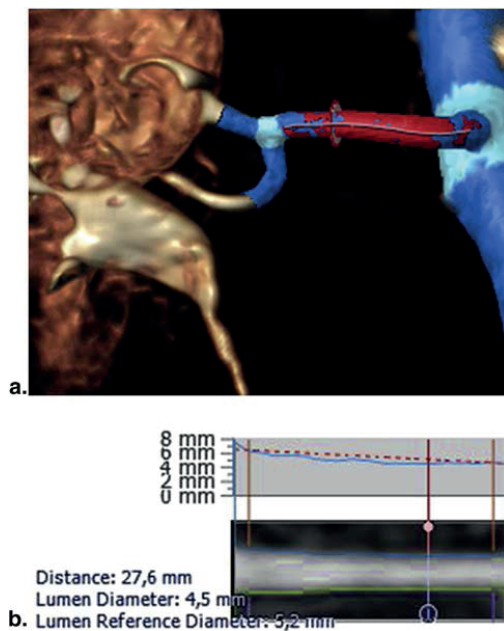


Figure 1. (a) Example renal artery measured with MRA. (b) Typical longitudinal cross-section of an analyzed renal artery. Blue lines represent renal artery borders. The pink line can be manually moved to measure luminal dimensions at a specific cross section. Orange lines represent reference lines for stenosis measurements. MRA, magnetic resonance angiography.

IVUS Acquisition

Renal arteries were examined with an IVUS system with automatic pullback at 0.5 mm/s (Atlantis SR Pro Imaging Catheter; Boston Scientific, Natick, MA) before renal denervation in all vessels. Spatial resolution was 100 μ m. A total dose of 200 μ g of nitrates was locally administered before invasive imaging to prevent catheter-induced spasm. Retrieved IVUS images were digitally stored and analyzed offline.

IVUS Analysis

Volumetric analysis of the region of interest was performed at 0.5-mm fixed intervals throughout the segment between the renal artery ostium and the first major bifurcation using dedicated software (QCU-CMS, LKEB, Leiden University, The Netherlands). In cases where the guiding catheter was located deeper than the anatomic renal artery ostium or that the first major bifurcation was not visualized, IVUS analysis was performed in the entire pullback. In analyzed frames, the lumen contour was segmented with the help of a semiautomatic algorithm, using manual corrections where necessary (Fig 2). As in MRA, mean diameter was calculated in each frame by the lumen area, as the equivalent diameter based on the assumption of circularity.

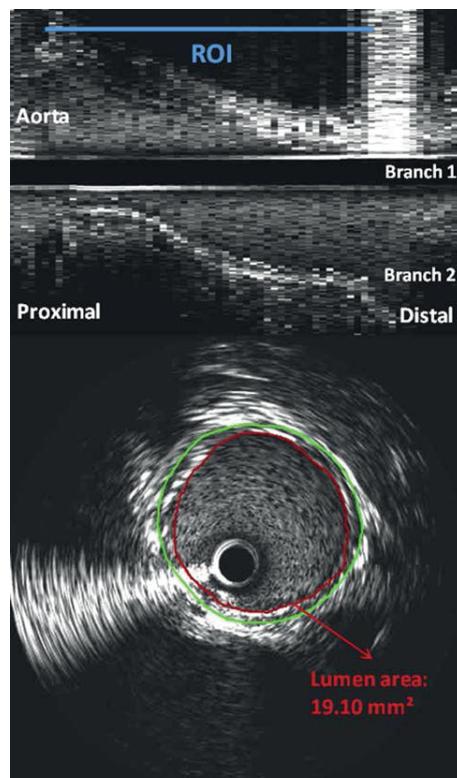


Figure 2. Intravascular ultrasound renal artery. Black line represents intravascular ultrasound catheter. White band is guidewire artifact. Red line represents the lumen area. Green line represents the external elastic membrane. ROI, region of interest.

Statistical Analysis

Continuous data with normal distribution are presented as mean standard deviation (SD). Bland–Altman plots were drawn to assess intraobserver and interobserver variability of MRA and IVUS measurements. Intraobserver and interobserver variability was calculated as the absolute value of the difference between two measurements divided by the average value of the pairs of interest. Associations of MRA measurements with

IVUS measurements were estimated with the Pearson correlation coefficient. Paired *t* tests were performed to test significant differences between the means values for MRA and IVUS measurements. Statistical analyses were performed using the IBM SPSS Statistics, version 20.0.01 (SPSS, Chicago, IL). Bland–Altman plots were made with GraphPad Prism version 4.00 (GraphPad Software Inc, La Jolla, CA).

RESULTS

Segmentation Algorithm and Renal Artery Dimensions

In nine patients, 17 renal arteries were analyzed to study intra- observer and interobserver reproducibility. In three renal arteries by observer 1 and in 3 renal arteries by observer 2, the bifurcation was selected manually. The segmentation was not possible in two matched renal arteries. Minimum lumen diameter, mean lumen diameter, and total lumen volume measured by MRA and IVUS are summarized in Table 1 and Supplementary Tables 1 and 2.

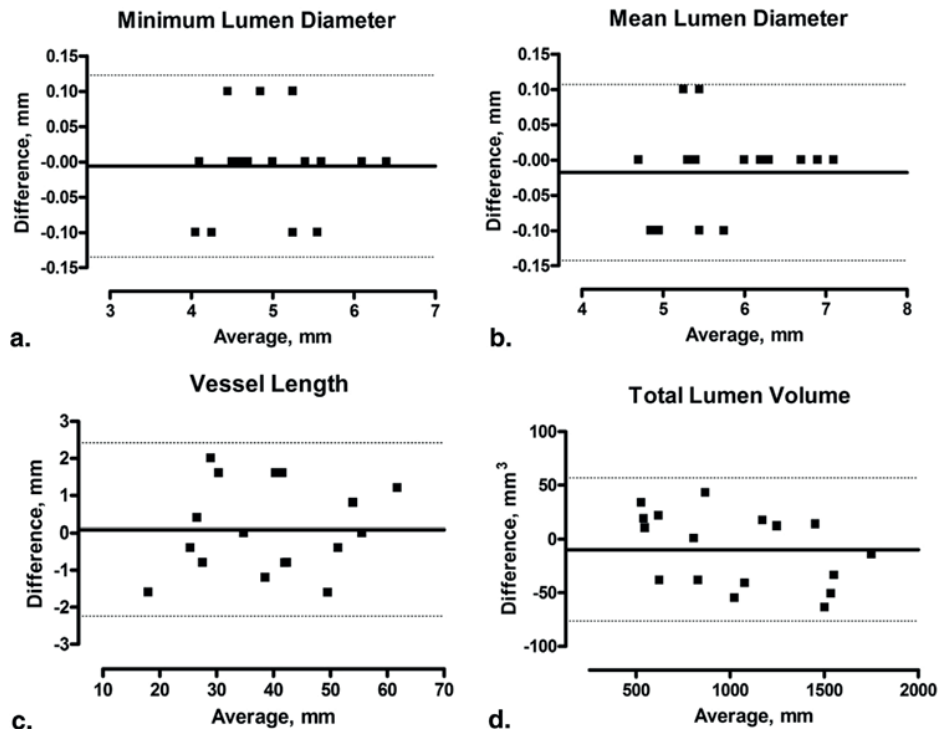
Table 1. Renal Artery Dimensions After Adjustments with IVUS Ref

Parameter	MRA, Mean \pm SD; <i>n</i> = 14	MRA Range	IVUS, Mean \pm SD; <i>n</i> = 14	IVUS Range	<i>P</i> value
Minimum lumen diameter (mm)	5.2 \pm 0.7	4.1–6.4	5.2 \pm 0.7	4.2–6.7	0.947
Mean lumen diameter (mm)	5.8 \pm 0.7	4.6–7.1	5.9 \pm 0.6	4.7–7.0	0.485
Total lumen volume (mm ³)	861.9 \pm 407.3	406.2–1687.2	902.9 \pm 369.4	471.3–1527.5	0.248

IVUS, intravascular ultrasound; MRA, magnetic resonance angiography; SD, standard deviation. A paired *t* test is used to test differences between the mean values for MRA and IVUS

Intraobserver Reproducibility MRA

Mean minimum lumen diameter was 5.1 \pm 0.8 mm. Bias of minimum lumen diameter was 0 mm; standard deviation (SD) of bias, 0.1 mm (95% limits of agreement, 0.1 to 0.1 mm). Intraobserver variability was 0.8%. Mean lumen diameter was 5.8 \pm 0.7 mm. Bias of mean lumen diameter was 0 mm; SD of bias, 0.1 mm (95% limits of agreement) -0.1 to 0.1 mm). Intraobserver variability was 0.7%. Mean vessel length was 39.4 \pm 12.3 mm. Bias of vessel length was 0.1 mm; SD of bias, 1.2 mm (95% limits of agreement, -2.2 to 2.4 mm). Intraobserver variability was 2.5%. Mean total lumen volume was 1035.3 \pm 403.6 mm³. Bias of total lumen volume was -9.7 mm³; SD of bias, 34.0 mm³ (95% limits of agreement, -76.4 to 57.0 mm³). Intraobserver variability was 2.9%. Bland–Altman plots are shown in Figure 3.

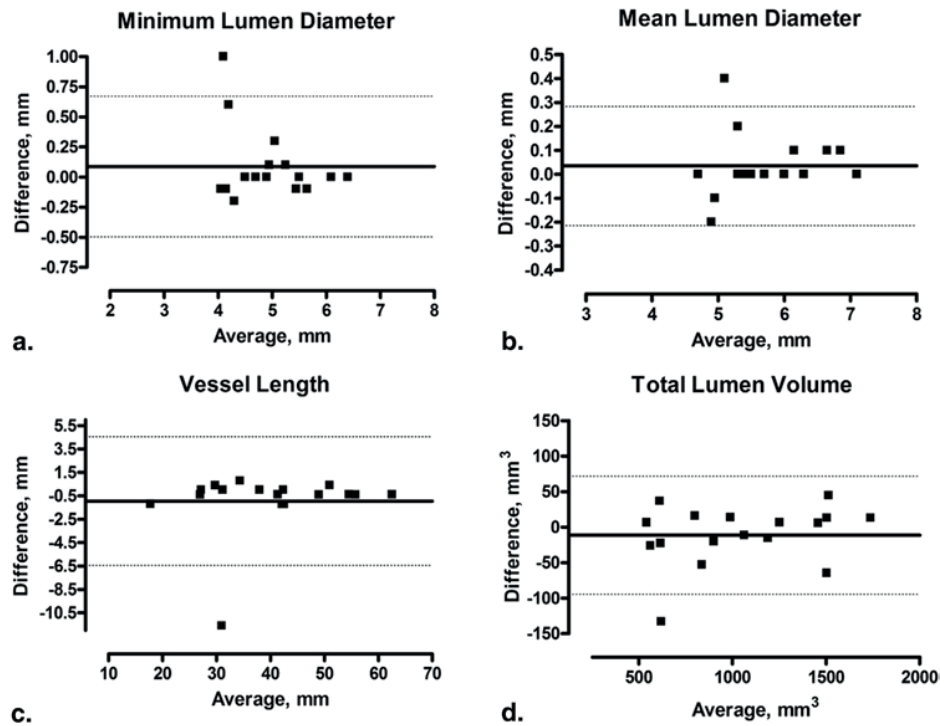


	Minimum Lumen Diameter	Mean Lumen Diameter	Vessel Length	Total Lumen Volume
Bias	0 mm	0 mm	0.1 mm	-9.7 mm ³
SD of Bias	0.1 mm	0.1 mm	1.2 mm	34.0 mm ³
95% Limits of Agreement	-0.1 – 0.1 mm	-0.1 – 0.1 mm	-2.2 – 2.4 mm	-76.4 – 57.0 mm ³

Figure 3. Bland-Altman plots of minimum lumen diameter (a), mean lumen diameter (b), vessel length (c), and total lumen volume (d) of the renal arteries measured by magnetic resonance angiography. Dotted lines show 95% limits of agreement.

Interobserver Reproducibility MRA

Mean minimum lumen diameter was $5.0 \text{ mm} \pm 0.8 \text{ mm}$. Bias of minimum lumen diameter was 0.1 mm; SD of bias, 0.3 mm (95% limits of agreement, -0.5 to 0.7 mm). Inter-observer variability was 3.2%. Mean lumen diameter was $5.7 \pm 0.7 \text{ mm}$. Bias of mean lumen diameter was 0 mm; SD of bias, 0.1 mm (95% limits of agreement, -0.2 to 0.3 mm). Interobserver variability was 1.2%. Mean vessel length was $39.8 \pm 12.0 \text{ mm}$. Bias of vessel length was -0.9 mm; SD of bias, 2.8 mm (95% limits of agreement, -6.4 to 4.6 mm). Interobserver variability was 2.8%. Mean total lumen volume was 1041.0 ± 397.1



	Minimum Lumen Diameter	Mean Lumen Diameter	Vessel Length	Total Lumen Volume
Bias	0.1 mm	0 mm	-0.9 mm	-11.4 mm ³
SD of Bias	0.3 mm	0.1 mm	2.8 mm	42.4 mm ³
95% Limits of Agreement	-0.5 – 0.7 mm	-0.2 – 0.3 mm	-6.4 – 4.6 mm	-94.5 – 71.7 mm ³

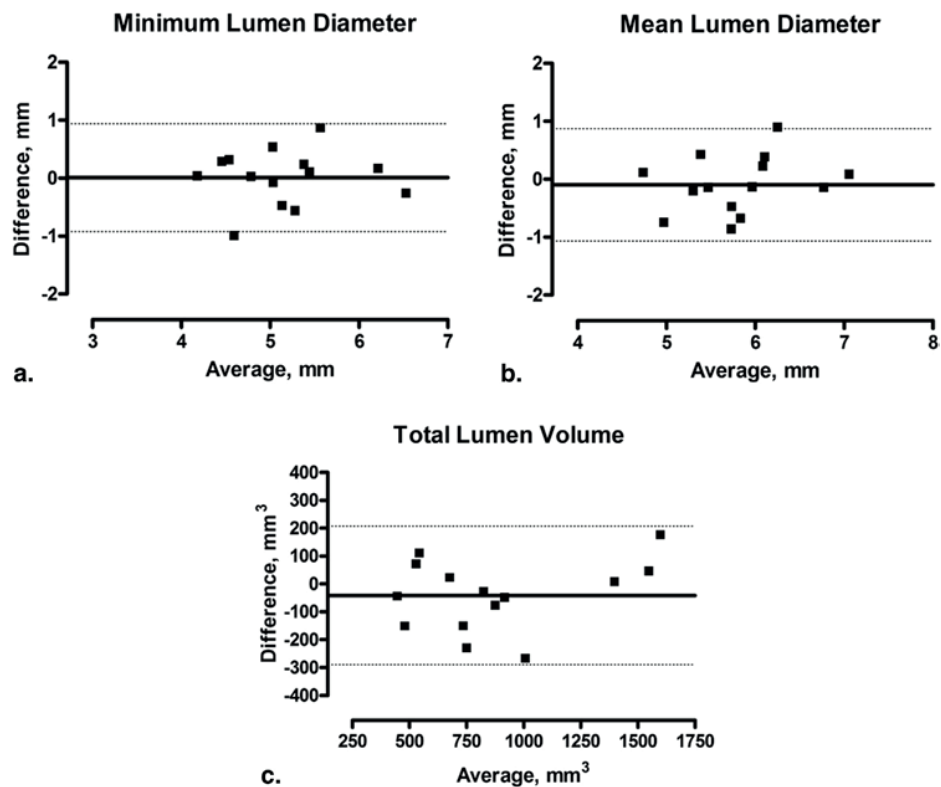
Figure 4. Interobserver variability magnetic resonance angiography (MRA). Bland-Altman plots of minimum lumen diameter (a), mean lumen diameter (b), vessel length (c), and total lumen volume (d) of the renal arteries measured by MRA. Dotted lines show 95% limits of agreement.

mm³. Bias of total lumen volume was -11.4 mm³; SD of bias, 42.4 mm³ (95% limits of agreement, -94.5 to 71.7 mm³). Interobserver variability was 2.8%. Bland-Altman plots are shown in Figure 4.

Validation of MRA Dimensions Against IVUS

Mean vessel length measured with MRA was 32.3 ± 11.4 and measured with IVUS 32.8 ± 11.4 . Mean minimum lumen diameter was 5.2 ± 0.7 mm. Bias of minimum lumen diameter was 0 mm; SD, 0.5 mm (95% limits of agreement, -0.9 to 0.9 mm). Minimum lumen

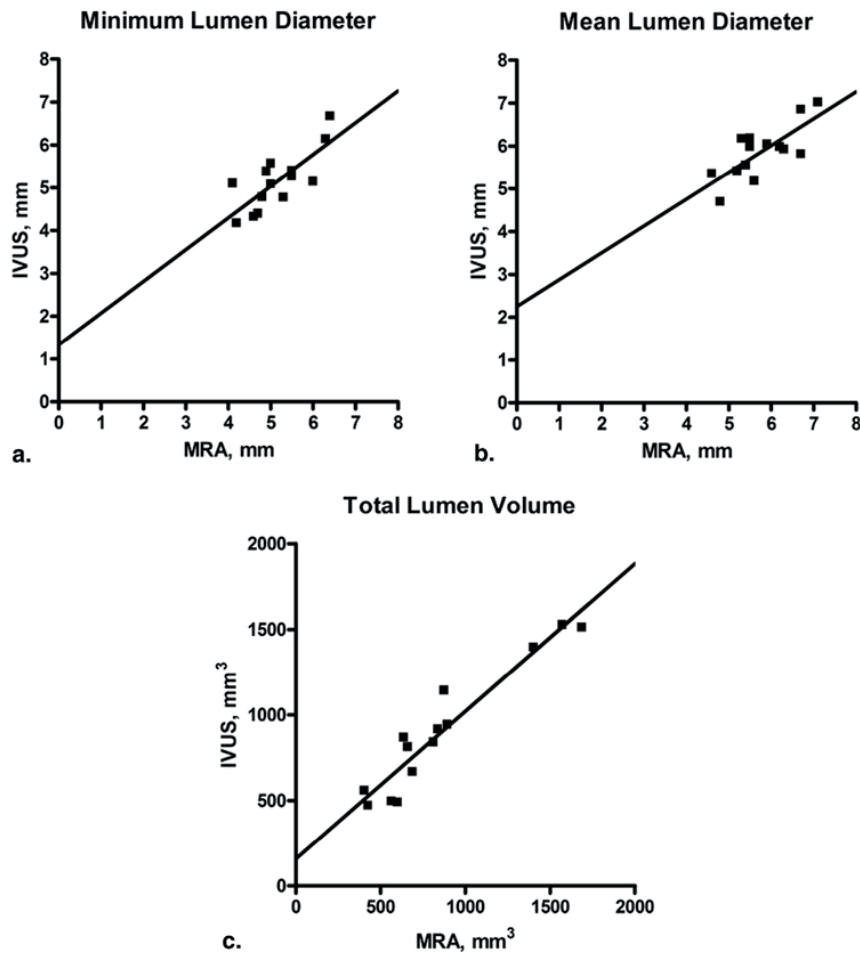
diameter measured by MRA was correlated with minimum lumen diameter measured by IVUS (R value, 0.771; $P = .001$). Mean lumen diameter was 5.8 ± 0.6 mm. Bias of mean lumen diameter was -0.1 mm; SD, 0.5 mm (95% limits of agreement, -1.1 to 0.9 mm). Mean lumen diameter measured by MRA was correlated with mean lumen diameter measured by IVUS (R value, 0.750; $P = .002$). Mean total lumen volume was 882.4 ± 383.6



	Minimum Lumen Diameter	Mean Lumen Diameter	Total Lumen Volume
Bias	0 mm	-0.1 mm	-40 mm ³
SD of Bias	0.5 mm	0.5 mm	126.7 mm ³
95% Limits of Agreement	-0.9 – 0.9 mm	-1.1 – 0.9 mm	-289.4 – 207.5 mm ³

Figure 5. Bland-Altman plots of minimum lumen diameter (a), mean lumen diameter (b), and total lumen volume (c) in mm³ of the renal arteries measured by magnetic resonance angiography and intravascular ultrasound. Dotted lines show 95% limits of agreement

mm³. Bias of total lumen volume was -40 mm³; SD, 126.7 mm³ (95% limits of agreement -289.4 to 207.5 mm³). Total lumen volume measured by MRA was correlated with the IVUS measurement (R value, 0.951; P < .001). Bland-Altman and correlation plots are shown in Figures 5 and 6.



	Minimum Lumen Diameter	Mean Lumen Diameter	Total Lumen Volume
R value	0.771	0.750	0.951
P value	0.001	0.002	< 0.001

Figure 6. Correlation of MRA dimensions with IVUS. Correlation of minimum lumen diameter (a), correlation of mean lumen diameter (b), correlation of total lumen volume (c). MRA, magnetic resonance angiography; IVUS, intravascular ultrasound.

DISCUSSION

Our study demonstrates that quantitative MRA can measure the renal artery dimensions (vessel length, minimum lumen diameter, mean lumen diameter, and renal artery volumes) reproducibly and with good intraobserver and interobserver variability. Intraobserver variability using semiautomatic MRA analysis was excellent for minimum lumen diameter and mean lumen diameter (0.8% and 0.7%, respectively). For vessel length and total lumen volume was slightly higher but were still well (2.5% and 2.9%, respectively). Interobserver variability was excellent for minimum lumen diameter and mean lumen diameter (3.2% and 1.2%, respectively) and good for vessel length and total lumen volume (2.8% and 2.8%, respectively).

MRA Technique

Automatic analysis of MRA and CTA (13-15) has been developed over the last years. The described quantitative MRA software requires minimal of user interaction to select the vessel segment of interest. By standardizing marker points for ostium and bifurcation identification, the used algorithm achieves excellent reproducibility which is important when baseline and follow-up imaging have to be compared. As well as CTA, renal duplex ultrasound, and invasive renal angiography, MRA is widely used for the detection of RAS (16). The advantage of MRA is that it does not require the use of ionizing radiation or iodinated contrast material that are required by CTA (17, 18), nor is MRA hampered by a higher body mass as may the case with duplex ultrasound. Various magnetic resonance imaging techniques have been developed to visualize the aorta and its branches, including “black blood” sequences, 2D and 3D TOF methods, phase-contrast techniques, and 3D contrast-enhanced methods using a gadolinium-based agent (19). The most commonly used sequences are the 2D TOF MRA and 3D contrast-enhanced methods. Nevertheless, the quality of the images in MRA depends on proper breath-hold and accurate timing of the contrast bolus. MRA cannot be performed in patients with implanted devices or claustrophobia.

Validation with IVUS

To the best of our knowledge, this is the first study validating MRA measurements of the renal arteries against IVUS measurements. Because of difficulties in engaging the tip of the IVUS catheter beyond the first large renal artery bifurcation (53% of the cases) and inability to fully visualize the ostium of the renal artery due to engagement of the tip of the guiding catheter (47%), IVUS pullback length was on average 5.9 mm shorter than the length of renal artery as assessed by MRA. To be able to validate the MRA volumetric measurements with IVUS, the segment of interest was matched by using either the ostium or bifurcation of the renal artery as a land mark. In this way, we were able to

validate the volume measurements of the renal artery segment between MRA and IVUS. Quantitative MRA renal artery measurements correlated well with IVUS, with a Pearson $R > 0.5$ for all measurements. MRA slightly underestimated vessel dimensions compared with IVUS, but the mean differences were small and not significant. One potential cause could have been the use of perprocedural intra-arterial nitrates directly before the IVUS pullback.

Clinical Applicability

Noninvasive quantitative measurements of renal artery dimension might be useful in preprocedural planning. The significance of the proper assessment of luminal dimensions has been demonstrated by recent data showing that oversizing with balloon-based RDN devices significantly increases the risk of intimal dissections of the renal artery as detected by OCT. Particularly, the measurement of minimum lumen diameter can be helpful in helping the treating physician in selecting the proper device and especially in selecting the balloon size to avoid oversizing (9). MRA may thus be important to the selection of patients for RDN procedure. Quantitative MRA analyses might allow accurate follow-up of renal arteries after renal artery interventions, allowing precise estimates of the vascular lumen and possible stenoses. The latter supports the use of MRA over duplex ultrasound, which is known to be highly operator dependent and which has a diagnostic accuracy in detecting stenosis that ranges from 60% to 90% (20). MRA, in contrast, has a sensitivity of 93% and specificity of 91% to detect renal artery stenosis compared with digital subtraction arteriography with invasive measurements (21). Current rates of stenosis after RDN depend strongly on the definitions and the methods of follow-up. For example, the Symplicity HTN-3 trial (which used the Medtronic Symplicity Flex RDN system) showed that the occurrence of RAS (defined as $>70\%$) was low (1 of 332 [0.3%]) within 6 months after renal denervation. Conversely, an emerging number of case reports have been published on RAS related to RDN (22-24), and recent data on the use of optical coherence tomography after RDN showed dissections in up to 35% of the arteries (9). In our study, MRA measurements demonstrated a low intraobserver variability of 0.8% for minimum lumen diameter, 2.9% for total lumen volume, and low interobserver variability of 3.2% for minimum lumen diameter, and 2.8% for total lumen volume. This allows the assessment of changes well in the range of a 10–40% change in luminal dimensions that might be clinically relevant at the long term. This dedicated quantitative analyses software requires minimal user input and might help to examine subtle changes renal artery integrity after RDN. The presented technology could help to achieve a more accurate evaluation of renal artery integrity at the medium- and long-term after renal artery interventions, especially in an era with an emerging number of newer generation devices.

Limitations

Our study has several limitations. First, interstudy variability was not tested by performing repeated MRAs. Second, as we were unable to treat small renal arteries with the current generation devices used in our site, patients with a renal artery diameter <4 mm were not included in this study. Our results might therefore not be applicable to arteries <4 mm. A total dose of 200 μ g of nitrates was locally administered before IVUS to prevent catheter-induced spasm. This might change the artery size and might be an explanation for the small differences in renal artery dimensions. The slice thickness of 1.6 mm without overlap is a limitation of the acquisition but inherent to breath-hold period of 20 seconds used in our protocol. Different MRA protocols and interstudy repeatability of the renal artery dimension were not tested as we were interested in the segmentation algorithm. Another contrast-agent injection on a second day would also have been more invasive. A double dose (0.2 mmol/kg) of contrast agent for CE-MRA might have an impact on signal intensity (25). We opted for a single dose of contrast agent because kidney perfusion was part of the MRI protocol, which requires another 0.1 mmol/kg of contrast agent.

CONCLUSIONS

Renal artery dimensions acquired with MRA can be quantified with good reproducibility, and these measurements correlated well with IVUS measurements. The software is a promising tool to assess changes in renal artery dimension after renal artery intervention and for the selection of the proper device before the procedure.

ACKNOWLEDGMENTS

The authors thank Jean-Paul Aben, Pie Medical Imaging, Maastricht, The Netherlands, for his help with the detailed description of the segmentation algorithm.

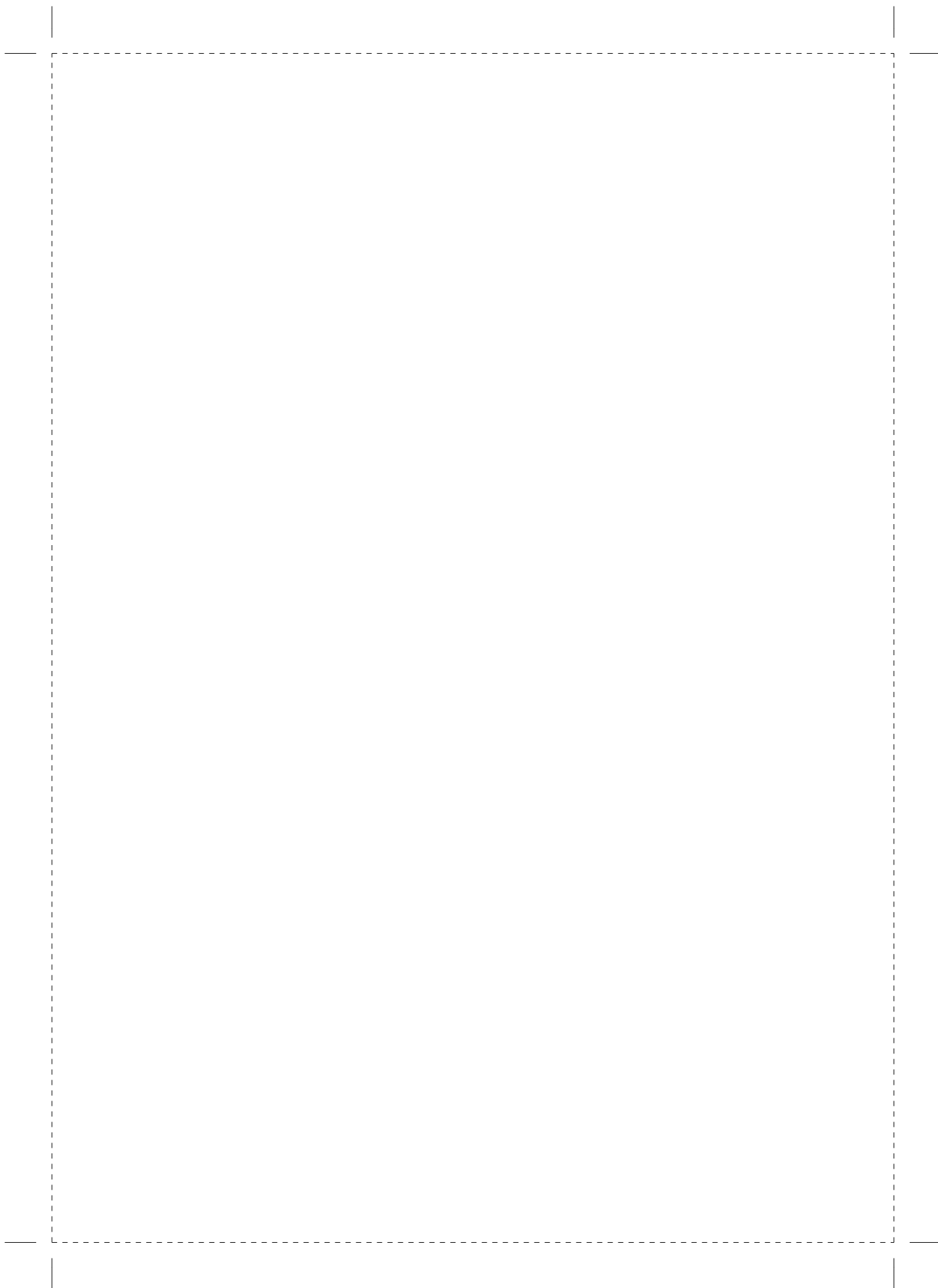
SUPPLEMENTARY DATA

Supplementary data related to this article can be found at <http://dx.doi.org/10.1016/j.acra.2015.03.014>.

REFERENCES

1. Bohm M, Linz D, Ukena C, Esler M, Mahfoud F. Renal denervation for the treatment of cardiovascular high risk-hypertension or beyond? *Circulation research*. 2014;115(3):400-9.
2. Daemen J, Mahfoud F. Renal denervation: expanding the indication. *EuroIntervention : journal of EuroPCR in collaboration with the Working Group on Interventional Cardiology of the European Society of Cardiology*. 2013;9 Suppl R:R101-4.
3. Davis MI, Filion KB, Zhang D, Eisenberg MJ, Afialo J, Schiffrin EL, et al. Effectiveness of renal denervation therapy for resistant hypertension: a systematic review and meta-analysis. *Journal of the American College of Cardiology*. 2013;62(3):231-41.
4. Bhatt DL, Kandzari DE, O'Neill WW, D'Agostino R, Flack JM, Katzen BT, et al. A controlled trial of renal denervation for resistant hypertension. *The New England journal of medicine*. 2014;370(15):1393-401.
5. Symplicity HTN1, Esler MD, Krum H, Sobotka PA, Schlaich MP, Schmieder RE, et al. Renal sympathetic denervation in patients with treatment-resistant hypertension (The Symplicity HTN-2 Trial): a randomised controlled trial. *Lancet*. 2010;376(9756):1903-9.
6. Krum H, Schlaich MP, Sobotka PA, Bohm M, Mahfoud F, Rocha-Singh K, et al. Percutaneous renal denervation in patients with treatment-resistant hypertension: final 3-year report of the Symplicity HTN-1 study. *Lancet*. 2014;383(9917):622-9.
7. Papademetriou V, Tsioufis CP, Sinhal A, Chew DP, Meredith IT, Malaipan Y, et al. Catheter-based renal denervation for resistant hypertension: 12-month results of the EnligHTN I first-in-human study using a multielectrode ablation system. *Hypertension*. 2014;64(3):565-72.
8. Karanasos A, Van Mieghem NM, Regar E, Daemen J. Serial imaging observations of vascular healing in a denervation-induced renal artery dissection. *European heart journal*. 2015;36(17):1040.
9. Karanasos A, Van Mieghem N, Bergmann MW, Hartman E, Ligthart J, van der Heide E, et al. Multimodality Intra-Arterial Imaging Assessment of the Vascular Trauma Induced by Balloon-Based and Nonballoon-Based Renal Denervation Systems. *Circulation Cardiovascular interventions*. 2015;8(7):e002474.
10. Delingette H, Cotin S, Ayache N. Efficient linear elastic models of soft tissues for real-time surgery simulation. *Studies in health technology and informatics*. 1999;62:100-1.
11. Antiga L, Steinman DA. Robust and objective decomposition and mapping of bifurcating vessels. *IEEE transactions on medical imaging*. 2004;23(6):704-13.
12. Girasis C, Schuurbiers JC, Muramatsu T, Aben JP, Onuma Y, Soekhradj S, et al. Advanced three-dimensional quantitative coronary angiographic assessment of bifurcation lesions: methodology and phantom validation. *EuroIntervention : journal of EuroPCR in collaboration with the Working Group on Interventional Cardiology of the European Society of Cardiology*. 2013;8(12):1451-60.
13. van 't Klooster R, de Koning PJ, Dehnavi RA, Tamsma JT, de Roos A, Reiber JH, et al. Automatic lumen and outer wall segmentation of the carotid artery using deformable three-dimensional models in MR angiography and vessel wall images. *Journal of magnetic resonance imaging : JMRI*. 2012;35(1):156-65.
14. Ahmed S, Zimmerman SL, Johnson PT, Lai H, Kawamoto S, Horton KM, et al. MDCT interpretation of the ascending aorta with semiautomated measurement software: improved reproducibility compared with manual techniques. *Journal of cardiovascular computed tomography*. 2014;8(2):108-14.

15. White JH, Bartlett ES, Bharatha A, Aviv RI, Fox AJ, Thompson AL, et al. Reproducibility of semi-automated measurement of carotid stenosis on CTA. *The Canadian journal of neurological sciences Le journal canadien des sciences neurologiques*. 2010;37(4):498-503.
16. Lao D, Parasher PS, Cho KC, Yeghiazarians Y. Atherosclerotic renal artery stenosis--diagnosis and treatment. *Mayo Clinic proceedings*. 2011;86(7):649-57.
17. Schoenberg SO, Rieger J, Weber CH, Michaely HJ, Waghershauser T, Ittrich C, et al. High-spatial-resolution MR angiography of renal arteries with integrated parallel acquisitions: comparison with digital subtraction angiography and US. *Radiology*. 2005;235(2):687-98.
18. Vasbinder GB, Nelemans PJ, Kessels AG, Kroon AA, Maki JH, Leiner T, et al. Accuracy of computed tomographic angiography and magnetic resonance angiography for diagnosing renal artery stenosis. *Annals of internal medicine*. 2004;141(9):674-82; discussion 82.
19. Leiner T, de Haan MW, Nelemans PJ, van Engelshoven JM, Vasbinder GB. Contemporary imaging techniques for the diagnosis of renal artery stenosis. *European radiology*. 2005;15(11):2219-29.
20. Zhang HL, Sos TA, Winchester PA, Gao J, Prince MR. Renal artery stenosis: imaging options, pitfalls, and concerns. *Progress in cardiovascular diseases*. 2009;52(3):209-19.
21. Eklof H, Ahlstrom H, Magnusson A, Andersson LG, Andren B, Hagg A, et al. A prospective comparison of duplex ultrasonography, captopril renography, MRA, and CTA in assessing renal artery stenosis. *Acta radiologica*. 2006;47(8):764-74.
22. Kaltenbach B, Id D, Franke JC, Sievert H, Hennersdorf M, Maier J, et al. Renal artery stenosis after renal sympathetic denervation. *Journal of the American College of Cardiology*. 2012;60(25):2694-5.
23. Jaen Aguila F, Mediavilla Garcia JD, Molina Navarro E, Vargas Hitos JA, Fernandez-Torres C. Bilateral renal artery stenosis after renal denervation. *Hypertension*. 2014;63(5):e126-7.
24. Pucci G, Battista F, Lazzari L, Dominici M, Boschetti E, Schillaci G. Progression of renal artery stenosis after renal denervation. Impact on 24-hour blood pressure. *Circulation journal : official journal of the Japanese Circulation Society*. 2014;78(3):767-8.
25. Heverhagen JT, Wright CL, Schmalbrock P, Knopp MV. Dose comparison of single versus double dose in contrast-enhanced magnetic resonance angiography of the renal arteries: intra-individual cross-over blinded trial using Gd-DTPA. *European radiology*. 2009;19(1):67-72.





Chapter 3

Serial quantitative magnetic resonance angiography follow-up of renal artery dimensions following treatment by four different renal denervation systems.

van Zandvoort L, **van Kranenburg M**, Karanasos A, van Mieghem N, Ouhlous M, van geuns RJM, van Domburg R. Daemen J

Eurointervention. 2017 Jan 3; 12(13)

ABSTRACT

Aims - renal sympathetic denervation (RDN) is being studied as a therapeutic option for patients with therapy resistant hypertension. It remains unclear if the procedure affects the renal arteries in such a way that luminal narrowing might occur at the mid- to longer-term.

Methods & results - In a prospective cohort of 27 patients referred for RDN, quantitative magnetic resonance angiography (MRA) was used to assess 52 vessels at baseline, 6-, and 12 months post treatment with one out of four different devices. No renal artery stenosis was seen at 6 or 12 months. The average mean lumen area was $26,6 \pm 7,3 \text{ mm}^2$ at baseline versus $25,0 \pm 7,1$ and $25,0 \pm 6,1$ at 6 and 12 months respectively resulting in a late loss of $1,6 \text{ mm}^2$ at 6 months and $1,9 \text{ mm}^2$ at 12 months. No differences were observed in the arterial response to RDN with the four different systems used. There was no correlation between post procedural dissections, edema or thrombi as detected with invasive imaging and luminal narrowing at follow-up.

Conclusions - Quantitative MRA of patients treated with RDN revealed no significant change in renal artery dimensions up to 12 months follow-up. The lack of a change in renal artery luminal dimensions was irrespective of the arterial response to the individual devices used.

Keywords: renal artery, renal artery denervation, MRA, hypertension

CONDENSED ABSTRACT

It remains unclear if percutaneous renal sympathetic denervation (RDN), a potential treatment for therapy resistant hypertension, might cause luminal narrowing at mid- to longer-term. A total of 52 vessels, treated with one out of four different RDN devices, were analyzed with quantitative magnetic resonance angiography (MRA) at baseline, 6 months and 12 months. Renal artery dimension did not change over time. No differences were observed in the arterial response to RDN with the four different systems used. There was no correlation between post procedural arterial damage as detected with invasive imaging and luminal narrowing at follow-up.

INTRODUCTION

Controlling blood pressure in hypertensive patients remains a challenge for all physicians and treatment targets are usually not achieved despite multiple antihypertensive drugs. (1) Percutaneous renal sympathetic denervation (RDN) is currently being studied as a potential treatment option in patients with therapy resistant hypertension. The indication spectrum is currently even being expanded towards several new indications (2-5). At present, over 53 devices are available to dismantle afferent and efferent renal nerves in the renal arterial wall. Although the body of evidence supporting the efficacy of several of both the 1st and 2nd generation devices is growing, long-term safety data is limited (6-8) and mostly restricted to duplex ultrasound findings, showing a low rate of adverse events, both at short and longer term follow-up (7, 9). A limited number of computed tomography angiography (CTA) or magnetic resonance angiography (MRA) follow-up observations revealed an absence of renal artery stenosis at 6 months. (10). However, recent high resolution intravascular imaging findings performed directly post procedure, demonstrated signs of small thrombi and/or dissections in almost 50% of the treated arteries, illustrating that binary outcome parameters of stenosis might not be sufficient. (11) The aim of the present study is to accurately assess renal artery integrity at the medium to long-term using recently validated quantitative Magnetic Resonance Angiography software in patients treated with 4 different RDN devices. (12, 13)

METHODS

Patient selection

We present a prospective study in which a total of 29 patients with therapy resistant hypertension, vasospastic angina and/or heart failure underwent RDN at the Erasmus Medical Center, Rotterdam, the Netherlands, between December 2012 and February 2014. RDN was performed by one out of four different systems: Symplicity Flex™ (Medtronic, Minneapolis, MN), Paradise™ (Recor Medical, Palo Alto, CA), Oneshot™ (Covidien, Campbell, CA), and Vessix V2™ (Boston Scientific, Natick, MA). Two patients were excluded because of the implantation of a non-MRI compatible pacemaker at 3 months (n=1) and 1 because of a missed follow-up scan (n=1). A total of 27 patients and 52 vessels were used for the final analyses at baseline and 6 months follow-up (in 2 patients only 1 vessel could be analysed at baseline because of insufficient contrast density). For the 12 months analyses, 33 vessel remained (MRA image quality was insufficient at 12 months follow-up (N=14), CTA at 12 months follow-up instead of MRA (N=1) and no follow-up MRA of 12 months follow-up post at the time of this research (N=4)).

Denervation procedure.

All patients were preloaded with 300mg aspirin, if naïve, and advised to continue with aspirin for at least 1 month. Pre-procedurally, 100IU heparin/kg were administered to achieve an active clotting time >250s. A total of 200mcg nitrates was locally administered before invasive imaging. Procedures were performed according to device-specific instructions for use. Additional peri-procedural invasive imaging was performed in 19 out of the 52 vessels used for the final analysis in the present study. Targeted renal arteries were examined with an intravascular ultrasound (IVUS) system with automatic pullback at 0.5 mm/s (Boston Scientific, Natick, MA) and optical coherence tomography (OCT) using the Illumien or C7XR system and Dragonfly or Dragonfly Duo catheter (all Lightlab/St Jude, Minneapolis, MN) as previously described. (11)

IVUS and OCT image acquisition

Targeted renal arteries were examined with an IVUS system with automatic pullback at 0.5 mm/s (Boston Scientific, Natick, MA) pre- and post-RDN. Retrieved IVUS images were stored and analyzed offline. OCT was performed after RDN. Images were acquired using the Illumien or C7XR system and Dragonfly or Dragonfly Duo catheter (all Lightlab/St Jude, Minneapolis, MN). The catheter was positioned distally to the examined segment (distal to the first major bifurcation) and automatically pulled back at 20mm/sec, acquiring images at 100m/sec, with simultaneous iso-osmolar contrast (Iodixanol 370, Visipaque™, GE Health Care, Ireland) administration at a flow rate of 4-6ml/sec, depending on artery size. The protocol used for detection of edema, thrombus or dissection using both IVUS and OCT has been published previously. (11)

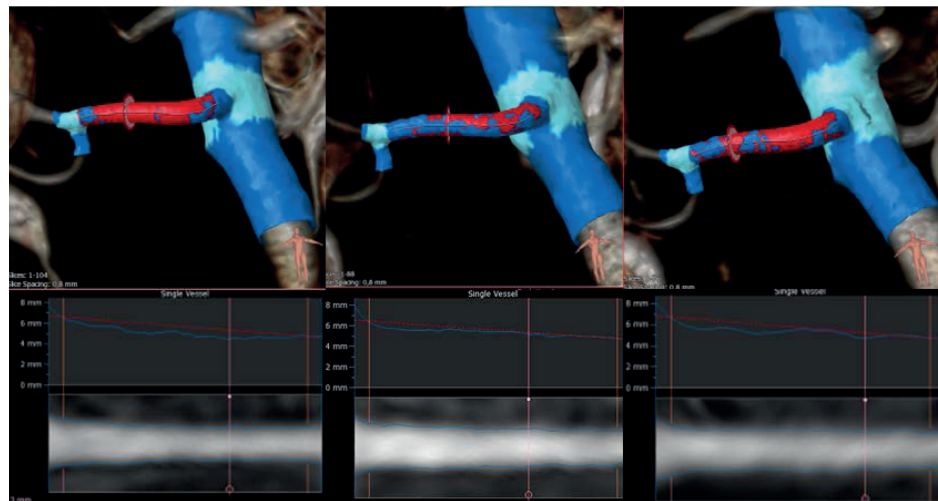
Magnetic resonance angiography acquisition

Magnetic resonance angiography was performed on a 1.5-T MRI scanner (Discovery MR450, GE Medical systems, Milwaukee, Wisconsin, USA) at baseline and 6 and 12 months follow-up according to a dedicated RDN imaging protocol. Patients were positioned in supine position and an 8-channel cardiac coil was placed on the thorax and upper-abdomen. As part of this MRI protocol, a 3D Vasc Fast TOF Spoiled Gradient Echo sequence was used to acquire images of the renal vasculature, after a test-bolus procedure. Images were acquired during a breath hold. The following parameters were used: field of view: 46 cm * 41.4 cm, matrix; 320 * 192, upsampled to 512 * 512, number of excitations; 0.75, pixel size; 0.89 * 0.89 mm, flip angle; 17 degrees, slice thickness; 1.6 mm, location per slab; 28 upsampled to 56 with ZIP2, repetition time; 3.2 ms, echo time; 1.2 ms, bandwidth; 83.33 Hz. The duration of the breathhold was approximately 20 seconds, depending on the locations per slab. A power injector (Medrad Spectris, Warrendale, Pennsylvania, U.S.A.) was used to inject gadobutrol (Gadovist 1.0 mmol/ml, Bayer, Mijdrecht, the Netherlands). Gadovist was injected, around 18 seconds before

acquisition, with a dose of 0.1 mmol/kg ml into an antecubital vein followed by 15 ml of saline at a rate of 2.5 ml/s to visualize the renal arteries.

Magnetic resonance angiography analysis

Quantitative magnetic resonance angiography was performed using dedicated imaging software CAAS MRA (Version 1.0, Pie Medical Imaging B.V, Maastricht, the Netherlands) according to a predefined algorithm. (13) The automatically segmented arteries were inspected and borders were manually corrected if necessary in the stretched multi-planar rendering and perpendicular view. Vessel length (mm), minimum lumen diameter (mm) mean lumen diameter (mm), minimum lumen area (mm^2), mean lumen area (mm^2), percent diameter stenosis and percent area stenosis were based on semi-automatic segmentation (Figure 1). One of the investigators (LZ) performed all of the analyses blinded to individual patients characteristics and treatment time.



	Baseline	6 months follow-up	12 months follow-up
Vessel Length, mm	36,8	35,2	36,8
Minimum lumen diameter, mm	4,5	4,3	4,0
Mean lumen diameter, mm	5,2	5,3	5,3
Minimum lumen area, mm^2	15,6	14,5	12,8
Mean lumen area, mm^2	21,6	23,0	22,4

Figure 1. Case example of a renal artery analysis with the use of CAAS quantitative MRA software. Baseline, 6 months follow-up and 12 months follow-up are depicted.

Statistical analysis

Statistical analyses were performed by using SPSS (version 21.0, SPSS Inc, Chicago Ill). Baseline, categorical variables are reported as either counts of percentages and compared using the Chi Squared test. Continuous variables are reported as mean \pm SD and were compared using a linear mixed model. All continuous variables were normally distributed. Categorical variables were reported as either percentages or frequencies. A P value < 0.05 was considered statistically significant. Between-device differences were examined using analysis of variance (ANOVA). When there was a significant difference between groups, the Bonferroni test was used as a post hoc comparison. Since our data included multiple observations per patient, crossed random effects modeling was used to account for the correlation between observations. (14) Luminal dimensions over time were assessed using crossed random effects with two random effects. The first random effect was the period (either 6 or 12 months), the second random effect was related to the fact whether either 1 or both vessels were assessed in each individual patients.

RESULTS

Patient demographics and baseline characteristics are depicted in Table 1. Mean age at the time of intervention was 64 ± 11 years and 56% of the patients were male. Diabetes was present in 26% and 70% of the patients had hypercholesterolemia. Baseline renal function was preserved in all patients with a baseline eGFR of 82.5 ± 28.0 ml/min/1.73m². Mean office blood pressure (BP) was $176 \pm 21/93 \pm 17$ mmHg. Mean ambulatory BP was $144 \pm 14/81 \pm 13$ mmHg. There was no significant difference between any of the baseline characteristics in patients treated with the four different devices used for RDN (table 1). Quantitative MRA at baseline and follow-up revealed no renal artery stenosis at either 6 or 12 months. The average mean lumen area was 26.6 ± 7.3 mm² at baseline versus 25.0 ± 7.1 and 25.0 ± 6.1 at 6 and 12 months respectively resulting in a late loss of 1.6 mm² at 6 months and 1.9 mm² at 12 months (Table 2). There was no significant increase in the area or diameter stenosis over time. By using three different cut-offs for diameter and area stenosis ($>25\%$, $>50\%$ and $>70\%$), no trend was observed towards an increased number of patients with renal artery stenosis over time (Figures 2 and 3). Only 5 out of 52 vessels showed an absolute increase in percent diameter stenosis $> 25\%$ at 6 months. If comparing baseline versus 12 months, no vessels were identified with a $>25\%$ increase in percent diameter stenosis. An absolute increase of $> 50\%$ in percent diameter stenosis was not observed at either time point in any of the patients. Comparing the differences in late loss in vessels treated with balloon (ReCor Paradise, BSc Vessix and Covidien OneShot) versus the MDT Symplicity Flex non-balloon based system did not result in any significant differences (P=NS for all) (Figure 4). Intravascular imaging using optical

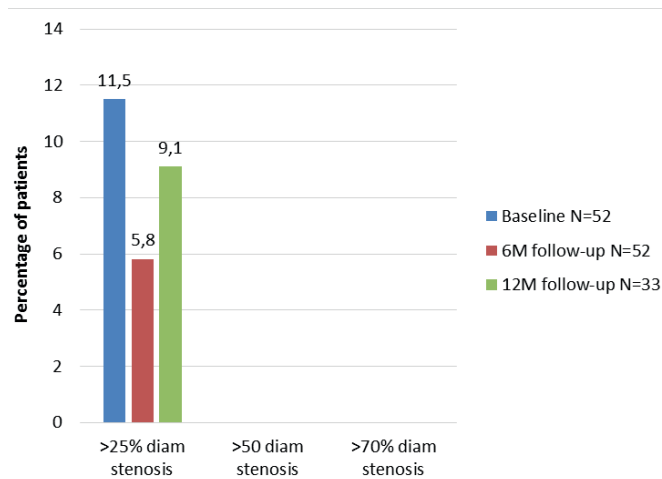
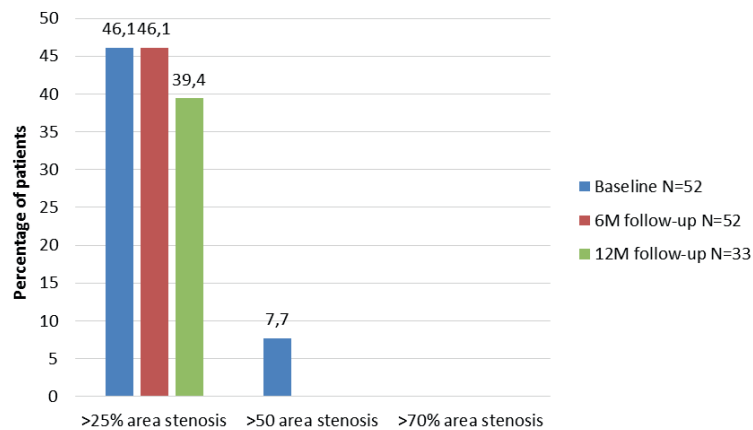
Table 1. Baseline characteristics (patient analyses)

	All patients (n=27)	Devices: MDT Symplicity Flex (n=10)	ReCor Paradise (n=12)	BSc Vessix (N=3)	Covidien OneShot (N=2)	p-value
Age, years (±SD)	64±11	67±12	64±11	56±2	66±13	0,540
Male % Race of patient, %	56	40	58	67	100	0,429
Caucasian	78	90	67	100	50	0,460
Afro American	15	0	25	0	50	0,460
Hindu	7	10	8	0	0	0,460
Length, cm (±SD)	172,2±10,9	168,4±9	172,9±11,8	180,7±13,6	174,5±9,1	0,386
Weight, kg (±SD)	87,1±16,1	84±13,5	88,8±19,8	91,7±15,3	86±12,7	0,875
BMI, kg/m ² (±SD)	29,3±4,1	29,5±3,8	29,6±4,7	28,2±5	28,1±1,2	0,934
DM, %	26	30	25	100	50	0,627
Hypertension, %	100	100	100	100	100	1
Hypercholesterolemia, %	70,4	70	75	33,3	100	0,401
Family history, %	56	60	50	67	50	0,939
Duration of the procedure (min)	84,7±16	98,5±35,3	72,6±31,7	85,7±30	100,5±46	0,364
Current smoking, %	26	20	17	67	50	0,272
eGFR, ml/min (±SD)	63,1±33,1	51,2±20,9	64,5±39,1	76,1±41,1	94,9±22,1	0,795
Mean ambulatory BP, mmHg (±SD/±SD)	144±14/ 81±13	146,6±13,1/ 79,4±15,4	138,3±15,8/ 78,5±10,6	150,7±9,1/ 94,7±12,5	152±14,1/ 86,5±16,3	0,333/ 0,270

Values are expressed as mean±SD, number or %; BP=blood pressure; eGFR=estimated glomerular filtration rate; BMI= body mass index

Table 2. Quantitative renal artery imaging results at baseline, 6 months and 12 months follow-up (vessel analyses)

Variables	Baseline N=52 (mean±SD)	6 Months follow-up N=52 (mean±SD)	12 months follow- up N=33 (mean±SD)	P-value Baseline – 6 months follow-up	P-value Baseline – 12 months follow-up
Vessel length, mm	40,3±12,6	40,3±12,7	39,2±12,1	,693	,878
Minimum lumen diameter, mm	4,9±0,8	4,7±0,8	4,8±0,7	,044	,124
Mean lumen diameter, mm	5,7±0,8	5,6±0,7	5,6±0,7	,086	,004
Minimum lumen area, mm ²	19,7±6,6	17,9±5,8	18,3±5,6	,051	,114
Mean lumen area, mm ²	26,6±7,3	25,0±7,1	25,0±6,1	,088	,003
Percent diameter stenosis	14,9±9,0	13,2±8,4	12,9±8,4	,159	,130
Percent area stenosis	26,9±14,9	23,9±14,4	23,4±14,6	,175	,152

**Figure 2.** % diameter stenosis subdivided in 3 categories**Figure 3.** % area stenosis subdivided in 3 categories

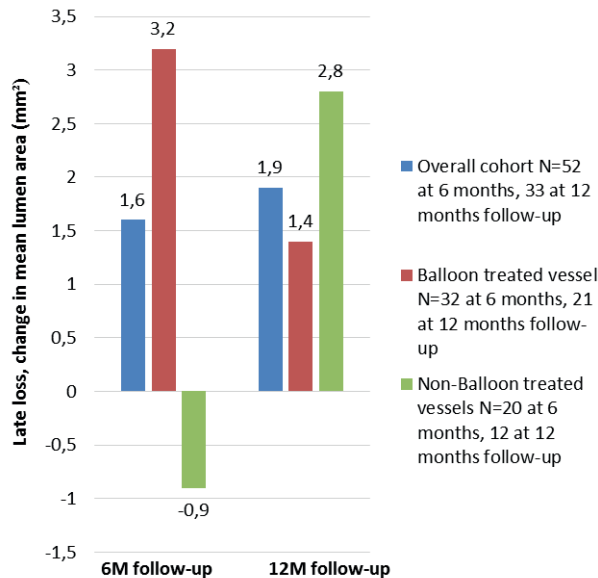


Figure 4. Late loss according to treatment device

coherence tomography directly post procedure revealed dissections in 6/19 vessels (32%) and thrombus in 13/19 vessels (68%). There was no correlation between these post procedural signs of vascular traumata and luminal narrowing at 6 or 12 months. Renal function slightly decreased over time. Mean baseline eGFR was 82.4ml/min and decreased to 77 ml/min/1.73m² at 6 months and 74.9 ml/min/1.73m² at 12 months (p-value=0.013). Although there was no correlation between late-loss and change in renal function at 6 or 12 months, a clear correlation was seen between contrast volume using peri-procedural and renal function decline over time. No new cases of renal impairment (eGFR<60ml/min) were observed.

DISCUSSION

Using quantitative MRA software we demonstrated an absence of renal artery stenosis at 6 and 12 months post procedure. More specifically, no decrease in renal artery dimensions post RDN could be found at either 6 or 12 months, irrespective of the device used.

The present study adds to previous observations reporting on the safety of RDN because of 3 reasons. At first, recent studies with a focus on follow-up of renal arteries 6 month after RDN used duplex ultrasound or occasionally CTA or MRA, and only focused on binary outcomes, namely the presence of stenosis or not. Using recently validated dedicated quantitative MRA software we were able to more accurately report on the

true vascular response of RDN.(13) Second, our study was not limited to the use of a single RDN device. Instead, the vascular response to treatment with both balloon and non-balloon based devices as well as radiofrequency versus ultrasounds devices was assessed. Third, we were able to extend the safety findings reported at 6 months to 1 year.

The need for a more precise method to assess renal artery dimensions was driven by the findings from several recent studies assessing the direct consequences of RDN on renal artery integrity.(11, 15, 16) Using dedicated intravascular imaging techniques like IVUS and OCT a significant proportion of renal arteries proved to be left with dissections, thrombus and edema, mostly not directly visible on standard post procedural angiography. Although in the vast majority of the cases these findings were not linked to direct clinical consequences, the effect on long-term vascular integrity and perhaps even renal function remains elusive. The importance however of a careful assessment of long-term vascular safety has been recently underlined by the report of a European expert consensus document on future trial design in renal denervation. (17)

In a recently published validation study we demonstrated that renal artery dimension can be accurately measured using CAAS MRA, with a good intraobserver and interobserver variability and a good correlation as compared to intravascular ultrasound. (13) Quantitative MRA facilitates non-invasive assessment of small changes in renal artery luminal dimensions and allowed us to study the correlation between peri-procedural renal artery damage and long-term luminal narrowing. Although we hypothesized that a small albeit significant change in luminal dimensions could be due to the cases in which the arterial lumen integrity was lost due to small dissections, thrombi and edema, we were not able to demonstrate a correlation. Additionally, no differences were observed between luminal narrowing at follow-up and the use of either of the individual RDN devices used.

In our study renal function slightly deteriorated over time. Although the technology has been previously hypothesized to improve renal function in patients with renal failure, the impact of the treatment on renal function over time has been disputed. While some single arm studies reported on an improvement in renal function, others demonstrate that renal function might slightly deteriorate over time. (18, 19) We further hypothesized that luminal narrowing might be responsible for a decrease in renal function. However, no correlation was found between the change in luminal dimensions at both 6 and 12 months follow-up and the change in eGFR. Further scrutinizing the pathophysiology of the renal function decline in our cohort revealed a clear correlation with contrast volume used during the procedure. Due to the learning curve in the initial cases performed at our site together with the use of OCT imaging to assess renal artery integrity contrast usage was substantially higher in the initial cases. It appears therefore unlikely that the RDN procedure itself causes a significant change in renal function over time.

Limitations

The sample size of our study was relatively small, which implicates that the conclusions on the inter-device differences should be interpreted with caution. Unfortunately, several follow-up scans could not be analyzed adequately due to the suboptimal quality of several MRA's with suboptimal harmonization of contrast delivery and scan time and movement- and breathing artefacts due to the need for a 20-second breath hold. Also, at the time of this study, not all patients reached the 12 months follow-up (N=2). Further research should focus on a larger study cohort and extended follow-up duration.

CONCLUSION

Quantitative MRA of patients treated with percutaneous renal denervation revealed no significant decrease in renal artery dimensions at both 6 and 12 months follow-up. The lack of a decrease in renal artery luminal dimensions was irrespective of the arterial response to the individual devices used.

Funding : None.

Take home message

Renal artery luminal dimension did not change after treatment with one out of four different renal denervation devices when measured using dedicated quantitative MRA software. There was no correlation between post procedural arterial damage as detected with invasive imaging and luminal narrowing at follow-up.

Conflict of interest statement

A.K. has received research support from St Jude Medical for OCT-related research.

N.M. is on the Advisory board of Abbott vascular.

JD received institutional research support from Boston Scientific, ReCor Medical, St. Jude Medical and Medtronic

REFERENCES

- Scheltens T, Bots ML, Numans ME, Grobbee DE, Hoes AW. Awareness, treatment and control of hypertension: the 'rule of halves' in an era of risk-based treatment of hypertension. *Journal of human hypertension*. 2007;21(2):99-106.
- Santiapillai GR, Ferro A. Renal denervation as an option for the management of hypertension. *J Biomed Res*. 2014;28(1):18-24.
- Castro Torres Y, Katholi RE. Renal denervation for treating resistant hypertension: current evidence and future insights from a global perspective. *Int J Hypertens*. 2013;2013:513214.
- Bohm M, Linz D, Ukena C, Esler M, Mahfoud F. Renal Denervation for the Treatment of Cardiovascular High Risk-Hypertension or Beyond? *Circ Res*. 2014;115(3):400-9.
- Daemen J, Mahfoud F. Renal denervation: expanding the indication. *EuroIntervention*. 2013;9 Suppl R:R101-4.
- Davis MI, Filion KB, Zhang D, Eisenberg MJ, Afilalo J, Schiffrin EL, et al. Effectiveness of renal denervation therapy for resistant hypertension: a systematic review and meta-analysis. *J Am Coll Cardiol*. 2013;62(3):231-41.
- Bhatt DL, Kandzari DE, O'Neill WW, D'Agostino R, Flack JM, Katzen BT, et al. A controlled trial of renal denervation for resistant hypertension. *N Engl J Med*. 2014;370(15):1393-401.
- Symplcity HTNI, Esler MD, Krum H, Sobotka PA, Schlaich MP, Schmieder RE, et al. Renal sympathetic denervation in patients with treatment-resistant hypertension (The Symplcity HTN-2 Trial): a randomised controlled trial. *Lancet*. 2010;376(9756):1903-9.
- Krum H, Schlaich MP, Sobotka PA, Bohm M, Mahfoud F, Rocha-Singh K, et al. Percutaneous renal denervation in patients with treatment-resistant hypertension: final 3-year report of the Symplcity HTN-1 study. *Lancet*. 2014;383(9917):622-9.
- Papademetriou V, Tsioufis CP, Sinhal A, Chew DP, Meredith IT, Malaipapan Y, et al. Catheter-Based Renal Denervation for Resistant Hypertension : 12-Month Results of the EnligHTN I First-in-Human Study Using a Multielectrode Ablation System. *Hypertension*. 2014.
- Karanasos A, Van Mieghem N, Bergmann MW, Hartman E, Ligthart J, van der Heide E, et al. Multimodality Intra-Arterial Imaging Assessment of the Vascular Trauma Induced by Balloon-Based and Nonballoon-Based Renal Denervation Systems. *Circ Cardiovasc Interv*. 2015;8(7).
- Schuurbiers JC, Lopez NG, Ligthart J, Gijzen FJ, Dijkstra J, Serruys PW, et al. In vivo validation of CAAS QCA-3D coronary reconstruction using fusion of angiography and intravascular ultrasound (ANGUS). *Catheter Cardiovasc Interv*. 2009;73(5):620-6.
- van Kranenburg M, Karanasos A, Chelu RG, van der Heide E, Ouhlous M, Nieman K, et al. Validation of Renal Artery Dimensions Measured by Magnetic Resonance Angiography in Patients Referred for Renal Sympathetic Denervation. *Acad Radiol*. 2015;22(9):1106-14.
- Lingsma H, Nauta S, van Leeuwen N, Borsboom G, Bruining N, Steyerberg E. Tools & Techniques: Analysis of clustered data in interventional cardiology: current practice and methodological advice. *EuroIntervention*. 2013;9(1):162-4.
- Templin C, Jaguszewski M, Ghadri JR, Sudano I, Gaehwiler R, Hellermann JP, et al. Vascular lesions induced by renal nerve ablation as assessed by optical coherence tomography: pre- and post-procedural comparison with the Simplicity catheter system and the EnligHTN multi-electrode renal denervation catheter. *Eur Heart J*. 2013;34(28):2141-8, 8b.
- Cordeanu ME, Gaertner S, Bronner F, Jahn C, Prinz E, Hannedouche T, et al. Neointimal thickening resulting in artery stenosis following renal sympathetic denervation. *Int J Cardiol*. 2014;177(3):e117-9.

17. Mahfoud F, Bohm M, Azizi M, Pathak A, Durand Zaleski I, Ewen S, et al. Proceedings from the European clinical consensus conference for renal denervation: considerations on future clinical trial design. *Eur Heart J*. 2015;36(33):2219-27.
18. Tsioufis CP, Papademetriou V, Dimitriadis KS, Kasiakogias A, Tsiachris D, Worthley MI, et al. Catheter-based renal denervation for resistant hypertension: Twenty-four month results of the EnLIGHTN I first-in-human study using a multi-electrode ablation system. *Int J Cardiol*. 2015;201:345-50.
19. Azizi M, Sapoval M, Gosse P, Monge M, Bobrie G, Delsart P, et al. Optimum and stepped care standardised antihypertensive treatment with or without renal denervation for resistant hypertension (DENERHTN): a multicentre, open-label, randomised controlled trial. *Lancet*. 2015;385(9981):1957-65.



Chapter 4

Qualitative grading of aortic regurgitation:
a pilot study comparing CMR 4D flow and
echocardiography.

Chelu RG, van den Bosch AE, **van Kranenburg M**, Hsiao A, van den Hoven AT, Ouhlous M, Budde RPJ, Beniest, KM, Swart LE, Coenen A, Lubbers MM, Wielopolski PA, Vasanawala SS, Roos-Hesselink JW, Nieman K.

Int J Cardiovasc Imaging. Springer Netherlands; 2015 Oct 24;32(2):301-7.

ABSTRACT

Over the past 10 years there has been intense research in the development of volumetric visualization of intracardiac flow by cardiac magnetic resonance (CMR). This volumetric time resolved technique called CMR 4D flow imaging has several advantages over standard CMR. It offers anatomical, functional and flow information in a single free-breathing, ten-minute acquisition. However, the data obtained is large and its processing requires dedicated software. We evaluated a cloud-based application package that combines volumetric data correction and visualization of CMR 4D flow data, and assessed its accuracy for the detection and grading of aortic valve regurgitation using transthoracic echocardiography as reference. Between June 2014 and January 2015, patients planned for clinical CMR were consecutively approached to undergo the supplementary CMR 4D flow acquisition. Fifty four patients (median age 39 years, 32 males) were included. Detection and grading of the aortic valve regurgitation using CMR 4D flow imaging were evaluated against transthoracic echocardiography. The agreement between 4D flow CMR and transthoracic echocardiography for grading of aortic valve regurgitation was good ($K = 0.73$). To identify relevant, more than mild aortic valve regurgitation, CMR 4D flow imaging had a sensitivity of 100 % and specificity of 98 %. Aortic regurgitation can be well visualized, in a similar manner as transthoracic echocardiography, when using CMR 4D flow imaging.

INTRODUCTION

In the management of valvular heart disease assessment of transvalvular flow by cardiac magnetic resonance (CMR) can provide valuable incremental information to echocardiography, either as an alternative imaging modality in patients with poor acoustic windows, complex anatomy or for quantification of transvalvular flow. By current CMR practices, valvular flow patterns are measured across two-dimensional cross-sections, which are manually placed in the position of interest. Over the past 10 years there has been intense research in the development of volumetric visualization of intracardiac flow by CMR (1). So-called CMR 4D flow imaging offers volumetric anatomical, functional and flow information during the entire cardiac cycle. It has several potential advantages over standard planar methods (2), including the ability to visualize complex flow patterns, select any plane when evaluating these CMR 4D flow datasets, without being limited to preselected planes and with the possibility to adapt the point of evaluation to the structural displacement throughout the cardiac cycle. Because all data is acquired during an uninterrupted ten-minute free-breathing scan, CMR 4D flow imaging is easy to perform and more comfortable for the patient. There are however a number of practical drawbacks that have prevented CMR 4D flow imaging from reaching the stage of widespread clinical implementation. While data acquisition was lengthy in the past, parallel imaging techniques (3, 4) have reduced the scan time to ten minutes or less. However, processing of the large data and correcting for eddy currents and gradient field distortions require dedicated software (5). Previously published experiences were achieved by using in-house developed software for volumetric data pre-processing (6-10). In this proof of concept study we evaluated the feasibility and performance of a cloud-based application that combines data pre-processing, including volumetric eddy currents correction, and visualization of CMR 4D flow data, and assessed its accuracy for the detection and grading of aortic valve regurgitation using echocardiography as reference.

METHODS

Study population

Between June 2014 and January 2015 adult patients planned for clinical contrast-enhanced CMR were consecutively approached to undergo the supplemental CMR 4D flow examination, and prospectively included in the study principles of the Declaration of Helsinki and approved by the institutional Medical Ethics Committee. All participants gave written informed consent.

Cardiac MR examination

The acquisition was performed using a 1.5 T or 3.0 T whole body scanners (Discovery MR450 and Discovery MR750, 45 mT/m, 200 T/ms, GE Medical Systems, Milwaukee, WI, USA) with a software version DV24.0, using dedicated 32-channel phased-array cardiac surface coils. Depending on the clinical request a variety of CMR examinations were performed including multi-planar cine steady-state free precession acquisitions, flow visualization using phase contrast sequence, contrast-enhanced angiography or delayed enhancement imaging.

CMR 4D flow data acquisition

The CMR 4D flow data was acquired immediately, or shortly after the bolus injection of 0.1-0.2 mmol/kg gadolinium-based contrast agent (Gadovist 1 mmol/ml, Bayer, Mijdrecht, The Netherlands), depending on the clinical indication for contrast administration. The sequence was prescribed in the axial plane, with a matrix of 192 x 144 and 2.8 mm slices interpolated to 1.4 mm slices, while the entire thorax was included in the field of view during a free-breathing, ECG gated scan. Patients were also asked to breath regularly during the acquisition. The median views per segment was 4 and the median repetition time was 3.9 ms, resulting in a temporal resolution of 63 ms. When necessary, the views per segment and temporal resolution were adapted to limit the scan duration to approximately ten minutes (Table 2). Following recommendations from literature, the velocity encoding value was set at 250 cm/s, which is a good compromise for the 4D flow to allow acquiring low and high velocities simultaneously (11).

Remote CMR 4D flow data correction, reconstruction and analysis

Because CMR 4D flow imaging is a phase contrast sequence, similar to planar flow acquisitions, magnitude images for anatomic information as well as images containing flow information may be reconstructed from the data. These large unreconstructed raw data sets (approximating 5 Gb per patient) were uploaded to a dedicated web-based software application (Arterys Inc., San Francisco, CA, USA) for data correction, visualization of the anatomical and flow components, and evaluation of the aortic regurgitation. As previously described (6), images were reconstructed for each cardiac temporal phase with a combined auto calibrating parallel imaging compressed sensing algorithm (L1-SPIRiT). Data was processed using large servers (Amazon Inc., Seattle, WA, USA). They are equipped with high frequency processors (Intel Xeon E5-2670, Intel Corporation, Santa Clara, CA, USA) and high-performance graphics processing units (NVIDIA Corporation, Santa Clara, CA, USA). The user logged into the application via internet connection from any type of computer or other device. Before the data sets were analyzed, the user could semi-automatically correct the images for encoding errors related to gradient field distortions and eddy currents. This approach is based on defining a threshold to identify

regions with static tissue. These were then used to estimate eddy current induced varying phase offset errors, which were subsequently subtracted from the entire image (12). Once the post-processing was complete and eddy currents correction performed the software facilitated interactive, real-time, manual navigation through the imaging volume using perpendicular multi-planar reformations and volume rendered reconstructions. The data could be reformatted into planes representing specific regions of interest (Fig. 1; Video 1). Flow could be displayed by color-coding of the velocity information or by vector rendering to display flow direction. For a red color on the color scale, a threshold of 150 cm/s was set.

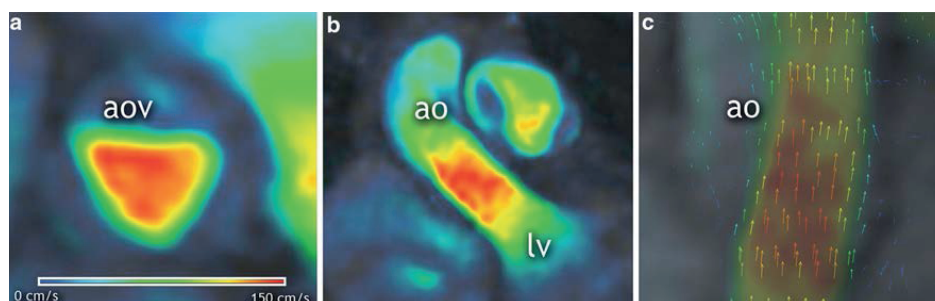


Figure 1. Aortic valve visualization with CMR 4D flow imaging. Short (a) and long-axis (b) cross-sectional views of the left ventricular outflow tract depicting systolic flow across the aortic valve. Because velocity-based color-coding lacks directional information, superimposed vectors display is used for confirmation of flow direction (c). The color scale can be manually modified as in this example where low velocities are displayed in dark blue color and equal or higher than 150 cm/s are displayed in red color. lv left ventricle, ao aorta

Evaluation of aortic valve function by CMR 4D flow imaging

The aortic valve was localized within the three dimensional anatomical dataset and displayed on three cross-sectional views that are perpendicular to each other. Using the cine display mode with superposition of flow onto the anatomy, the data was screened for the presence of reversed flow from the aortic valve during diastole. Identification of suspected aortic regurgitation was then evaluated using a temporally frame-by-frame approach. Because the velocity-based color-coded display of flow lacks directional information, the vector arrow display was used for confirmation (Fig. 1). Aortic valve regurgitation was defined as mild, moderate or severe. The grading criteria were adapted from echocardiographic recommendations (13, 14) using only the parameters available for both echocardiography and CMR 4D flow imaging: the ratios between the width of regurgitant jet and of the left ventricle outflow tract, and between the length of the regurgitant jet and of the left ventricle and the presence of reversal flow during diastole at the level of the descending aorta (Table 3). Two blinded readers (RGC and KN

with 4 and 7 years of CMR experience, respectively) independently assessed each case and graded aortic regurgitation. A joint consensus reading served to solve discordant interpretations.

Evaluation of aortic valve function by echocardiography

Two-dimensional transthoracic Doppler echocardiography was performed using a commercially available system (IE33, Philips Medical Systems, Best, The Netherlands). The gain settings were adapted to the patient's characteristics to obtain the best quality of color Doppler. Because usually in aortic regurgitation the velocities are higher than 2 m/s, it is not possible to correct for aliasing phenomenon even by changing the aliasing velocity settings. Thus practically aliasing is always present. We set the aliasing velocity at 1.2 m/s. Blinded to the CMR 4D flow imaging results, echocardiography images were independently evaluated by two cardiologists (AvdB and JR-H with 15 and 23 years of echocardiography experience, respectively), followed by a consensus reading. The presence of aortic regurgitation was graded using the same criteria as described above for the CMR 4D flow imaging. Because our paper focusses on the technical validation of 4D flow imaging we only considered parameters that could be assessed by both techniques.

Statistical analysis

Statistical analysis was performed using SPSS (version 21 IBM, Armonk, NY, USA) and MedCalc (version 13.0; MedCalc Software, Ostend, Belgium). Categorical variables were reported as totals and percentages and continuous variables with a normal distribution as means \pm standard deviations (SDs), or if data was skewed, as median with interquartile range. The diagnostic characteristics of CMR 4D flow imaging were evaluated against echocardiography by using C-statistics, including sensitivity, specificity, positive predictive value, negative predictive value with their corresponding 95 % confidence intervals (CIs), accuracy and Cohen's kappa agreement test.

RESULTS

Out of 59 eligible patients, the scan failed in five because of insufficient data storage capacity on the MR scanner, leaving 54 patients for inclusion in the study. Median age of the population was 39 years (range 18-76), 32 were males and 46 % were known with congenital heart disease (Table 1). 69 % were scanned on 1.5 T and 31 % on 3.0 T MR scanner. No patients were excluded due to poor image quality of CMR 4D flow imaging or echocardiography. The median time between echocardiography and CMR 4D flow acquisition was 2 months.

Table 1. Baseline characteristics of the study population

Characteristic	
Age (years) ^a	39 ± 15
Male gender	32 (59)
Body mass index (kg/m ²) ^a	24.7 ± 5.2
Heart rate (beats/min) ^b	66 (48 - 208)
Sinus rhythm	51 (94)
Systolic blood pressure (mmHg) ^a	124 ± 14
Diastolic blood pressure (mmHg) ^a	77 ± 10
Clinical history	
Congenital heart disease	25 (46.2)
Aortic valve stenosis (corrected)	4 (7.4)
Atrial septum defect	2 (3.7)
Bicuspid aortic valve	7 (12.9)
Coarctation – corrected	1 (1.8)
Marfan syndrome	1 (1.8)
Pulmonary valve stenosis – corrected	3 (5.5)
Tetralogy of Fallot – corrected	1 (1.8)?
Turner Syndrome	4 (7.4)
Ventricular septal defect (closed)	1 (1.8)
Cardiomyopathies (CMP)	26 (48.1)
Anthracyclines induced CMP	1 (1.8)
Amyloidosis	1 (1.8)
Dilated CMP	4 (7.4)
Hypertrophic CMP	13 (24)
Non-compaction CMP	4 (7.4)
Sarcoidosis	3 (5.5)
Other	3 (5.5)
Heart transplant	1 (1.8)
Hypertension	1 (1.8)
Post-cardiac arrest	1 (1.8)

Unless otherwise specified, data are numbers of patients, with percentages in parentheses

a Data are means ± standard deviations

b Medians with minimum and maximum values

Performance of CMR 4D flow imaging

The correction and visualization of the CMR 4D flow data and interpretation of aortic regurgitation required 10-15 minutes per patient. The agreement between CMR 4D flow imaging and echocardiography for the grading of regurgitation was good ($K = 0.73$; Table 4). Representative case examples are shown in Figs. 2, 3 and Video 2.

By CMR 4D flow imaging all four patients with moderate and 9 out of 15 patients with mild regurgitation were correctly identified. One case of mild regurgitation by echocardiography was interpreted as moderate by CMR 4D flow, and in 1 out of 35 cases CMR 4D flow identified mild regurgitation while echocardiography showed none. For the detection of any regurgitation, CMR 4D flow imaging demonstrated specificity of 97 % (95 % CI: 85-99 %), sensitivity of 74 % (CI: 49-91 %), positive predictive value of 93 %

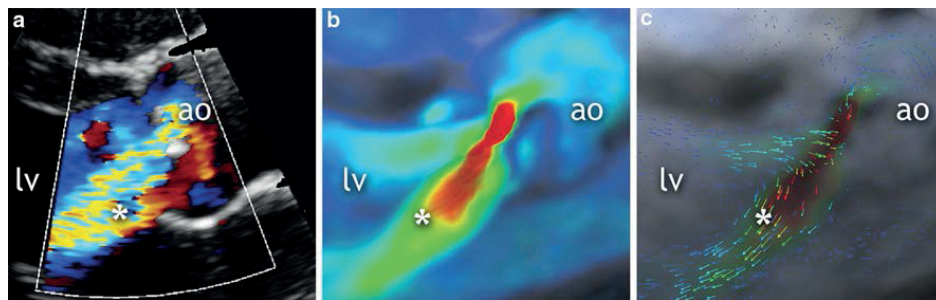


Figure 2. Aortic regurgitation by echocardiography and CMR 4D flow imaging. Case example of a 19-year-old man after balloon dilatation of the aortic valve for congenital aortic stenosis. Panel a Parasternal long axis view of aortic valve in diastole, showing moderate regurgitation (asterisk) demonstrated with color-flow Doppler echocardiography. Panels b and c Corresponding CMR 4D flow images showing the moderate aortic regurgitation. Asterisk regurgitant jet, lv left ventricle, ao aorta

Table 2. Imaging parameters of the CMR 4D flow acquisition

Imaging parameter	Value
Repetition time (ms) ^c	3.9
Echo time (ms) ^c	1.5
Flip angle (degrees)	15
Acquired matrix size	192 x 160 x 78
Reconstructed matrix	256 x 256 x 156
Acquired spatial resolution (mm)	1.77 x 2.12 x 2.80
Reconstructed spatial resolution (mm)	1.33 x 1.33 x 1.40
Views per segment ^a	4 (3-5)
Temporal resolution (ms) ^b	62.8 (51 - 65)
Velocity encoding	250 x 250 x 250
Sampling	Poisson
Acceleration ^c	2.0 x 2.0
Median scanning duration (min.s) ^b	8:52 (7.37 – 9:50)

A Medians with minimum and maximum values

B Medians with interquartile range in parenthesis

C Medians

(CI: 68-99 %) negative predictive value of 87 % (CI: 73-96 %), accuracy of 88 % and $K = 0.74$. To identify clinically relevant, more than mild regurgitation, CMR 4D flow imaging had sensitivity of 100 % (CI: 40-100 %), specificity of 98 % (CI: 89-100 %), positive predictive value of 80 % (CI: 29-97 %) and negative predictive value of 100 % (CI: 92-100 %), accuracy of 98 % and excellent agreement with echocardiography $K = 0.88$.

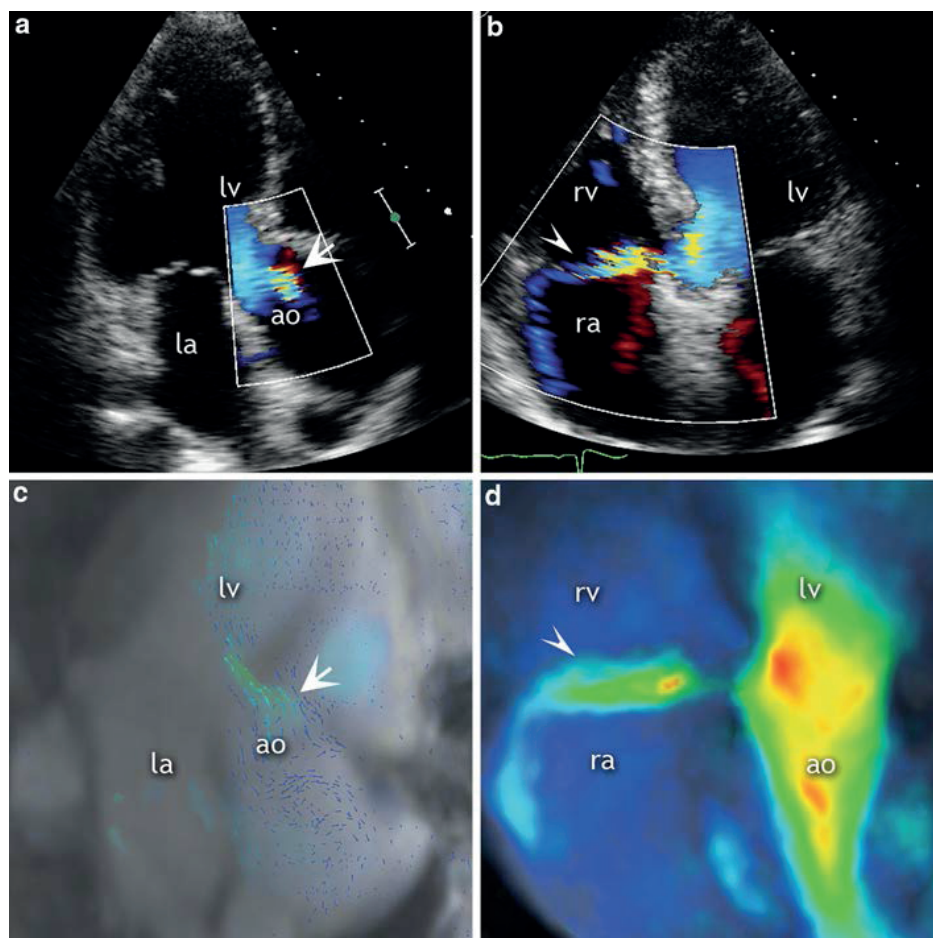


Figure 3. Mild aortic regurgitation and intracardiac shunt. A 47-year-old man post aortic valvotomy and Ross procedure for congenital aortic stenosis. Panel a Three chamber view with color-flow Doppler echocardiography showing a small aortic regurgitant jet (asterisk). Panel b Doppler echocardiography imaging, apical four chamber view, zoomed in on the basal septum and the right atrium; color flow through a typical Gerbode defect (arrows). Panels C and D CMR 4D flow imaging with corresponding views of the mild aortic regurgitation and the subvalvular, ventriculo-atrial jet, respectively. lv left ventricle, ao aorta, ra right atrium, rv right ventricle

Table 3. Aortic regurgitation grading criteria

Grade	Ratio between the width of the regurgitant jet and the left ventricle outflow tract	Ratio between the length of the regurgitant jet and the left ventricle outflow tract	Diastolic reversal flow in the descending aorta
Mild	<25%	<25%	Absent
Moderate	25-64%	25-50%	Trace
Severe	More than 65	More than 50%	Present holodiastolic

Adapted from echocardiographic recommendations for the assessment of native aortic valve regurgitation, only parameters available for both methods were used; the ratios between the width of regurgitant jet and of the left ventricle outflow tract and between the length of the regurgitant jet and of the left ventricle and the presence of reversal flow during diastole at the level of the descending aorta (13,14)

Table 4. Agreement between CMR 4D flow imaging and echocardiography

CMR 4D flow imaging	Echocardiography			
	None	Mild	Moderate	Total
None	34	5	0	39
Mild	1	9	0	10
Moderate	0	1	4	5
Total	35	15	4	54

The correlation between the two methods, when assessing the aortic regurgitation, was kappa = 0.73. When using a threshold of mild aortic regurgitation the correlation kappa = 0.74 and when using a threshold of moderate aortic regurgitation was kappa = 0.88.

DISCUSSION

In this study we report the first experiences with a cloud- based software application for pre- and post-processing CMR 4D flow data. We investigated its performance for the evaluation of aortic valve regurgitation. The novelty of storage capacity of the MR scanner caused difficulties, reconstruction and evaluation was successful in all other cases. For the detection and grading of aortic regurgitation, CMR 4D flow imaging correlated well with echocardiography and all patients with clinically relevant aortic regurgitation were correctly identified. There were two cases of overestimation, one mild aortic regurgitation graded as moderate with 4D flow and another one not visible with echocardiography which was graded as mild with 4D flow. There were also five mild regurgitations on echo, missed with 4D flow. We consider that CMR 4D flow is feasible and correlates well, but the population is not of sufficient size to conclude if there is systematic over- or underestimation. Out of the 5 underestimated regurgitations, two were scanned at 3.0 T and three at 1.5 T and from the two overestimated regurgitations one was scanned at 1.5 T and one at 3.0 T. Under the limitations of modest number of patients, we did not observe any indication that field strength was associated with accuracy.

In 2012, Hsiao et al. [6] used non-commercially available in-house software with a similar computational algorithm for data processing with color-speed overlay as in our paper, to evaluate valve regurgitation and intracardiac shunts with CMR 4D flow imaging against color Doppler echocardiography. The results are similar to our findings, good agreement ($K = 0.76$) was achieved when applying a threshold of at least mild regurgitation, and also a substantial agreement ($K = 0.69$) when using a threshold of more than mild regurgitation. The minor differences in agreement between both studies may be explained by the fact that in our study vector arrow overlay was used to help indicate the direction of the flow.

Clinical utility of CMR 4D flow imaging

Echocardiography has been the primary imaging technique for the care of patients with structural heart disease, offering advantages in ease of performance, safety and cost. However, in complex disease and after surgery echocardiography alone is frequently insufficient. CMR offers an alternative imaging option that is helpful in a number of specific applications, e.g. imaging of myocardial perfusion or scar, flow quantification, or when echocardiography cannot be performed adequately due to technical reasons, such as insufficient acoustic window. By the current standard of care, CMR measures flow using two-dimensional, velocity-encoded sequences, and it displays flow perpendicular to a manually selected plane. It can be a lengthy process that requires good cooperation from the patient. Potential advantages of CMR 4D flow protocol are that anatomical, functional and flow information are obtained during a free-breathing acquisition of 7-10 minutes, which is more comfortable for the patient and easier to perform. Without a need to specify beforehand, or expert assistance during the examination, flow can be measured anywhere and in any direction within the great vessels of the thorax after the data has been acquired. While 2D sequences acquire flow information in a static plane, CMR 4D flow imaging allows for dynamic alignment of the plane of interest to the position of moving structures (e.g. valve annulus) (15). Three-dimensional visualization of flow is also helpful for assessment of regurgitation jets that change direction during the heart cycle. However, clinical application of CMR 4D flow imaging is met by several technical challenges. Accurate representation of flow requires several pre-processing steps to correct for eddy currents and for magnetic field inhomogeneity. Experienced centers often rely on in-house developed solutions. To our knowledge this is the first report on the performance of a cloud-based software that applies volumetric eddy currents correction and direct, interactive flow visualization of CMR 4D flow data in a single tool package by internet connection, with remote processing of transferred raw datasets on high-performance workstations.

Study limitations

This is a relatively small, single-center study. As a proof of concept we limited the analysis to the qualitative evaluation of aortic valve regurgitation. Because demonstration of technical feasibility for flow visualization was the aim of this study, only parameters available for both echocardiography and CMR 4D flow imaging were used for assessment of the regurgitation severity. The prevalence of aortic regurgitation was 35 %, though none of the patients had severe regurgitation. Future studies should expand into quantitative analyses, as well as a wider range of valve pathologies. Future work is needed to determine optimal technical parameters for quantification of stenosis, regurgitation, shear stress, pressure gradients and other flow field derived metrics. To improve the contrast to noise ratio, we performed the CMR 4D flow acquisition after clinically indicated intravenous contrast agent administration. Future work may focus of determining diagnostic accuracy with- out the use of contrast agent.

CONCLUSION

In this study we showed that the use of a cloud-based reconstruction application with advanced eddy currents correction, integrated with interactive imaging evaluation tools allowed for remote visualization and interpretation of CMR 4D flow data and is sufficient for gross visualization of aortic valve regurgitation.

Acknowledgments The trial was funded by the Dutch Heart Foundation. We thank all participating patients and medical personnel who made this study possible. We thank Mihai Strachinaru, Andrea Pezzato, Kevin Were Wanambiro, Frans Blok, Artemis Westenberg, John Axerio-Cilies and Fabien Beckers for their support.

Funding Dutch Heart Foundation, Grant Number 2013T093.

Compliance with ethical standards

Conflict of interest A.H., S.S.V. are founders and shareholders of Arterys Inc., San Francisco, CA, USA. K.N. reports non-financial support from Siemens Medical Solutions, grants from GE Healthcare, from Bayer Healthcare, outside the submitted work. J.W.R.-H. reports grant from Dutch Heart Foundation. R.G.C., A.E.v.d.B., M.v.K., A.T.v.d.H., M.O., R.P.B., K.B., A.C., M.M.L., P.A.W.: none declared.

REFERENCES

1. Pelc NJ, Bernstein MA, Shimakawa A, Glover GH. Encoding strategies for three-direction phase-contrast MR imaging of flow. *Journal of magnetic resonance imaging : JMRI*. 1991;1(4):405-13.
2. Vasanaawala SS, Hanneman K, Alley MT, Hsiao A. Congenital heart disease assessment with 4D flow MRI. *Journal of magnetic resonance imaging : JMRI*. 2015;42(4):870-86.
3. Baltes C, Kozerke S, Hansen MS, Pruessmann KP, Tsao J, Boesiger P. Accelerating cine phase-contrast flow measurements using k-t BLAST and k-t SENSE. *Magnetic resonance in medicine*. 2005;54(6):1430-8.
4. Jung B, Stalder AF, Bauer S, Markl M. On the undersampling strategies to accelerate time-resolved 3D imaging using k-t-GRAPPA. *Magnetic resonance in medicine*. 2011;66(4):966-75.
5. Hsiao A, Alley MT, Massaband P, Herfkens RJ, Chan FP, Vasanaawala SS. Improved cardiovascular flow quantification with time-resolved volumetric phase-contrast MRI. *Pediatric radiology*. 2011;41(6):711-20.
6. Hsiao A, Lustig M, Alley MT, Murphy MJ, Vasanaawala SS. Evaluation of valvular insufficiency and shunts with parallel-imaging compressed-sensing 4D phase-contrast MR imaging with stereoscopic 3D velocity-fusion volume-rendered visualization. *Radiology*. 2012;265(1):87-95.
7. van der Hulst AE, Westenberg JJ, Kroft LJ, Bax JJ, Blom NA, de Roos A, et al. Tetralogy of fallot: 3D velocity-encoded MR imaging for evaluation of right ventricular valve flow and diastolic function in patients after correction. *Radiology*. 2010;256(3):724-34.
8. Westenberg JJ, Roes SD, Ajmone Marsan N, Binnendijk NM, Doornbos J, Bax JJ, et al. Mitral valve and tricuspid valve blood flow: accurate quantification with 3D velocity-encoded MR imaging with retrospective valve tracking. *Radiology*. 2008;249(3):792-800.
9. Hope MD, Meadows AK, Hope TA, Ordovas KG, Saloner D, Reddy GP, et al. Clinical evaluation of aortic coarctation with 4D flow MR imaging. *Journal of magnetic resonance imaging : JMRI*. 2010;31(3):711-8.
10. Weigang E, Kari FA, Beyersdorf F, Luehr M, Etz CD, Frydrychowicz A, et al. Flow-sensitive four-dimensional magnetic resonance imaging: flow patterns in ascending aortic aneurysms. *European journal of cardio-thoracic surgery : official journal of the European Association for Cardio-thoracic Surgery*. 2008;34(1):11-6.
11. Tariq U, Hsiao A, Alley M, Zhang T, Lustig M, Vasanaawala SS. Venous and arterial flow quantification are equally accurate and precise with parallel imaging compressed sensing 4D phase contrast MRI. *Journal of magnetic resonance imaging : JMRI*. 2013;37(6):1419-26.
12. Walker PG, Cranney GB, Scheidegger MB, Waseleski G, Pohost GM, Yoganathan AP. Semiautomated method for noise reduction and background phase error correction in MR phase velocity data. *Journal of magnetic resonance imaging : JMRI*. 1993;3(3):521-30.
13. Lancellotti P, Tribouilloy C, Hagendorff A, Popescu BA, Edvardsen T, Pierard LA, et al. Recommendations for the echocardiographic assessment of native valvular regurgitation: an executive summary from the European Association of Cardiovascular Imaging. *European heart journal cardiovascular Imaging*. 2013;14(7):611-44.
14. Nishimura RA, Otto CM, Bonow RO, Carabello BA, Erwin JP, 3rd, Guyton RA, et al. 2014 AHA/ACC guideline for the management of patients with valvular heart disease: a report of the American College of Cardiology/American Heart Association Task Force on Practice Guidelines. *The Journal of thoracic and cardiovascular surgery*. 2014;148(1):e1-e132.
15. Roes SD, Hammer S, van der Geest RJ, Marsan NA, Bax JJ, Lamb HJ, et al. Flow assessment through four heart valves simultaneously using 3-dimensional 3-directional velocity-encoded magnetic resonance imaging with retrospective valve tracking in healthy volunteers and patients with valvular regurgitation. *Investigative radiology*. 2009;44(10):669-75.

PART 3

**CARDIAC MAGNETIC RESONANCE
IMAGING IN ISCHEMIC HEART DISEASE
TRIALS**

3.1 ANIMAL STUDIES



Chapter 5

VEGF165A microsphere therapy for myocardial infarction suppresses acute cytokine release and increases microvascular density but does not improve cardiac function.

Uitterdijk A, Springeling T, **van Kranenburg M**, van Duin RWB, Krabbendam-Peters I, Gorsse-Bakker C, Sneep S, van Haeren R, Verrijck R, van Geuns RJM, van der Giessen WJ*, Markkula T, Duncker DJ, van Beusekom HMM.

Am J Physiol Heart Circ Physiol. 2015 Aug 309(3):H396–406.

*deceased 6 june 2011

ABSTRACT

VEGF165A microsphere therapy for myocardial infarction suppresses acute cytokine release and increases microvascular density but does not improve cardiac function. *Am J Physiol Heart Circ Physiol* 309: H396 –H406, 2015. First published May 29, 2015; doi:10.1152/ajpheart.00698.2014.—Angiogenesis induced by growth factor-releasing microspheres can be an off-the-shelf and immediate alternative to stem cell therapy for acute myocardial infarction (AMI), independent of stem cell yield and comorbidity-induced dysfunction. Reliable and prolonged local delivery of intact proteins such as VEGF is, however, notoriously difficult. Our objective was to create a platform for local angiogenesis in human-sized hearts, using polyethylene-glycol/polybutylene-terephthalate (PEG-PBT) microsphere-based VEGF165A delivery. PEG-PBT microspheres were biocompatible, distribution was size dependent, and a regimen of 10×10^6 15- μ m microspheres at 0.5×10^6 /min did not induce cardiac necrosis. Efficacy, studied in a porcine model of AMI with reperfusion rather than chronic ischemia used for most reported VEGF studies, shows that microspheres were retained for at least 35 days. Acute VEGF165A release attenuated early cytokine release upon reperfusion and produced a dose-dependent increase in microvascular density at 5 wk following AMI. However, it did not improve major variables for global cardiac function, left ventricular dimensions, infarct size, or scar composition (collagen and myocyte content). Taken together, controlled VEGF165A delivery is safe, attenuates early cytokine release, and leads to a dose-dependent increase in microvascular density in the infarct zone but does not translate into changes in global or regional cardiac function and scar composition.

INTRODUCTION

STEM CELL THERAPY for acute myocardial infarction (AMI), sought after to facilitate cardiac repair, has shown promise to improve cardiac function and patient outcome (1). However, outcome parameters vary widely (2) and are not always reported well (3). Rather than trans-differentiation of stem cells into cardiomyocytes, the postulated mechanism of stem cell action is through paracrine factors, inducing antiapoptotic effects, immunomodulation, and regional angiogenesis (4). Improved angiogenesis or maintenance of the preexisting microvascular bed is a prerequisite for, not only cardiac regeneration, but also cardiac healing through improved or maintained perfusion. It allows for access of leukocytes and facilitates scar-stabilizing processes such as fibrosis and debridement. Autologous stem cell therapy, however, is delayed hours to days because of cell harvesting and cell culture steps, and quality and viability may vary with comorbidities (5, 6). In addition, it has been suggested that early post-AMI regional inflammation may impair stem cell function. This implies that stem cell therapy depends heavily on quality of the cells and, importantly, cannot be used immediately following a primary percutaneous coronary intervention (pPCI), which is the preferred AMI treatment. This leaves acute and reperfusion-induced injury such as no reflow untreated. Microsphere (MSP) therapy, releasing angiogenic or other therapeutic factors, could be an off-the-shelf alternative to stem cells. It would make it independent from comorbidity-induced. This timing is of particular importance, as delivery of therapeutic agents before the occurrence of no-reflow-induced perfusion deficits should allow optimal distribution of MSPs and widens its therapeutic potential beyond angiogenesis to prolonged local delivery of other pharmaceuticals.

We used an amphiphilic biomaterial composed of polyethylene glycol and polybutylene terephthalate (PEG-PBT) with adjustable release kinetics (PolyActive). It is designed especially for stable protein delivery (7-11) and can theoretically harbor more than one growth factor per MSP for simultaneous release. Adjustable release kinetics of MSPs allows control of diffusion, and, subsequently, sequential release of multiple growth factors is possible when a mixture of growth factor-specific MSPs with dedicated release characteristics is given. PolyActive MSP delivery keeps proteins intact, protects them against proteolytic degradation, and has shown excellent biocompatibility in implants (12). PolyActive can be stored as an off-the-shelf therapy without loss of activity.

Many studies of growth factor-induced angiogenesis have been performed in the past, but these models invariably used chronic ischemia through permanent occlusion of a coronary artery. However, the clinical reality in Western Europe is that patients suffering an AMI are referred for pPCI where possible, to relieve ischemia by immediate reperfusion. We therefore studied the efficacy of MSP-induced angiogenesis using VEGF165A as a model drug in a setting similar to that used for pPCI by using a translational animal model of ischemia-reperfusion.

MATERIALS AND METHODS

Source of VEGF165A

Growth factor VEGF165A, used for both cell culture studies and preparation of loaded MSPs, was sourced from one supplier (Peprotech, Rocky Hill, NJ). Growth factor for cell culture studies was diluted from fresh stock.

Preparation of VEGF165A-Loaded PolyActive MSPs

Monodisperse formulations of placebo, high-dose (-0.3 pg), and low-dose (-0.1 pg) VEGF165A-loaded PolyActive MSPs (OctoPlus, Leiden, The Netherlands) were prepared by a double-emulsion (water in oil in water) method. VEGF165A aqueous solution (0.5% wt/vol) was emulsified by high shear mixing (Ultra-Turrax) into a solution of PolyActive, a copolymer of PEG-PBT with compositions 1000PEGT80PBT20 or 1500PEGT77PBT23 (Polyvation, Groningen, The Netherlands) in dichloromethane (10% wt/vol). This emulsion was pushed through a membrane (Nanomi, Oldenzaal, The Netherlands) with a uniform pore size specific for each desired MSP size, using nitrogen into a 0.5% solution of polyvinyl alcohol (13–23 kDa; Sigma, Zwijndrecht, The Netherlands), resulting in a suspension of uniformly sized microdroplets. Extraction and evaporation of the organic solvent resulted in formation of hardened MSPs. After the washing and final sieving through an absolute 20- μ m sieve to remove aggregated samples, suspended MSPs were frozen in water for injection and stored at -80°C until use.

MSP Size Distribution and Surface Characteristics

Size distribution and the number of MSPs per milliliter were determined by Coulter counter analysis (Coulter Counter Multisizer 3; Beckman Coulter, Mijdrecht, The Netherlands). MSP shape and surface characteristics were studied by scanning electron microscopy (Jeol JSM6610LV at 5 KV). Hydrated MSPs were dried through graded ethanol series followed by a chemical drying step using hexamethyldisilazane (Sigma). Fully dried MSPs were mounted using double-sided conductive carbon tape and sputter coated (gold) before examination.

In Vitro Release Kinetics of VEGF165A MSPs

Because small increments in systemic VEGF levels are difficult to determine (13), release kinetics of drug-laden MSPs were only determined in vitro. Release kinetics were assessed by placing 10×10^6 MSP in a gently and continuously swirled extraction medium at 37°C (PBS + 0.05% Tween20) that precludes aggregation of proteins and stabilizes them for later analysis (14). Total VEGF165A release was measured at <1 min (mimicking acute release), 2.5 h (mimicking early reperfusion), then every day for 14 days followed by 21, 28, and 35 days postincubation. These time points were selected to mimic timing

of the efficacy study described below. Eluted VEGF165A was measured by ELISA according to manufacturer's instructions for human VEGF165A (R&D Systems, Abingdon, Oxfordshire, United Kingdom). Absorbance was measured at 450 nm with a microplate photometer and converted to concentration using a standard calibration curve. MSP size was measured before and after the release kinetics studies by Coulter counter analysis.

In Vitro Angiogenic VEGF165A Efficacy

To study the lower threshold of VEGF165A efficacy in cardiac network formation, cultured human cardiac microvascular endothelial cells (HCMVECs; Lonza, Breda, The Netherlands) were starved for 20 h [0.5% heat-inactivated FBS in basal endothelial cell growth medium (EBM2)] (Lonza) for synchronization. Starved cells were isolated by contemporary trypsinization and centrifugation, and 2.6×10^4 cells/cm² were resuspended into EBM2 + 0.5% heat-inactivated FBS. According to the manufacturer's instructions, microslides for angiogenesis (IBIDI, Martinsried, Germany) were filled with 10 μ l growth factor-reduced MatriGel (BD Biosciences, Breda, The Netherlands) per well. Then 50 μ l of cell suspension with incremental VEGF165A (Peprotech; 0, 30, or 100 ng/g) was added to every well (n 5), and equal distribution was ascertained. Angiogenesis was subsequently allowed for 18 h at 37°C under hypoxic (PO₂: 2%) cell culture conditions and photographically documented. Total tube length and number of junctions were quantified (Angiosys 1.0; TCS Cellworks, Buckingham, Buckinghamshire, United Kingdom) for statistical analysis.

In Vivo Size Finding for MSP Retention, Safety, and Biocompatibility

The MSP size generally used for determination of myocardial blood flow is 15 μ m, as it is retained by the organ without inducing arteriolar obstruction (15). However, because biomaterials can show specific behavior, we decided to test both smaller (12 μ m) and larger (17 μ m) MSPs to confirm retention and determine potential arteriolar obstruction with PolyActive MSPs. These experiments were performed in 5–6-mo-old Yorkshire-Landrace swine of either sex (34.2 ± 0.9 kg). All animal experiments were conducted in compliance with the Guide for the Care and Use of Laboratory Animals and after written approval of the Animal Ethics Committee of the Erasmus MC. In short, swine were sedated with an intramuscular injection of midazolam (1 mg/kg) and ketamine (20 mg/kg). Following an intravenous ear catheter placement, anesthesia was induced with an intravenous injection of 600 mg pentobarbital. Animals were intubated and mechanically ventilated (O₂:N₂ 1:3, vol:vol). Anesthesia was maintained with pentobarbital ($15 \text{ mg} \cdot \text{kg}^{-1} \cdot \text{h}^{-1}$), and animals were instrumented as described before (16). For size finding (myocardial MSP retention), $1\text{--}5 \times 10^6$ placebo MSPs ranging from 12–17 μ m were injected via intracoronary method in 11 animals for dispersion into the healthy myocardium with an infusion rate up to $1.5 \times 10^6/\text{min}$. After 2 h, animals were eutha-

nized, and excised hearts were conventionally processed for infarct size determination by triphenyltetrazolium chloride (TTC) (16) and histological MSP quantification by Resorcin-Fuchsin staining, which stains MSPs black. To determine whether myocardial microinfarctions were produced by MSP infusion, we investigated the acute effects of placebo MSP infusion in four healthy swine. Under fluoroscopic guidance, distally to the first marginal branch of the left circumflex coronary artery (LCx, to mimic the delivery as planned for the efficacy study), 15- μ m placebo MSPs were infused in anesthetized swine through a micro-catheter. Numbers of infused MSPs varied from 5×10^6 to 20×10^6 and were infused with a rate of 0.5 or 1.0×10^6 MSPs/min (Table 1). Serial blood sampling and quantification of markers for necrosis and follow-up infarct size measurements were executed as described before (16). For biocompatibility studies, the subacute and chronic inflammatory response to placebo MSPs were assessed in six swine infused with 5×10^6 15- μ m MSPs (0.5×10^6 /min). After 5 days (n 3) or 28 days (n 3), animals were killed as described above, and tissues were retrieved and prepared for routine hematoxylin and eosin histology.

Table 1. Dose tolerance

No. of Microspheres	5×10^6	10×10^6	10×10^6	20×10^6
Infusion Parameters				
Infusion volume	10 ml	20 ml	40 ml	40 ml
Infusion density	5×10^5 /ml	5×10^5 /ml	2.5×10^5 /ml	5×10^5 /ml
Infusion speed	2 ml/min	2 ml/min	2 ml/min	2 ml/min
Infusion rate	1×10^6 /min	1×10^6 /min	0.5×10^6 /min	1×10^6 /min
Myocardial Damage				
Infarct size, % MTA	0.00	2.54	0.00	9.67
[hsTnI], ng/ml	0.42	2.03	0.30	8.68
[hFABP], ng/ml	6.44	12.10	0.48	28.99

MTA, microsphere-treated areal hsTnI (baseline: below detectable levels); hFABP = heart-specific acid-binding protein (baseline: 6.1 ± 1.1 ng/ml)

Efficacy of VEGF-Eluting MSP Therapy for AMI

Thirty-two swine (31.4 ± 0.4 kg) were sedated as above, and anesthesia was maintained with fentanyl ($20 \mu\text{g}\cdot\text{kg}^{-1}\cdot\text{h}^{-1}$ iv). Maximal transient coronary vasodilatation was induced for quantitative angiography (selective infusion of 1 mg isosorbidedinitrate) to determine optimal balloon sizing. Coronary diameters were measured using a nonionic contrast agent (Iodixanol) and dedicated software (CAAS; Pie Medical Imaging, Eindhoven, The Netherlands). The occlusion and infusion sites were carefully selected by at least two investigators and were always selected distal to the first marginal branch. An appropriately sized coronary angioplasty balloon with a standard guide wire was carefully

positioned under fluoroscopic guidance at the selected site of infusion. The LCx was occluded for 2 h followed by reperfusion. Upon occlusion, anesthesia was switched from fentanyl to isoflurane inhalation anesthesia (17, 18). Immediately upon reperfusion by deflation of the angioplasty balloon, 10×10^6 15- μ m MSPs containing placebo, low-dose, or high-dose VEGF165A were infused (in 40 ml saline, 2 ml/min, 0.5×10^6 particles/min). The route of administration and the area of distribution of the MSPs are illustrated in Fig. 1 and show that MSPs are given through the lumen of the angioplasty balloon upon deflation while remaining at the original location, leading to MSP treatment of the area at risk only (i.e., subjected to ischemia) and not outside the area at risk. Anesthetized animals were monitored for 2.5 h following reperfusion to serially assess biomarker release. Catheters were removed, the wound was closed, and animals received antibiotic prophylaxis (a mixture of procainebenzylpenicillin and dihydrostreptomycin sulfate, 20 mg/kg and 25 mg/kg im, respectively) and were then allowed to recover.

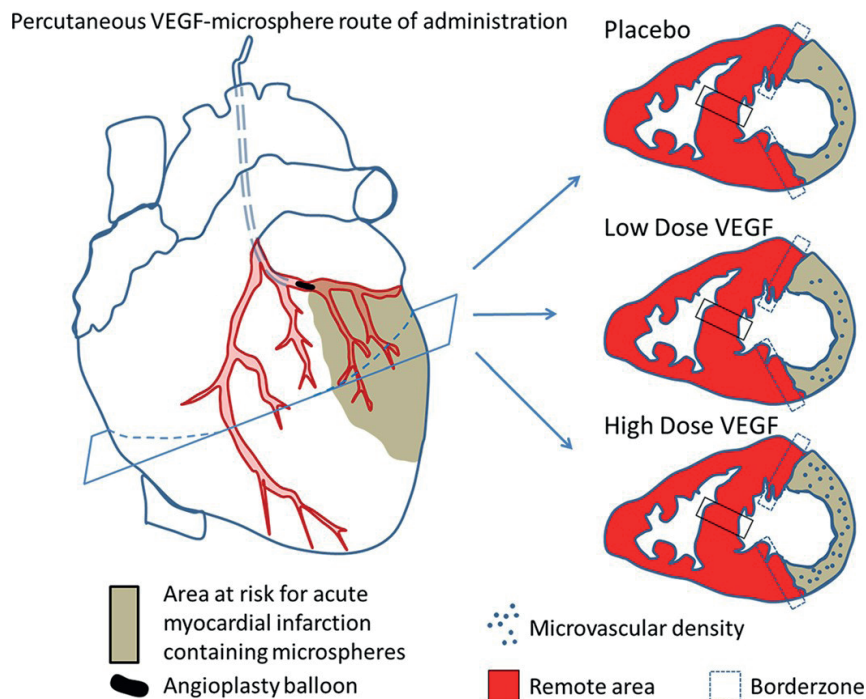


Figure 1. Graphic representation of the acute myocardial infarction (AMI) model showing the route of microsphere (MSP) administration. MSPs were administered via the guidewire lumen following deflation of the "over-the-wire" angioplasty balloon used to induce ischemia. Hence, MSPs were only delivered to the area at risk. The cross-sections at the right indicate the areas of interest used for histological analysis.

Global and Regional Cardiac Function by MRI

Global and regional cardiac function including microvascular obstruction was assessed, processed, and analyzed in a blinded manner at 1 and 5 wk after myocardial infarction and therapy using MRI as described before (25, 38). In short, animals were sedated and intubated as described above. Anesthesia was maintained with fentanyl ($20 \mu\text{g}\cdot\text{kg}^{-1}\cdot\text{h}^{-1}$) and, when necessary, supported with thiopental sodium (100-mg bolus). Mechanical ventilation and peri-imaging breath-holds were performed using a mobile ventilator (Carina; Draeger, Zoetermeer, The Netherlands). When necessary, and always in absence of pain reflexes, muscle relaxation was achieved using pancuronium bromide (2–4-mg bolus). Cardiac MRI examinations were performed on a 1.5-Tesla clinical scanner (Signa HD; GE Medical Systems, Milwaukee, WI) using a dedicated cardiac four-channel phased array cardiac receiver coil. Repeated breath-holds and gating to the electrocardiogram were applied to minimize the influence of cardiac and respiratory motion on data collection. All cardiac MRI (CMR) protocols consisted of cine-MRI (myocardial function) and delayed enhancement MRI (DE-MRI, infarct size and no reflow). Cine-MRI was performed using a steady-state, free-precession technique (FIESTA, GE Medical System). With the use of standard techniques to identify the major cardiac axes, two-chamber and four-chamber cine-CMR images were obtained. The two- and four-chamber end-diastolic images provided the reference images to obtain a series of short-axis views. This resulted in 8–12-cine breath-hold short-axis images to cover the entire left ventricle. Delayed enhancement imaging was performed with a gated breath-hold two-dimensional T1-inversion recovery gradient-echo sequence minimally 10 min after infusion of gadolinium-diethyl-triamine-penta-acetic-acid (0.2 mmol/kg iv, Gadobutrol, 1.0 mmol/ml ; Bayer, Mijdrecht, the Netherlands) (19). After MRI imaging, animals were allowed to recover as described above (1 wk post-AMI) or transported back to the operating theatre for follow-up death.

MRI Image Processing and Analysis

All images were transferred to a Microsoft Windows-based personal computer for blind analysis using the CAAS-MRV program (version 3.3.1; Pie Medical Imaging). Cine and delayed-enhancement images were acquired during the same imaging session and were matched using identical slice positions. Registration of follow-up and baseline cine and delayed-enhancement images was achieved by consensus of two observers using anatomic landmarks such as papillary muscles and right ventricular insertion sites. The images were analyzed in a blind matter using the additional information of the long axis to limit the extent of volume at the base and the apex of the heart. Left ventricular end-diastolic volume (LVEDV), LV end-systolic volume (LVESV), LV ejection fraction (LVEF), LV mass, and LV end-diastolic wall thickness of the infarct were measured by semiautomatically drawing the endocardial and epicardial contour in end-systolic and end-diastolic

phase of the two- and four-chamber images with automatic segmentation to the short axis and if necessary corrected manually. Papillary muscles and trabeculations were considered part of the blood pool volume and excluded from myocardial mass. LVEF was calculated as $(LVEDV - LVESV)/LVEDV$. Infarct size (IS m/m) was determined on short-axis delayed-enhancement images using semiquantitative analyses for the detection of the delayed-enhancement regions (8).

Histology

At death of the anesthetized animal, a sternotomy was performed, and the pericardium was carefully opened; after an overdose of pentobarbital, the aorta was cross-clamped, and the vena cava was opened. Immediately upon euthanasia, proximally to the aorta clamp, an infusion setup was placed to flush the arrested heart with approximately 1 l of ice-cold saline to remove blood and plasma from the heart. The flushed heart was excised and cut into five transversal slices on a cooled cutting board. Slices were sectioned into remote, border zone, and infarct tissue and subsequently fixed in 3.5–4.0% buffered formaldehyde, in preparation for paraffin embedding. Area at risk (see Fig. 1) is defined as the area subjected to ischemia and is the only area containing MSP. Infarct area is defined as the area showing extensive fibrosis and lack of cardiomyocytes. Border zone is defined as the area bordering the infarct and does not contain MSPs. For microvascular density of the remote area, tissue was taken from the LV wall opposite of the infarcted area (i.e., septum).

Microvascular Density Measurement

As arteriolar density does not change as a result of myocardial infarction (20), we measured total microvascular density in the MSP-treated infarct area reflecting changes in capillary density. To quantify microvascular density in myocardial tissue, 4- μ m sections of paraffin-embedded infarct, border zone, and remote tissue were stained with the biotin-labeled lectin *Dolichos Biflorus* (DBA, L6533; 1:100, Sigma) followed by streptavidin-horseradish peroxidase (1:4,000, Sigma) and diaminobenzidine-H₂O₂ as a chromogen. With the use of a X40 magnification, four MSP-containing, nonoverlapping images were taken of every section (Clemex Vision 4.0; Clemex Technologies, Longueuil, Quebec, Canada). Microvascular density was quantified using an adapted Chalkley grid to rapidly and reliably quantify angiogenesis despite tortuosity (21) with a custom-built ImageJ macro (version 1.46r; National Institutes of Health, Bethesda, MD). The adapted Chalkley grid was manually placed over every image, with an MSP in the center of the image in case of infarcted tissue. With increments of 4°, the automated Chalkley grid was then rotated 90 times for each image to determine its maximum Chalkley score. Chalkley scores were converted to absolute microvascular densities with a calibration curve.

Extracellular Matrix and Regional Cardiomyocyte Presence

Collagen area and cardiomyocyte presence within the infarct region were quantified using a Resorcin-Fuchsin staining. MSP-containing areas (designated as having been subjected to ischemia) were divided into six nonoverlapping sections. Every section was analyzed to determine the percentage of collagen (red-stained areas) and cardiomyocytes (yellow-stained cardiomyocytes).

Biomarkers for Necrosis and Inflammation

Serial blood samples were analyzed for markers of necrosis as described before (16). Also, to assess the acute anti-inflammatory response of VEGF165A drug-laden MSP therapy, TNF- α and IL-6 levels were quantified in blood samples obtained at baseline, at 2.5 h of reperfusion, and at 5 wk of follow-up using similar procedures and performed according to manufacturer's instructions (R&D Systems).

Cumulative Regional VEGF Concentration per Gram of Infarct Tissue

The cumulative VEGF concentration eluted by 10×10^6 low- and high-dose MSPs was calculated by dividing the mean in vitro VEGF release in 35 days (i.e., 0.9 μg and 2.8 μg) by the weight of each

Statistical Analysis

Data are presented as means \pm SE. Data were analyzed with Sigmaplot (Version 11.0; Sigmaplot, Drunen, The Netherlands) and SPSS (IBM SPSS statistics 21). Two-way (time \times treatment) repeated-measures ANOVA or paired-sample t-test was used followed by post hoc Bonferroni's correction when appropriate. Statistical significance was accepted when $P < 0.05$.

RESULTS

In Vitro Studies of Size Distribution, Surface Characteristics, and Release Kinetics of VEGF165A MSPs

Determination of MSP size showed a similar diameter in all formulations in the therapy study (placebo: $15.2 \pm 0.01 \mu\text{m}$; low dose: $15.3 \pm 0.01 \mu\text{m}$; high dose: $15.3 \pm 0.00 \mu\text{m}$). Scanning-electron microscopy was used to visually ascertain MSP integrity for the three formulations and showed an intact and smooth surface. The release patterns of the 15- μm VEGF-containing formulations is illustrated in Fig. 2. Cumulative dose for low- and high-dose MSP was 0.92 ± 0.05 and $2.80 \pm 0.17 \mu\text{g}$ VEGF165A per 10×10^6 MSPs. Importantly, the release pattern was not statistically different between the two active formulations. All MSPs showed a decrease in diameter at the end of a period of 35 days, but this was similar in all formulations (placebo: $-9.8 \pm 0.1\%$; low dose: $-10.3 \pm 0.7\%$; high dose: $-10.5 \pm 0.1\%$).

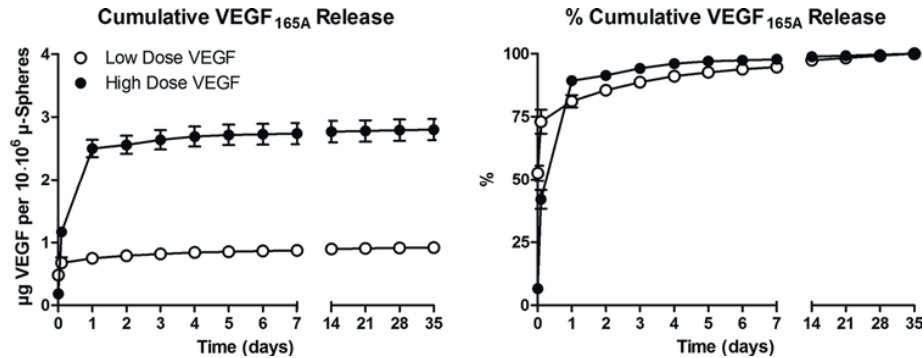


Figure 2. Cumulative in vitro release curves ($n = 3$) of 10×10^6 MSPs in low- and high-dose drug-laden formulations, showing an early release burst of VEGF, followed by a steady increase in the cumulative release. *Left:* absolute values. *Right:* release expressed as a percentage of the total cumulative dose. Data are shown as means \pm SE. \square , low-dose VEGF MSPs. \bullet , high-dose VEGF MSPs.

In Vitro Angiogenic Effects of VEGF165A

The HCMVEC tube-formation assay under hypoxic conditions (Fig. 3), as a marker for angiogenesis, showed a clear dose response to VEGF165A in terms of significantly increased tube length ($P = 0.007$) and number of junctions ($P = 0.021$). Post hoc analysis showed that this was dictated by the difference between 100 and 0 ng/g with a trend for 30 ng/g toward improved network formation. The low-dose VEGF165A group reflects this value, and therapy was steered toward a cumulative VEGF dose approximating 100 ng/g.

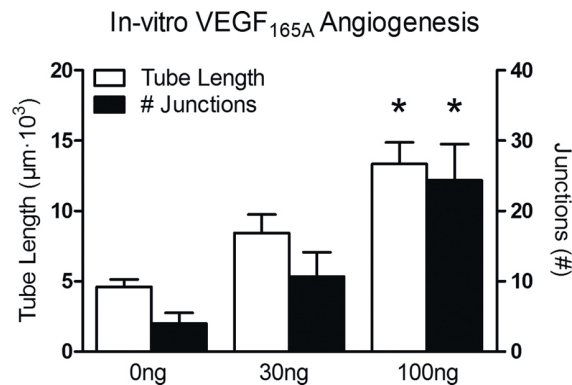


Figure 3. In vitro angiogenic response of human cardiac microvascular endothelial cells in a tube-formation assay ($n = 5$) under ischemic conditions to indicate the lower threshold of VEGF165A efficacy in the no-reflow zones. Data show a dose response with statistically significant effects at 100 ng/g, and this value was subsequently used to steer the low-dose VEGF165A group. Data are shown as means \pm SE. Open bars represent tube length, and solid bars represent number of junctions. * $P < 0.05$ vs. corresponding 0-ng measurement.

Size Finding, Safety, and Biocompatibility

The size-finding study data obtained by intracoronary infusion of MSPs of different size in swine myocardium confirmed that smaller MSPs of 12 μm were not well retained ($6 \pm 1\%$ compared with 17- μm spheres). The latter showed impaired distribution with congestion of the microvasculature although TTC staining was negative. Therefore, 15- μm -diameter MSPs were selected for subsequent studies of safety and biocompatibility. In the safety or dose-tolerance study with 15- μm spheres, the average MSP-treated area (MTA) was $21.4 \pm 3.3\%$ of the left ventricle (17.5 ± 3.2 g cardiac tissue) in all groups. Data show that infusion of 10 and 20×10^6 MSP at 1×10^6 MSP/min resulted in a macroscopically detectable TTC-stained infarct area of respectively 2.5 and 9.7% MTA. However, MSP infusion of 5×10^6 ($1 \times 10^6/\text{min}$) and 10×10^6 ($0.5 \times 10^6/\text{min}$) showed no macroscopic myocardial necrosis, which was confirmed by absence of hFABP and high-sensitivity troponin I release (Table 1). Histology confirmed adverse effects produced by the two high-dose and faster MSP infusion rates as hemorrhagic events. In contrast, the 5×10^6 ($1 \times 10^6/\text{min}$) and the 10×10^6 ($0.5 \times 10^6/\text{min}$) groups did not show microbleedings. Analysis of the biocompatibility following intracoronary infusion of MSPs revealed no inflammation, either at 5 or at 28 days following infusion of the MSPs (Fig. 4) without signs of microvascular damage. These safety and biocompatibility results formed the basis for the longitudinal functional assessment of MSP therapy for myocardial infarction using 10×10^6 MSP at a rate of 0.5×10^5 MSP/min.

Efficacy of VEGF-Eluting MSP Therapy for AMI

Mortality following myocardial infarction was observed in eight swine (25%) who died prematurely. Mortality was not different between groups; nonconvertible ventricular fibrillation during the infarct-reperfusion protocol occurred in four swine, two during coronary artery occlusion and two during reperfusion. No animals died during infusion of MSPs. Two animals died within 48 h postinfarction of subacute cardiac complications. One animal died at 1 wk because of severe heart failure, and one animal died because of technical failure. All remaining 24 swine ($n = 8$ per group) completed the protocol and were included for final blinded analyses. Baseline Characteristics and Cumulative VEGF Exposure Infarct mass at baseline by markers of necrosis. To ascertain that infarct mass at baseline was similar in all groups, circulating hFABP levels were taken at 50 min of reperfusion to calculate infarct mass (41). Infarct masses did not differ between groups (placebo: 13 ± 2 g; low dose: 14 ± 2 g; high dose: 16 ± 1 g; $P = 0.40$). Cumulative VEGF exposure. Cumulative local VEGF concentration per infarct mass (infarct mass at baseline by hFABP divided by VEGF dose) showed that, per gram of infarcted myocardium, the low-dose group received 0.07 ± 0.01 μg VEGF165A, and the high-dose group received 0.35 ± 0.06 μg VEGF165A. Placebo MSP-treated animals received no VEGF165A.

Global and Regional Cardiac Function at 1 and 5 wk Post- AMI

To understand the early effects of VEGF therapy on cardiac function, 1 wk post-AMI, global and regional myocardial functions were assessed with cardiac MRI. Results (Table 2) clearly show that global and regional myocardial functions are similar compared with placebo therapy. Global and regional myocardial functions were assessed again at 5 wk post-AMI. Importantly, no significant differences were found between VEGF groups and placebo, suggesting that VEGF did not have an effect on global and regional myocardial function either early (1 wk) or late (5 wk) post- AMI.

Inflammatory Biomarker Release

To understand the effect of VEGF therapy on inflammation, TNF- α and IL-6 were quantified at baseline, 2.5 h of reperfusion, and 5 wk of follow-up. Data are illustrated in Fig. 5 and show that, whereas placebo spheres showed a significant increase in TNF- α release during reperfusion ($P < 0.01$), levels decreased significantly to normal at 5 wk of follow-up ($P < 0.01$). TNF- α levels in both VEGF- containing MSP formulations remained at baseline levels. A similar pattern for placebo was observed for IL-6, and, although the high-dose group showed an increase at early reperfusion, this did not reach levels of statistical significance ($P 0.15$).

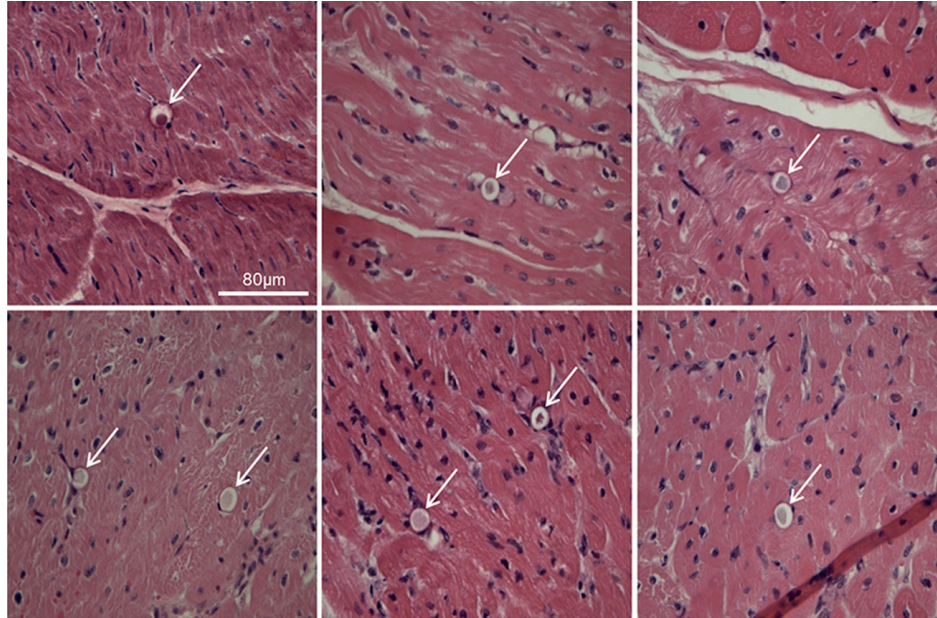


Figure 4. Histological analysis of in vivo bio- compatibility to assess safety of MSP ther- apy, illustrated for 6 different hearts, shows absence of MSP-induced inflammation at 5 days (*top*) and 28 days (*bottom*) following infusion in healthy, nonischemic myocar- dium. MSPs are light pink (arrow). Hema- toxylin and eosin stain, bar 80 μ m.

Histological Analysis

Microvascular density measurements.

To study the effect of VEGF on microvascular density in the infarct zone, Chalkley counts of the infarct area were normalized to the non-infarcted remote areas. In contrast to placebo treatment ($13 \pm 7\%$ decrease in Chalkley score vs. remote, Fig. 6),

Table 2. global and regional myocardial characteristics by MRI

LV function and Remodeling	Treatment	Post-AMI 1 wk	Post-AMI 5 wk
Heart rate, beats/min	Placebo	77 ± 8	80 ± 4
	Low dose	71 ± 4	71 ± 4
	High dose	64 ± 5	75 ± 7
End-diastolic volume, ml	Placebo	104 ± 7	$120 \pm 7^*$
	Low dose	106 ± 3	$126 \pm 6^*$
	High dose	107 ± 8	$125 \pm 9^*$
Stroke volume, ml	Placebo	46 ± 2	$54 \pm 2^*$
	Low dose	42 ± 3	$58 \pm 3^*$
	High dose	48 ± 2	$49 \pm 3^{\dagger}$
Ejection fraction, %	Placebo	46 ± 3	46 ± 2
	Low dose	40 ± 2	$46 \pm 2^*$
	High dose	46 ± 2	$40 \pm 4^*$
LV mass, g	Placebo	49 ± 2	$54 \pm 2^*$
	Low dose	49 ± 2	$54 \pm 2^*$
	High dose	48 ± 3	$52 \pm 3^*$
Infarct Characteristics			
Infarct mass, g	Placebo	8.0 ± 2.0	$6.4 \pm 1.6^*$
	Low dose	9.3 ± 0.9	$6.9 \pm 0.6^*$
	High dose	9.6 ± 1.6	$7.6 \pm 1.2^*$
Infarct size, % LV	Placebo	15.5 ± 3.3	$11.2 \pm 2.3^*$
	Low dose	19.4 ± 2.2	$13.3 \pm 1.6^*$
	High dose	19.4 ± 2.4	$14.4 \pm 1.8^*$
End-diastolic wall thickness, mm	Placebo	4.2 ± 0.2	4.1 ± 0.2
	Low dose	3.9 ± 0.1	3.6 ± 0.3
	High dose	4.2 ± 0.1	$3.6 \pm 0.3^*$
No reflow, % IM	Placebo	9.5 ± 4.9	-
	Low dose	10.1 ± 4.6	-
	High dose	7.7 ± 2.7	-

Data are mean \pm SE; n = 8 per group. AMI, acute myocardial infarction; LV, left ventricular; IM infarct mass; -, not detectable. *P < 0.05 vs. corresponding week 1; † p < 0.10 vs. corresponding low dose. At 5 wk post-AMI, no reflow can no longer be detected.

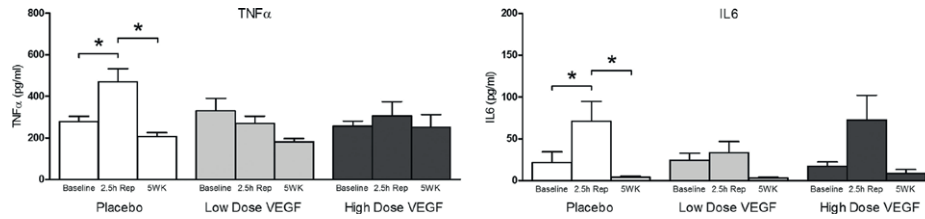


Figure 5. Longitudinal assessment for release of inflammatory markers TNF- α and IL-6 in plasma as measured by ELISA shows that the VEGF release by the MSPs attenuates cytokine release at 2.5-h reperfusion, having returned to baseline at 5 wk of follow-up. Data are presented as means \pm SE, n 8 per group. * P < 0.01. Rep, reperfusion. IL-6 levels at 2.5-h reperfusion were not statistically different from baseline and 5 wk of follow-up (P 0.15).

high-dose treatment resulted in a significantly higher Chalkley score ($10 \pm 6\%$, P < 0.04 vs. placebo). This corresponds to a difference of -739 ± 278 vessels/mm² (P < 0.05). The low-dose group remained similar to the remote area, indicating a dose-response effect. In Fig. 6, typical examples of microvascular density in the infarcted area are shown. Capillary density in the border zones in the placebo, low-dose VEGF, and high-dose VEGF group ($2,045 \pm 125$; $2,168 \pm 115$; $2,223 \pm 134$ vessels/mm, respectively) were similar to the remote area and showed no signs of VEGF effects. Chalkley scores of infarcted tissue with an MSP-containing viable rim, reliably measureable in a few animals (n 4 to 5/group), similarly did not show differences with remote tissue in paired analyses.

Collagen and regional cardiomyocyte presence.

To study whether differences in microvascular density affected infarct healing, we quantified the presence of collagen and cardiomyocytes in the area at risk, defined as the area containing MSP (Fig. 7). VEGF165A therapy at 5 wk post-AMI did not result in differences in total collagen content (placebo: $24 \pm 5\%$; low dose: $25 \pm 3\%$; high dose: $33 \pm 3\%$ surface area; P 0.25) or changes in cardiomyocyte presence compared with placebo (placebo: $41 \pm 7\%$; low dose $37 \pm 5\%$; high dose $27 \pm 5\%$; P 0.21).

DISCUSSION

The present study was performed to test the safety, biocompatibility, and efficacy of controlled VEGF165A release from degradable MSPs as an off-the-shelf therapy for regional angiogenic therapy following AMI in a setting of PCI. Intracoronary delivery was initiated directly upon reperfusion of the infarct tissue to allow delivery of drug-loaded MSPs before onset of reperfusion injury and no reflow. This approach allows optimal

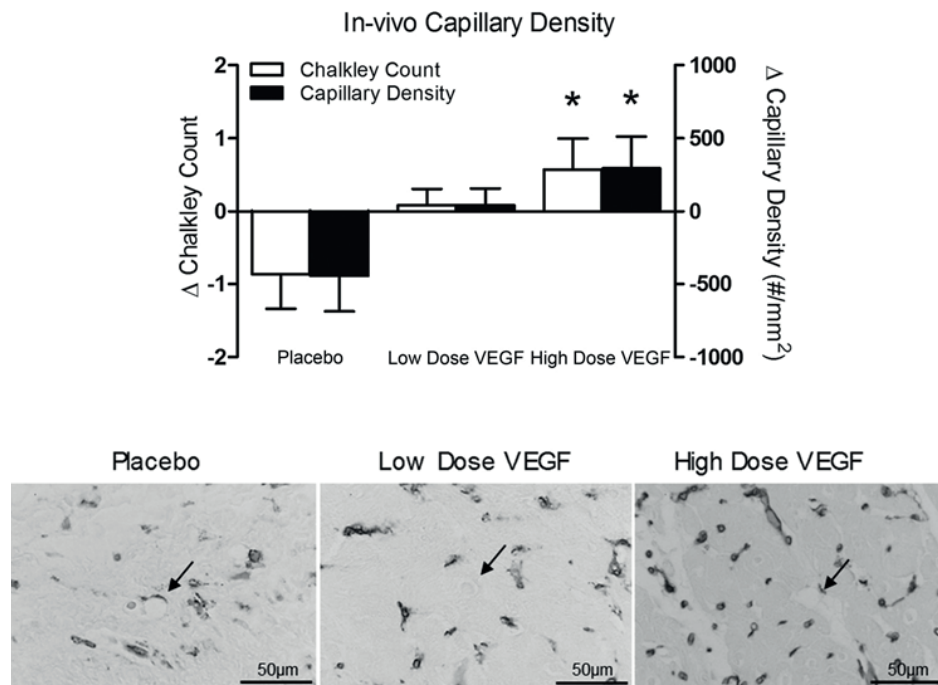


Figure 6. *Top:* in vivo relative microvascular density measurements in the area at risk as a result of VEGF165A therapy at 5 wk of follow-up. Data, given as the difference between infarct and remote area, are shown as means \pm SE. Open bars represent differences in the Chalkley counts, and solid bars represent the differences in the absolute number of capillaries $*P < 0.05$ vs. placebo. *Bottom:* microvascular staining of the area at risk in placebo (*left*), low-dose VEGF (*middle*), and high-dose VEGF (*right*) MSPs by horseradish peroxidase (HRP)-labeled lectin Dolichos Biflorus. MSPs were used to center the Chalkley grid before automated measurements of the microvasculature. HRP was visualized with diaminobenzidine-H₂O₂. Bar 50 μ m.

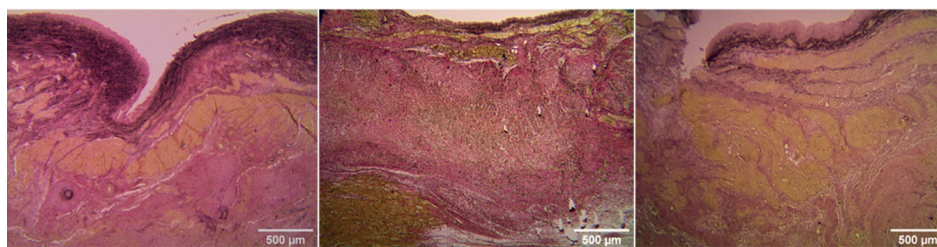


Figure 7. Endocardial border of the infarct area in the 3 groups showing extensive fibrosis with endocardial survival of cardiomyocytes, with collagen stained red and cellular elements such as muscle stained yellow. Resorcin-Fuchsin stain. Bar 500 μ m.

Table 3. Animal studies on the cardiotherapeutic effects of regional VEGF therapy for myocardial infarction

Author	Species	I/R time	Route of administration	Start of therapy	Duration of Therapy	Cumulative VEGF Dose	Effect on vascular density	Effect on global function
Dicks et al. (13)	Dog	Permanent occlusion	IM	3 days post AMI	47 days	0, Control -, VEGF	- ↑*	- ↑*781
Saeed et al (16)	Dog	Permanent occlusion	IM	3 days post AMI	50 days	0, Control -, VEGF	- ↑*	↔792 ↑*†
Ferrarini et al. (16)	Dog	Permanent occlusion	IM	240 min after onset ischemia	28 days	0, Control -, VEGF	- ↑*	- ↔
Vera Janavel et al. (43)	Sheep	Permanent occlusion	IM	60 min after onset ischemia	15 days	0, Control -, VEGF	- ↑*	- ↔
Bougioukas (8)	Rabbit	Permanent occlusion	IM	5 min after onset ischemia	Bolus	0, Control 10 microgram, VEGF	- ↑*	- -
Wu et al. (44)	Rat	Permanent occlusion	IM	7 days post-MI	35 days	0, Control -, VEGF	- ↑*	- ↑*
Rufaihah et al. (32)	Rat	Permanent occlusion	IM	Early after onset ischemia	30 days	-, Control 25 microgram/ml, VEGF	- ↑*	↓* ↔
Hao et al. (22)	Rat	Permanent occlusion	IM	7 days post MI	28 days	0, Control -, VEGF	- ↔	↓† ↑*
Gao et al. (20)	Rat	Permanent occlusion	IM	Immediately after onset ischemia	28 days	0, Control -, VEGF	- ↑*	- ↔
Zhang et al. (45)	Rat	Permanent occlusion	IM	Immediately after onset ischemia	Several hours	0, Control 11 microgram VEGF	- ↑*	↓ ↑*
Oh et al. (29)	Rat	Permanent occlusion	IM	14 days post-MI	28 days	0 Control, -, VEGF	- ↑*	- ↔
Su et al. (39)	Mouse	60 min/32 days	IM	Immediately after onset ischemia	56 days	0, Control -, VEGF	- ↑*	- ↑*

Table 3. Animal studies on the cardiotherapeutic effects of regional VEGF therapy for myocardial infarction (continued)

Author	Species	I/R time	Permanent occlusion	Route of administration	Start of therapy	Duration of Therapy	Cumulative VEGF Dose	Effect on vascular density	Effect on global function
Formiga et al. (17)	Rat	Permanent occlusion	IM		4 days post-MI	28 days	0, Control 0.9 microgram VEGF	- ↑*	- ↑*
Simon-Yarza et al. (37)	Rat	Permanent occlusion	IM		1 wk post- MI	90 days	0.51 microgram VEGF 1.02 microgram VEGF 0, control	↑* ↑* -	↑* ↑* ↓
Scott et al. (36)	Rat	Permanent occlusion	IV		Immediately after onset ischemia	Bolus	0 control, - 24 microgram VEGF	↑* -	↑* -
Zhigang et al. (46)	Rat	Permanent occlusion	IV		3 days post MI	14 days	-control, VEGF	↑* ↔	- ↔
Sato et al. (35)	Pig	Ameroid constrictor	IV IC IC/IV		3 wk after onset constriction	40-200 min 40 min	10 microgram/ kg, 2 microgram/kg VEGF, 10 microgram/kg VEGF, 0 Control	↔ ↔ ↔ ↑ [‡]	↔ ↔ ↔ ↔
Uitterdijk et al.	Swine	120 min/5 wk	IC		Onset reperfusion	35 days	0 microgram Control, 0.9 microgram VEGF, 2.8 microgram VEGF	↓ ↔ ↑*	↔ ↔ ↔

I/R, Infarct/reperfusion time; IM, intramyocardial (endo or epicardially); IV, intravenous; IC, intracoronary; MI, myocardial infarction; -, not reported. *P < 0.05 vs. control; †P < 0.05 vs. baseline functional measurements; ‡ effects assessed as increased regional coronary flow, not as vascular density.

MSP distribution within the area at risk before development of perfusion defects as a result of no reflow.

Major Findings

We observed that 15- μ m MSPs were effectively retained and distributed within the myocardium without inducing an acute or chronic local inflammatory response or (micro)infarction. MSP presence did not negatively affect cardiac function compared with historic data with similar infarct size (heart rate 84 ± 19 vs. 80 ± 4 beats/min, stroke volume 60 ± 11 vs. 54 ± 2 ml) (28). VEGF-loaded MSP delivery in infarcted myocardium significantly reduced the acute release of the proinflammatory cytokines TNF- α and IL-6 during reperfusion. At follow-up, histology revealed dose-dependent changes in microvascular density within the MTA compared with the intrinsic nonischemic control area. Per gram of infarcted myocardium, a dose of 0.07 ± 0.01 μ g VEGF165A maintained microvascular density, whereas 0.35 ± 0.06 μ g VEGF165A increased microvascular density. However, these changes did not translate to changes in scar composition (collagen and cardiomyocyte presence) or global and regional myocardial function by cardiac MRI at 1 or 5 wk after AMI.

MSP Composition and Size

We found that 15- μ m diameter MSPs were effectively retained by the porcine myocardium, whereas 12- μ m MSPs were not, and 17- μ m MSPs impaired optimal distribution. MSP retention may be dictated by, not only size, but also material properties because poly(lactide-co-glycolide) MSPs of 7- μ m diameter were described to be retained well (22). Thus every (bio)material for local drug delivery needs to be tailored individually to the intended microvascular bed for optimal MSP sizing. Especially in case of angiogenic MSPs, it is prudent to regulate MSP retention to prevent angiogenesis in unwanted areas.

Timing of MSP Delivery

The timing of infusion, immediately upon reperfusion of the ischemic myocardium, allows distribution before the major onset of reperfusion injury and no reflow (23). This opens up new therapeutic options for treatment of no reflow, as systemic drug delivery will be limited by the development of microvascular perfusion defects within half an hour after onset of reperfusion. The timing of MSP therapy upon reperfusion is of great clinical potential, as MSPs can be infused directly following PCI, thus limiting additional procedural risks to the patient.

Inhibition of Acute Inflammation

Reperfusion following myocardial infarction is typically associated with the release of proinflammatory cytokines such as TNF- α and IL-6 (24). The main source of TNF- α is

suggested to be the monocyte/macrophage, whereas others indicate that mast cells are the initial source of TNF- α that subsequently gives rise to influx of monocyte/macrophages, with the latter as the main source for IL-6 (22, 24). However, cardiomyocytes and endothelium can also release TNF- α when stimulated (25). Given the chronic nature of our study, we were unable to assess the acute effect of VEGF MSP infusion on cardiac macrophage accumulation and mast cell degranulation in tissue. Consequently, we were unable to identify the source of these cytokines. Whether reduction of TNF- α and IL-6 is detrimental or protective for the reperfused myocardium is difficult to say. TNF- α reduction can attenuate infarct size, but TNF- α can also increase the expression of cytoprotective proteins (25). In our study, it did not translate to differences in myocardial function.

VEGF Therapy and Global Function

VEGF165A therapy in our study resulted in a dose-dependent increase in microvascular density, but this did not translate into global or regional improvements of cardiac function as measured by cardiac MRI. However, we induced relatively small infarcts, and 5 wk of follow-up may be considered short. Previous results from our laboratory indicate that, indeed, these conditions may not result in measurable global functional improvements at the short term, despite regional improvements (18). Our study is the first to report MSP-based VEGF release for AMI in a setting of reperfused myocardial infarction in a large-animal model. Interestingly, ~57% of small-animal VEGF studies that include functional measurements report improvements in global cardiac function, and 50% of large-animal studies show global functional improvements (Table 3); however, these are mostly studied in a setting of chronic ischemia. No clear therapeutic optima, including timing of administration and total cumulative dosage, can be distilled from this previous work. Thus differences in experimental conditions, including animal model, infarct size, and therapeutic protocol, may underlie differences in therapeutic outcome.

VEGF Elicits a Dose-Dependent Increase in Cardiac Microvascular Density

It is remarkable that so few studies report the total cumulative dose of administered VEGF or the dose normalized to body weight or infarct mass. Consequently, an effective VEGF dosage remains to be established and may be species dependent. For example, two rat studies that applied a bolus-like administration of VEGF both report positive effects on global function while administering a striking 458-fold difference in cumulative growth factor dosage (11 μ g vs. 24 ng) (26, 27). These results suggest that at least a broad range of therapeutic efficacy of VEGF for chronic myocardial infarction exists. Our study, using a model of reperfused myocardial infarction, shows that, whereas placebo treatment resulted in loss of microvascular density in the infarct zone, a cumulative dose of 0.9 μ g VEGF (0.07 ± 0.01 μ g/g myocardium) preserved microvascular density and 2.8

μg ($0.35 \pm 0.06 \mu\text{g/g}$ myocardium) resulted in an increased microvascular density compared with remote tissue. This demonstrates that VEGF indeed elicits dose-dependent angiogenesis in the infarcted tissue. When we place this outcome in perspective, it is striking that the effect of VEGF therapy in all previous studies consistently resulted in a significantly higher microvascular density of the infarct zone compared with the microvascular density of control infarcts. This effect appears independent of dosage, therapeutic protocol, or timing of administration. It must be noted, however, that we were the only group to compare microvascular density within the infarct region to the intrinsic control (remote area). It may well be that, although VEGF increased microvascular density in infarcted tissue compared with control infarctions, it could still be lower than in the remote zone, which could affect long-term outcome.

Route of Administration and AMI Model

From a translational point of view, it is evident that an intravenous or intracoronary route of administration is less invasive as opposed to injecting growth factors directly into the myocardium. Considering the potential tumorigenic potency and blood pressure-lowering effects of VEGF (28), any bolus, either intravenous, intracoronary, or intramyocardially, is less appropriate, as it inevitably recirculates. VEGF, distributed via the microcirculation, binds avidly to endothelium and fibrin, where bound to the latter it still supports endothelial proliferation (29, 30). Slow and sustained VEGF delivery via degradable biomaterials following intracoronary delivery therefore seems a viable therapy as the growth factor can be more easily bound to the tissue, and subsequent circulating levels should remain low. So far, none of the studies in Table 3 used the clinically relevant intracoronary route of biomaterial-mediated VEGF administration, and no conclusions can be drawn whether the outcome would have differed. We speculate, however, that optimal growth factor delivery and retention will be carrier dependent and needs to be tailored, as is true for cell therapy (31). Clearly a permanent occlusion, as used in the vast majority of the studies summarized in Table 3, is not representative for the clinical situation where interventions to restore perfusion of the ischemic territory are the golden standard in many countries. As a consequence, results obtained from these nonreperfused infarct studies will less likely predict the true effects of VEGF therapy following PCI for AMI.

Clinical Relevance

In our model of reperfused myocardial infarction, intracoronary delivery of VEGF by degradable MSPs clearly resulted in an increased microvascular density but not in improved cardiac function. Whether the changes in microvascular density would translate to a better long-term outcome beyond our 5-wk period is unknown. Thus the long-term benefit of increased microvascular density remains to be determined. The present

study does serve as a proof of principle that chronic delivery of active protein using biocompatible polymers in the broader context is feasible. It is a versatile methodology that is not limited to regional and global cardiac scar remodeling therapy or to one specific protein but rather might serve as a general platform for local drug delivery via the microvascular bed.

Limitations

The present formulation of MSPs showed an early (burst) release of VEGF in the in vitro study, which may have protected or stabilized the vascular bed from the acute ischemic insult, resulting in attenuated release of inflammatory cytokines, but also results in lower sustained VEGF levels. We cannot exclude that this may have affected efficacy of angiogenesis. In addition, multiple growth factors might also have improved efficacy of angiogenic therapy. It is also generally accepted that comorbidities, such as hypertension, diabetes, and atherosclerosis, often present in patients suffering AMI, can affect angiogenesis. Therefore, studies in large-animal models in which these risk factors are present would be useful before testing angiogenic strategies in clinical trials.

CONCLUSIONS

Regional, controlled VEGF delivery leads to a dose-dependent increase in microvascular density in infarcted tissue. This increase did not translate to changes in global or regional cardiac function or scar composition. Controlled regional VEGF delivery, however, is safe and feasible and supports the development of novel adjunctive off-the-shelf therapeutic applications.

ACKNOWLEDGMENTS

The authors cordially acknowledge the indispensable contributions of Ayla Hoogendoorn, Frank-Jan Drost, Felix Kienjet, and Bas Wijenberg. Klazina Kooiman and Tom van Rooij are thanked for their contributions in particle sizing.

GRANTS

This work was funded by SenterNovem/AgenstschapNL for “A NOVEL APPROACH TO CARDIAC THERAPY: Development of a platform technology for local sustained delivery.”

DISCLOSURES

Coauthors Ruud Verrijk and Tommi Markkula were employees of OctoPlus at the time of the study. The authors confirm that there are no known conflicts of interest associated with this publication and there has been no significant financial support for this work that could have influenced its outcome.

REFERENCES

1. Delewi R, Hirsch A, Tijssen JG, Schachinger V, Wojakowski W, Roncalli J, et al. Impact of intracoronary bone marrow cell therapy on left ventricular function in the setting of ST-segment elevation myocardial infarction: a collaborative meta-analysis. *European heart journal*. 2014;35(15):989-98.
2. de Jong R, Houtgraaf JH, Samiei S, Boersma E, Duckers HJ. Intracoronary stem cell infusion after acute myocardial infarction: a meta-analysis and update on clinical trials. *Circulation Cardiovascular interventions*. 2014;7(2):156-67.
3. Szady AD, Pepine CJ, Sharma SV, Cogle CR, Perin EC, Ellis SG, et al. A critical analysis of clinical outcomes reported in stem cell trials for acute myocardial infarction: some thoughts for design of future trials. *Current atherosclerosis reports*. 2013;15(8):341.
4. Pavo N, Charwat S, Nyolczas N, Jakab A, Murlasits Z, Bergler-Klein J, et al. Cell therapy for human ischemic heart diseases: critical review and summary of the clinical experiences. *Journal of molecular and cellular cardiology*. 2014;75:12-24.
5. Dimmeler S, Leri A. Aging and disease as modifiers of efficacy of cell therapy. *Circulation research*. 2008;102(11):1319-30.
6. Fadini GP, Albiero M, Vigili de Kreutzenberg S, Boscaro E, Cappellari R, Marescotti M, et al. Diabetes impairs stem cell and proangiogenic cell mobilization in humans. *Diabetes care*. 2013;36(4):943-9.
7. Bezemer JM, Grijpma DW, Dijkstra PJ, van Blitterswijk CA, Feijen J. A controlled release system for proteins based on poly(ether ester) block-copolymers: polymer network characterization. *Journal of controlled release : official journal of the Controlled Release Society*. 1999;62(3):393-405.
8. Bezemer JM, Grijpma DW, Dijkstra PJ, van Blitterswijk CA, Feijen J. Control of protein delivery from amphiphilic poly(ether ester) multiblock copolymers by varying their water content using emulsification techniques. *Journal of controlled release : official journal of the Controlled Release Society*. 2000;66(2-3):307-20.
9. Bezemer JM, Radersma R, Grijpma DW, Dijkstra PJ, Feijen J, van Blitterswijk CA. Zero-order release of lysozyme from poly(ethylene glycol)/poly(butylene terephthalate) matrices. *Journal of controlled release : official journal of the Controlled Release Society*. 2000;64(1-3):179-92.
10. Bezemer JM, Radersma R, Grijpma DW, Dijkstra PJ, van Blitterswijk CA, Feijen J. Microspheres for protein delivery prepared from amphiphilic multiblock copolymers. 2. Modulation of release rate. *Journal of controlled release : official journal of the Controlled Release Society*. 2000;67(2-3):249-60.
11. Bezemer JM, Radersma R, Grijpma DW, Dijkstra PJ, van Blitterswijk CA, Feijen J. Microspheres for protein delivery prepared from amphiphilic multiblock copolymers. 1. Influence of preparation techniques on particle characteristics and protein delivery. *Journal of controlled release : official journal of the Controlled Release Society*. 2000;67(2-3):233-48.
12. van Dijkhuizen-Radersma R, Hesseling SC, Kaim PE, de Groot K, Bezemer JM. Biocompatibility and degradation of poly(ether-ester) microspheres: in vitro and in vivo evaluation. *Biomaterials*. 2002;23(24):4719-29.
13. Henry TD, Rocha-Singh K, Isner JM, Kereiakes DJ, Giordano FJ, Simons M, et al. Intracoronary administration of recombinant human vascular endothelial growth factor to patients with coronary artery disease. *American heart journal*. 2001;142(5):872-80.
14. Bondos SE, Bicknell A. Detection and prevention of protein aggregation before, during, and after purification. *Analytical biochemistry*. 2003;316(2):223-31.
15. Krueger MA, Huke SS, Glenny RW. Visualizing regional myocardial blood flow in the mouse. *Circulation research*. 2013;112(9):e88-97.

16. Uitterdijk A, Sneep S, van Duin RW, Krabbendam-Peters I, Gorse-Bakker C, Duncker DJ, et al. Serial measurement of hFABP and high-sensitivity troponin I post-PCI in STEMI: how fast and accurate can myocardial infarct size and no-reflow be predicted? *American journal of physiology Heart and circulatory physiology*. 2013;305(7):H1104-10.
17. Cason BA, Gamperl AK, Slocum RE, Hickey RF. Anesthetic-induced preconditioning: previous administration of isoflurane decreases myocardial infarct size in rabbits. *Anesthesiology*. 1997;87(5):1182-90.
18. Moelker AD, Baks T, van den Bos EJ, van Geuns RJ, de Feyter PJ, Duncker DJ, et al. Reduction in infarct size, but no functional improvement after bone marrow cell administration in a porcine model of reperfused myocardial infarction. *European heart journal*. 2006;27(24):3057-64.
19. Springeling T, Kirschbaum SW, Rossi A, Baks T, Karamermer Y, Schulz C, et al. Late cardiac remodeling after primary percutaneous coronary intervention-five-year cardiac magnetic resonance imaging follow-up. *Circulation journal : official journal of the Japanese Circulation Society*. 2013;77(1):81-8.
20. Haitsma DB, Bac D, Raja N, Boomsma F, Verdouw PD, Duncker DJ. Minimal impairment of myocardial blood flow responses to exercise in the remodeled left ventricle early after myocardial infarction, despite significant hemodynamic and neurohumoral alterations. *Cardiovascular research*. 2001;52(3):417-28.
21. Fox SB, Leek RD, Weekes MP, Whitehouse RM, Gatter KC, Harris AL. Quantitation and prognostic value of breast cancer angiogenesis: comparison of microvessel density, Chalkley count, and computer image analysis. *The Journal of pathology*. 1995;177(3):275-83.
22. Arras M, Mollnau H, Strasser R, Wenz R, Ito WD, Schaper J, et al. The delivery of angiogenic factors to the heart by microsphere therapy. *Nature biotechnology*. 1998;16(2):159-62.
23. Reffelmann T, Kloner RA. Microvascular reperfusion injury: rapid expansion of anatomic no reflow during reperfusion in the rabbit. *American journal of physiology Heart and circulatory physiology*. 2002;283(3):H1099-107.
24. Frangogiannis NG, Smith CW, Entman ML. The inflammatory response in myocardial infarction. *Cardiovascular research*. 2002;53(1):31-47.
25. Kleinbongard P, Schulz R, Heusch G. TNFalpha in myocardial ischemia/reperfusion, remodeling and heart failure. *Heart failure reviews*. 2011;16(1):49-69.
26. Scott RC, Rosano JM, Ivanov Z, Wang B, Chong PL, Issekutz AC, et al. Targeting VEGF-encapsulated immunoliposomes to MI heart improves vascularity and cardiac function. *FASEB journal : official publication of the Federation of American Societies for Experimental Biology*. 2009;23(10):3361-7.
27. Zhang J, Ding L, Zhao Y, Sun W, Chen B, Lin H, et al. Collagen-targeting vascular endothelial growth factor improves cardiac performance after myocardial infarction. *Circulation*. 2009;119(13):1776-84.
28. Sato K, Wu T, Laham RJ, Johnson RB, Douglas P, Li J, et al. Efficacy of intracoronary or intravenous VEGF165 in a pig model of chronic myocardial ischemia. *Journal of the American College of Cardiology*. 2001;37(2):616-23.
29. Jakeman LB, Winer J, Bennett GL, Altar CA, Ferrara N. Binding sites for vascular endothelial growth factor are localized on endothelial cells in adult rat tissues. *The Journal of clinical investigation*. 1992;89(1):244-53.
30. Sahni A, Francis CW. Vascular endothelial growth factor binds to fibrinogen and fibrin and stimulates endothelial cell proliferation. *Blood*. 2000;96(12):3772-8.
31. Campbell NG, Suzuki K. Cell delivery routes for stem cell therapy to the heart: current and future approaches. *Journal of cardiovascular translational research*. 2012;5(5):713-26.



Chapter 6

Multiple common co-morbidities produce left ventricular diastolic dysfunction associated with coronary microvascular dysfunction, cardiac oxidative stress and myocardial stiffening.

O. Sorop, I. Heinonen, **M. van Kranenburg**, V.J. de Beer, Y. Octavia, R.W.B. van Duin, K. Stam, R.J. van Geuns, A.H. van den Meiracker, A.H. Danser, W.J. Paulus, J. van der Velden, D. Merkus and D.J. Duncker,

submitted to Journal of Molecular and Cellular Cardiology

ABSTRACT

Aim - More than 50% of patients with heart failure have preserved ejection fraction (HFpEF) characterized by diastolic dysfunction. HFpEF usually occurs in female patients with multiple comorbidities such as hypertension (HT), obesity, hypercholesterolemia (HC) and diabetes mellitus (DM), but its pathophysiological basis is still incompletely understood. These co-morbidities have been proposed to induce systemic inflammation, cardiac microvascular dysfunction and oxidative stress, leading to myocardial fibrosis and myocyte stiffening and ultimately diastolic dysfunction. Here we tested this hypothesis in a swine model chronically exposed to three common comorbidities.

Methods and Results – DM (induced by streptozotocin), HC (high fat diet) and HT (resulting from renal artery embolization), (DM+HC+HT) were produced in ten female swine, which were followed for 6 months. Eight female healthy swine on normal pig-chow served as controls (CONTROL). The DM+HC+HT group showed hyperglycemia, hypercholesterolemia, hypertriglyceridemia and hypertension, which were associated with systemic inflammation and impaired coronary small artery endothelium-dependent vasodilation. Myocardial superoxide production was markedly increased, due to increased NOX activity and eNOS uncoupling, and associated with reduced NO production. These abnormalities were accompanied by increased myocardial collagen content, reduced capillary/fiber ratio and elevated passive cardiomyocyte stiffness, resulting in a reduced E/A ratio (as measured with cardiac MRI), and an increased left ventricular end-diastolic stiffness (as measured with a pressure-volume catheter), while ejection fraction was maintained.

Conclusion - The combination of three common comorbidities leads to systemic inflammation, myocardial oxidative stress and coronary microvascular dysfunction, which may be associated with myocardial stiffening and diastolic dysfunction with preserved ejection fraction.

Keywords: diastolic dysfunction, inflammation, coronary arteries, LV stiffness, oxidative stress

INTRODUCTION

More than 50% of patients with heart failure, present with heart failure with preserved ejection fraction (HFpEF) (1, 2). Hospitalized patients with HFpEF have high mortality and rehospitalization rates, and there is currently no effective treatment available for these patients (3, 4). Common metabolic and cardiovascular risk factors appear to be critical in the development of HFpEF, as the incidence of HFpEF rises with increasing prevalence of obesity, hypertension, chronic kidney disease, female sex and type 2 diabetes (5-7). Furthermore, studies in HFpEF patients have shown alterations in myocardial structure, function and cell signaling that are unique to this form of heart failure (8-11). However, the pathophysiological basis of HFpEF is still not fully understood, particularly at the myocardial tissue level. Consequently, findings from these earlier studies have led to the proposition of a novel paradigm, in which multiple comorbidities for HFpEF, including obesity, hypertension, hypercholesterolemia and diabetes induce a systemic pro-inflammatory state, that leads to coronary microvascular dysfunction and oxidative stress, which in turn, result in myocardial stiffening and ultimately left ventricular dysfunction (12). However, direct experimental evidence for this unifying hypothesis is still lacking. Consequently, we set out to investigate the chain of events as proposed in this novel paradigm, using a large animal model chronically exposed to three common comorbidities that associate with HFpEF, i.e. hyperglycemia, hypercholesterolemia and hypertension. Since the prevalence of HFpEF is predicted to increase in our aging Western societies, (13) such a large animal model may offer a much needed platform for testing novel drug and lifestyle therapies for the treatment of HFpEF.

MATERIALS AND METHODS

Animals

The study was performed in accordance with the "Guiding Principles in the Care and Use of Laboratory Animals" as approved by the Council of the American Physiological Society, and with approval of the Animal Care Committee at Erasmus University Medical Center, Rotterdam, The Netherlands, complying with the institutional and national guidelines for the care and use of laboratory animals. Ten female (21.7 ± 0.3 kg) Yorkshire x Landrace pigs were studied. Eight healthy female pigs, of similar age were studied as controls (Control). In addition, 6 fresh control hearts from slaughterhouse female pigs of similar body weight as the control animals (~ 100 kg at sacrifice) were studied to compare vascular function characteristics.

Induction of risk factors

The animals were made diabetic (DM) by injection of streptozotocin (Bio-connect B. V., Huissen, The Netherlands), given for 3 consecutive days (50 mg/kg/day i.v.) to destroy approximately 70-80% of the pancreatic β -cell islets(14). Pigs were housed in metabolic cages and their diabetic status was regularly monitored by measurements of urinary and venous blood glucose and ketones levels.

One-and-a-half week after DM-induction, hypertension (HT) was produced by micro-embolization of afferent glomerular arteries in the kidneys. The animals were sedated with zoletil (Tiletamine/Zolazepam; 5 mg/kg), rompun (Xylazine; 2.25 mg/kg) and atropine (2 ml, i.m.), and artificially ventilated with a mixture of O₂ and N₂ (1:2) to which 1–2% (vol/vol) isoflurane was added. Arterial access was obtained via a 9F sheath in the right carotid artery, allowing measurement of blood pressure and heart rate. A Swan-Ganz catheter (Corodyn™ TD, B. Braun Melsungen, Germany) was advanced towards the renal arteries and 75 mg of polyethylene microspheres (38-42 μ m, Cospheric, Santa Barbara, CA, USA) were infused separately in the right kidney as well as the bottom half of the left kidney. A port-a-cath catheter (Port-a-cath II POWER P.A.C., Smiths Medical International Ltd., UK) was then advanced via the carotid artery in the descending aorta and tunneled subcutaneously to the back. Thereafter the wound was closed and animals were allowed to recover. The catheter was flushed and blood pressure was measured in the awake state every 2 weeks for the rest of the study duration.

One week after HT induction, a high fat diet, with 25% of fat and 1% of cholesterol (HC), was gradually introduced. The animals were fed two meals/day during which they had unlimited access to 600-800 grams of food for one hour. The diet was supplemented with 10g salt/day. All animals completed 6 months of study duration.

Hemodynamic assessment

At sacrifice, animals were sedated with zoletil (Tiletamine/Zolazepam; 5 mg/kg) rompun (Xylazine; 2.25 mg/kg) and atropine (2 ml i.m.), anesthetized with pentobarbital (20 mg/kg i.v.) and artificially ventilated. In the morning, animals underwent cardiac magnetic resonance imaging (MRI) for assessment of left ventricular (LV) dimensions and function as detailed below. Thereafter, a 9F sheath was placed in the left carotid artery and catheters were implanted for measurement of mean aortic pressure (MAP), and LV pressure (Millar catheter, LVP), pulmonary artery pressure (PAP), pulmonary capillary wedge pressure (PCWP), cardiac output (CO, by thermodilution) and for blood sampling. The pressure-volume loops and end diastolic (EDPVR) and end systolic pressure-volume relationships (ESPVR) were constructed using a pressure/volume catheter placed in the LV (CD Leycom, The Netherlands), both during baseline hemodynamic conditions and during preload reduction after complete obstruction of the inferior vena cava by inflation of a Fogarty balloon (8/10F, Edwards Life sciences, Amsterdam, The Netherlands).

Following thoracotomy, LV anterior wall transmural biopsies were taken for single myocyte passive force measurements.

Contrast-enhanced cardiovascular magnetic resonance acquisition and analysis

Contrast-enhanced cardiovascular magnetic resonance was performed using a 1.5-Tesla scanner (Discovery MR450, GE Medical System, Milwaukee, Wisconsin, USA). Swine were placed in lateral position and a dedicated 32-channel phased-array surface coil (GE Medical Systems, Milwaukee, Wisconsin, U.S.A.) was placed on the thorax. Four leads were placed subcutaneously and connected to the MRI's ECG system to create a vectorcardiogram for consistent ECG gating. For assessment of the LV function, a breath hold, ECG gated, steady state free precession sequence (SSFP) was used. The field of view was adjusted to prevent fold-over artefacts. Reconstructed pixel size was 0.70 x 0.70 mm, slice thickness; 6 mm, slice gap; 0 mm, with a temporal resolution of 42 ms. Two and four chamber views were acquired to cover the long axis of the LV. Using these orientations on the diastolic phase, the short axis functional scan was planned covering the entire length of the heart using approximately 17 slices. For the assessment of mitral valve flow, a 2D vascular phase contrast, breath hold, ECG gated sequence was used. Reconstructed pixel size; 1.41 x 1.41 mm, slice thickness; 7 mm, with a temporal resolution 42 ms, velocity encoding; 120 cm/s. Plane of acquisition was at the tip of the mitral valve leaflets, perpendicular to the flow and positioned during the (systolic or diastolic) phase. For myocardial fibrosis detection, late gadolinium enhancement imaging was performed. Slices covering the LV were acquired 10 minutes after intravenous injection of an bolus of 0.20 mmol/kg Gadovist (Gadovist 1.0 mmol/ml, Bayer, Mijdrecht, the Netherlands), using an inversion recovery prepared radio-frequency spoiled gradient echo pulse sequence (IR-SPGR). The inversion time was selected to null out the myocardial muscle signal. Typical inversion times ranged between 200-300 ms. The reconstructed pixel size was 1.40 x 1.40 mm. LV function and mass, transmitral flow and late gadolinium enhancement were analysed on a remote workstation using dedicated software. For evaluation of LV function CAAS MRV, 3.4, Pie Medical Imaging, 2011, Maastricht, the Netherlands was used. For the assessment of mitral valve flow CAAS MR Flow 1.2, (Pie Medical Imaging, 2011, Maastricht, the Netherlands) was used. LV end-diastolic volume (EDV) and LV end-systolic volume (ESV) were short axis-based and calculated using a combination of long and short axis images and are expressed in millilitres (15). Epicardial and endocardial contours were automatically detected on short axis images and manually corrected. The papillary muscles and trabecula were considered to be part of the blood pool. LV mass was calculated as the differences in epicardial and endocardial EDV multiplied by 1.05 g/cm³ and was expressed in grams(15). To measure E/A ratio, peak velocities were measured within a region of interest placed at the orifice of the mitral valve for all cardiac phases (16).

Plasma measurements

Fasting arterial blood samples were obtained at sacrifice for determination of plasma glucose, triglycerides, total cholesterol, low-density lipoprotein (LDL), high-density lipoprotein (HDL), aspartate aminotransferase (ASAT), alanine aminotransferase (ALAT), and creatinine. Arterial plasma concentrations of interleukin-6 (IL-6, R&D Systems Europe Ltd., Abingdon, UK) and tumor necrosis factor alpha (TNF- α , R&D Systems Europe Ltd., Abingdon, UK), were determined using ELISA kits.

Small artery function in vitro

After the LV biopsies were obtained, hearts were arrested, immediately excised and placed in cold, Krebs bicarbonate buffer solution. Epicardial small coronary arteries (~300 μ m diameter) were isolated from the LV apex and studied in vitro using a Mulvany wire myograph (DMT, Aarhus, Denmark) as previously described (17). In short, vascular segments (~2mm length) were mounted on wires, and maintained at 37°C, in Krebs buffer. After a 30 minutes stabilization period, the internal diameter was set to a tension equivalent to 90% of the estimated diameter at 100 mmHg effective transmural pressure(18), followed by depolarization by 10^{-1} mol/l potassium chloride (KCl, Sigma-Aldrich, Zwijndrecht, The Netherlands) to achieve the maximal contractile response. The concentration-response curves (CRC) for the different substances were performed on separate segments, adjacent to each other in vivo. Endothelial-dependent vasodilator capacity was tested in response to bradykinin (BK, 10^{-10} to 10^{-6} mol/l, Sigma-Aldrich, Zwijndrecht, The Netherlands) upon precontraction by 10^{-6} mol/l thromboxane- A_2 analogue U46619 (Sigma-Aldrich, Zwijndrecht, The Netherlands). Smooth muscle cell relaxation was tested using the exogenous NO-donor, S-nitroso-N-acetylpenicillamine (SNAP, 10^{-10} to 10^{-5} mol/l, Sigma-Aldrich, Zwijndrecht, The Netherlands).

Reactive Oxygen Species (ROS) and cardiac nitric oxide (NO) production measurements

To evaluate cardiac oxidative stress, basal superoxide generation from the endocardium of the anterior LV, was measured by lucigenin-enhanced chemiluminescence (Sigma Aldrich; 5 μ mol/L) in a 96-well microplate using a luminometer (Luminoskan Ascent, ThermoLabsystem) in which dark-adapted lucigenin was added via an auto-dispenser as previously described.(19) Besides total superoxide production, nitric oxide synthase (NOS)-dependent superoxide production was determined by incubating the samples from the same homogenized LV for 20 minutes with the NOS inhibitor L-NAME (Sigma Aldrich; 1 mmol/l), while NADPH oxidase contribution to superoxide production was assessed using the NADPH oxidase inhibitor VAS2870, (10 μ M). The experiment was repeated upon stimulation of superoxide production by 300 μ M NADPH. The temperature was maintained at 37°C and light emission was recorded and expressed as Tiron-

inhibitable relative light units (RLU) per mg per second. All samples were measured in duplicate. Myocardial NO production in the same area was evaluated by measuring the production of NO metabolites NO_2^- and NO_3^- using the Griess reaction colorimetric assay (Cayman Chemical).

Endothelial Nitric Oxide Synthase regulations

Total endothelial nitric oxide synthase (eNOS) protein expression, phosphorylated eNOS and eNOS monomer and dimer protein expression were determined in homogenized LV tissue samples. For detection of eNOS monomer and dimer fraction, low temperature SDS-PAGE was performed as previously described (20). Briefly, gels and buffers were equilibrated at 4°C before electrophoresis, and the buffer tank was placed in an ice bath during electrophoresis to maintain the low temperature. SDS-PAGE for phosphorylated eNOS, total eNOS protein content and housekeeping protein glyceraldehyde 3-phosphate dehydrogenase (GAPDH) was performed at room temperature. Subsequent to SDS-PAGE, the proteins were transferred to nitrocellulose membranes and the blots were probed with primary anti-phospho eNOS Ser1177 (1:1000, Cell Signaling), anti-eNOS (1:500, Transduction Laboratory) and anti-GAPDH (1:10000, Imgenex). All blots were analysed using the Odyssey system (LI-COR).

Histology and immunohistochemistry

After excision of the heart, LV anterior myocardial tissue samples were cut, fixated in 4% buffered formaldehyde and embedded in paraffin. 4.5 µm thick slides were cut, deparaffinized and stained for histological analyses. 6-10 fields were examined in the endocardial and in the epicardial part of each slide, at ×20 magnification. Collagen deposition was quantified using picrosirius red staining. Using a linear polarization filter, the area occupied by collagen type I, collagen type III fibers, as well as total collagen was measured and expressed as percentage of the myocardial area. Myocyte size was quantified with a Gomori silver stain. Cross-sectional areas of 300-350 cells with clearly visible nuclei were measured in total per slide. Capillary density was quantified in the same area as used for measurements of myocyte size and collagen. Endothelial cells were stained with biotin-labeled lectin (lectin 1/100 diluted in 1% bovine serum albumin in PBS, Sigma-Aldrich Chemie®, Zwijndrecht, The Netherlands). All vessels smaller in diameter than 10 µm were counted. Capillary-to-fiber ratio was calculated as the number of capillaries per tissue area and corrected for the total number of cardiomyocytes present in the same field. All measurements were performed using a microscopy image analysis system (Impak C, Clemex Vision Image analysis system, Clemex Technologies, Quebec, Canada).

Cardiomyocyte Measurements

Single cardiomyocytes were obtained via mechanical isolation in cold relaxing solution containing (in mM) free Mg^{2+} 1, KCl 100, EGTA 2, Mg-ATP 4, imidazole 10 (pH 7.0, adjusted with KOH). Subsequently, cells were incubated for 5 min in relaxing solution with Triton X-100 (0.5%) to remove all membranes as described previously(21). Isometric force was measured at maximal calcium concentration ($31.6 \mu\text{mol/L}$) at 15°C and sarcomere length of $2.2 \mu\text{m}$ to determine the maximal force generating capacity of single cardiomyocytes. The diameters of the cardiomyocyte were measured microscopically, in two perpendicular directions. Cross-sectional area was calculated assuming an elliptical cross-section. Isometric force was measured after the preparation was transferred from relaxing to activating solution. When steady force was reached, the myocyte length was reduced by 20% within 2 ms using the piezoelectric motor and restretched after 30 ms (slack test). As a result, force first dropped to zero and then quickly redeveloped to the original steady-state level. Subsequently, the myocyte was returned to the relaxing solution, and a second slack test (10 s duration) was performed allowing the determination of passive force (F_{pas}). Active maximal isometric force, (F_{act}), was calculated from the total force level in activating solution – F_{pas} and corrected for cross-sectional area. F_{pas} measurement were performed at sarcomere lengths ranging from 1.8 to $2.2 \mu\text{m}$.

Data analysis

Data are presented as mean \pm SEM. Comparison of variables between the two groups was performed by Student t-test (StatView 5.0 SAS Institute Inc.). Vasodilator responses to BK and SNAP were expressed as percentage of the precontraction to U46619. Vasoconstrictor responses to U46619 were normalized to 10^{-1} mol/l KCl. Statistical analysis of CRCs, MAP changes over time and F_{pas} was performed using two-way ANOVA. $P < 0.05$ was considered statistically significant.

RESULTS

Model characteristics

At 6-months follow-up, significant increases in glucose, cholesterol, LDL- and HDL-cholesterol values, and the LDL/HDL ratio, and to a lesser extent in triglycerides ($P=0.07$), were observed in DM+HC+HT animals compared to controls (Table 1). TNF- α plasma levels were significantly higher than those of healthy controls, consistent with a chronic inflammatory status in these animals. No differences in plasma creatinine or urea values were observed between the groups. However, DM+HC+HT animals had lower body weights ($79 \pm 3 \text{ kg}$) than the age-matched control animals ($102 \pm 4 \text{ kg}$, $P < 0.05$). Plasma levels of ASAT were similar between groups (42 ± 11 in DM+HC+HT vs $40 \pm 2 \text{ U/l}$ in Control),

but ALAT was significantly lower in the DM+HC+HT animals as compared to the controls (24 ± 4 vs 51 ± 2 U/l, $P < 0.05$). MAP, measured under general anesthesia, immediately prior to and following infusion of the polyethylene beads in the kidneys, rose from 62 ± 3 mmHg to 87 ± 4 mmHg ($P < 0.05$). The increase in MAP was well maintained over time, as indicated by the biweekly measurements in the awake state, with animals standing quietly in the cage (Fig. 1).

Table 1. Arterial Blood characteristics in DM + HC + HT swine group versus healthy control swine (control) obtained at fasting state under anesthesia.

Parameter	Control (n=8)	DM + HC + HT (n = 10)
Glucose (mmol/l)	6.1 ± 0.7	$22.7 \pm 0.9^*$
Cholesterol (mmol/l)	2.2 ± 0.12	$16.8 \pm 3.4^*$
LDL-cholesterol (mmol/l)	1.1 ± 0.1	$14.0 \pm 3.2^*$
HDL-cholesterol (mmol/l)	1.1 ± 0.1	$5.1 \pm 0.7^*$
LDL/HDL-Cholesterol	1.1 ± 0.1	$2.7 \pm 0.4^*$
Triglycerides (mmol/l)	0.35 ± 0.05	$1.16 \pm 0.36^\#$
Urea (mmol/l)	4.2 ± 0.5	3.8 ± 0.4
Creatinine ($\mu\text{mol/l}$)	130 ± 6	129 ± 11
TNF- α (pg/ml)	74 ± 24	$231 \pm 64^*$
IL-6 (pg/ml)	21 ± 8	67 ± 32

LDL=low density lipoprotein, HDL=high density lipoprotein, TNF- α =tumor necrosis factor alpha, IL-6=interleukin-6, * $P < 0.05$, # $P = 0.07$, DM+HFD+HT vs Control

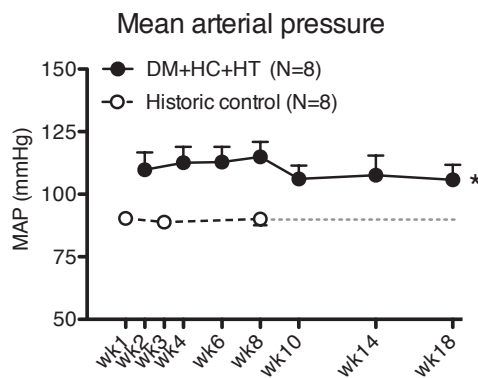


Figure 1. Mean arterial pressure, measured in resting awake state, was increased in time in DM+HC+HT animals in comparison to historic healthy control animals. * $P < 0.05$ in DM+HC+HT versus historic healthy control by two-way ANOVA.

Coronary small artery function in vitro

Small arteries from the DM+HC+HT animals showed similar precontraction to 10^{-6} M U46619 as compared to control vessels, i.e. $65 \pm 6\%$ vs $70 \pm 16\%$ of the response to 10^{-1} mol/l KCl in the BK experiments, and $62 \pm 8\%$ vs $64 \pm 8\%$ in DM+HC+HT vs Control in the SNAP experiments, (both $P = \text{NS}$). The vasorelaxation to the endothelium-dependent

vasodilator BK was significantly blunted in DM+HC+HT pigs (Fig. 2A), whereas the vaso-relaxation to the endothelium-independent vasodilator SNAP was maintained (Fig. 2B), indicative of endothelial dysfunction.

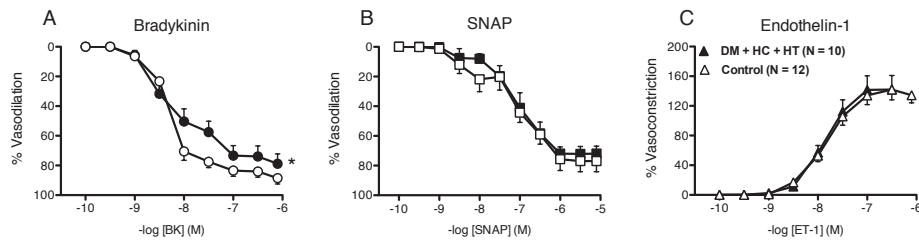


Figure 2. Response to bradykinin (BK), the exogenous NO-donor, S-nitroso-N-acetylpenicillamine (SNAP) and endothelin-1 (ET-1) in small arteries isolated from the DM+HC+HT animals and healthy control hearts. BK-induced response was significantly impaired in the diseased animals, while no differences were recorded in the SNAP and ET-1 mediated responses. * $P < 0.05$ DM+HC+HT versus Control by two-way ANOVA.

ROS measurements

Myocardial production of the NO metabolites NO_2^- and NO_3^- was significantly lower in the DM+HC+HT animals compared to controls, suggesting reduced NO production (Fig. 3A). Conversely, basal superoxide production was 3-fold increased in DM+HC+HT animals. This increase was suppressed by both L-NAME and VAS2870 ($P < 0.05$ in the presence of L-NAME or VAS2870 versus baseline measurements), indicating that both NOS and NADPH oxidase contributed to superoxide production (Fig. 3B). NADPH resulted in aggravated – and VAS2870-inhibitable but not L-NAME-inhibitable – superoxide production in DM+HC+HT animals as compared to controls (Fig. 3C), confirming NADPH oxidase as a major source of superoxide anion in DM+HC+HT animals. Moreover, although

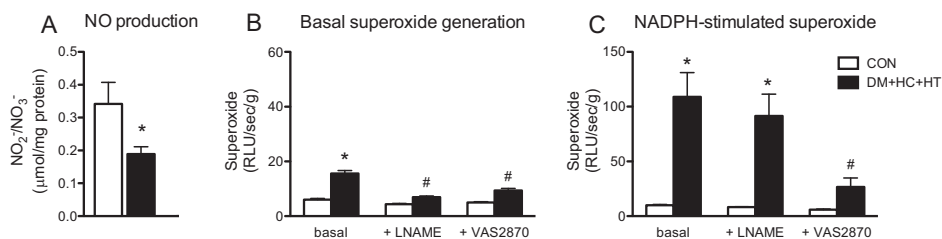


Figure 3. Basal NO production was significantly lower (Fig. 3A) while superoxide generation was significantly higher in the endocardial layer of the left ventricle of DM+HC+HT animals as compared to healthy controls. This superoxide generation was significantly suppressed by L-NAME and VAS2870, (Fig. 3B). Upon NADPH oxidase stimulation, the superoxide anion production was dramatically increased (Fig. 3C), this response being fairly independent of NOS, and significantly impaired by VAS2870 treatment, suggesting that NADPH oxidase is the major source of superoxide anion in the DM+HC+HT animals. * $P < 0.05$ DM+HC+HT versus Control; # $P < 0.05$ vs corresponding basal level.

total eNOS expression was increased in DM+HC+HT as compared to control, (Fig. 4A), this increase was principally due to an increase in eNOS monomer, as the monomer/dimer ratio was markedly higher than in controls (Fig. 4B). Also, eNOS phosphorylation on residue Ser1177 was higher (possibly phosphorylation of the eNOS monomer(22)), suggesting that not only expression, but also eNOS activity was increased, (Fig. 4C). The increase in monomer/dimer ratio in the DM+HC+HT animals points to uncoupling of eNOS as the mechanism behind increased NOS-dependent superoxide production

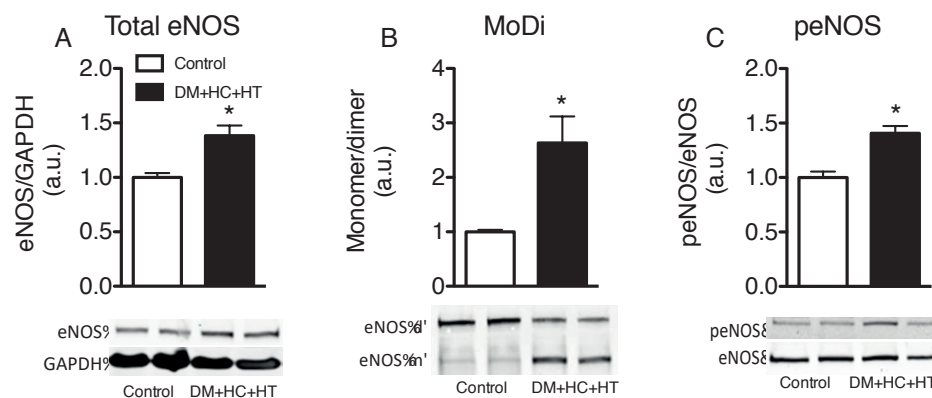


Figure 4. eNOS expression was increased in the diseased animals (Fig. 4A), as was the monomer/dimer ratio (Fig. 4B), suggesting that eNOS uncoupling contributes to superoxide anion production. Phosphorylation of eNOS was also significantly increased in the diseased animals, (Fig. 4C). *P<0.05 DM+HC+HT versus Control.

Myocardial structural changes: Collagen deposition, myocyte cross-sectional area and capillary density

Figure 5 summarizes the histological findings in the subendocardial layer of the LV anterior wall of animals from both groups. Total collagen deposition (collagen type I + III), were assessed in the subendocardial and subepicardial layers of the LV. Collagen deposition was significantly increased in DM+HC+HT animals as compared to the healthy controls, (Fig. 5A). No difference was seen between the endocardium and the epicardium, (data not shown). The measurement of the cardiomyocytes cross-sectional area revealed that cardiomyocytes from the DM+HC+HT animals were significantly smaller than those of control pigs (Fig. 5B). No significant difference in cardiomyocyte size was found between the endocardium and epicardium in DM+HC+HT animals ($413 \pm 42 \mu\text{m}^2$ in endo vs $379 \pm 29 \mu\text{m}^2$ in epi), whereas in Control animals the endocardial cells tended to be smaller than the epicardial cells ($598 \pm 23 \mu\text{m}^2$ in endo and $676 \pm 31 \mu\text{m}^2$ in epi, $P=0.06$). When normalized to body weight, the difference in myocyte area between Control and DM+HC+HT disappeared. Capillary density was similar between the groups (Fig. 5C) and also between the subendocardium and subepicardium in each group (data not

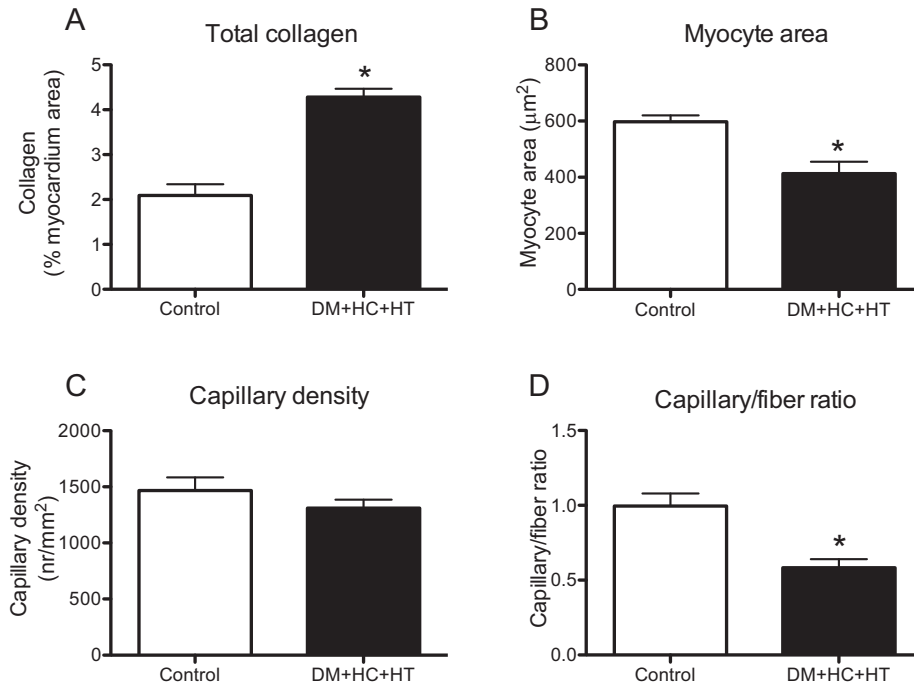


Figure 5. Increased collagen deposition (Fig. 5A) but no myocyte hypertrophy (Fig. 5B) was recorded in endocardium of LV anterior wall of the DM+HC+HT animals when compared to healthy controls. Capillary density was similar between groups (Fig. 5C), however the capillary-to-fibre ratio was significantly reduced in DM+HC+HT (Fig. 5D), indicative of capillary rarefaction. * $P < 0.05$ DM+HC+HT versus Control

shown). However, the capillary-to-fiber ratio was significantly lower in the DM+HC+HT group as compared to Control animals, suggestive of capillary rarefaction (Fig. 5D). No differences were observed between the subendocardium and subepicardium of either group (not shown). Figure 6 presents typical examples of the LV subendocardium stained with picrosirius red for collagen (Fig. 6A, D), Gomori for myocyte size (Fig. 6B, C) and lectine for capillary density (Fig. 6C, E) in Control versus DM+HC+HT animals.

in press

Figure 6. Typical examples of the endocardial layer of the LV stained with picrosirius red for collagen (Fig. 6A, D), Gomori for myocyte size (Fig. 6B, C) and lectine for capillary density (Fig. 6C, E) in DM+HC+HT versus Control.

Single myocyte passive and maximal force

Increased passive stiffness (F_{pas} , Fig. 7A) as well as increased maximal force (F_{max} , Fig. 7B) of the cardiomyocytes isolated from the subendocardium of the LV anterior wall of DM+HC+HT animals was observed as compared to the healthy controls.

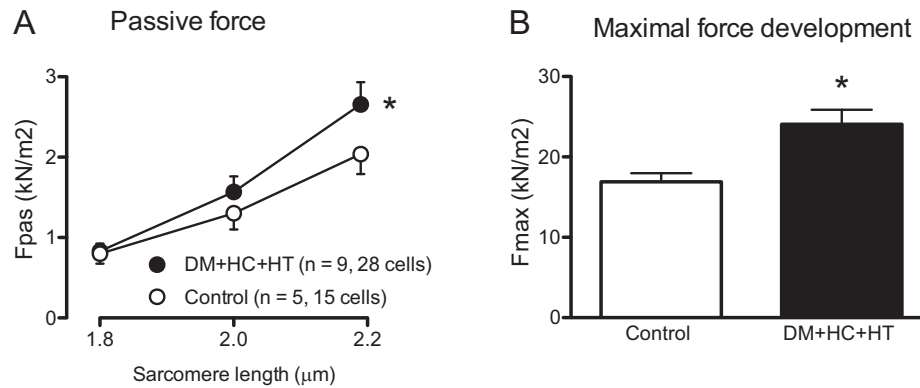


Figure 7. Increased passive (Fig. 7A) and maximal force (Fig. 7B), was seen in DM+HC+HT group as compared to healthy animals. * $P < 0.05$ DM+HC+HT versus Control.

Cardiac MRI and global LV function

MRI variables are shown in Table 2. LV EDV, was similar while SV was smaller in DM+HC+HT as compared to Control animals, while ejection fraction was not changed, (Fig. 8A). Late gadolinium enhancement did not show any difference despite an increased collagen content in the LV of DM+HC+HT animals as measured histologically, (data not shown). However, E/A ratio tended to be lower in the DM+HC+HT group, suggestive of early diastolic dysfunction (Fig. 8B), although LV dP/dt_{min} or the time constant of relaxation tau were not different. These findings were complemented by the pressure-volume data, showing that DM+HC+HT animals had increased LV end-diastolic elastance, indicative of increased passive stiffness of the LV in vivo (Fig. 8D, $P < 0.05$). LV end-systolic elastance also tended to be higher in these animals, although this failed to reach statistical significance (Fig. 8C, $P = 0.10$). No significant group differences were observed in LV end-diastolic pressure, dP/dt_{max} or tau (Table 2). The LV EDV was significantly lower in the DM+HC+HT animals as measured by the pressure-volume catheter and showed a similar behavior when measured in the MRI, although it did not reach statistical significance. Similarly, the stroke volume was also significantly lower in the DM+HC+HT group versus Control animals, as measured by both pressure-volume catheter and MRI.

Atrial, ventricular and renal weights

No group differences were detected in LV, right ventricle, left or right atrium mass, either in absolute terms or when normalized for body weight (Supplemental Table 1). Kidneys of the DM+HC+HT animals were smaller than kidneys of control healthy animals, however, when corrected for body weight, these differences were no longer apparent (Supplemental Table 1).

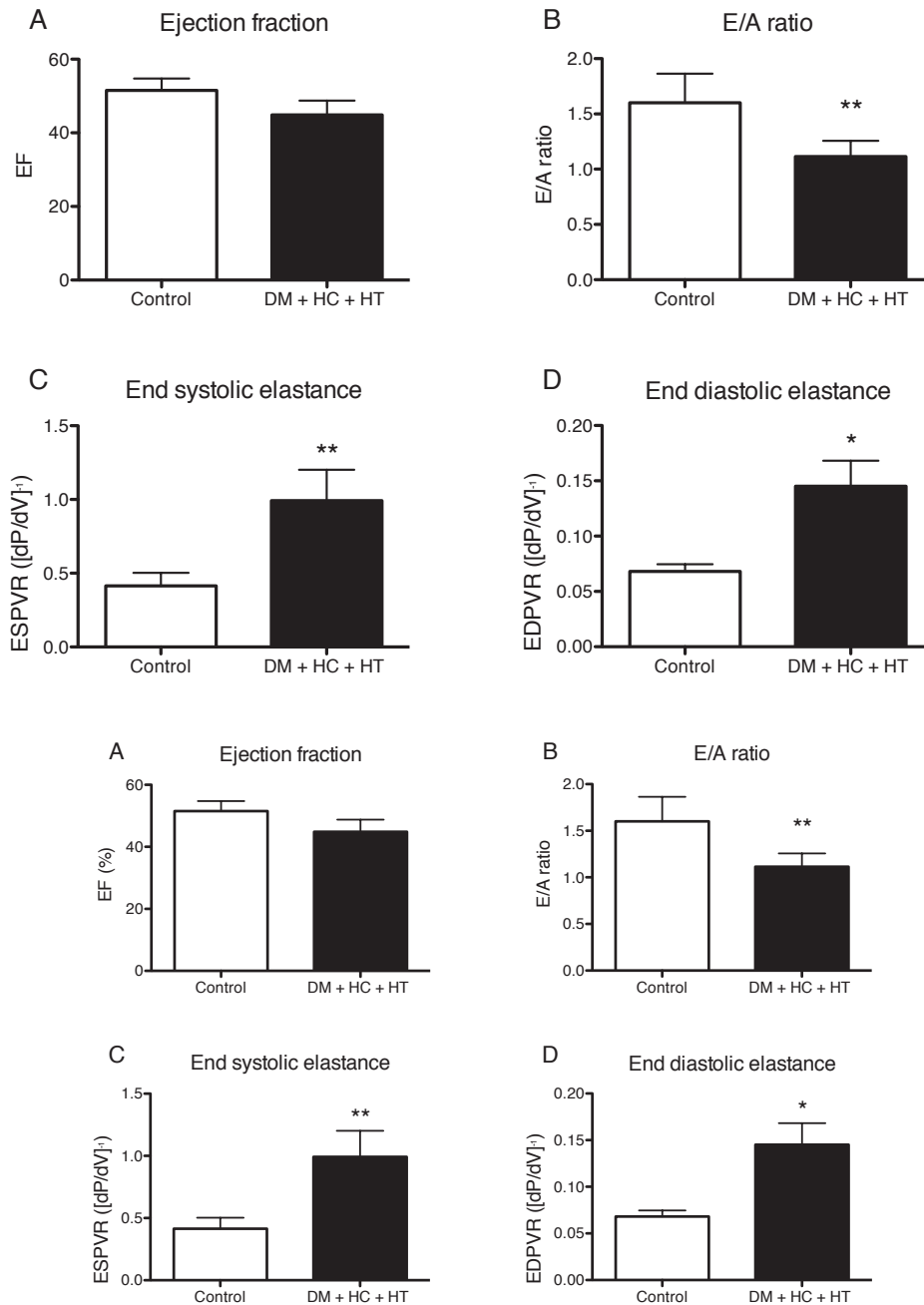


Figure 8. No difference in ejection fraction (EF) was seen between groups as measured with MRI (Fig. 8A). However, the early-to-late filing velocity ratio of blood during diastole (E/A ratio) was significantly reduced in the DM+HC+HT animals (Fig. 8B). In accordance to these findings, increased end diastolic elastance was seen in these animals (Fig. 8D), while a trend towards significance in the end systolic elastance was recorded (Fig. 8C). * $P < 0.05$ DM+HC+HT versus Control. ** $P < 0.05$ DM+HC+HT versus Control by one sided t-test.

Table 2. Left ventricular function in Control and DM + HC + HT groups under anesthesia

	Control	DM + HC + HT
Body weight (kg)	102±4	79±3*
Pressure/Volume Catheter	N=8	N=10
Heart rate (bpm)	85±3	91±5
LV EDV (ml)	174±22	113±11*
SV (ml)	75±3	55±4*
Ejection fraction (%)	47±5	50±3
Millar Catheter	N=8	N=10
Heart rate (bpm)	88±4	85±3
dP/dt max (mmHg/s)	1470±138	1604±214
dP/dt min (mmHg/s)	-2510±322	-2687±266
Tau (ms)	49±3	48±3
LV EDP (mmHg)	9±2	9±2
MRI	N=6	N=7
Heart rate	89±7	71±3*
LV EDV (ml)	189±12	162±11
SV	98±9	73±7*
Ejection fraction (%)	51±3	45±4

LV= left ventricle, SV=stroke volume, EDV=End-diastolic volume, ESV= End-systolic volume, dP/dT min and dP/dT max = minimum and maximum rate of pressure change in the left ventricle, LV EDP=left ventricle end diastolic pressure, Tau=time constant of isovolumic relaxation; *P<0.05 compared to Controls

DISCUSSION

In the present study, we report that in the absence of major geometrical alterations in the heart, the coexistence of three common comorbidities leads to LV diastolic dysfunction as evidenced by reduced LV diastolic early-to-late filling velocities as well as increased passive LV stiffness in vivo, while EF was still preserved. The cascade of events leading to diastolic dysfunction included the presence of chronic systemic inflammation and decreased endothelium-dependent vasodilation in the coronary arteries as assessed in vitro. We also observed reduced capillary-to-fiber ratio, higher superoxide production due to NOX activation and eNOS uncoupling and reduced cardiac NO production, all likely to be important mechanisms for the observed increased collagen content in the LV contributing to LV stiffening and thereby reduced diastolic function (12).

Paulus and Tschope (12) recently proposed that a systemic inflammatory state produced by cardiovascular comorbidities or risk factors is common in many HF patients including those with HFpEF (23, 24). The inflammatory state promotes coronary microvascular endothelial dysfunction, which characterized by generation of reactive oxygen species and reduced NO bioavailability, leading to a cascade of signaling events that ulti-

mately promote cardiac fibrosis and myocyte stiffness. Indeed, it is now well established that multiple common comorbidities, including obesity, diabetes and hypertension, are strongly associated with HFpEF (5-7, 25-27). This cascade of events could be faithfully recapitulated in the present study. Thus, firstly, a pro-inflammatory state as documented by markedly elevated levels of circulating TNF- α in diseased animals. Secondly, coronary small artery endothelial dysfunction was also evident as relaxation responses to bradykinin were diminished, while smooth muscle cell function was preserved as responses to the exogenous NO donor SNAP were intact. Thirdly, and perhaps most importantly, ROS production paralleled by a decreased cardiac NO production was markedly increased. Specifically, the basal superoxide production was increased 3-fold in the DM+HC+HT animals as compared to controls. This increase was significantly suppressed by L-NAME as well as by VAS2870, indicating that both NOS and NADPH oxidase were the principal sources of superoxide production. Upon stimulation of NADPH oxidase, the superoxide production was markedly increased as compared to controls, confirming NADPH oxidase major source of superoxide anion. Furthermore, although increased eNOS expression and phosphorylation levels were observed in DM+HC+HT animals, the monomer/dimer ratio was increased almost 3-fold, indicating that eNOS-uncoupling accounted for the aggravated NOS-dependent superoxide production.

In addition to these functional alterations, structural vascular impairments were also present in the myocardium of DM+HC+HT animals. We observed capillary rarefaction as evidenced by lower capillary-to-fiber ratio in the diseased hearts. Capillary rarefaction has only been sparsely investigated in previous studies, but our findings are well in accordance with a recent study by Mohammed et al. who reported a reduced capillary density in the myocardium of HFpEF patients (28). This capillary rarefaction may have important clinical implications, particularly when occurring simultaneously with the observed coronary arterial endothelial dysfunction, as it will impair myocardial oxygenation especially during physical exercise (29). These microvascular alterations, at the level of both small arteries and capillaries may contribute to reduced exercise tolerance in HFpEF patients (30). The observed vascular changes were accompanied by an increase in the total collagen, which together with the increased passive stiffness of single cardiac myocytes translated into a higher LV stiffness (31, 32) as demonstrated by an increased LV end-diastolic elastance and increased E/A ratio, both clear indicators of diastolic dysfunction. Interestingly, maximal force of single cardiomyocytes was increased accompanied by a trend towards increased LV end-systolic elastance. It could be speculated that the increase in contractility acted as a compensatory mechanisms to maintain LV function particularly in the face of the elevated blood pressure in the absence of LV hypertrophy (33).

The animal model presented here is complementary to a recently reported porcine model of diastolic dysfunction (34). Thus, Schwarzl et al. produced hypertension and

hypercholesterolemia using DOCA-salt and western diet containing high amounts of salt, fat and cholesterol. An important difference between the two studies, besides the longer follow-up (6 months versus 12 weeks), was the induction of diabetes in our model. Although Schwarzl et al (34) reported several similar findings, including LV end-diastolic stiffness, increased superoxide production and eNOS uncoupling, some findings are distinctly different. Diabetes, which is a common comorbidity in HFpEF patients, likely contributed to the endothelial dysfunction and activation of NOX, which are also observed in HFpEF patients (22). Moreover, whereas concentric LV hypertrophy occurred in response to the pressure-overload in the study of Schwarzl et al. cardiomyocyte area was reduced in our model. The latter is in accordance with the concept that severe hyperglycemia induces muscle cell atrophy both in skeletal (35, 36) and cardiac muscle (37, 38). Additionally, increased LV fibrosis was documented in the present study but not in the study by Schwarzl et al., most likely because hyperglycemia in addition to inflammation is an important trigger for extracellular matrix remodeling in HFpEF (39, 40). Further, diabetes is also known to lead to vascular deficiency, mediated by miR-320 according to a recent study (41) as also documented here as capillary rarefaction. Conversely, in the study by Schwarzl et al. (34) the contribution of titin, the giant molecular “spring” that is considered as one of the most important factors responsible for cardiomyocyte passive stiffness, was comprehensively addressed. Reduced total titin phosphorylation and a shift towards its stiffer isoform N2B were reported, supporting the concept that both collagen and titin contribute to myocardial stiffness in HFpEF patients (31). Clearly, both models identified potential targets for study and treatment of the observed structural and functional alterations in the LV.

CONCLUSIONS

The present study demonstrates that in a large animal, chronic exposure to multiple common co-morbidities results in endothelium-dependent coronary artery dysfunction, capillary rarefaction, oxidative stress, and perturbed nitric oxide production, which are associated with increased myocardial fibrosis and passive cardiomyocyte stiffness, resulting in LV diastolic dysfunction. This large animal model provides an excellent translational tool for improving our understanding of the pathophysiology of heart failure with preserved ejection fraction and for testing novel therapeutic interventions, including drugs, exercise and diet interventions, for the treatment of the patients with this form of heart failure.

Supplemental data

In online Supplemental data section kidney and heart weights are reported.

Acknowledgments

The authors thank Wies Lommen (VUMC, Amsterdam), Ilona Krabbendam, Lau Blonden, Ruben van Drie (ErasmusMC, Rotterdam, The Netherlands) for their technical support. This study was supported by grants from the European Commission FP7-Health-2010 grant MEDIA-261409, the Netherlands CardioVascular Research Initiative CVON-ARENA CVON2011-11, CVON-PHAEDRA CVON2012-08, CVON-RECONNECT CVON2014-11 and The Academy of Finland 251272, Finnish Diabetes Research Foundation, and Finnish Foundation for Cardiovascular Research.

Disclosures: None

Supplemental Table 1. Kidneys and heart weights at sacrifice in Control and DM+HC+HT animals.

		Controls (N=8)	DM+HC+HT (N=10)
Body weight (kg)		102±4	79±3*
Kidneys			
Left kidney	- absolute (g)	176±12	127±7*
	- relative (g/kg)	1.69±0.09	1.64±0.10
Right kidney	- absolute (g)	173±14	132±10*
	- relative (g/kg)	1.66±0.12	1.71±0.14
Heart			
LV	- absolute (g)	231±17	184±9*
	- relative (g/kg)	2.2±0.1	2.3±0.1
RV	- absolute (g)	73±8	58±3
	- relative (g/kg)	0.68±0.08	0.74±0.02
LA	- absolute (g)	21±1	16±1*
	- relative (g/kg)	0.20±0.01	0.21±0.01
RA	- absolute (g)	14±1	13±1
	- relative (g/kg)	0.13±0.01	0.17±0.01*

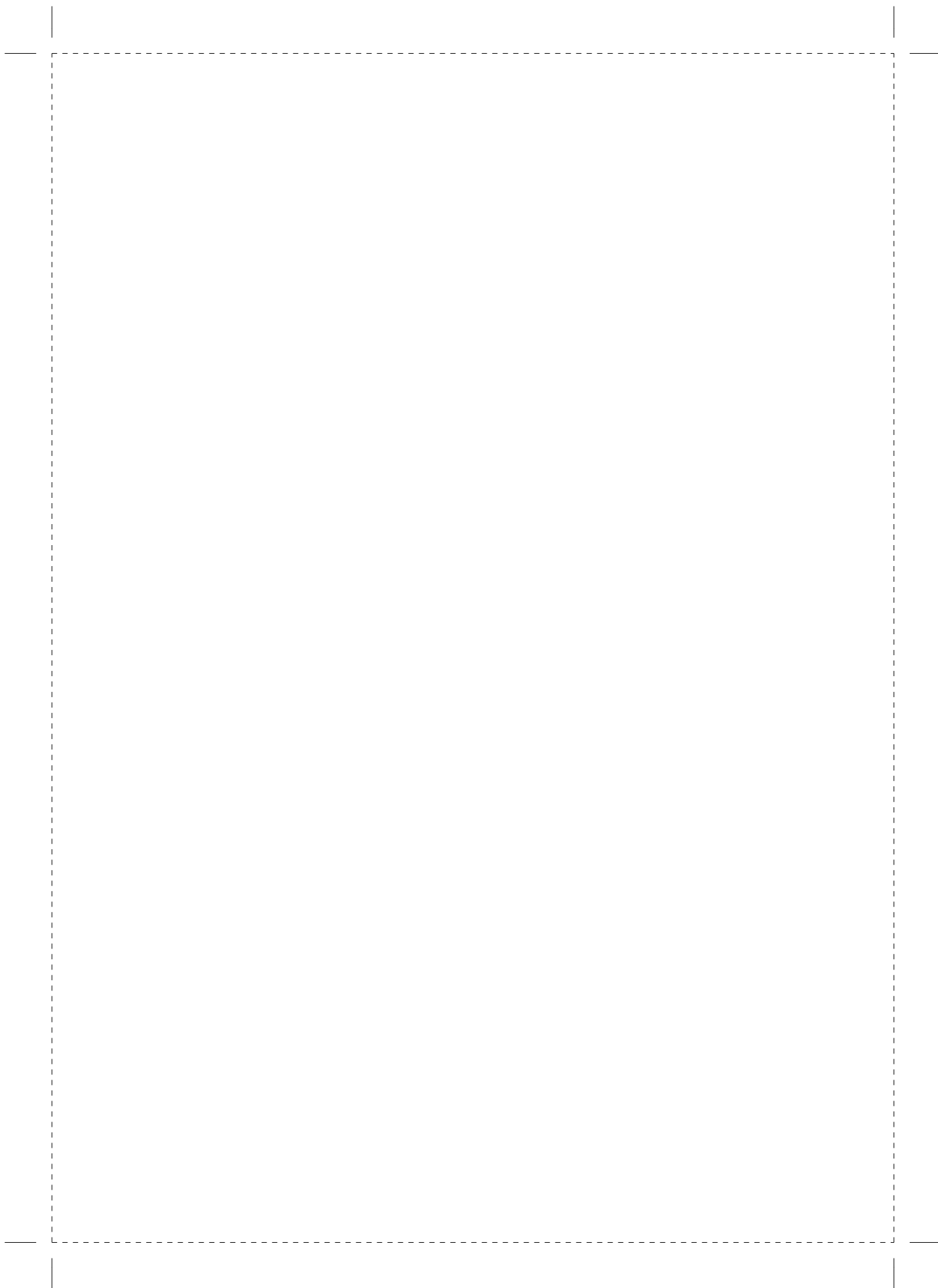
LV= left ventricle, RV= right ventricle, LA= left atrium, RA= right atrium. The data is presented as absolute value and also relative to the body weight. *P<0.05 compared to Controls.

REFERENCES

1. Dickstein K, Cohen-Solal A, Filippatos G, McMurray JJ, Ponikowski P, Poole-Wilson PA, et al. ESC Guidelines for the diagnosis and treatment of acute and chronic heart failure 2008: the Task Force for the Diagnosis and Treatment of Acute and Chronic Heart Failure 2008 of the European Society of Cardiology. Developed in collaboration with the Heart Failure Association of the ESC (HFA) and endorsed by the European Society of Intensive Care Medicine (ESICM). *European heart journal*. 2008;29(19):2388-442.
2. Borlaug BA, Paulus WJ. Heart failure with preserved ejection fraction: pathophysiology, diagnosis, and treatment. *European heart journal*. 2011;32(6):670-9.
3. Ambrosy AP, Fonarow GC, Butler J, Chioncel O, Greene SJ, Vaduganathan M, et al. The global health and economic burden of hospitalizations for heart failure: lessons learned from hospitalized heart failure registries. *Journal of the American College of Cardiology*. 2014;63(12):1123-33.
4. Butler J, Fonarow GC, Zile MR, Lam CS, Roessig L, Schelbert EB, et al. Developing therapies for heart failure with preserved ejection fraction: current state and future directions. *JACC Heart failure*. 2014;2(2):97-112.
5. Lam CS, Carson PE, Anand IS, Rector TS, Kuskowski M, Komajda M, et al. Sex differences in clinical characteristics and outcomes in elderly patients with heart failure and preserved ejection fraction: the Irbesartan in Heart Failure with Preserved Ejection Fraction (I-PRESERVE) trial. *Circulation Heart failure*. 2012;5(5):571-8.
6. Taylor AL. Heart failure in women. *Current heart failure reports*. 2015;12(2):187-95.
7. Ather S, Chan W, Bozkurt B, Aguilar D, Ramasubbu K, Zachariah AA, et al. Impact of noncardiac comorbidities on morbidity and mortality in a predominantly male population with heart failure and preserved versus reduced ejection fraction. *Journal of the American College of Cardiology*. 2012;59(11):998-1005.
8. Zile MR, Baicu CF, Gaasch WH. Diastolic heart failure - Abnormalities in active relaxation and passive stiffness of the left ventricle. *New Engl J Med*. 2004;350(19):1953-9.
9. Falcao-Pires I, Gavina C, Hamdani N, Van Der Velden J, Stienen GJM, Niessens HWM, et al. Mechanisms underlying diastolic dysfunction induced by pressure overload differ between aortic valve stenosis and hypertension. *Cardiovascular research*. 2012;93:S107-S.
10. Czuriga D, Musters RJP, Borbely A, Falcao-Pires I, Bogaards SJP, Leite-Moreira AF, et al. High diastolic stiffness modifies sarcomeric structure in failing human cardiomyocytes. *European heart journal*. 2011;32:904-5.
11. Czuriga D, Paulus WJ, Czuriga I, Edes I, Papp Z, Borbely A. Cellular Mechanisms for Diastolic Dysfunction in the Human Heart. *Curr Pharm Biotechno*. 2012;13(13):2532-8.
12. Paulus WJ, Tschope C. A Novel Paradigm for Heart Failure With Preserved Ejection Fraction Comorbidities Drive Myocardial Dysfunction and Remodeling Through Coronary Microvascular Endothelial Inflammation. *Journal of the American College of Cardiology*. 2013;62(4):263-71.
13. Owan TE, Hodge DO, Herges RM, Jacobsen SJ, Roger VL, Redfield MM. Trends in prevalence and outcome of heart failure with preserved ejection fraction. *The New England journal of medicine*. 2006;355(3):251-9.
14. Gerrity RG, Natarajan R, Nadler JL, Kimsey T. Diabetes-induced accelerated atherosclerosis in swine. *Diabetes*. 2001;50(7):1654-65.
15. Kirschbaum SW, Baks T, Gronenschild EH, Aben JP, Weustink AC, Wielopolski PA, et al. Addition of the long-axis information to short-axis contours reduces interstudy variability of left-ventricular analysis in cardiac magnetic resonance studies. *Investigative radiology*. 2008;43(1):1-6.

16. Caudron J, Fares J, Bauer F, Dacher JN. Evaluation of left ventricular diastolic function with cardiac MR imaging. *Radiographics : a review publication of the Radiological Society of North America, Inc.* 2011;31(1):239-59.
17. van Ditzhuijzen NS, Karanasos A, Bruining N, van den Heuvel M, Sorop O, Ligthart J, et al. The impact of Fourier-Domain optical coherence tomography catheter induced motion artefacts on quantitative measurements of a PLLA-based bioresorbable scaffold. *The international journal of cardiovascular imaging.* 2014;30(6):1013-26.
18. Halpern W, Mulvany MJ, Warshaw DM. Mechanical properties of smooth muscle cells in the walls of arterial resistance vessels. *The Journal of physiology.* 1978;275:85-101.
19. Kim YM, Guzik TJ, Zhang YH, Zhang MH, Kattach H, Ratnatunga C, et al. A myocardial Nox2 containing NAD(P)H oxidase contributes to oxidative stress in human atrial fibrillation. *Circulation research.* 2005;97(7):629-36.
20. Moens AL, Champion HC, Claeys MJ, Tavazzi B, Kaminski PM, Wolin MS, et al. High-dose folic acid pretreatment blunts cardiac dysfunction during ischemia coupled to maintenance of high-energy phosphates and reduces postreperfusion injury. *Circulation.* 2008;117(14):1810-9.
21. Boontje NM, Merkus D, Zaremba R, Versteilen A, de Waard MC, Mearini G, et al. Enhanced myofilament responsiveness upon beta-adrenergic stimulation in post-infarct remodeled myocardium. *Journal of molecular and cellular cardiology.* 2011;50(3):487-99.
22. Franssen C CS, Unger A, Korkmaz HI, De Keulenaer GW, Tschöpe C, Leite-Moreira AF, Musters R, Niessen HWM, Linke WA, Paulus WJ, Hamdani N. Myocardial Microvascular Inflammatory Endothelial activation in heart failure with preserved ejection fraction. *JACC Heart failure.* 2015.
23. Rauchhaus M, Doehner W, Francis DP, Davos C, Kemp M, Liebenthal C, et al. Plasma cytokine parameters and mortality in patients with chronic heart failure. *Circulation.* 2000;102(25):3060-7.
24. Deswal A, Petersen NJ, Feldman AM, Young JB, White BG, Mann DL. Cytokines and cytokine receptors in advanced heart failure: an analysis of the cytokine database from the Vesnarinone trial (VEST). *Circulation.* 2001;103(16):2055-9.
25. Alagiakrishnan K, Banach M, Jones LG, Datta S, Ahmed A, Aronow WS. Update on diastolic heart failure or heart failure with preserved ejection fraction in the older adults. *Annals of medicine.* 2013;45(1):37-50.
26. Mentz RJ, Kelly JP, von Lueder TG, Voors AA, Lam CS, Cowie MR, et al. Noncardiac comorbidities in heart failure with reduced versus preserved ejection fraction. *Journal of the American College of Cardiology.* 2014;64(21):2281-93.
27. Bhatia RS, Tu JV, Lee DS, Austin PC, Fang J, Haouzi A, et al. Outcome of heart failure with preserved ejection fraction in a population-based study. *The New England journal of medicine.* 2006;355(3):260-9.
28. Mohammed SF, Hussain S, Mirzoyev SA, Edwards WD, Maleszewski JJ, Redfield MM. Coronary microvascular rarefaction and myocardial fibrosis in heart failure with preserved ejection fraction. *Circulation.* 2015;131(6):550-9.
29. Laughlin MH, Davis MJ, Secher NH, van Lieshout JJ, Arce-Esquivel AA, Simmons GH, et al. Peripheral circulation. *Comprehensive Physiology.* 2012;2(1):321-447.
30. Borlaug BA, Melenovsky V, Russell SD, Kessler K, Pacak K, Becker LC, et al. Impaired chronotropic and vasodilator reserves limit exercise capacity in patients with heart failure and a preserved ejection fraction. *Circulation.* 2006;114(20):2138-47.
31. Zile MR, Baicu CF, Ikonomidis JS, Stroud RE, Nietert PJ, Bradshaw AD, et al. Myocardial stiffness in patients with heart failure and a preserved ejection fraction: contributions of collagen and titin. *Circulation.* 2015;131(14):1247-59.

32. Yarbrough WM, Mukherjee R, Stroud RE, Rivers WT, Oelsen JM, Dixon JA, et al. Progressive induction of left ventricular pressure overload in a large animal model elicits myocardial remodeling and a unique matrix signature. *The Journal of thoracic and cardiovascular surgery*. 2012;143(1):215-23.
33. Kawaguchi M, Hay I, Fetis B, Kass DA. Combined ventricular systolic and arterial stiffening in patients with heart failure and preserved ejection fraction: implications for systolic and diastolic reserve limitations. *Circulation*. 2003;107(5):714-20.
34. Schwarzl M, Hamdani N, Seiler S, Alogna A, Manninger M, Reilly S, et al. A porcine model of hypertensive cardiomyopathy: implications for heart failure with preserved ejection fraction. *American journal of physiology Heart and circulatory physiology*. 2015;309(9):H1407-18.
35. Hulmi JJ, Silvennoinen M, Lehti M, Kivela R, Kainulainen H. Altered REDD1, myostatin, and Akt/mTOR/FoxO/MAPK signaling in streptozotocin-induced diabetic muscle atrophy. *American journal of physiology Endocrinology and metabolism*. 2012;302(3):E307-15.
36. Jakobsen J, Reske-Nielsen E. Diffuse muscle fiber atrophy in newly diagnosed diabetes. *Clinical neuropathology*. 1986;5(2):73-7.
37. Kawaguchi M, Asakura T, Saito F, Nemoto O, Maehara K, Miyake K, et al. [Changes in diameter size and F-actin expression in the myocytes of patients with diabetes and streptozotocin-induced diabetes model rats]. *Journal of cardiology*. 1999;34(6):333-9.
38. Kawaguchi M, Techigawara M, Ishihata T, Asakura T, Saito F, Maehara K, et al. A comparison of ultrastructural changes on endomyocardial biopsy specimens obtained from patients with diabetes mellitus with and without hypertension. *Heart and vessels*. 1997;12(6):267-74.
39. Hutchinson KR, Lord CK, West TA, Stewart JA, Jr. Cardiac fibroblast-dependent extracellular matrix accumulation is associated with diastolic stiffness in type 2 diabetes. *PloS one*. 2013;8(8):e72080.
40. Zhao J, Randive R, Stewart JA. Molecular mechanisms of AGE/RAGE-mediated fibrosis in the diabetic heart. *World journal of diabetes*. 2014;5(6):860-7.
41. Wang X, Huang W, Liu G, Cai W, Millard RW, Wang Y, et al. Cardiomyocytes mediate anti-angiogenesis in type 2 diabetic rats through the exosomal transfer of miR-320 into endothelial cells. *Journal of molecular and cellular cardiology*. 2014;74:139-50.



PART 3

3.2 HUMAN STUDIES



Chapter 7

Prognostic value of microvascular obstruction and infarct size, as measured by CMR in STEMI patients.

van Kranenburg M, Magro M, Thiele H, de Waha S, Eitel I, Cochet A, Cottin Y, Atar D, Buser P, Wu E, Lee D, Bodi V, Klug G, Metzler B, Delewi R, Bernhardt P, Rottbauer W, Boersma E, Zijlstra F, van Geuns RJM.

JACC Cardiovasc Imaging. 2014 Sep;7(9):930–9.

ABSTRACT

The aim of this study was to evaluate the value of microvascular obstruction (MO) and infarct size as a percentage of left ventricular mass (IS%LV), as measured by contrast-enhanced cardiac magnetic resonance, in predicting major cardiovascular adverse events (MACE) at 2 years in patients with ST-segment elevation myocardial infarction reperfused by primary percutaneous coronary intervention. Individual data from 1,025 patients were entered into the pooled analysis. MO was associated with the occurrence of MACE, defined as a composite of cardiac death, congestive heart failure, and myocardial re-infarction (adjusted hazard ratio: 3.74; 95% confidence interval: 2.21 to 6.34). IS% LV 25% was not associated with MACE (adjusted hazard ratio: 0.90; 95% confidence interval: 0.59 to 1.37). The authors conclude that MO is an independent predictor of MACE and cardiac death, whereas IS%LV is not independently associated with MACE.

INTRODUCTION

In the setting of ST-segment elevation myocardial infarction (STEMI), primary percutaneous coronary intervention (pPCI) is the preferred reperfusion strategy and a cornerstone in the treatment of patients with STEMI (1). A substantial proportion of STEMI patients display a “no-reflow” phenomenon despite successful epicardial reperfusion (2). This phenomenon is characterized by either absent or inadequate myocardial tissue reperfusion despite successful reopening of the infarct-related artery (3). No-reflow is thought to be a consequence of microvascular obstruction (MO), caused by numerous components, including distal atherothrombotic embolization, ischemic injury, reperfusion injury, and susceptibility of the coronary microcirculation to injury (2). No-reflow can be assessed with cine coronary angiography, ST-segment resolution measured on electrocardiography, and noninvasive imaging techniques such as myocardial contrast echocardiography and contrast-enhanced cardiac magnetic resonance (CE-CMR). In patients with STEMI, the presence and magnitude of MO are visualized by CE-CMR, with accurate and reproducible measurements of left ventricular ejection fraction (LVEF) and infarct size (IS) (4). Compared with myocardial segments without MO, segments with MO are more likely to demonstrate wall thinning and are less likely to demonstrate improvement of segmental wall thickening during follow-up study (5). Moreover, MO is an important predictor of global functional recovery after STEMI (6). Several studies suggest that MO is associated with worse prognosis (7-13). However, previous studies in this regard have been hampered by a limited number of patients, evaluated a combined clinical endpoint, and were single-center studies. Furthermore, although intuitively IS measured within 2 weeks after STEMI is an important independent determinant of outcome, there is conflicting evidence to support its independent predictive value for major adverse cardiac events (MACE) (9, 12, 14).

We performed a meta-analysis of individual patient data to evaluate the hypotheses that MO and IS expressed as a percentage of left ventricular (LV) mass (IS%LV) are independent predictors of MACE and cardiac death in patients with STEMI undergoing pPCI.

METHODS

Study Selection

The MEDLINE database was searched for citations of in-human studies published in English from January 2004 to April 2012, using the following terms: microcirculation(MESH), magnetic resonance imaging, myocardial infarction, and microvascular obstruction. A total of 134 publications were identified. Related studies from the reference Lower Late Angioplasty Complications) risk score (15), the Zwolle primary PCI index(16), and the

Thrombolysis in Myocardial Infarction (TIMI) risk score(17); baseline CE-CMR variables; and clinical outcomes (MACE) were mentioned before- hand in a protocol, along with study rationale and study design. The protocol was sent to participating centers. Previous approval of the individual study design by a local ethics committee was necessary for participation. Datasets from participating centers were merged by the coordinating center (Erasmus Medical Center, Rotterdam, the Netherlands). Queries were sent to the primary investigators in cases in which further data and clarification were needed.

Definitions/ce-cmr.

STEMI was defined on the basis of the definitions used by the authors of the primary publications (8–13) (18, 19). All clinical and angiographic variables were study based. Angiographic left main coronary artery lesions were categorized as left anterior descending artery lesions. Imaging was performed in different centers on 1.5-T scanners from different vendors (Online Table 1). The scanning protocols, CE-CMR parameters, and data analysis have been described in the included studies (8–13,18,19). All investigators but one used a steady-state, free-precession sequence for cine CMR (Online Table 1). LV end-diastolic volume, LV end- systolic volume, and LVEF were short-axis based, as provided by the investigators. If LV end-diastolic and end-systolic volume were not indexed, the Mosteller equation was used to adjust these for body surface area. Late gadolinium enhancement was performed by the different centers by use of a (phase-sensitive) inversion recovery gradient echo sequence. MO, as visualized with late gadolinium enhancement, was defined as any region of hypo- enhancement within the hyperenhanced area. IS was determined on short-axis images. IS was expressed both in grams and as a percentage of the LV mass (IS% LV). IS%LV was determined by manual or automated tracing of the infarct border. In patients with MO, regions of hypoenhancement were included in the IS. In 2 studies, patients with prior infarction were included (8,12). In patients with prior myocardial infarction, only the region indicative of acute infarction (8), corresponding with edema in T2-weighted imaging (12), was measured in delayed-enhancement images.

Endpoints.

The primary endpoint was the prevalence of major adverse cardiovascular events (MACE), defined as a composite of cardiac death, myocardial re-infarction, and new congestive heart failure, at 2 years. The secondary endpoint was cardiac mortality. Congestive heart failure was defined as any symptom of cardiac decompensation requiring hospitalization. The individual study investigators provided previously defined and used events (Online Table 1). If a patient experienced more than one event, the first event was chosen for the combined clinical endpoint. Patients were considered at risk from the time of admission for the treatment of STEMI.

Statistical Analysis.

Continuous data with normal distribution are presented as mean \pm SD. Non-normally distributed variables are reported as median with corresponding interquartile range (IQR). Categorical variables are represented by frequencies and percentages. Patients were categorized according to the presence of MACE. Differences in continuous variables between categories of patients were studied by the unpaired Student *t* test or the Mann-Whitney *U* test (in cases of non-normal distribution). Proportions were compared using the chi-square test or the Fisher exact test, where applicable. The incidences of the primary and secondary endpoints are reported as Kaplan-Meier estimates at a follow-up of 2 years. As small infarcts and minor decreases in LVEF might not have an impact on outcome, the relationship between these variables on outcome was investigated by plotting IS%LV and LVEF against event-free survival. A log-rank test was used to evaluate differences in freedom from study endpoints between categories of patients. Univariate and multivariate Cox regression analyses, stratified by study, were used to determine the prognostic value of MO, IS%LV, and LVEF with respect to the primary and secondary endpoints. Predictors of cardiac death and MACE in published reports—namely, age (>65 years); sex (female); the presence of diabetes, hypertension, anterior myocardial infarction (culprit lesion in the left anterior descending artery), or multivessel disease; TIMI flow grade after PCI (reference: TIMI flow grade after PCI of 0 or 1); and CMR-based LVEF (12,16,17)—were entered into the univariate regression model, along with MO, IS%LV, LV end-diastolic volume index, and LV end-systolic volume index (9). Variables that resulted in a *p* value of <0.10 in the univariate Cox model were entered into the multivariate Cox proportional hazards model, with respect to multicollinearity. LV end-systolic volume index was not entered into the multivariate model due to a collinear relation with LVEF (Pearson correlation: -0.774). We applied the method of backward selection; all variables with a *p* value of <0.05 remained. The proportional hazards assumption was validated graphically. In cases of missing data (the requested variable data were unavailable in >5.0% of the cohort), these variables were not taken into account in the regression analysis (e.g., time to reperfusion and Killip class). We report unadjusted hazard ratios (HRs) and adjusted hazard ratios (aHRs), 95% confidence intervals (CIs), and *p* values. We determined the *c*-index (20) to report on the performance of the models to discriminate between patients with and without the study endpoints. The incremental value of IS%LV, LVEF, and MO was compared with that from a model with established clinical variables. *c*-Index models were developed on the basis of multivariate Cox models. We applied, for these models, a backward variable-selection method; all variables with a *p* value of <0.05 remained. Two-sided probability values with an α level of ≤ 0.05 were considered to be statistically significant. Statistical analysis was performed using the statistical packages IBM SPSS Statistics version 20.0.01 (IBM SPSS Statistics, IBM Corporation, Armonk, New York) and SAS version 9.2 (SAS Institute Inc., Cary, North Carolina). Kaplan-Meier curves were drawn with GraphPad Prism version 4.00 (GraphPad Software Inc., San Diego, California).

Table 1. Patient Characteristics

	Entire Cohort (n = 1025)	MACE (n = 130)	No MACE (n = 895)	P Value
Demographics				
Age, yrs	59.7 ± 12.7	61.8 ± 13.3	59.4 ± 12.6	0.04
Male	796 (77.7)	94 (72.3)	702 (78.4)	0.12
BMI, kg/m ² *	27.0 ± 3.8	27.2 ± 4.1	27.0 ± 3.7	0.60
CV risk factors				
Hypertension	530/1,012 (52.4)	70/128 (54.7)	460/884 (52.0)	0.58
Hypercholesterolemia	380/1,010 (37.6)	57/128 (44.5)	323/882 (36.6)	0.08
Current or prior smoking	507/1,203 (49.6)	54/130 (41.5)	455/893 (51.0)	0.02
Family history of MI [†]	278/937 (29.7)	37/121 (30.6)	241/816 (29.5)	0.81
Diabetes	176/1,012 (17.4)	35/128 (27.3)	141/884 (16.0)	<0.001
Prior MI [‡]	47/948 (5.0)	12/123 (9.8)	35/825 (4.2)	0.009
Prior CABG [§]	10/947 (1.1)	2/123 (1.6)	8/824 (1.0)	0.51
Angiographic variables				
Time to reperfusion	3.3 (2.1-4.9)	3.5 (2.1-4.9)	3.2 (2.1-4.9)	0.57
Infarct-related artery				
LAD	514/1,023 (50.2)	73/128 (57.0)	441/895 (49.3)	0.10
RCA	413/1,023 (40.4)	43/128 (33.6)	370/895 (49.3)	0.10
LCA	96/1,023 (9.4)	12/128 (9.4)	84/895 (9.4)	0.99
N-vessel disease				
1	563/1,004 (56.1)	53/126 (42.1)	510/878 (58.1)	<0.001
2	280/1,004 (27.9)	39/126 (31.0)	241/878 (27.4)	0.41
3	161/1,004 (16.0)	34/126 (27.0)	127/878 (14.5)	<0.001
Multivessel disease	441/1,013 (43.5)	73/127 (57.5)	368/886 (41.5)	<0.001
TIMI flow grade after PCI				
0	14/1,019 (1.4)	6/129 (4.7)	8/890 (0.9)	<0.001
1	14/1,019 (1.4)	5/129 (3.9)	9/890 (1.0)	0.009
2	64/1,019 (6.3)	9/129 (7.0)	55/890 (6.2)	0.73
3	927/1,019 (91.0)	109/129 (84.5)	818/890 (91.9)	0.006
Enzymatic IS				
Maximal CK	2,161 (1,040-4,160)	2,729 (1,169-6,024)	2,109 (1,031-3,913)	0.04
CE-CMR variables				
Time from MI to CE-CMR, days [¶]	4 (2-6)	4 (2-6)	4 (2-6)	0.57
Presence of MO	577 (56.3)	109 (83.8)	468 (52.3)	<0.001
IS, %LV	18.5 (9.2-28.3)	24.9 (14.4-37.4)	18.0 (8.9-26.7)	<0.001
IS, g	22.3 (10.8-37.4)	33.7 (15.3-54.1)	21.0 (10.2-34.7)	<0.001
LVEF, %	48.0 ± 12.3	41.4 ± 13.3	48.9 ± 11.9	<0.001
LVESV, ml	80.5 ± 35.7	94.7 ± 42.0	78.4 ± 34.2	<0.001
LVESV index, ml/m ²	41.3 ± 17.2	48.4 ± 19.6	40.3 ± 16.6	<0.001

Table 1. Patient Characteristics (continued)

	Entire Cohort (n = 1025)	MACE (n = 130)	No MACE (n = 895)	P Value
LVEDV, ml	150.5 ± 42.4	156.3 ± 45.3	149.6 ± 41.9	0.09
LVEDV index, ml/m ²	77.4 ± 19.6	80.5 ± 20.9	77.0 ± 19.4	0.05

Values are mean ± SD, n/N (%), or median (IQR). Data missing in the following number of cases: *124 (12.1%), †88 (8.6%), ‡77 (7.5%), §78 (7.6%), |||278 (27.1%), and ¶446 (43.5%) (reperfusion within 12 h). Data missing in > 7.5% of the cohort.

BMI = body mass index; CABG = coronary artery bypass grafting; CE-CMR = contrast-enhanced cardiac magnetic resonance; CK = creatine kinase; CV = cardiovascular; IQR = interquartile range; IS = infarct size; LAD = left anterior descending; LCA = left circumflex artery; %LV = percentage of LV mass; LVEDV = left ventricular end-diastolic volume; LVEF = left ventricular ejection fraction; LVESV = left ventricular end-systolic volume; MI = myocardial infarction; MO = microvascular obstruction; PCI = percutaneous intervention; RCA = right coronary artery; TIMI = Thrombolysis in Myocardial Infarction.

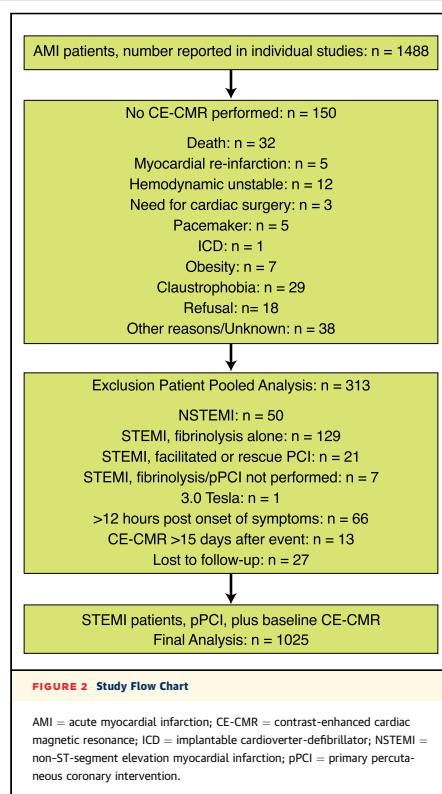
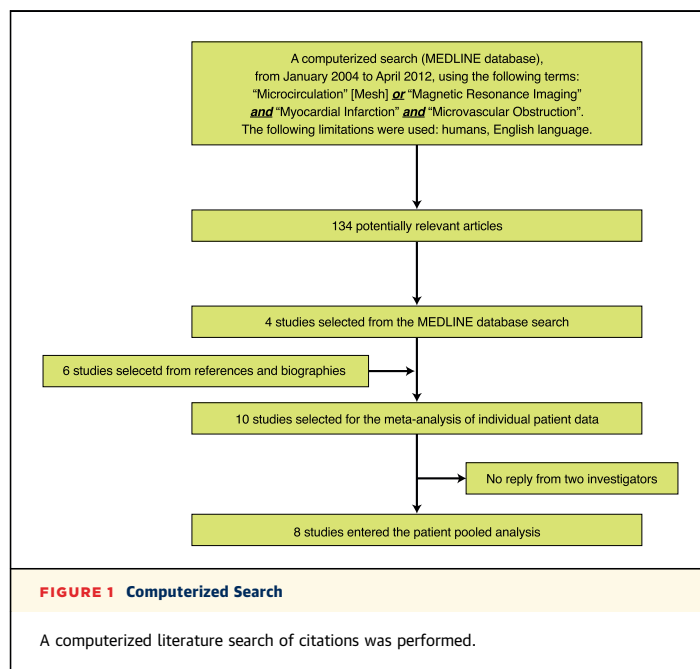
RESULTS

Patient Characteristics.

We identified 10 eligible observational and experimental studies. The principal investigators of these studies were invited to participate in this collaborative analysis. Eight of 10 investigators provided individual patient data (Figure 1). In this pooled analysis, 2 studies with 193 potentially eligible patients were not included due to investigator unresponsiveness (14) (21). The individual study characteristics are summarized in Online Table 1. The inclusion procedure is shown in Figure 2. Of 1,488 AMI patients, 150 patients (10.1%) were unable to have a CMR examination, and 313 patients were excluded due to other reasons (Figure 2). Consequently, data from 1,025 STEMI patients who underwent reperfusion by pPCI between April 9, 1999 and September 28, 2008 were included in the patient pooled analysis. The mean age at inclusion was 59.7 ± 12.7 years, and 77.7% of the cohort were men (n = 796). The median time to reperfusion was 3.3 h (IQR: 2.1 to 4.9 h). CE-CMR was performed within a median of 4 days (IQR: 2 to 6 days) after the occurrence of STEMI. MO was present in 56.3% of patients in the overall cohort. Of patients with TIMI flow grade after PCI of 3 (927 of 1,019 [91.0%]), MO was present in 54.9%. The mean LVEF was 48.0 ± 12.3%. Of the entire cohort, 14.7% had a severely depressed (<35%) LVEF. The baseline characteristics of patients with MACE and patients without MACE are compared in Table 1. The median duration of available follow-up was 12 months (IQR: 4 to 21 months).

Predictors Of Mace.

The composite endpoint occurred in 130 patients within 2 years of follow-up. In 9 patients, an event occurred between the index event and the CE-CMR study. Cardiac death occurred in 25 patients; myocardial re-infarction, in 47 patients; and congestive heart



failure, in 58 patients. The Kaplan-Meier estimate of freedom from MACE at 2 years was 76.5% in patients with MO versus 93.0% in patients without MO ($p < 0.001$). For both LVEF and IS%LV, nonlinear relationships were observed (Figures 3 and 4). Therefore, these 2 variables were categorized using tertiles, which provides a large number of events per category while respecting nonlinearity. For LVEF, the first tertile (cutoff: 42.7%, simplified to $\leq 40\%$, used in the CADILLAC risk score [15]) was compared to the reference group (LVEF $> 40\%$). For IS%LV, the last tertile (cutoff: 24.7%, simplified to $\geq 25\%$) was compared to the reference group (IS%LV $< 25\%$). The Kaplan-Meier estimate of freedom from MACE at 2 years was 74.3% in patients with IS%LV $> 25\%$ versus 87.4% in patients with IS%LV $< 25\%$ ($p < 0.001$). Kaplan-Meier curves for MACE by MO and IS%LV in the entire cohort, and grouped by MO and IS%LV, are depicted in Figures 5 to 7. The Kaplan-Meier estimate of freedom from MACE was 71.3% in patients with IS%LV $> 25\%$ with MO versus 94.9% in patients with IS%LV $< 25\%$ without MO ($p < 0.001$). Univariate Cox regression is summarized in Table 2. MO (HR: 4.68; 95% CI: 2.86 to 7.66), IS%LV $\geq 25\%$ (HR: 2.04; 95% CI: 1.42 to 2.92), and LVEF $\leq 40\%$ (HR: 3.45; 95% CI: 2.40 to 4.97) were associated with MACE on univariate Cox regression analysis. Sex (HR: 1.34; 95% CI: 0.89 to 2.00) and anterior myocardial infarction (HR: 1.30; 95% CI: 0.90 to 1.87) were not associated with MACE on univariate Cox regression analysis. Multivariate Cox regression is summarized in Table 3. MO (aHR: 3.74; 95% CI: 2.21 to 6.34) and LVEF $\leq 40\%$ (aHR: 2.30; 95% CI: 1.48 to 3.58)

Table 2. Association of patient characteristics with MACE at 2 years univariate Cox regression analysis

	HR	95% CI	p Value
Demographics			
Age	1.60	1.11-2.31	0.01
Sex	1.34	0.89-2.00	0.16
CV risk factors			
Diabetes	1.66	1.09-2.53	0.02
Hypertension	0.97	0.67-1.42	0.89
Anterior MI	1.30	0.90-1.87	0.16
Angiographic variables			
Multivessel disease	1.65	1.13-2.40	0.009
TIMI flow grade after PCI	3.31	1.70-6.43	< 0.001
CE-CMR variables			
Presence of MO	4.68	2.86-7.66	< 0.001
IS%LV	2.04	1.42-2.92	< 0.001
LVEF	3.45	2.40-4.97	< 0.001
LVESV index	1.03	1.02-1.04	< 0.001
LVEDV index	1.02	1.01-1.02	< 0.001

CI = confidence interval; HR = hazard ratio; MACE = major cardiovascular events; other abbreviations as in Table 1.

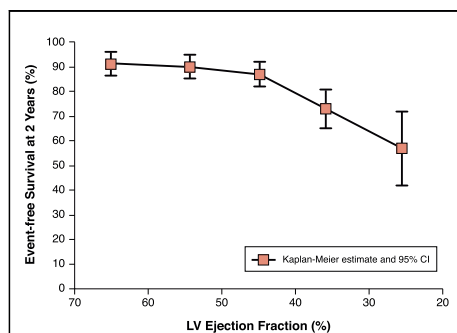


FIGURE 3 Relationship Between LV Ejection Fraction and Event-Free Survival

Values are Kaplan-Meier estimates (95% confidence interval), by LV ejection fraction category (>60%, 50% to ≤60%, 40% to ≤50%, 30% to ≤40%, or <30%). LV = left ventricular.

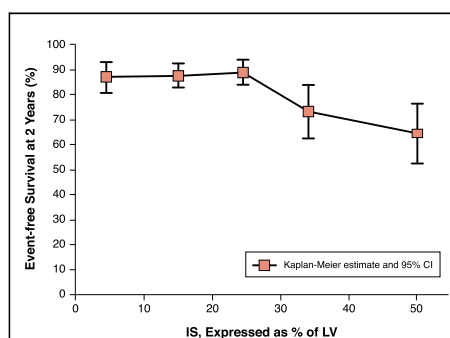


FIGURE 4 Relationship Between IS%LV and Event-Free Survival

Values are Kaplan-Meier estimates (95% confidence interval), by IS%LV category (0 to ≤10%, 10% to ≤20%, 20% to ≤30%, 30 to ≤40%, or >40%). IS%LV = infarct size expressed as a percentage of left ventricular mass.

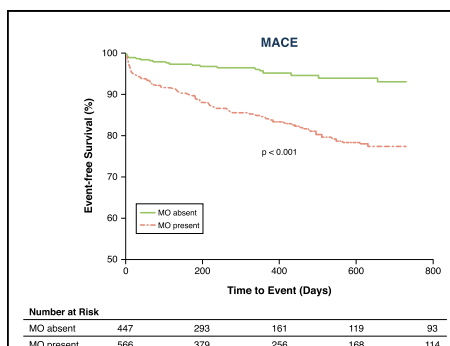


FIGURE 5 Relationship Between MO and Event-Free Survival

Values are Kaplan-Meier estimates in patients with microvascular obstruction (MO) versus patients without MO, indicating the time to major adverse cardiovascular events (MACE), follow-up 2 years.

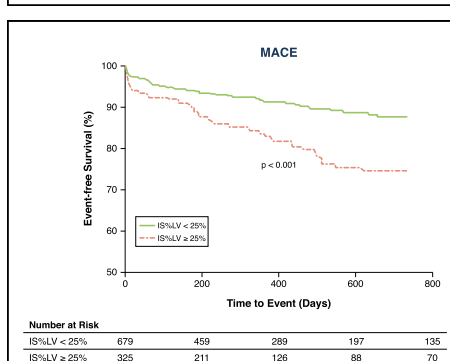


FIGURE 6 Relationship Between IS%LV and Event-Free Survival

Values are Kaplan-Meier estimates in patients with IS%LV ≥25% versus <25%, indicating the time to MACE, follow-up 2 years. Abbreviations as in Figures 4 and 5.

were associated with MACE, whereas IS%LV ≥25% and diabetes were not independently associated with MACE (model I). After the application of the backward variable-selection method, five variables (age, multi-vessel disease, TIMI flow grade after PCI, MO, and LVEF ≤40%) remained significant (model II). In a separate analysis, IS%LV, unadjusted for MO and LVEF, but adjusted for age, multivessel disease, and TIMI flow grade after PCI, was associated with the occurrence of MACE (aHR: 1.82; 95% CI: 1.26 to 2.63) (data not shown). The addition of IS%LV ≥25% to a model with age, multivessel disease, and TIMI flow grade after PCI (model a) resulted in an increase of the c-index from 0.59 to 0.61 (model b) in the prediction of MACE. The addition of LVEF ≤40% resulted in an increase from 0.59 to 0.66 (model c), with a further increase to 0.70 (model e) when MO was added (Table 4).

Predictors Of Cardiac Death.

The Kaplan- Meier estimate of freedom from cardiac death at 2 years was 96.7% (MO vs. no MO: 99.8% vs. 94.6%; $p < 0.001$). The Kaplan-Meier estimate of freedom from cardiac death at 2 years was 95.2% in patients with IS%LV $\geq 25\%$ versus 97.3% in patients with IS%LV $< 25\%$ ($p < 0.21$) (data not shown). Univariate Cox regression is summarized in Table 5. MO (HR: 15.02; 95% CI: 2.01 to 112.24) and LVEF $\leq 0\%$ (HR: 2.26; 95% CI: 1.01 to 5.05) were associated with cardiac death on univariate Cox regression analysis. IS%LV $\geq 25\%$ was not associated with cardiac death in a univariate Cox model (HR: 1.77; 95% CI: 0.80 to 3.89). Independent predictors on multivariate Cox regression and their respective aHRs for cardiac death at 2 years are summarized in Table 6. MO was associated with the occurrence of cardiac death (aHR: 13.22; 95% CI: 1.75 to 99.82) when adjusted for age (aHR: 2.21; 95% CI: 0.96 to 5.06) and LVEF $\leq 40\%$ (aHR: 1.66; 95% CI: 0.74 to 3.75).

Table 3. Association of patient characteristics with MACE at 2 years multivariate Cox regression analysis

	aHR	95% CI	p Value
Model I*			
Age	1.54	1.04-2.27	0.03
Diabetes	1.25	0.80-1.94	0.33
Multivessel disease	1.56	1.07-2.28	0.02
TIMI flow grade after PCI	2.11	1.04-4.27	0.04
Presence of MO	3.74	2.21-6.34	<0.001
IS%LV $\geq 25\%$	0.90	0.59-1.37	0.63
LVEF $\leq 40\%$	2.30	1.48-3.58	<0.001
LVEDV index	1.00	0.99-1.01	0.58
Model II ‡			
Age	1.58	1.08-2.30	0.02
Multivessel disease	1.56	1.08-2.27	0.02
TIMI flow grade after PCI	2.25	1.14-4.45	0.02
Presence of MO	3.72	2.22-6.25	<0.001
LVEF $\leq 40\%$	2.40	1.63-3.53	<0.001

*Before backward variable selection in 970 patients, 118 events. ‡ Backward variable selection in 984 patients, 118 events.

aHR = adjusted hazard ratios; other abbreviations as in Tables 1 and 2.

Table 4. Incremental value of MO, IS%LV, and LVEF $\leq 40\%$, in the prediction of MACE at 2 years

Model a: age + multivessel disease + TIMI flow grade after PCI	0.59
Model b: age + multivessel disease + TIMI flow grade after PCI + IS%LV $\geq 25\%$	0.61
Model c: age + multivessel disease + TIMI flow grade after PCI + LVEF $\leq 40\%$	0.66
Model d: age + multivessel disease + TIMI flow grade after PCI + LVEF $\leq 40\%$ + IS%LV $\geq 25\%$	0.66
Model e: age + multivessel disease + TIMI flow grade after PCI + LVEF $\leq 40\%$ + MO	0.70

Abbreviations as in Tables 1 and 2.

Table 5. Association of Patient Characteristics With Cardiac Death at 2 Years: Univariate Cox Regression Analysis

	HR	95% CI	p Value
Demographics			
Age	2.18	0.95-5.01	0.07
Sex	1.33	0.50-3.54	0.57
CV risk factors			
Diabetes	2.25	0.96-5.25	0.06
Hypertension	1.05	0.44-2.49	0.91
Anterior MI	1.41	0.64-3.10	0.40
Angiographic variables			
Multivessel disease	0.78	0.35-1.76	0.55
TIMI flow grade after PCI	2.51		0.22
CE-CMR variables			
Presence of MO	15.02	2.01-112.24	0.01
IS%LV \geq 25%	1.77	0.80-3.89	0.16
LVEF \leq 40%	2.26	1.01-5.05	0.05
LVESV index	1.01	0.99-1.04	0.22
LVEDV index	1.00	0.98-1.02	0.91

Abbreviations as in Tables 1 and 2.

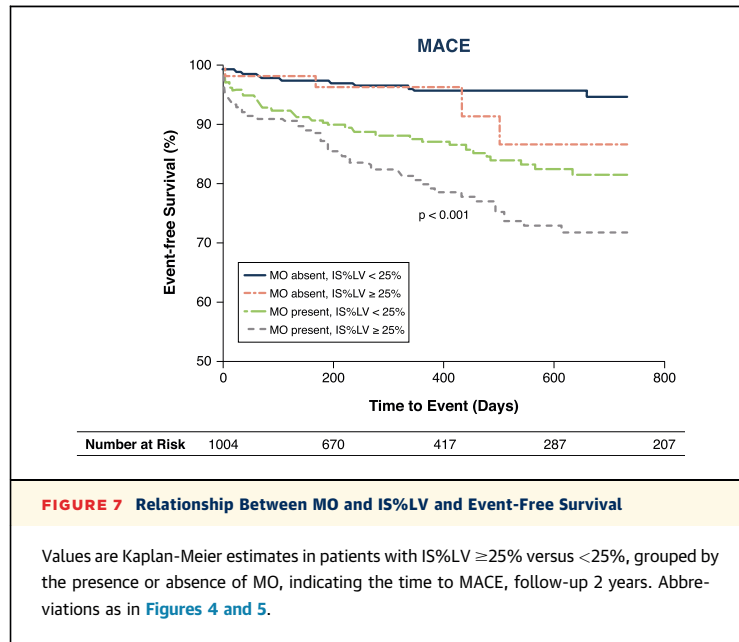
Table 6. Association of Age, MO, and LVEF \leq 40% With Cardiac Death at 2 Years: Multivariate Cox Regression Analysis

	aHR	95% CI	p Value
Age	2.21	0.96 – 5.06	0.06
Presence of MO	13.22	1.75 – 99.82	0.01
LVEF \leq 40%	1.66	0.74 – 3.75	0.22

N = 760 patients, 25 events. Abbreviations as in Tables 1, 2, and 3.

DISCUSSION

The main findings of this study were that: 1) MO was present in >50% of patients with STEMI reperfused by pPCI (even in patients with TIMI flow grade post pPCI of 3, MO was present in >50% of patients); 2) MO, IS%LV, and LVEF were predictors for MACE, with value added to clinical risk factors; 3) MO was associated with cardiac death when adjusted for age and LVEF; and 4) IS%LV, adjusted for MO and LVEF, was not an independent predictor of MACE or cardiac death. Previous studies that evaluated the prognostic value of MO, IS%LV, and LVEF in STEMI patients were limited by the inclusion of relatively small study sample sizes; evaluated composite clinical endpoints with “soft” components, including revascularization or angina; and were single-center studies (7–13). In the present inter-



nationally representative patient pooled analysis, we were able to assess the impact of CE-CMR variables on more clinically relevant events. With a sample size of 1,025 patients, the statistical power of the present pooled analysis was increased compared with that of previous single-center studies, which led to more robust predictions.

Our finding that the value of IS%LV, measured within 14 days after STEMI, is secondary to those of MO and LVEF is remarkable. It is important to realize that IS%LV is correlated with LVEF; however, LVEF is affected by additional factors, such as previous cardiovascular conditions, which might explain the importance of LVEF as a predictor of MACE in the present study. However, the univariate association of IS with MACE, its correlation with LVEF, and its contribution to the model as shown by an improvement in the c-index suggest that IS%LV is an attractive option as an endpoint in studies investigating new treatments. The measurement of LVEF is influenced by the presence of stunned myocardium, the relevance of which remains a topic of research, because most CMR studies are performed 4 to 7 days after STEMI, when stunning may be only partially resolved. The finding that MO was, in addition to IS%LV and LVEF, an independent predictor of MACE is in concordance with findings from previous single-center studies. In the largest study to date, by de Waha et al. (12), IS adjusted for TIMI risk score, MO, and LVEF was not an independent predictor of adverse outcomes. We draw the same conclusion in the present study, in which IS%LV and LVEF were analyzed as continuous variables. The cause of the detrimental effect of MO remains speculative. Baks et al. (5) demonstrated that the presence of MO in dysfunctional myocardial segments was associated with significantly

greater thinning of the myocardium compared with that in segments without MO at follow-up. In contrast to segments without MO, segments with MO demonstrated no improvement in segmental wall thickening in a follow-up study at 5 months. Nijveldt et al. (6) found that a significant proportion of patients with MO developed a significant increase in LV end-diastolic volume, with no improvement in LVEF, whereas patients without MO showed a significant improvement in LVEF, at 4 months of follow-up. Both of those studies suggest an important relation between MO and LV remodeling that potentially might result in heart failure used as a MACE, as in the present study. In addition to having predictive value for congestive heart failure, MO seems to be an important predictor of cardiac death. Reasons for cardiac death in patients with MO have been demonstrated by Ito et al. (22). Patients with no-reflow more often had malignant arrhythmias, cardiac tamponade, and early congestive heart failure compared with patients without no-reflow. An explanation of those findings might have been the reduced end-diastolic wall thickness in MO-positive segments, which might result in an increase in wall stress in the affected and adjacent segments (5). The findings from the present study demonstrate, in a large cohort, the prognostic value of MO in patients who sustained a STEMI. MO was present in >50% of the study population, even, importantly, in a large subgroup of patients with angiographic TIMI flow grade after PCI of 3. These findings suggest that pPCI is not optimal yet and that there is a need for future novel treatment strategies. Of the current variables, MO is still the best predictor and probably indicates which patients should be investigated further. Screening for arrhythmias and progressive dilation, with follow-up echocardiography or CE-CMR, could potentially identify a high risk for cardiac death. The findings of this study are relevant in CMR trial design for the evaluation of the effects of, for example, thrombectomy devices, vasodilators, coronary post-conditioning, cell therapy, and glycoprotein IIb/IIIa inhibitors (23) in patients with STEMI. It is advisable to use, in addition to the measurement of LVEF and IS%LV, MO as surrogate endpoint in CMR trials in STEMI patients as MO and IS%LV might be variables that represent separate pathophysiological processes.

STUDY LIMITATIONS.

The results of our study should be viewed in light of limitations inherent to the design of meta-analyses of individual patient data. These limitations include publication bias, data-availability bias, unmeasured heterogeneity in the patients included, and the use of event adjudication by different clinical events committees (24). CE-CMR was performed at a wide range of days (up to 14) after STEMI, at different time points after contrast injection, and with different concentrations of gadolinium-based contrast agents (25). These variations may have influenced the detection of MO and may have influenced the

measurement of IS (26). CE-CMR analysis was conducted in different ways, which also might have influenced the measurements of IS and MO. In this analysis, we evaluated the prognostic value of MO only, without investigation of the extent of MO. A previous study (12) showed that the extent of MO provided incremental prognostic information. Unfortunately, this variable was available in only one study and therefore could not be included in the pooled analysis. In cases of missing data, variables that may have influenced the primary endpoint (e.g., extent of MO, myocardial salvage (27), and the presence of a hypo- intense infarct core (28)) were not taken into account. Due to a low cardiac death rate, we were not able to add more variables in the multivariate Cox regression analysis.

CONCLUSIONS

MO is an independent predictor of the occurrence of MACE and cardiac death at 2 years in patients with STEMI. IS%LV is not independently associated with the occurrence of MACE, but might be used, in addition to MO and LVEF, as a surrogate endpoint in clinical trials investigating new treatment options.

SUPPLEMENTAL

Editorial

Meta-analysis of MACE in MI: What's the MO?* Nathaniel Reichel

JACC Cardiovasc Imaging. 2014 Sep; 7(9):953-5.

<http://www.sciencedirect.com/science/article/pii/S1936878X14005397>

REFERENCES

1. Task Force on the management of ST-segment elevation myocardial infarction, Steg PG, James SK, Atar D, Badano LP, Blomstrom-Lundqvist C, et al. ESC Guidelines for the management of acute myocardial infarction in patients presenting with ST-segment elevation. *European heart journal*. 2012;33(20):2569-619.
2. Niccoli G, Burzotta F, Galiuto L, Crea F. Myocardial no-reflow in humans. *Journal of the American College of Cardiology*. 2009;54(4):281-92.
3. Kloner RA, Ganote CE, Jennings RB. The "no-reflow" phenomenon after temporary coronary occlusion in the dog. *The Journal of clinical investigation*. 1974;54(6):1496-508.
4. Thiele H, Kappl MJ, Conradi S, Niebauer J, Hambrecht R, Schuler G. Reproducibility of chronic and acute infarct size measurement by delayed enhancement-magnetic resonance imaging. *Journal of the American College of Cardiology*. 2006;47(8):1641-5.
5. Baks T, van Geuns RJ, Biagini E, Wielopolski P, Mollet NR, Cademartiri F, et al. Effects of primary angioplasty for acute myocardial infarction on early and late infarct size and left ventricular wall characteristics. *Journal of the American College of Cardiology*. 2006;47(1):40-4.
6. Nijveldt R, Beek AM, Hirsch A, Stoel MG, Hofman MB, Umans VA, et al. Functional recovery after acute myocardial infarction: comparison between angiography, electrocardiography, and cardiovascular magnetic resonance measures of microvascular injury. *Journal of the American College of Cardiology*. 2008;52(3):181-9.
7. Wu KC, Zerhouni EA, Judd RM, Lugo-Olivieri CH, Barouch LA, Schulman SP, et al. Prognostic significance of microvascular obstruction by magnetic resonance imaging in patients with acute myocardial infarction. *Circulation*. 1998;97(8):765-72.
8. Hombach V, Grebe O, Merkle N, Waldenmaier S, Hoher M, Kochs M, et al. Sequelae of acute myocardial infarction regarding cardiac structure and function and their prognostic significance as assessed by magnetic resonance imaging. *European heart journal*. 2005;26(6):549-57.
9. Wu E, Ortiz JT, Tejedor P, Lee DC, Bucciarelli-Ducci C, Kansal P, et al. Infarct size by contrast enhanced cardiac magnetic resonance is a stronger predictor of outcomes than left ventricular ejection fraction or end-systolic volume index: prospective cohort study. *Heart*. 2008;94(6):730-6.
10. Bodi V, Sanchis J, Nunez J, Mainar L, Lopez-Lereu MP, Monmeneu JV, et al. Prognostic value of a comprehensive cardiac magnetic resonance assessment soon after a first ST-segment elevation myocardial infarction. *JACC Cardiovascular imaging*. 2009;2(7):835-42.
11. Cochet AA, Lorgis L, Lalande A, Zeller M, Beer JC, Walker PM, et al. Major prognostic impact of persistent microvascular obstruction as assessed by contrast-enhanced cardiac magnetic resonance in reperfused acute myocardial infarction. *European radiology*. 2009;19(9):2117-26.
12. de Waha S, Desch S, Eitel I, Fuernau G, Zachrau J, Leuschner A, et al. Impact of early vs. late microvascular obstruction assessed by magnetic resonance imaging on long-term outcome after ST-elevation myocardial infarction: a comparison with traditional prognostic markers. *European heart journal*. 2010;31(21):2660-8.
13. Klug G, Mayr A, Schenk S, Esterhammer R, Schocke M, Nocker M, et al. Prognostic value at 5 years of microvascular obstruction after acute myocardial infarction assessed by cardiovascular magnetic resonance. *Journal of cardiovascular magnetic resonance : official journal of the Society for Cardiovascular Magnetic Resonance*. 2012;14:46.
14. Larose E, Rodes-Cabau J, Pibarot P, Rinfret S, Proulx G, Nguyen CM, et al. Predicting late myocardial recovery and outcomes in the early hours of ST-segment elevation myocardial infarction traditional measures compared with microvascular obstruction, salvaged myocardium, and necrosis characteristics by cardiovascular magnetic resonance. *Journal of the American College of Cardiology*. 2010;55(22):2459-69.

15. Halkin A, Singh M, Nikolsky E, Grines CL, Tchong JE, Garcia E, et al. Prediction of mortality after primary percutaneous coronary intervention for acute myocardial infarction: the CADILLAC risk score. *Journal of the American College of Cardiology*. 2005;45(9):1397-405.
16. De Luca G, Suryapranata H, van 't Hof AW, de Boer MJ, Hoorntje JC, Dambrink JH, et al. Prognostic assessment of patients with acute myocardial infarction treated with primary angioplasty: implications for early discharge. *Circulation*. 2004;109(22):2737-43.
17. Morrow DA, Antman EM, Charlesworth A, Cairns R, Murphy SA, de Lemos JA, et al. TIMI risk score for ST-elevation myocardial infarction: A convenient, bedside, clinical score for risk assessment at presentation: An intravenous nPA for treatment of infarcting myocardium early II trial substudy. *Circulation*. 2000;102(17):2031-7.
18. Atar D, Petzelbauer P, Schwitter J, Huber K, Rensing B, Kasprzak JD, et al. Effect of intravenous FX06 as an adjunct to primary percutaneous coronary intervention for acute ST-segment elevation myocardial infarction results of the F.I.R.E. (Efficacy of FX06 in the Prevention of Myocardial Reperfusion Injury) trial. *Journal of the American College of Cardiology*. 2009;53(8):720-9.
19. Hirsch A, Nijveldt R, van der Vleuten PA, Tijssen JG, van der Giessen WJ, Tio RA, et al. Intracoronary infusion of mononuclear cells from bone marrow or peripheral blood compared with standard therapy in patients after acute myocardial infarction treated by primary percutaneous coronary intervention: results of the randomized controlled HEBE trial. *European heart journal*. 2011;32(14):1736-47.
20. Harrell FE, Jr., Lee KL, Mark DB. Multivariable prognostic models: issues in developing models, evaluating assumptions and adequacy, and measuring and reducing errors. *Statistics in medicine*. 1996;15(4):361-87.
21. Ott I, Schulz S, Mehilli J, Fichtner S, Hadamitzky M, Hoppe K, et al. Erythropoietin in patients with acute ST-segment elevation myocardial infarction undergoing primary percutaneous coronary intervention: a randomized, double-blind trial. *Circulation Cardiovascular interventions*. 2010;3(5):408-13.
22. Ito H, Maruyama A, Iwakura K, Takiuchi S, Masuyama T, Hori M, et al. Clinical implications of the 'no reflow' phenomenon. A predictor of complications and left ventricular remodeling in reperfused anterior wall myocardial infarction. *Circulation*. 1996;93(2):223-8.
23. Eitel I, Wohrle J, Suenkel H, Meissner J, Kerber S, Lauer B, et al. Intracoronary compared with intravenous bolus abciximab application during primary percutaneous coronary intervention in ST-segment elevation myocardial infarction: cardiac magnetic resonance substudy of the AIDA STEMI trial. *Journal of the American College of Cardiology*. 2013;61(13):1447-54.
24. Riley RD, Lambert PC, Abo-Zaid G. Meta-analysis of individual participant data: rationale, conduct, and reporting. *Bmj*. 2010;340:c221.
25. Wagner A, Mahrholdt H, Thomson L, Hager S, Meinhardt G, Rehwald W, et al. Effects of time, dose, and inversion time for acute myocardial infarct size measurements based on magnetic resonance imaging-delayed contrast enhancement. *Journal of the American College of Cardiology*. 2006;47(10):2027-33.
26. Gruszczynska K, Kirschbaum S, Baks T, Moelker A, Duncker DJ, Rossi A, et al. Different algorithms for quantitative analysis of myocardial infarction with DE MRI: comparison with autopsy specimen measurements. *Academic radiology*. 2011;18(12):1529-36.
27. Eitel I, Desch S, Fuernau G, Hildebrand L, Gutberlet M, Schuler G, et al. Prognostic significance and determinants of myocardial salvage assessed by cardiovascular magnetic resonance in acute reperfused myocardial infarction. *Journal of the American College of Cardiology*. 2010;55(22):2470-9.
28. Eitel I, Kubusch K, Strohm O, Desch S, Mikami Y, de Waha S, et al. Prognostic value and determinants of a hypointense infarct core in T2-weighted cardiac magnetic resonance in acute reperfused ST-elevation-myocardial infarction. *Circulation Cardiovascular imaging*. 2011;4(4):354-62.



Chapter 8

Prognostic significance of microvascular obstruction and infarct size measured by cardiovascular magnetic resonance for the prediction of adverse left ventricular remodelling in patients with ST-segment elevation myocardial infarction: insight from a pooled analysis of individual patient data.

M. van Kranenburg, O.C. Manintveld, T. Yetgin, V. Bodi, D. Atar, P. Buser, E. Wu, D. Lee, P. Bernhardt, W. Rottbauer, A.C. van Rossum, E. Boersma, G.P. Krestin, F. Zijlstra, R.J.M. van Geuns.

Submitted

ABSTRACT

Background - Left ventricular remodeling and dilatation is a precursor of the development of heart failure and is an important predictor of morbidity and mortality after ST-elevation myocardial infarction (STEMI). Data on functional outcome assessed by contrast-enhanced cardiovascular magnetic resonance (CE-CMR) are scarce and limited to small single-centre data. We sought to gain insight in whether microvascular obstruction (MO) and infarct size (IS) determined by CE-CMR are predictors of adverse left ventricular (LV) remodeling patients with STEMI in a large pooled data set.

Methods - A network meta-analysis of individual patient data was performed. LV adverse remodeling measured by CE-CMR was defined as more than 20% increase in LV end-diastolic volume index (LVEDVi) between baseline and follow-up imaging.

Results - Individual data of 392 STEMI patients enrolled in five studies were analysed. Baseline CE-CMR was performed in 5 days (interquartile range [IQR]: 3-7) after the occurrence of STEMI. Follow-up CE-CMR was performed in 4 months (IQR: 3-6 months). Adverse LV remodeling was present in 16.3% (N=64) and absent in 83.7% (N=328) of the patients. Baseline LVEDVi (hazard ratio [HR]: 0.97, 95% confidence interval [CI]: 0.96-0.99, $p<0.001$), baseline LV ejection fraction (HR: 2.53, 95%CI: 1.44-4.45, $p<0.001$), IS (HR: 1.04, 95% CI: 1.02-1.05, $p<0.001$), and MO (HR: 1.73, 95%CI: 1.01-2.96, $p=0.05$) were significantly associated with adverse LV remodeling in univariate logistic regression analysis. In multivariate logistic regression, all of these parameters were associated with adverse LV remodeling and notably IS and MO were independent related with adverse LV remodeling.

Conclusion - In this so far largest reported multi-center cohort evaluating LV remodeling with CE-CMR, both IS and the presence of MO were independently associated with LV adverse remodeling besides early dilatation and reduced ejection fraction in patients with STEMI.

Keywords: Cardiovascular magnetic resonance, Infarct size, Left ventricular remodeling, Microvascular obstruction, ST-segment elevation myocardial infarction

INTRODUCTION

Left ventricular (LV) remodeling after ST-segment elevation myocardial infarction (STEMI) is a precursor of the development of heart failure and is also a predictor for mortality (1,2). The term ventricular remodeling refers to alteration in ventricular architecture, with associated increased volume and altered chamber configuration. The armamentarium to measure LV remodeling after cardiac injury includes repeated measurements of 2-dimensional echocardiography, single-photon emission computed tomography and contrast-enhanced cardiovascular magnetic resonance (CE-CMR), or a combination of these modalities. In patients with STEMI, CE-CMR provides information about infarct size (IS) and microvascular obstruction (MO) as visualized with delayed enhancement in the same session with accurate and reproducible measurements of functional measurements, using a gadolinium based contrast agent (3).

The clinical value of MO, as measured by CE-CMR, was first introduced in 1998 (4) and has been associated with worse prognosis in one study (5) and subsequently in a robust pooled patient-level analysis performed by our network (6). In patients with STEMI, the myocardial segments exhibiting MO are associated with wall thinning and an absence of improvement of segmental wall thickening compared with segments without MO during follow-up (7). MO is also an important predictor of global functional recovery after STEMI (8) and an ominous indicator of adverse LV remodeling (8,9). Although there is a strong relation between IS and MO in small-sized studies, it is not clear whether IS and MO (8,10-14) play an independent role in LV remodeling.

Comprehension of the temporal associations between IS, MO and LV remodeling is imperative, not only for our understanding of the pathophysiology following acute myocardial infarction, but also for optimizing treatment strategies in this population, especially when considering that IS and MO are used as surrogate endpoints in clinical trials (15,16). Therefore, we sought to identify CE-CMR variables for the prediction of LV remodeling and to evaluate whether LV remodeling measured by CE-CMR determines outcome after STEMI in a pooled patient-level dataset, thereby potentially providing valuable insights in the process of LV remodeling.

METHODS

Study selection

A computerized literature search of citations ranging from January 2004 to April 2012 in the MEDLINE database was performed using the following terms: "Microcirculation" [Mesh] OR "Magnetic Resonance Imaging" AND "Myocardial Infarction" AND "Microvascular Obstruction", with the following limitations: humans, English language, resulting

in 134 publications. Related articles from reference lists of retrieved articles, and the bibliographies of the co-authors were included. Observational studies including STEMI patients reperfused by primary percutaneous coronary intervention (pPCI) within 12 h of symptom onset, followed by CE-CMR within 14 days were eligible. Studies with more than 60 participants were invited to participate. In case of experimental studies; only the placebo group was included in the analysis.

Data collection

Requested variables comprised baseline characteristics, variables used in the CADILLAC risk score (17), Zwolle pPCI index (18) and Thrombolysis in Myocardial Infarction risk score (19), baseline CE-CMR variables and clinical outcomes (MACE). These variables were stated beforehand in a protocol, along with study rationale and study design, sent to participating centers. Previous approval of the individual study design by a local ethics committee was necessary for participation. Data sets from participating centers were merged by the coordinating center: Erasmus MC, Rotterdam, the Netherlands. The merged database was checked for completeness and consistency of definitions in variables by the coordinating center. Queries were sent to the primary investigators, in case of need of further data and clarification.

Definitions / contrast enhanced cardiovascular magnetic resonance

The definition of STEMI was based on those used by the authors of the primary publications(20). All clinical and angiographic variables were study based. Angiographic left main coronary artery lesions were categorized as left anterior descending artery (LAD) lesions. Imaging was performed in different centers on 1.5 Tesla scanners from different vendors (table X1 supplemental table). The scan protocols, CE-CMR parameters and data analysis have been described in the included studies. For functional imaging Steady-state free precession gradient echo sequences were used. LV end-diastolic volume, LV end-systolic volume and LV ejection fraction were short-axis based, as provided by the investigators. If not indexed, the Mosteller equation was used to adjust LV end-diastolic volume and LV end-systolic volume for body surface area. Late gadolinium enhancement (LGE) was performed by the different centers by use of an inversion recovery gradient echo sequence. MO visualized with LGE was defined as any region of hypo-enhancement within the hyper-enhanced area. IS was determined in short axis images. IS was expressed as a percentage of the LV mass (IS%LV). IS%LV was determined by manual or automatic tracing of the infarct border. In patients with MO, regions of hypoenhancement were included in the IS.

Objectives and endpoints

The primary objective was to determine independent predictors for adverse LV remodeling. Adverse LV remodeling was defined as the occurrence of >20% increase in left ventricular end diastolic volume index (LVEDVi). The relationship between adverse LV remodeling and the occurrence of MACE was explored. MACE was defined as any of the following events: cardiac death and congestive heart failure. Congestive heart failure was defined as any symptom of cardiac decompensation requiring hospitalization. The individual study investigators provided previously defined and used events (table X1: supplemental table). When a patient experienced more than one event, the first event was chosen for the combined clinical endpoint. Patients were considered at risk from the time of admission for treatment of STEMI.

Statistical analysis

Continuous data with normal distribution are presented as mean \pm standard deviation (SD). Non-normally distributed variables are reported as medians with the corresponding interquartile range (IQR). Categorical variables are represented by frequencies and percentages. Patients were categorized according to the presence of MACE. Differences in continuous variables between categories of patients were studied by unpaired Student's *t* test or Mann-Whitney U test (in case of a non-normal distribution). Proportions were compared using the chi-square test or the Fisher's exact test, where applicable. The incidences of the primary and secondary endpoints are reported as Kaplan-Meier estimates at a follow-up of 2 years. A univariate and multivariate logistic regression analysis was used to determine CE-CMR predictors of adverse LV remodeling. Variables associated with adverse LV remodeling in previous studies (in univariate and multivariate analysis) namely; age (11), anterior myocardial infarction (21), multi-vessel disease (22), infarct size (10), baseline LV ejection fraction (10), MO (9,11), in addition to LV end-diastolic volume index and LV end-systolic volume index entered the univariate logistic regression analysis. Variables that resulted in a $P < 0.10$ in the univariate logistic regression model entered the multivariate logistic regression model using the backward variable selection method. In case of missing data (variable data in > 7.5% of cohort not present), these variables were not taken into account in the regression analysis. Hazard ratios, 95% confidence intervals (CI) and P-values were reported. Two-sided *P*-values values with $\alpha \leq 0.05$ were considered to be statistically significant. Statistical analysis was performed using the statistical package IBM SPSS Statistics (version 20.0.01 (SPSS, Chicago, IL). A Kaplan-Meier curve was drawn with GraphPad Software Inc, GraphPad Prism 6, version 6.02 (La Jolla, Ca)

RESULTS

Patient characteristics

We identified ten eligible observational (7) and experimental studies (3). The principal investigators of these studies were invited to participate in this collaborative analysis. Eight out of ten investigators provided individual patient data (figure 1). In five out of eight a follow-up CE-CMR scan was performed (23-27). The study flowchart is shown in figure 1. Of 672 enrolled acute myocardial infarction (AMI) patients, paired CE-CMR examinations were available in 392 STEMI patients. Between April 1999 and April 2008 (IQR: March 2003 - May 2007), these patients were admitted to a coronary care unit. Patients with adverse LV remodeling were compared to patients without adverse LV remodeling in table 1. Adverse LV remodeling was present in 64/392 (16.3%) of patients and absent in 328 (83.7%) of the patients. pPCI was performed in 295/392 (75.3%) of the patients. Age at inclusion was 57.4 ± 11.5 and 83.4% of the cohort was men. Patients in the two groups had no significant differences between baseline characteristics.

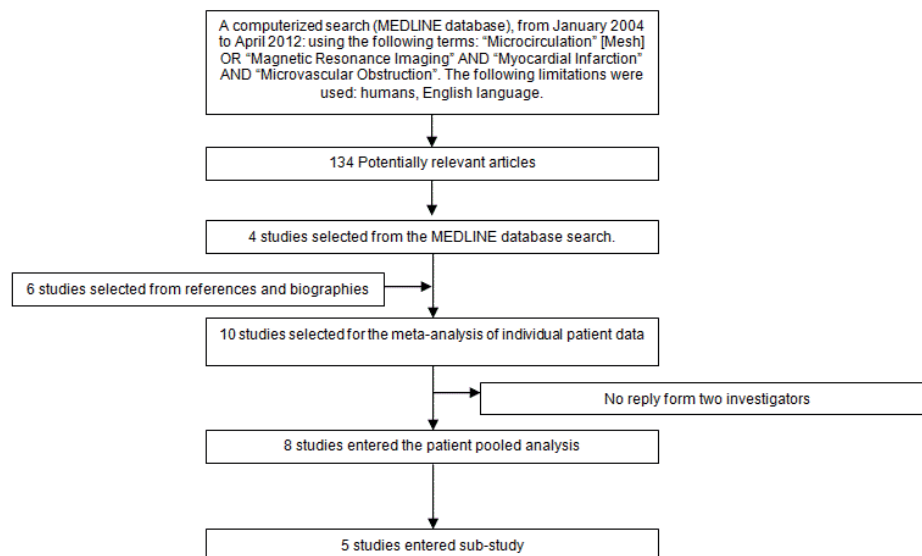


Figure 1. flow chart: systematic search process in the MEDLINE database

Contrast-enhanced cardiovascular magnetic resonance

Baseline and follow-up CE-CMR variables were compared in table 2. Baseline CE-CMR was performed in 5 days (IQR: 3-7) after the occurrence of STEMI. IS%LV was 26.2% (IQR: 15.7%-45%) in patients with adverse LV remodeling versus 19.4 (IQR: 10.1%-28.0%) in patients without adverse adverse LV remodeling ($P < 0.001$). MO was more prevalent in

Table 1. patient characteristics.

Variable	Entire cohort	LV remodeling	LV remodeling absent	P-value
	392	64 (16.3%)	328 (83.7%)	
Treatment				
pPCI	295/392 (75.3%)	48/64 (75.0%)	247/328 (75.3%)	0.96
Fibrinolysis	90/392 (23.0%)	16/64 (25.0%)	74/328 (22.6%)	0.67
Rescue or Facilitated PCI	10/392 (2.6%)	1/64 (1.6%)	9/328 (2.7%)	0.58
Cardiovascular Risk Factors				
Age	57.4 ± 11.5	57.5 ± 11.1	57.3 ± 11.5	0.94
Male	327/392 (83.4)	55/64 (85.9%)	272/328 (82.9%)	0.55
BMI	27.2 ± 3.5	27.7 ± 3.5	27.1 ± 3.5	0.26
Diabetes	43/381 (11.3%)	7/59 (11.9%)	36/322 (11.2%)	0.88
Hypertension	158/381 (41.5%)	23/59 (39.0%)	135/322 (41.9%)	0.67
Hypercholesterolemia	128/379 (33.8%)	22/59 (37.3%)	106/320 (33.1%)	0.53
Smoking/prior smoking	238/391 (60.9%)	41/63 (65.1%)	197/328 (60.1%)	0.46
Family history of myocardial infarction	81/257 (31.5%)	10/33 (30.3%)	71/224 (31.7%)	0.87
History of myocardial infarction	8/267 (3.0%)	8/230 (3.5%)	0/37 (0%)	0.60
Angiographic variables				
Time to reperfusion	3.3 (IQR: 2.2-4.7)	3.3 (IQR: 2.2-4.9)	3.0 (2.1-4.3)	0.68
Infarct-related artery				
Right coronary	134/391 (34.3%)	21/64 (32.8%)	113/327 (34.6%)	0.79
Left anterior descending	222/391 (56.8%)	40/64 (62.5%)	182/327 (55.7%)	0.31
Left circumflex	35/391 (9.0%)	3/64 (4.7%)	32/327 (9.8%)	0.19
N-vessel disease				
1	238/381 (62.5%)	33/60 (55.0%)	205/321 (63.9%)	0.30
2	89/381 (23.4%)	17/60 (28.3%)	72/321 (22.4%)	0.26
3	45/381 (11.8%)	7/60 (11.7%)	38/321 (11.8%)	0.96
Multi-vessel disease	134/381 (35.2%)	24/60 (40.0%)	110/321 (34.3%)	0.39
TIMI flow grade post PCI				
0	5/385 (1.3%)	1/62 (1.6%)	4/323 (1.2%)	0.59
1	1/385 (0.3%)	0/62 (0%)	1/323 (0.3%)	1.00
2	32/385 (8.3%)	8/62 (12.9%)	24/323 (7.4%)	0.15
3	347/385 (90.1%)	53/62 (85.5%)	294/323 (91.0%)	0.18
Enzymatic infarct size				
Maximal Creatine Kinase	1603 (IQR: 859-3311)	2818 (IQR: 1321-5658)	1500 (IQR: 782-3138)	0.30

Values are means ± SD, if applicable medians and IQR are reported, pPCI; primary percutaneous coronary intervention, BMI; body mass index * missing in 124 cases (12.1%), Family history of myocardial infarction * missing in 88 cases (8.6%), prior myocardial infarction * missing in 77 cases (7.5%), Time to reperfusion is ischemic time * missing in 446 cases, 446 cases reperfusion within 12 hours (43.5%), LV; left ventricular, TIMI; thrombolysis in myocardial infarction, Maximal Creatine Kinase * missing in 278 cases (27.1%),

Table 2. CE-CMR variables

	Baseline CE-CMR Entire cohort	Follow-up CE-CMR Entire cohort	Baseline CE-CMR LV remodeling	Follow-up CE-CMR LV remodeling	Baseline CE-CMR No LV remodeling	Follow-up CE-CMR No LV remodeling	P-values Comparing baseline CE-CMR variables	P-values Comparing follow-up CE-CMR variables
Time between myocardial infarction and CE-CMR	5 days (IQR: 3-7)	4 months (IQR: 3-6)	5 days (IQR: 3-7)	5 months (IQR: 4-7)	5 days (IQR: 3-7)	4 months (IQR: 3-6)	0.98	0.10
LV end-diastolic volume, ml	157.5 ± 42.8 (IQR: 3-7)	161.4 ± 52.9 (IQR: 3-6)	141.7 ± 49.3 (IQR: 3-7)	188.4 ± 64.2 (IQR: 4-7)	160.6 ± 40.8 (IQR: 3-7)	156.1 ± 48.8 (IQR: 3-6)	0.005	< 0.001
LV end-diastolic volume index, ml/m ²	80.3 ± 19.3	83.6 ± 24.6	72.1 ± 22.4	96.5 ± 29.8	81.9 ± 18.2	80.9 ± 22.5	< 0.001	0.001
LV end-systolic volume, ml	84.2 ± 35.0	81.7 ± 41.6	80.5 ± 41.4	104.1 ± 56.6	84.9 ± 33.6	77.3 ± 36.5	0.43	< 0.001
LV end-systolic volume index, ml/m ²	42.8 ± 16.7	41.7 ± 20.6	41.0 ± 19.6	53.2 ± 28.5	43.2 ± 16.1	39.4 ± 17.9	0.40	< 0.001
LV ejection fraction, %	47.8 ± 11.8	51.5 ± 12.5	45.4 ± 13.7	47.4 ± 14.4	48.3 ± 11.4	52.4 ± 11.9	0.12	0.01
MO	158/392 (40.3%)		33/64 (51.6%)		125/328 (38.1%)		0.045	
IS%LV	20.6 (IQR: 10.9-30.5)	12.7 (IQR: 6.0-19.0)	26.2 (IQR: 15.7-45.0)	16.0 (IQR: 6.0-34.9)	19.4 (IQR: 10.1-28.0)	12.6 (IQR: 6.0-17.3)	0.005	0.659
IS	26.5 (IQR: 14.0-42.3)	15.0 (IQR: 6.5-26.0)	33.0 (IQR: 17.3-59.5)	19.0 (IQR: 6.5-46.7)	25.6 (IQR: 13.5-40.7)	15.0 (IQR: 6.5-25.0)	0.095	0.934

Values are means ± SD, if applicable medians and IQR are reported, CE-CMR; contrast-enhanced cardiac magnetic resonance, LV; left ventricular, MO; microvascular obstruction, IS%LV; infarct size expressed as percentage of LV mass. * missing data: in > 10% of cohort data not present

patients with LV adverse remodeling 51.6% versus 38.1% in patients without adverse LV remodeling ($p = 0.05$). Follow-up CE-CMR was performed in 4 months (IQR: 3-6 months) after performance of the baseline CE-CMR. Follow-up LV ejection fraction was $47.3\% \pm 14.4$ in patients with adverse LV remodeling versus 52.4 ± 11.9 in patients without adverse LV remodeling (0.012). Baseline IS%LV and MO were associated with the occurrence of LV remodeling (figure 2 and figure 3). Follow-up LV ejection fraction increased both in patients without MO (baseline LV ejection fraction $51.9\% \pm 10.9$, follow-up LV ejection fraction $55.9\% \pm 11.0$, $p \leq 0.001$) and in patients with MO (baseline LV ejection fraction $42.2\% \pm 10.6$, follow-up LV ejection fraction $45.2\% \pm 11.8$, $p \leq 0.001$, figure 4).

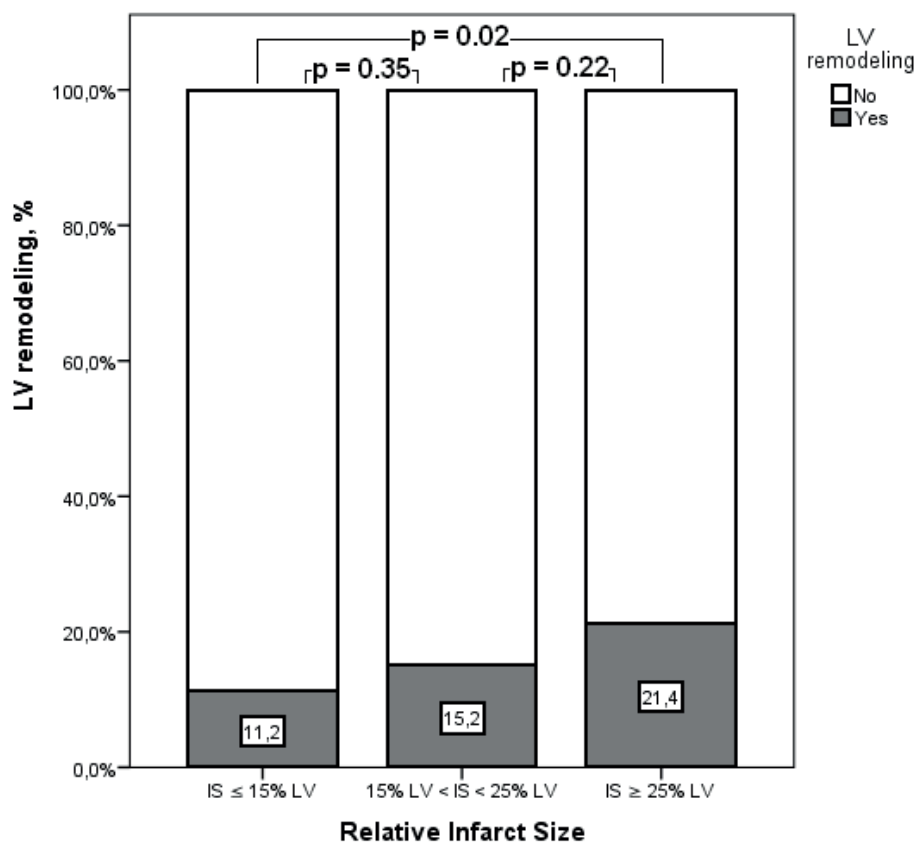


Figure 2. Occurrence of adverse LV remodeling related to IS%LV
LV; left ventricular, IS; infarct size.

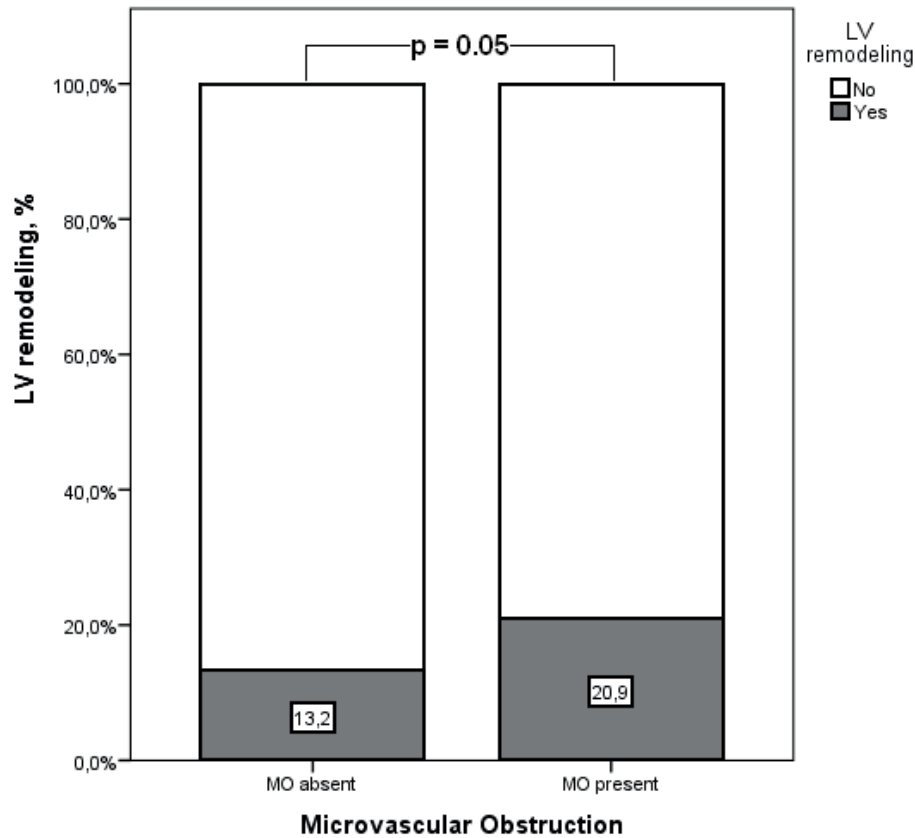


Figure 3. Occurrence of adverse LV remodeling related to presence of MO
LV; left ventricular, MO; microvascular obstruction,

Predictors of LV remodeling

Univariate logistic regression is summarized in table 3. Variables associated with the occurrence of LV remodeling were LVEDVI [HR = 0.97 (95% CI: 0.96-0.99)], baseline LV ejection fraction (ref: >40%) [HR = 2.53 (95% CI: 1.44-4.45)], baseline IS%LV [HR = 1.04 (95% CI: 1.02-1.05)], MO [HR = 1.73 (95% CI: 1.01-2.96)] while Age, anterior myocardial infarction, multi-vessel disease, TIMI flow grade post PCI and LV end-systolic volume index were not associated with the occurrence of LV remodeling. In the multivariable logistic regression analysis baseline LV end-diastolic volume index, baseline IS%LV, baseline LV ejection fraction and MO were independently associated with the occurrence of LV remodeling, where the independency between the last two is most remarkable (Table 4).

Clinical outcome

The combined endpoint occurred in 24 patients, including 3 cardiac deaths and 21 patients with admission for congestive heart failure (LV remodeling vs. no LV remodel-

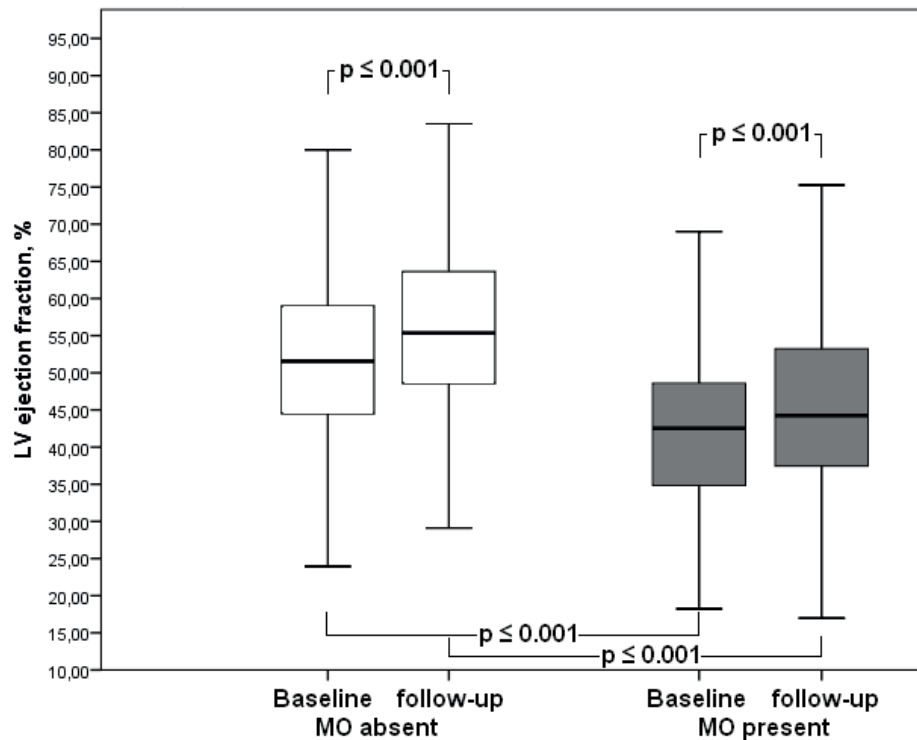


Figure 4. changes in LV ejection fraction from baseline to follow-up in patients without microvascular obstruction versus with microvascular obstruction

Table 3. univariate Logistic – regression for LV remodelling

Variable	HR	95% CI	P-value
Age	0.91	0.50-1.64	0.74
Anterior myocardial infarction	1.33	0.77-2.30	0.31
Multi-vessel disease	1.28	0.73-2.25	0.39
TIMI flow grade post PCI	1.04	0.12-9.08	0.97
Baseline LV end-systolic volume index	0.99	0.98-1.01	0.34
Baseline LV end-diastolic volume index	0.97	0.96-0.99	<0.001
Baseline LV ejection fraction, >40%	2.53	1.44-4.45	<0.001
Baseline IS%LV	1.04	1.02-1.05	<0.001
MO	1.73	1.01-2.96	0.05

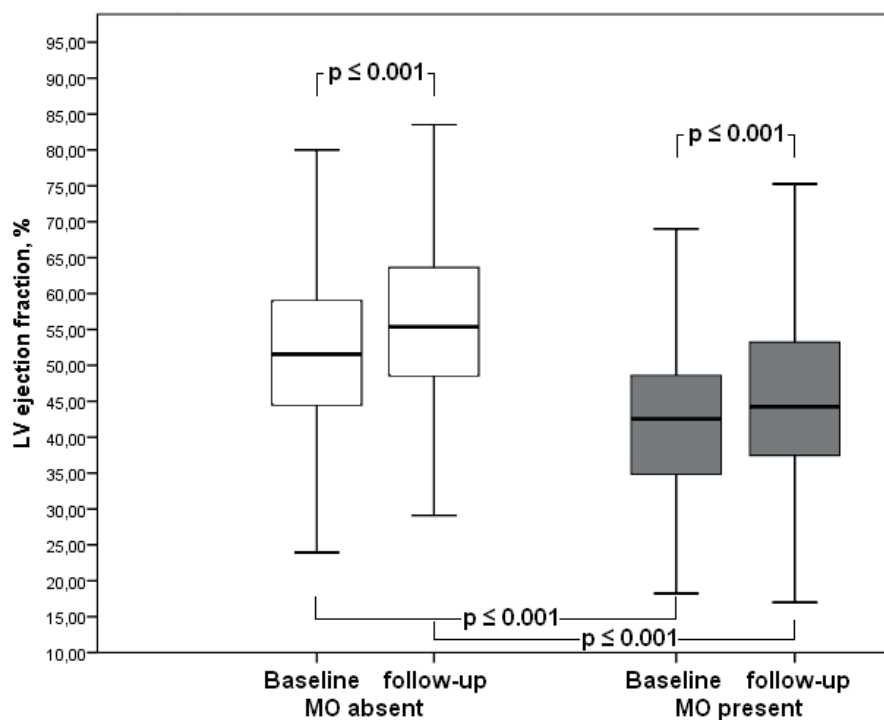
CI; confidence interval HR; hazard ratio, IS%LV: infarct size expressed as percentage of LV mass LV; left ventricular, MO: microvascular obstruction, TIMI: thrombolysis in myocardial infarction.

ing, $n = 17$ vs. $n = 7$) within 2 years of follow-up. The Kaplan-Meier estimate of MACE grouped by LV remodeling was 73.5% in patients with adverse LV remodeling and 87.3% in patients without adverse LV remodeling ($P = 0.121$).

Table 4. multivariate logistic – regression analysis for LV remodeling.

Variable	HR	95% CI	P-value
LV end-diastolic volume index, ml/m ²	0.95	0.94-0.97	<0.001
Baseline LV ejection fraction, >40%	2.47	1.22-4.99	0.012
Baseline IS%LV, continuous	1.03	1.00-1.05	0.018
MO	2.13	1.09-4.18	0.027

CI; confidence interval, HR; hazard ratio, IS%LV: infarct size expressed as percentage of LV mass, LV; left ventricular, MO microvascular obstruction.

**Figure 5.** changes in LV ejection fraction from baseline to follow-up in patients without microvascular obstruction versus with microvascular obstruction.

LV; left ventricular, MO; microvascular obstruction.

DISCUSSION

The main findings of the study were that: (i) mean LV ejection fraction (EF) improved after reperfusion therapy for acute MI, whereas the majority of the patients still showed increased end-diastolic volumes during follow-up with significant LV remodeling in 16.3%; (ii) baseline LV ejection fraction, baseline IS%LV, MO and baseline LV end-diastolic volume index are important predictors for the occurrence of adverse LV remodeling; (iii) and IS%LV and MO independently correlate with LV dilatation.

To our knowledge, the present study represents the largest patient pooled analysis investigating LV remodeling which evaluates clinical and CE-CMR variables in patients with STEMI. These observations extend findings obtained from previous studies evaluating paired CE-CMR examinations for LV remodeling, which were single-center studies (5,7-11),(28) and provide important insight into the determinants of LV remodeling, therefore potentially guiding the direction of development of novel therapies.

LV ejection fraction measured shortly after primary PCI is of limited value for primary prevention of acute death due to ventricular fibrillation. In this regard, the current study shows an independent prediction for adverse remodeling post STEMI both for IS%LV and MO in the era of primary PCI. An average of 4-5% of improvement in LV EF post reperfusion therapy is seen in most studies with CMR but variability is large. Although the mean LV EF is improving during follow-up, remodeling is standard for all patients and about 1/3 of the patients show progressive dilatation in the long-term, increasing the risk of arrhythmias and heart failure in these patients (29). Identification of these patients in an early phase is valuable in efficient healthcare strategies post STEMI and pPCI where CMR with both measurement of MO and IS could be applied.

Furthermore, Previous studies on IS and MO as predictors for MACE were mainly driven by re-MI and heart failure with a minority on cardiac death. We previously showed that MO eliminated IS as predictor of cardiac death and the combined endpoint (6). In the current analysis IS remained an independent predictor for remodeling as a precursor of heart failure. Previous studies linked multivessel disease (6) and SyntaxScore (30) (both representing the extent of atherosclerotic disease) to the presence of MO and might explain the stronger relation between MO and repeat-myocardial infarction. Our results are in-line with a recent large single center study where both %IS and MO predicted remodeling(28). In this study remodeling was defined as >10% increase in left ventricular end systolic volume index, selecting also patients with less extensive remodeling and potentially less clinical impact.

Myocardial remodeling by itself in the era of reperfusion therapy is mainly a phenomenon of the remote area. In an animal experiment with detailed CMR analysis the circumferential area of the MI was not increasing with only a reduction of the wall thickness during the remodeling process (31). The general increase in EDVi could be attributed to increase in the circumferential length of the remote area with an associated decrease in wall thickness in these areas. Importantly, however, remodeling after AMI is also a process with alterations in structure and function in response to hemodynamic load and/or cardiac injury involving both infarcted and non-infarcted myocardium. The infarct area is characterized by acute ischemic injury, MO and with persistent ischemia after restoration of coronary artery flow and reperfusion injury. Finally the remote area is also effected by the systemic inflammatory and immunological responses. All these steps can potentially be improved with additional pharmacological therapies and assessed by different CMR techniques. Despite optimal treatment of STEMI with pPCI, remodeling still

occurs in numerous patients, which is a major determinant of heart failure (32). In addition there is evidence that leucocyte recruitment (33), leucocyte infiltration with upregulation of inflammation markers and increased edema also occur in the remote myocardium and not just in the infarct region (34) and (35). The combination of these factors can lead to decreased cell-cell interaction and result in diminished wall contraction. In the following days/weeks, edema will resolve and fibroblasts will be removed and the remote myocardial cells will adjust to the increased wall stress by compensatory increase of contractile intracellular structures causing increased remote circumferential length which will improve remote pump function. In this sense, a recent elegant study using T1 measurement in humans of the remote myocardium demonstrated an increased T1 time in the remote zone in patients with incomplete ST segment resolution and inflammation markers on admission. Prolonged T1-time in remote areas represents edema and hypercellularity and was associated with remodeling and signs of heart failure. (36)

Study Limitations

There are several limitations inherent to the design of a meta-analysis that deserve comment. Study authors may not be contactable or willing to collaborate, definitions might vary along studies, individual participant data might have been not retrievable or there might be qualitative or quantitative differences between included studies. Furthermore, the study-design might be prone to publication, selection and data availability bias (37). Several limitations we need to specifically address for this meta-analysis: CMR was performed in a wide range up to 14 days post STEMI, on different time points after contrast injection with different concentrations of gadolinium based contrast agents. This may influence the detection of MO and might influence the “extension” of IS (38-40). CMR analysis did not take place in one center and different ways of analysis were performed which also influences the measured infarct size (3). Transmurality and the presence of hemorrhage were not available from all studies and could not be included as potential parameter for the prediction of adverse LV remodeling.

CONCLUSIONS

In this so far largest reported multi-center cohort evaluating LV remodeling with CE-CMR, both IS and the presence of MO were independently associated with LV dilatation in patients with STEMI

Conflict of interest

None declared.

Table X. Study Characteristics.

Author	Journal	Year of publication	Single - Multicenter study	Vendor	STEMI, pPCI patients pooled analysis	Delayed Enhancement Sequence	Definition MO	Acquisition parameters Delayed Enhancement Sequence	Determination IS%LV
Hombach et al.	Eur Heart Journal	2005	Single-center	Philips 1.5 Tesla	35	3D-gradient spoiled turbo fast-field-echo sequence with a selective 180 inversion recovery pre-pulse	MO was defined as late hypo-enhancement within a hyper-enhancement region on LE images	6-12 minutes after gadolinium injection (0.2 mmol/kg)	Manual delineation
Wu et al.	Heart	2008	Single-center	Siemens 1.5 Tesla	89	T1-weighted inversion recovery, fast gradient-echo pulse sequence	Dark areas of absent contrast surrounded by hyper-enhanced infarct tissue	10 minutes after gadolinium injection (0.2 mmol/kg)	Manual delineation, areas of microvascular obstruction were included in the total infarct size
Bodi et al.	JACC Cardiovasc Imaging	2009	Single-center	Siemens 1.5 Tesla	75	Inversion recovery steady state free precession imaging sequence	Visually defined in delayed enhancement sequences as a lack of contrast uptake in the core of a segment surrounded by tissue showing delayed enhancement	10 minutes after gadolinium injection (0.1 mmol/kg)	Manual delineation?
Atar et al.	JACC	2009	Multi-center	1.5 Tesla multivendor	104	Inversion recovery gradient-echo pulse sequence	Dark core, where there is no penetration of contrast medium, surrounded by necrotic bright area.	20 minutes after gadolinium injection (0.25 mmol/kg)	Manual delineation?
Hirsch et al.	Eur Heart Journal	2010	Multi-center	1.5 Tesla multivendor	59	Inversion recovery gradient-echo pulse sequence	Central dark surrounded by areas of hyper enhancement	10-15 minutes after gadolinium injection (0.15 mmol/kg)	Manual delineation

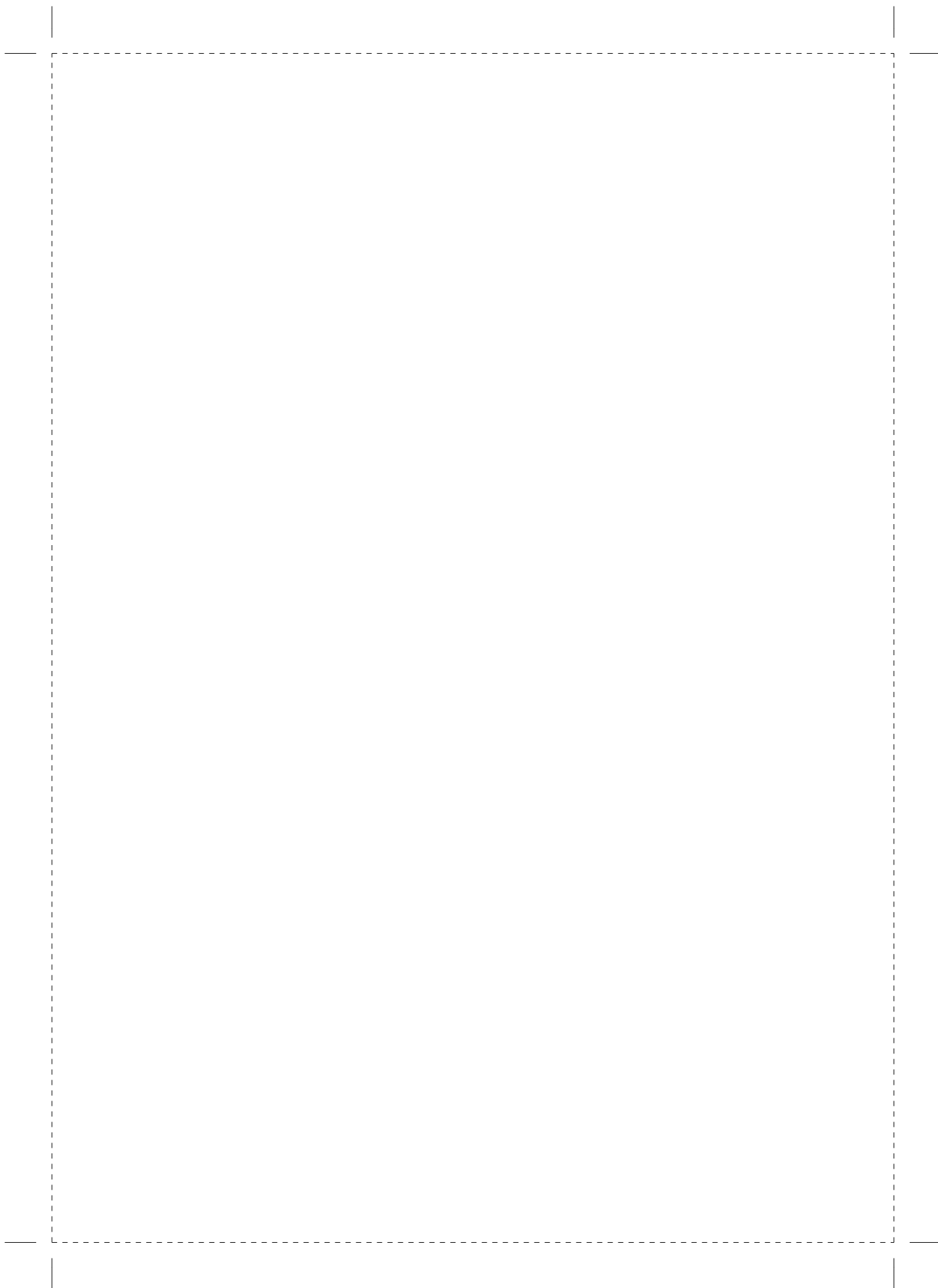
MO: microvascular obstruction, MAC(O)E: major adverse cardiovascular (and cerebrovascular) events.

REFERENCES

1. Pfeffer MA, Braunwald E. Ventricular remodeling after myocardial infarction. Experimental observations and clinical implications. *Circulation* 1990;81:1161-72.
2. St John Sutton M, Pfeffer MA, Plappert T et al. Quantitative two-dimensional echocardiographic measurements are major predictors of adverse cardiovascular events after acute myocardial infarction. The protective effects of captopril. *Circulation* 1994;89:68-75.
3. Gruszczynska K, Kirschbaum S, Baks T et al. Different algorithms for quantitative analysis of myocardial infarction with DE MRI: comparison with autopsy specimen measurements. *Acad Radiol* 2011;18:1529-36.
4. Wu KC, Zerhouni EA, Judd RM et al. Prognostic significance of microvascular obstruction by magnetic resonance imaging in patients with acute myocardial infarction. *Circulation* 1998;97:765-72.
5. de Waha S, Desch S, Eitel I et al. Impact of early vs. late microvascular obstruction assessed by magnetic resonance imaging on long-term outcome after ST-elevation myocardial infarction: a comparison with traditional prognostic markers. *Eur Heart J* 2010;31:2660-8.
6. van Kranenburg M, Magro M, Thiele H et al. Prognostic value of microvascular obstruction and infarct size, as measured by CMR in STEMI patients. *JACC Cardiovasc Imaging* 2014;7:930-9.
7. Baks T, van Geuns RJ, Biagini E et al. Effects of primary angioplasty for acute myocardial infarction on early and late infarct size and left ventricular wall characteristics. *J Am Coll Cardiol* 2006;47:40-4.
8. Nijveldt R, Beek AM, Hirsch A et al. Functional recovery after acute myocardial infarction: comparison between angiography, electrocardiography, and cardiovascular magnetic resonance measures of microvascular injury. *J Am Coll Cardiol* 2008;52:181-9.
9. Weir RA, Murphy CA, Petrie CJ et al. Microvascular obstruction remains a portent of adverse remodeling in optimally treated patients with left ventricular systolic dysfunction after acute myocardial infarction. *Circ Cardiovasc Imaging* 2010;3:360-7.
10. Springeling T, Kirschbaum SW, Rossi A et al. Late cardiac remodeling after primary percutaneous coronary intervention-five-year cardiac magnetic resonance imaging follow-up. *Circ J* 2012;77:81-8.
11. Ahn KT, Song YB, Choe YH et al. Impact of transmural necrosis on left ventricular remodeling and clinical outcomes in patients undergoing primary percutaneous coronary intervention for ST-segment elevation myocardial infarction. *Int J Cardiovasc Imaging* 2012.
12. Ganame J, Messalli G, Dymarkowski S et al. Impact of myocardial haemorrhage on left ventricular function and remodelling in patients with reperfused acute myocardial infarction. *Eur Heart J* 2009;30:1440-9.
13. Tarantini G, Razzolini R, Cacciavillani L et al. Influence of transmural, infarct size, and severe microvascular obstruction on left ventricular remodeling and function after primary coronary angioplasty. *Am J Cardiol* 2006;98:1033-40.
14. Baks T, van Geuns RJ, Biagini E et al. Recovery of left ventricular function after primary angioplasty for acute myocardial infarction. *Eur Heart J* 2005;26:1070-7.
15. Orn S, Manhenke C, Greve OJ et al. Microvascular obstruction is a major determinant of infarct healing and subsequent left ventricular remodelling following primary percutaneous coronary intervention. *Eur Heart J* 2009;30:1978-85.
16. Kim HW, Farzaneh-Far A, Kim RJ. Cardiovascular magnetic resonance in patients with myocardial infarction: current and emerging applications. *J Am Coll Cardiol* 2009;55:1-16.

17. Halkin A, Singh M, Nikolsky E et al. Prediction of mortality after primary percutaneous coronary intervention for acute myocardial infarction: the CADILLAC risk score. *J Am Coll Cardiol* 2005;45:1397-405.
18. De Luca G, Suryapranata H, van 't Hof AW et al. Prognostic assessment of patients with acute myocardial infarction treated with primary angioplasty: implications for early discharge. *Circulation* 2004;109:2737-43.
19. Morrow DA, Antman EM, Charlesworth A et al. TIMI risk score for ST-elevation myocardial infarction: A convenient, bedside, clinical score for risk assessment at presentation: An intravenous nPA for treatment of infarcting myocardium early II trial substudy. *Circulation* 2000;102:2031-7.
20. Task Force on the management of ST-segment elevation myocardial infarction of the European Society of Cardiology, Steg PG, James SK et al. ESC Guidelines for the management of acute myocardial infarction in patients presenting with ST-segment elevation. *Eur Heart J* 2012;33:2569-619.
21. Gaudron P, Eilles C, Kugler I, Ertl G. Progressive left ventricular dysfunction and remodeling after myocardial infarction. Potential mechanisms and early predictors. *Circulation* 1993;87:755-63.
22. Bolognese L, Neskovic AN, Parodi G et al. Left ventricular remodeling after primary coronary angioplasty: patterns of left ventricular dilation and long-term prognostic implications. *Circulation* 2002;106:2351-7.
23. Hombach V, Grebe O, Merkle N et al. Sequelae of acute myocardial infarction regarding cardiac structure and function and their prognostic significance as assessed by magnetic resonance imaging. *Eur Heart J* 2005;26:549-57.
24. Wu E, Ortiz JT, Tejedor P et al. Infarct size by contrast enhanced cardiac magnetic resonance is a stronger predictor of outcomes than left ventricular ejection fraction or end-systolic volume index: prospective cohort study. *Heart* 2008;94:730-6.
25. Bodi V, Sanchis J, Nunez J et al. Prognostic value of a comprehensive cardiac magnetic resonance assessment soon after a first ST-segment elevation myocardial infarction. *JACC Cardiovasc Imaging* 2009;2:835-42.
26. Atar D, Petzelbauer P, Schwitter J et al. Effect of intravenous FX06 as an adjunct to primary percutaneous coronary intervention for acute ST-segment elevation myocardial infarction: results of the F.I.R.E. (Efficacy of FX06 in the Prevention of Myocardial Reperfusion Injury) trial. *J Am Coll Cardiol* 2009;53:720-9.
27. Hirsch A, Nijveldt R, van der Vleuten PA et al. Intracoronary infusion of mononuclear cells from bone marrow or peripheral blood compared with standard therapy in patients after acute myocardial infarction treated by primary percutaneous coronary intervention: results of the randomized controlled HEBE trial. *Eur Heart J* 2011;32:1736-47.
28. Bodi V, Monmeneu JV, Ortiz-Perez JT et al. Prediction of Reverse Remodeling at Cardiac MR Imaging Soon after First ST-Segment-Elevation Myocardial Infarction: Results of a Large Prospective Registry. *Radiology* 2016;278:54-63.
29. Springeling T, Kirschbaum SW, Rossi A et al. Late cardiac remodeling after primary percutaneous coronary intervention-five-year cardiac magnetic resonance imaging follow-up. *Circ J* 2013;77:81-8.
30. Magro M, Nauta ST, Simsek C et al. Usefulness of the SYNTAX score to predict "no reflow" in patients treated with primary percutaneous coronary intervention for ST-segment elevation myocardial infarction. *Am J Cardiol* 2012;109:601-6.
31. Springeling T, Uitterdijk A, Rossi A et al. Evolution of reperfusion post-infarction ventricular remodeling: new MRI insights. *Int J Cardiol* 2013;169:354-8.

32. Dixon JA, Spinale FG. Myocardial remodeling: cellular and extracellular events and targets. *Annu Rev Physiol* 2011;73:47-68.
33. Ruparelia N, Digby JE, Jefferson A et al. Myocardial infarction causes inflammation and leukocyte recruitment at remote sites in the myocardium and in the renal glomerulus. *Inflamm Res* 2013;62:515-25.
34. Rolf A, Assmus B, Schachinger V et al. Maladaptive hypertrophy after acute myocardial infarction positive effect of bone marrow-derived stem cell therapy on regional remodeling measured by cardiac MRI. *Clin Res Cardiol* 2011;100:983-92.
35. Yang Z, Berr SS, Gilson WD, Toufektsian MC, French BA. Simultaneous evaluation of infarct size and cardiac function in intact mice by contrast-enhanced cardiac magnetic resonance imaging reveals contractile dysfunction in noninfarcted regions early after myocardial infarction. *Circulation* 2004;109:1161-7.
36. Carrick D, Haig C, Rauhalammi S et al. Pathophysiology of LV Remodeling in Survivors of STEMI: Inflammation, Remote Myocardium, and Prognosis. *JACC Cardiovasc Imaging* 2015;8:779-89.
37. Riley RD, Lambert PC, Abo-Zaid G. Meta-analysis of individual participant data: rationale, conduct, and reporting. *BMJ* 2010;340:c221.
38. Rochitte CE, Lima JA, Bluemke DA et al. Magnitude and time course of microvascular obstruction and tissue injury after acute myocardial infarction. *Circulation* 1998;98:1006-14.
39. Oshinski JN, Yang Z, Jones JR, Mata JF, French BA. Imaging time after Gd-DTPA injection is critical in using delayed enhancement to determine infarct size accurately with magnetic resonance imaging. *Circulation* 2001;104:2838-42.
40. Wagner A, Mahrholdt H, Thomson L et al. Effects of time, dose, and inversion time for acute myocardial infarct size measurements based on magnetic resonance imaging-delayed contrast enhancement. *J Am Coll Cardiol* 2006;47:2027-33.





Chapter 9

Ischemic postconditioning after routine thrombus aspiration during primary percutaneous coronary intervention: rationale and design of the POstconditioning Rotterdam Trial.

Yetgin T, **van Kranenburg M**, ten Cate T, Duncker DJ, de Boer MJ, Diletti R, van Geuns RJM, Zijlstra F, Manintveld OC.

Catheterization and Cardiovascular Interventions. 2015 Sept. DOI: 10.1002/ccd.26239

ABSTRACT

Background: Whether ischemic postconditioning (IPOC) immediately after routine thrombus aspiration (TA) reduces infarct size (IS) in patients with ST-segment elevation myocardial infarction (STEMI) undergoing primary percutaneous coronary intervention (PPCI) has not been established. Study design: The POstconditioning Rotterdam Trial (PORT) is a dual-center, prospective, open-label, randomized trial with blinded end-point evaluation enrolling 72 subjects with first-time STEMI, and an occluded infarct-related artery (IRA) without collaterals undergoing PPCI. Subjects are randomized 1:1 to a strategy of IPOC immediately after TA followed by stenting of the IRA or to conventional percutaneous coronary intervention (PCI), including TA followed by stenting of the IRA (controls). Cardiac magnetic resonance imaging (MRI) is performed at 3–5 days after STEMI and at 3 months. The primary endpoint is IS at 3 months measured by delayed enhancement MRI. Other secondary endpoints include MRI-derived micro-vascular obstruction (MVO), left ventricular ejection fraction, myocardial salvage index, enzymatic IS, ST-segment resolution, myocardial blush grade, microcirculatory resistance, inflammation markers, and clinical events through 3-month follow-up. Conclusions: PORT is testing the hypothesis that adding IPOC (against lethal reperfusion injury) to TA (against distal embolization and MVO) is cardioprotective and reduces ultimate IS in STEMI patients undergoing PPCI (Dutch Trial Register identifier: NTR4040).

INTRODUCTION

Prompt restoration of coronary blood flow by primary percutaneous coronary intervention (PPCI) is essential to salvage viable myocardium and limit myocardial infarct size (IS) in patients presenting with ST-segment elevation myocardial infarction (STEMI), thereby preserving left ventricular (LV) systolic function and improving clinical outcomes. However, reperfusion itself initiates a cascade of harmful events, resulting not only in mitochondrial dysfunction and cardiomyocyte death, termed lethal reperfusion injury (1, 2), but also major ultrastructural damage to capillary endothelium, leading to microvascular obstruction (MVO), termed no-reflow (3). Consequently, the full benefits of myocardial reperfusion are not realized with reperfusion-mediated injury constituting a key therapeutic target

Lethal Reperfusion Injury and Ischemic Postconditioning

Ischemic postconditioning (IPOC) is an interventional strategy in which controlled, brief, intermittent episodes of reocclusions in the first few minutes of reperfusion can protect myocardium from lethal reperfusion injury. In 2003, Zhao et al. (4) reported that interrupting reperfusion of previously ischemic myocardium by three short-lived episodes (of 30 sec each) of coronary artery reocclusion reduced myocardial IS in canine hearts by 44% following 60 min of left anterior descending artery occlusion. Importantly, the reduction in IS was associated with decreased myocardial edema, reduced neutrophil accumulation, attenuation of apoptotic cell death, and improved endothelial function, factors associated with myocardial reperfusion injury (4). Further mechanisms by which IPOC alters the pathophysiology of reperfusion injury involves physiological effects (e.g., reducing oxidative stress, delaying rapid restoration of normal pH, reducing calcium overload) and molecular effects (e.g., triggering release of autacoids and activation of their cell-surface receptors, thereby, recruiting signal transduction pathways) (2, 5-7). Ultimately, both the physiological and molecular mechanisms seem to converge on the mitochondria and result in prevention of cardiomyocyte hypercontracture and inhibition of opening of the mitochondrial permeability transition pore (2). Within 2 years after the initial discovery in 2003 (4), the first clinical studies of IPOC in small groups of patients with STEMI were published. In these studies, it was reported that interrupting reperfusion with four cycles of 1-min low pressure inflations and deflations of the angioplasty balloon immediately after direct stenting of the infarct-related artery (IRA) improved myocardial reperfusion, reduced myocardial IS both acutely and at 6 months, and improved LV ejection fraction up to 7% (percent points) at 1 year (8-10). However, recent (larger) trials were not able to confirm the initially observed benefits with IPOC and provide inconsistent results (11-14). The reasons for the contradictory findings have been comprehensively reviewed elsewhere (15) and briefly, may be related to a number

of factors, such as the inability to take into account the major determinants of IS; choice of inappropriate endpoints; brief window of protection against reperfusion injury; and impact of comorbidities and concurrent treatments on IPOC. Importantly and of additional concern, the potential interaction between the application of thrombus aspiration (TA) and the IPOC protocol might represent another crucial factor in achieving cardioprotection which is further discussed below.

Microvascular Obstruction and TA

Impaired myocardial perfusion after ischemia was first observed by Krug et al. (16) and described as “the inability to reperfuse a previously ischemic region.” Many factors may contribute to this phenomenon, including capillary damage with impaired vasodilation, compression of capillaries by swollen cardiomyocytes, blebbing of endothelial cells into the lumen, capillary plugging by neutrophils, and distal embolization of friable material released from the ruptured atherosclerotic plaque (17). Measures that prevent at least one of these components of MVO are, therefore, likely to improve microcirculatory flow. Moreover, MVO has been shown to be an independent predictor of MACE and cardiac death at 2 years after STEMI (18). In this regard, TA has emerged as a useful tool to further enhance the benefit of reperfusion during PPCI. The landmark TAPAS trial (19) demonstrated that TA prior to stenting resulted in improved myocardial reperfusion, as indicated by myocardial blush grade and ST-segment resolution, and clinical outcome (20) compared with conventional PCI after STEMI, which facilitated the use of this modality as an important myocardial adjunct in this setting. However, although manual TA was associated with significantly lower mortality and reduced major adverse cardiac events in the TAPAS trial (20) and subsequent meta-analyses (21, 22), a recent large trial (23) was not able to confirm the benefit of TA with respect to mortality or other clinical outcome measures at 1 year.

TA and IPOC

Until now, none of the conducted IPOC trials randomly assigned the use of TA which was applied in a small proportion of patients with its use being at operator discretion. Yet, these interventions have the potential to undermine the magnitude of benefit of one another. TA usually re-establishes a significant blood flow in the IRA and the delay between applying the procedure and initiating the IPOC protocol might exceed the very short time frame in which IPOC has been shown to be efficient, potentially modifying the efficiency of IPOC (24). Conversely, the application of the IPOC protocol (before TA) at an inappropriate site might dislodge atherosclerotic plaque or thromboemboli, inducing distal embolization of this material. In this regard, particular attention was paid to execution of the IPOC algorithm upstream of the culprit lesion to preclude inadvertent microembolization during the IPOC protocol in trials led by Ovize and his group [9,10,

(25, 26)], although the application of TA, if performed, and its sequence in relation to the IPOC protocol was not randomized or routinely implemented. In contrast, when the IPOC protocol was performed at the site of the index lesion, where thrombus is maximal, a detrimental effect of IPOC on IS and MVO was reported (11). Thus, distal embolization might have counterbalanced the potential beneficial effects of IPOC and might even have exaggerated final myocardial damage (27). For these reasons, it is of paramount importance to apply TA and IPOC in an appropriate manner and sequence not interfering with each other's merits. The two modalities might even lead to an increased effectiveness resulting from their cumulative action when properly combined in a (routine) standardized fashion, in contrast to previous IPOC trials.

Study Rationale

With multiple etiologies of reperfusion-mediated injury, a strategy aimed at minimizing one part of the process may not have much impact, especially, considering that management of STEMI has evolved substantially over the past decades (e.g., STEMI network activation decreasing treatment delays, more potent antiplatelet and antithrombotic agents maintaining patency of the IRA, and advances in PCI improving its efficacy). Thus, with TA offering the potential to reduce thrombus burden, distal embolization and MVO, and IPOC lethal reperfusion injury, it is hypothesized that combining these two interventions adequately in a standardized fashion would act in concert to modulate multiple components of reperfusion-mediated injury, and in turn, would increase myocardial salvage and reduce ultimate IS in STEMI patients undergoing PPCI. To test this hypothesis, we designed the POstconditioning Rotterdam Trial (PORT).

METHODS

Study Design and Patient Population

The PORT (Dutch Trial Register unique identifier: NTR4040) is a dual-center, prospective, open-label, randomized trial with blinded evaluation of outcomes. The study has been approved by the ethics committee of the participating centers and will take place at the cardiology departments of the Erasmus University Medical Centre in Rotterdam and the Radboud University Medical Centre in Nijmegen, the Netherlands (Appendix 1). All patients with STEMI and candidates for PPCI are considered for participation in the study. The eligibility criteria are outlined in Table I.

Study Objectives and Endpoints

The primary objective of this study is to evaluate whether IPOC immediately after routine TA but before stent implantation results in reduced IS, as measured by delayed

enhancement (DE) cardiac magnetic resonance imaging (MRI) at 3 months, compared with conventional treatment (including routine TA before stent implantation) in STEMI patients. Secondary objectives include investigating whether IPOC after routine TA improves myocardial salvage index; reduces MVO by MRI at 3–5 days, enzymatic IS, micro-circulatory resistance; enhances reperfusion and inflammation markers; and improves clinical outcomes at 1 and 3 months. The primary and secondary endpoints of the study are detailed in Table II.

Randomization and Treatment Protocol

All patients will receive aspirin 250–500 mg intravenously, 5,000 IU heparin and either 600 mg clopidogrel, 60 mg prasugrel, or 180 mg ticagrelor. Notably, the treatment guidelines of the participating hospitals include prasugrel and ticagrelor as first-line treatment options for antiplatelet therapy. After written informed consent and emergent coronary angiography, eligible patients are randomized 1:1 to a strategy of IPOC immediately after manual TA using the Export aspiration catheter (Medtronic, Inc., Minneapolis, MN) followed by stenting of the IRA or to conventional PCI, including TA followed by stenting of the IRA (controls). Randomization will be performed at the catheterization laboratory by a computer-generated random sequence, integrated in a dedicated web-based case report form, and stratified by infarct location and gender. All patients will receive procedural anticoagulation according to practice guideline recommendations (28) and local standards of care. The use of glycoprotein IIb/IIIa inhibitors as a bailout therapy or bivalirudin will be left to operator discretion. In the control group, no additional intervention will be performed after TA during the first 8 min of reperfusion. In the IPOC group, immediately after successful TA but within 1 min of reflow, 4 cycles of 1-min balloon occlusions (4–6 atm) proximal or distal to the culprit lesion will be performed, each separated by 1-min reperfusion intervals (Fig. 1). During inflation of the balloon, one film will be made with a small bolus of contrast to ensure coronary artery occlusion. After completion of the IPOC protocol in the IPOC group and at 8 min of reperfusion in the control group, pre- and poststenting intracoronary hemodynamic measurements (Table II) will be performed using a guidewire tipped with pressure and temperature sensors (PressureWire™ Certus™; St. Jude Medical, Inc., St. Paul, MN) positioned distal to the culprit lesion. Hereafter, coronary angiography will be performed in both groups to assess coronary patency and to estimate the myocardial perfusion index using the blush grade evaluation (29). Standard pharmacological therapies after the procedure will include aspirin, P2Y₁₂ inhibitors, beta-blockers, lipid-lowering agents, and angiotensin-converting enzyme inhibitors or angiotensin-II receptor blockers, according to current guide lines (28).

Table 1. Eligibility Criteria.

Eligibility criteria

Inclusion criteria

Written informed consent

Delay between onset of chest pain and percutaneous coronary intervention ≤ 6 hr in case of inferolateral wall infarction and ≤ 12 hr in case of anterior wall infarction

An occluded infarct-related artery must be demonstrated (TIMI 0-1)

Successful treatment of a culprit artery lesion in the LAD, RCA, or LCX (segment 1,2,3,6,7,11,12, or 13) according to the CASS quantification)

Exclusion criteria

Younger than 18 or older than 75 years of age

Cardiogenic shock defined as a sustained systolic blood pressure ≤ 80 mm Hg despite fluid hydration and/or the inability to discontinue vasopressors in less than 1 hr before

Postcardiac resuscitation

Thrombolytic therapy in the previous week

Myocardial infarction biomarkers at admission > 5 times the upper limit of normal since this implies longer lasting myocardial infarction

TIMI > 1 before intervention or TIMI < 2 after initial thrombus aspiration

Significant collateral blood flow to the distal vasculature of the occluded vessel (Rentrop grade ≥ 2)

An extended myocardial infarction, as evidenced by a new episode of chest pain with new ST-segment elevations and a new CK/CK-MB peak

Documented hospital admission for heart failure

Known pre-existent left ventricular dysfunction measured by any technique (ejection fraction $< 45\%$ prior to current admission for myocardial infarction)

History of known previous myocardial infarction

Prior coronary artery bypass grafting

Moderate to severe cardiac valve disease

Known cardiomyopathy

Congenital cardiac disease

Blood transfusion in the previous 24 hr.

Stroke or transient ischemic attack within the previous 24 hr

Any contra-indication for magnetic resonance imaging, that is

Pacemaker

Cerebrovascular clips

Claustrophobia

Chronic use of anti-inflammatory medication, except for the use of nonsteroidal anti-inflammatory drugs

Serious known concomitant disease with a life expectancy of less than 1 year

Follow-up impossible (no fixed abode)

Previous participation in this study of any other trial within the previous 30 days

CK indicates creatine kinase; CK-MB, creatine kinase myocardial bound; LAD, left anterior descending coronary artery; RCA, right coronary artery; LCX, left circumflex coronary artery; and TIMI, thrombolysis in myocardial infarction. ^{aa}Residual stenosis of culprit lesion $< 50\%$ and TIMI 2-3 after intervention.

MRI Protocol

Contrast-enhanced MRI will be performed early (3–5 days) after STEMI and after 3 months using a 1.5-T, or 3-T scanner using dedicated cardiac surface coils. For LV function cine steady-state free-precession sequences will be used in standard orientations (2-chamber, 4-chamber, and a stack of short-axis slices). Field of view and imaging matrix will be optimized to achieve a resolution of $<1.5 \times 1.5$ mm and a maximum temporal resolution of 50 ms. Slice thickness will be set to 8 mm with for the set of short axis images a gap of 2 mm. We will also evaluate the area at risk (identified with myocardial oedema), applying a breath-hold, black-blood, T2-weighted triple inversion recovery sequence. Orientation of acquisition will be equal to short axis cine imaging with the same slice thickness and gap. For early no-reflow rest first-pass myocardial perfusion will be performed during administration of a gadolinium-based contrast agent (0.10 mmol/kg, Gadovist, Bayer, Mijdrecht, the Netherlands) at a rate of 4.0 ml/s, using a single-shot saturation recovery gradient-echo pulse sequence. Three slices will cover the infarct area as seen during cine imaging over a period of 20–30 sec. Immediately after first-pass perfusion, an additional 0.1 mmol/kg gadolinium-based contrast agent will be administered (cumulative dose 0.2 mmol/kg) for IS and late no-reflow quantification. Late gadolinium enhancement images will be acquired 10–15 min after the second contrast administration using a 2D segmented inversion recovery gradient-echo pulse sequence, with slice position identical to the cine images, including long-axis views. The inversion time will be set to null the signal of viable myocardium (typical range 200–300 ms).

MRI Analysis

All the studies will be analyzed on a remote work-station. For evaluation of LV, T2-weighted, and late gadolinium enhancement images dedicated software: CAAS MRV, 3.4, Pie Medical Imaging, 2011, Maastricht, the Netherlands will be used. LV functional analysis: LV end-diastolic volume and LV end-systolic volume are expressed in milliliters will be calculated using a combination of long axis and short axis images (30). Epicardial and endocardial contours will be automatically detected on short axis images and manually corrected (31). The papillary muscles and trabeculations will be considered to be part of the blood pool. Regional systolic function will be determined using a modified 17-segment model. First-pass perfusion will be evaluated qualitatively for early MVO which will be identified by the presence of a hypoenhancement region. Area at risk will be determined in the T2-weighted short axis images by manual contouring and expressed in mass (g) and as percentage of the LV volume (%). IS will be determined in short axis late enhancement images using semiautomatic contouring (32). In patients with MVO, regions of hypoenhancement will be included in the IS. IS will be expressed in mass (g) and as a percentage of the LV mass (IS%LV). Quantitative analysis of no-reflow will be done in the same slices with manual contouring of the hypoenhanced regions.

Myocardial salvage will be calculated as the difference between the area at risk (in g) minus the IS (in g). Myocardial salvage index will be calculated as the difference between area at risk (g) minus IS (g) divided by the area at risk (g).

Blood Sampling

Blood sampling will be performed before the angiographic procedure and during PCI (from the arterial cannula) and every 6 hr during the first 24 hr after reperfusion, every 12 hr during day 2, once daily on day 3, and at the visits to the outpatient clinic at 1 and 3 months. For cardiac biomarkers, including creatine kinase and its myocardial bound, high-sensitivity troponin T and heart-specific fatty acid binding protein, both peak values and the area under the curve will be determined. Analysis of other biomarkers, including markers of inflammation and NT-proBNP will also be performed (Table II).

Clinical Follow-Up

All patients will be followed up with clinical examination and blood analyses during hospitalization and at 1 and 3 months. All major adverse clinical events during follow-up period will be recorded (Table II).

Statistical Considerations

Primary analyses will be performed according to the intention-to-treat principle for the whole population. An analysis per protocol will also be performed. Continuous variables will be summarized as mean and standard deviation or median and interquartile range, depending on normal distribution and will be compared using the Student's t-test or Mann-Whitney U-test, as appropriate. Categorical variables will be summarized as proportions and compared using the chi-square test or Fisher exact test. Linear regression will be used for comparing IS in relation to the area at risk between treatment groups. The Cox regression will be used to evaluate differences in clinical outcomes between groups. A two-tailed $P < 0.05$ will be considered statistically significant. The primary study endpoint is the IS at 3 months by DE MRI. In a previous series of unselected PPCI-treated STEMI patients in our institution who underwent DE MRI (33), anatomical IS was 35 ± 21 gr at baseline and 24 ± 17 gr at follow-up. Based on an expected relative reduction in IS of 20% by IPOC to 19 ± 9 gr (assuming IS is not normally distributed), 56 patients in each group will be needed to achieve $P < 0.05$ with a power of 80% and a two-tailed test. Assuming a drop-out rate of 10%, the total sample size will consist of (2 x 62) 124 patients randomized equally to the two groups. However, based on a previous trial (34) showing a 12% dropout rate due to the inability to obtain paired cine MRI images, among others, this study will continue enrollment until 124 patients are included with paired MRI studies.

Table 2. Study Endpoints.

Study endpoints
MRI-derived endpoints
Infarct size at 3 months (primary endpoint)
Microvascular obstruction at 3-5 days post-intervention
Myocardial salvage measured as AAR on T2-weighted MRI minus final infarct size on delayed enhancement MRI
Regional myocardial function at 3 months
Left ventricular ejection fraction at 3 months
Cardiac biomarkers
Creatine kinase
Creatine kinase myocardial bound ^a
High sensitivity troponine t ^a
Heart-specific fatty acid binding protein ^b
Reperfusion markers
ST-resolution 60 and 90 min postintervention
Myocardial blush grade
TIMI flow grade
Corrected TIMI frame count
Coronary physiology ^c
Index microcirculatory resistance
Coronary flow reserve
Fractional flow reserve
Inflammation and other markers ^d
Cytokines (interleukins 1 β , 6, 8, 10, 12; tumor necrosis factor- α ; p 70)
N-terminal pro-brain natriuretic peptide
Tissue macrophages
Clinical outcomes
MACE defined as cardiac death, myocardial infarction, coronary bypass grafting or a repeat percutaneous intervention during 3-month follow-up

AAR indicates area at risk; MACE, major adverse cardiac events; MRI, cardiac magnetic resonance imaging; and TIMI, thrombolysis in myocardial infarction.^aboth peak value and 72-hr area under the curve determination.^bmeasurement at 30, 45, and 60 min post-reflow. ^cMeasurement pre- and poststenting.^dChange in concentrations at 3 months relative to 24 hr.

SUMMARY AND CONCLUSION

Currently, there is no effective clinical therapy to limit myocardial reperfusion-mediated injury. PORT will enroll patients undergoing PPCI for STEMI in the early hours of infarct evolution, a time during which myocardial salvage should be possible. It will provide data primarily regarding the efficacy of IPOC immediately after routine TA compared to conventional treatment including TA on MRI-derived MVO at 3–5 days and IS determi-

nation at 3 months. In essence, the trial will provide important information regarding the question whether two interventions offering the potential to modulate different components of reperfusion-mediated injury are able to act jointly and augment their magnitude of benefit by potentially increasing myocardial salvage and reducing ultimate IS in STEMI patients undergoing PPCI.

APPENDIX 1: STUDY ORGANIZATION

Principal investigators: O.C. Manintveld, MD, PhD and F. Zijlstra, MD, PhD, Erasmus MC, Rotterdam. Coordinating investigators: O.C. Manintveld, MD, PhD, Erasmus MC, Rotterdam; T. ten Cate, MD, PhD, UMC St Radboud, Nijmegen.

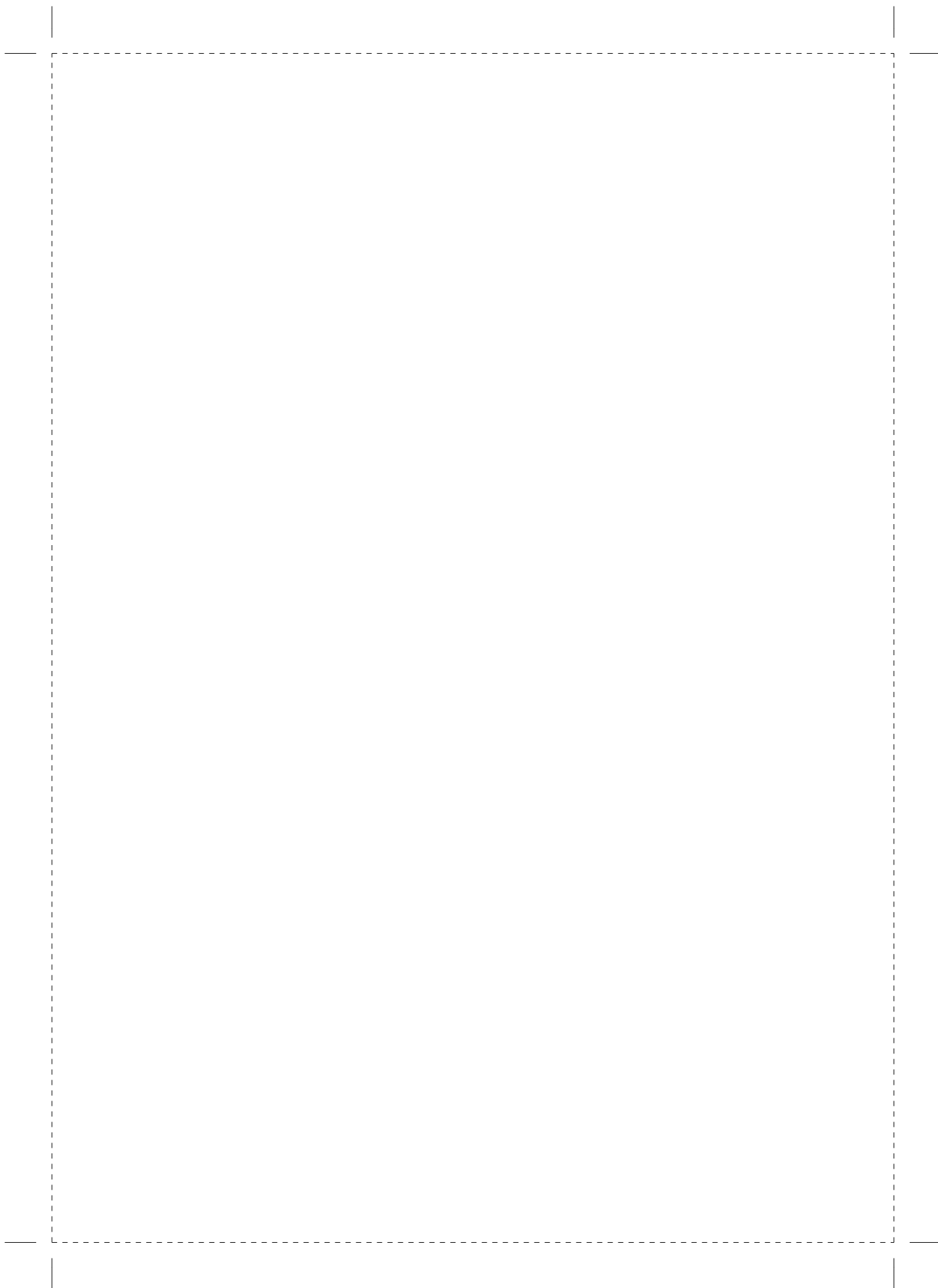
Combined clinical event committee and data safety monitoring board: M.L. Simoons, MD, PhD; A.H.M.M. Balk, MD, PhD and C.A.G.M van Montfort

REFERENCES

1. Braunwald E, Kloner RA. Myocardial reperfusion: a double-edged sword? *The Journal of clinical investigation*. 1985;76(5):1713-9.
2. Yellon DM, Hausenloy DJ. Myocardial reperfusion injury. *The New England journal of medicine*. 2007;357(11):1121-35.
3. Kloner RA, Ganote CE, Jennings RB. The "no-reflow" phenomenon after temporary coronary occlusion in the dog. *The Journal of clinical investigation*. 1974;54(6):1496-508.
4. Zhao ZQ, Corvera JS, Halkos ME, Kerendi F, Wang NP, Guyton RA, et al. Inhibition of myocardial injury by ischemic postconditioning during reperfusion: comparison with ischemic preconditioning. *American journal of physiology Heart and circulatory physiology*. 2003;285(2):H579-88.
5. Yetgin T, Manintveld OC, Duncker DJ, van der Giessen WJ. Postconditioning against ischaemia-reperfusion injury: ready for wide application in patients? *Netherlands heart journal : monthly journal of the Netherlands Society of Cardiology and the Netherlands Heart Foundation*. 2010;18(7-8):389-92.
6. Manintveld OC, Hekker M, van der Ploeg NT, Verdouw PD, Duncker DJ. Interaction between pre- and postconditioning in the in vivo rat heart. *Experimental biology and medicine*. 2009;234(11):1345-54.
7. Manintveld OC, Verdouw PD, Duncker DJ. The RISK of ROCK. *American journal of physiology Heart and circulatory physiology*. 2007;292(6):H2563-5.
8. Laskey WK. Brief repetitive balloon occlusions enhance reperfusion during percutaneous coronary intervention for acute myocardial infarction: a pilot study. *Catheterization and cardiovascular interventions : official journal of the Society for Cardiac Angiography & Interventions*. 2005;65(3):361-7.
9. Staat P, Rioufol G, Piot C, Cottin Y, Cung TT, L'Huillier I, et al. Postconditioning the human heart. *Circulation*. 2005;112(14):2143-8.
10. Thibault H, Piot C, Staat P, Bontemps L, Sportouch C, Rioufol G, et al. Long-term benefit of postconditioning. *Circulation*. 2008;117(8):1037-44.
11. Freixa X, Bellera N, Ortiz-Perez JT, Jimenez M, Pare C, Bosch X, et al. Ischaemic postconditioning revisited: lack of effects on infarct size following primary percutaneous coronary intervention. *European heart journal*. 2012;33(1):103-12.
12. Tarantini G, Favaretto E, Marra MP, Frigo AC, Napodano M, Cacciavillani L, et al. Postconditioning during coronary angioplasty in acute myocardial infarction: the POST-AMI trial. *International journal of cardiology*. 2012;162(1):33-8.
13. Hahn JY, Song YB, Kim EK, Yu CW, Bae JW, Chung WY, et al. Ischemic postconditioning during primary percutaneous coronary intervention: the effects of postconditioning on myocardial reperfusion in patients with ST-segment elevation myocardial infarction (POST) randomized trial. *Circulation*. 2013;128(17):1889-96.
14. Limalanathan S, Andersen GO, Klow NE, Abdelnoor M, Hoffmann P, Eritsland J. Effect of ischemic postconditioning on infarct size in patients with ST-elevation myocardial infarction treated by primary PCI results of the POSTEMI (Postconditioning in ST-Elevation Myocardial Infarction) randomized trial. *Journal of the American Heart Association*. 2014;3(2):e000679.
15. Ovize M, Thibault H, Przyklenk K. Myocardial conditioning: opportunities for clinical translation. *Circulation research*. 2013;113(4):439-50.
16. Krug A, Du Mesnil de R, Korb G. Blood supply of the myocardium after temporary coronary occlusion. *Circulation research*. 1966;19(1):57-62.

17. Hausenloy DJ, Yellon DM. Myocardial ischemia-reperfusion injury: a neglected therapeutic target. *The Journal of clinical investigation*. 2013;123(1):92-100.
18. van Kranenburg M, Magro M, Thiele H, de Waha S, Eitel I, Cochet A, et al. Prognostic value of microvascular obstruction and infarct size, as measured by CMR in STEMI patients. *JACC Cardiovascular imaging*. 2014;7(9):930-9.
19. Svilaas T, Vlaar PJ, van der Horst IC, Diercks GF, de Smet BJ, van den Heuvel AF, et al. Thrombus aspiration during primary percutaneous coronary intervention. *The New England journal of medicine*. 2008;358(6):557-67.
20. Vlaar PJ, Svilaas T, van der Horst IC, Diercks GF, Fokkema ML, de Smet BJ, et al. Cardiac death and reinfarction after 1 year in the Thrombus Aspiration during Percutaneous coronary intervention in Acute myocardial infarction Study (TAPAS): a 1-year follow-up study. *Lancet*. 2008;371(9628):1915-20.
21. Burzotta F, De Vita M, Gu YL, Isshiki T, Lefevre T, Kaltoft A, et al. Clinical impact of thrombectomy in acute ST-elevation myocardial infarction: an individual patient-data pooled analysis of 11 trials. *European heart journal*. 2009;30(18):2193-203.
22. De Luca G, Suryapranata H, van 't Hof AW, de Boer MJ, Hoorntje JC, Dambrink JH, et al. Prognostic assessment of patients with acute myocardial infarction treated with primary angioplasty: implications for early discharge. *Circulation*. 2004;109(22):2737-43.
23. Lagerqvist B, Frobert O, Olivecrona GK, Gudnason T, Maeng M, Alstrom P, et al. Outcomes 1 year after thrombus aspiration for myocardial infarction. *The New England journal of medicine*. 2014;371(12):1111-20.
24. Yetgin T, Magro M, Manintveld OC, Nauta ST, Cheng JM, den Uil CA, et al. Impact of multiple balloon inflations during primary percutaneous coronary intervention on infarct size and long-term clinical outcomes in ST-segment elevation myocardial infarction: real-world postconditioning. *Basic research in cardiology*. 2014;109(2):403.
25. Thuny F, Lairez O, Roubille F, Mewton N, Rioufol G, Sportouch C, et al. Post-conditioning reduces infarct size and edema in patients with ST-segment elevation myocardial infarction. *Journal of the American College of Cardiology*. 2012;59(24):2175-81.
26. Mewton N, Thibault H, Roubille F, Lairez O, Rioufol G, Sportouch C, et al. Postconditioning attenuates no-reflow in STEMI patients. *Basic research in cardiology*. 2013;108(6):383.
27. Heusch G, Kleinbongard P, Bose D, Levkau B, Haude M, Schulz R, et al. Coronary microembolization: from bedside to bench and back to bedside. *Circulation*. 2009;120(18):1822-36.
28. Task Force on the management of STsegmentESoC, Steg PG, James SK, Atar D, Badano LP, Blomstrom-Lundqvist C, et al. ESC Guidelines for the management of acute myocardial infarction in patients presenting with ST-segment elevation. *European heart journal*. 2012;33(20):2569-619.
29. van 't Hof AW, Liem A, Suryapranata H, Hoorntje JC, de Boer MJ, Zijlstra F. Angiographic assessment of myocardial reperfusion in patients treated with primary angioplasty for acute myocardial infarction: myocardial blush grade. *Zwolle Myocardial Infarction Study Group*. *Circulation*. 1998;97(23):2302-6.
30. Kirschbaum SW, Baks T, Gronenschild EH, Aben JP, Weustink AC, Wielopolski PA, et al. Addition of the long-axis information to short-axis contours reduces interstudy variability of left-ventricular analysis in cardiac magnetic resonance studies. *Investigative radiology*. 2008;43(1):1-6.
31. van Geuns RJ, Baks T, Gronenschild EH, Aben JP, Wielopolski PA, Cademartiri F, et al. Automatic quantitative left ventricular analysis of cine MR images by using three-dimensional information for contour detection. *Radiology*. 2006;240(1):215-21.

32. Gruszczynska K, Kirschbaum S, Baks T, Moelker A, Duncker DJ, Rossi A, et al. Different algorithms for quantitative analysis of myocardial infarction with DE MRI: comparison with autopsy specimen measurements. *Academic radiology*. 2011;18(12):1529-36.
33. Baks T, van Geuns RJ, Biagini E, Wielopolski P, Mollet NR, Cademartiri F, et al. Recovery of left ventricular function after primary angioplasty for acute myocardial infarction. *European heart journal*. 2005;26(11):1070-7.
34. Hirsch A, Nijveldt R, van der Vleuten PA, Tio RA, van der Giessen WJ, Marques KM, et al. Intracoronary infusion of autologous mononuclear bone marrow cells in patients with acute myocardial infarction treated with primary PCI: Pilot study of the multicenter HEBE trial. *Catheterization and cardiovascular interventions : official journal of the Society for Cardiac Angiography & Interventions*. 2008;71(3):273-81.



PART 4

OUTCOME STUDIES IN CONGENITAL HEART DISEASE



Chapter 10

Atrial-based pacing has no benefit over ventricular pacing in preventing atrial arrhythmias in adults with congenital heart disease.

Opic P, Yap S-C, **Van Kranenburg M**, Van Dijk AP, Budts W, Vliegen HW, van Erven L, Can A, Sahin G, de Groot NMS, Witsenburg M, Roos-Hesselink JW.

Europace. 2013 Dec;15(12):1757–62.

ABSTRACT

Aims - To determine whether atrial-based pacing prevents atrial arrhythmias in adults with congenital heart disease (CHD) compared with ventricular pacing

Methods and Results - All adult CHD patients from four participating centres with a permanent pacemaker were identified. Patients with permanent atrial arrhythmias at pacemaker implantation and patients who received a pacemaker for treatment of drug-refractory atrial arrhythmias were excluded. The final study population consisted of 211 patients (52% male, 36% complex CHD) who received a first pacemaker for sick sinus dysfunction (n = 82) or atrioventricular block (n = 129) at a median age of 24 years [interquartile range (IQR), 12 - 34]. A history of atrial arrhythmias at implantation was present in 49 patients (23%). Atrial-based pacing was the initial pacing mode in 139 patients (66%) while the others (34%) received ventricular pacing. During a median follow-up of 13 years (IQR, 7 - 21), 90 patients (43%) developed an atrial arrhythmia. Multivariate analysis demonstrated no significant effect of atrial-based pacing on subsequent atrial arrhythmias [hazard ratio (HR), 1.53; 95% confidence interval (CI), 0.91 - 2.56; P = 0.1]. Independent predictors of atrial arrhythmia were history of atrial arrhythmias (HR, 5.55; 95% CI, 3.47 - 8.89; P < 0.0001), older age (18 years) at pacemaker implantation (HR, 2.29; 95% CI, 1.29 - 4.04; P = 0.005), and complex CHD (HR, 1.57; 95% CI, 1.01 - 2.45; P = 0.04)

Conclusion - In contrast to the general population, atrial-based pacing was not associated with a lower incidence of atrial arrhythmia in adults with CHD.

INTRODUCTION

Atrial arrhythmias play an important role in the management of adults with congenital heart disease (CHD) (1). The prevalence of atrial arrhythmias is 15% in the adult CHD population, and the risk of developing atrial arrhythmias increases steadily with age (2). Atrial arrhythmias contribute significantly to morbidity and mortality in this population (2-4). Therefore, strategies to reduce the burden of atrial arrhythmias in this population are highly welcome. An interesting subgroup is the adult CHD population with bradycardia indications for permanent pacemaker implantation. In the general population, several prospective randomized trials have clearly demonstrated that atrial-based pacing ('physiological pacing') reduces the incidence of atrial fibrillation compared with ventricular pacing (5-10). This is not surprising, as loss of atrioventricular (AV) synchrony due to ventricular pacing is associated with increased natriuretic peptide levels, sympathetic nervous activation, and atrial pressures; all factors associated with the development of atrial fibrillation (11, 12). Whether atrial-based pacing is also beneficial in the adult CHD population is not clear (13). The aim of the present multicentre study is to investigate whether atrial-based pacing prevents atrial arrhythmias in adults with CHD.

METHODS

For the present retrospective observational study, all adults with CHD and pacemaker implantation were identified using the nationwide CONgenital CORvita (CONCOR) registry in the Netherlands, and a Belgian tertiary care adult CHD database (14). The central medical ethics committee in the Netherlands and the local Belgian Ethics Board approved the protocol. This study complies with the declaration of Helsinki. Data were collected from medical records and pacemaker databases. Baseline data prior to pacemaker implantation were registered from the patient records including gender, congenital anatomic diagnosis, surgical procedures, and history of atrial arrhythmias. The complexity of the CHD diagnosis was defined as simple, moderate, or complex according to the classification adopted at the American Heart Association Task Force on Adults with CHD (15). Detailed information concerning pacemaker implantation was recorded and included age at implantation, indication for pacemaker implantation, method of implant (endocardial/ epicardial), pacing mode (AAI/VVI/DDD/VDD), and the occurrence of sustained atrial arrhythmias during follow-up. Atrial-based pacing, which includes AAI, DDD, and VDD, was compared with ventricular pacing (VVI). The endpoint was the occurrence of sustained atrial arrhythmias (i.e. intra-atrial reentrant tachycardia, atrial tachycardia, and atrial fibrillation) documented by electrocardiogram, Holter, or stored logs.

Statistical analysis

Continuous data are presented as mean \pm SD or median with interquartile ranges (IQRs) as appropriate. Categorical variables are represented by frequencies and percentages. Comparison of continuous variables between groups was made by unpaired Student's t-tests. In the case of a skewed distribution, the Mann - Whitney U test was used. When comparing frequencies, the χ^2 test or Fisher's exact test was used, where appropriate. Cumulative freedom from atrial arrhythmias was constructed with the use of the Kaplan - Meier method and groups were compared by log-rank statistics. To determine predictors of sustained atrial arrhythmias during follow-up, univariate and multivariate Cox proportional hazard models were constructed after proportional hazard assumptions were verified. The patient was set as unit of analysis and time to first atrial arrhythmia was determined. Candidate variables included: atrial-based pacing, older age (≥ 18 years) at pacemaker implantation, complex CHD, female gender, history of atrial arrhythmia, endocardial pacing system, and sick sinus syndrome. Two-tailed probability values of <0.05 were considered statistically significant. Statistical analysis was performed using the statistical package R (64 bit) for Mac, version 2.14.2.

RESULTS

Patient characteristics

Crosscheck with local pacemaker registries of the four participating tertiary centres revealed a total of 274 patients. After exclusion of 63 patients with permanent or drug-refractory atrial arrhythmias at implantation, 211 patients comprised the final study population. The baseline characteristics of the included patients are summarized in Table 1. Patients with complex CHD comprised 37% of the population, and were mainly patients with transposition of the great arteries and single ventricle physiology. The majority of patients (66%) received atrial-based pacing at initial implantation (Figure 1). There were important baseline differences between patients with atrial-based pacing and those with ventricular pacing. Patients with ventricular pacing more often had the first pacemaker implantation at paediatric/adolescent age (64 vs. 22%, $P < 0.001$) and in an older era (before 1994) (75 vs. 21%, $P < 0.001$). Furthermore, an epicardial pacing system was more often used in patients with ventricular pacing (49 vs. 25%, $P < 0.001$). There was no difference in the complexity of the underlying CHD or the prevalence of a history of atrial arrhythmias between the two groups.

Atrial arrhythmias during follow-up

During a median follow-up of 13 years, 90 patients (43%) developed atrial arrhythmias. Of these 90 patients, 58 patients (64%) had intra-atrial reentrant tachycardia/atrial

Table 1. Baseline Characteristics at first pacemaker implantation

Variable	Total (n = 211)	Atrial based pacing (n = 139)	Ventricular pacing (n = 72)	P value
Age at first implantation (years) a	24 (12-34)	26 (19-39)	12 (7-26)	<0.001
First implant < 18 years	77 (36%)	31 (22%)	46 (64%)	<0.001
Male gender	110 (52%)	72 (52%)	38 (53%)	0.9
Complex CHD	79 (37%)	52 (37%)	27 (38%)	1.0
History of atrial arrhythmias	49 (23%)	36 (26%)	13 (18%)	0.2
Pacemaker implantation before 1994	83 (39%)	29 (21%)	54 (75%)	<0.001
Indication of pacemaker				
Acquired sick sinus syndrome	78 (37%)	45 (32%)	33 (46%)	0.05
Acquired atrioventricular block	69 (33%)	51 (37%)	18 (25%)	0.09
Surgical atrioventricular block	60 (28%)	41 (29%)	19 (26%)	0.6
Surgical sick sinus syndrome	4 (2%)	2 (1%)	2 (3%)	0.6
Pacing mode				
AAI (R)	14 (7%)	14 (10%)	-	< 0.001
DDD (R)	120 (57%)	120 (86%)	-	
VDD (R)	5 (2%)	5 (4%)	-	
VVI (R)	72 (34%)	-	72 (100%)	
Implantation technique				
Endocardial leads	141 (67%)	104 (75%)	37 (51%)	< 0.001
Epicardial leads	70 (33%)	35 (25%)	35 (49%)	

CHD: congenital heart disease

a: expressed as median with IQR

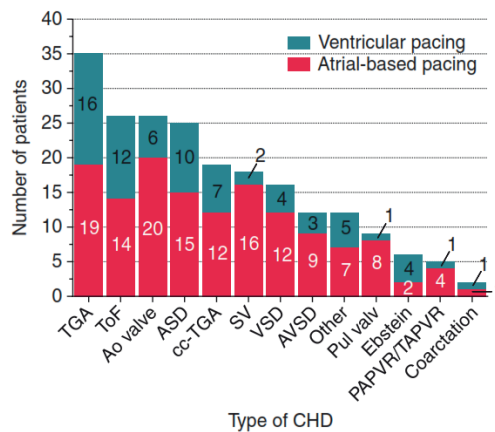


Figure 1. Congenital heart disease (CHD) diagnosis stratified by pacing mode at initial implantation. Ao valve, aortic valve disease; ASD, atrial septal defect; AVSD, atrioventricular septal defect; cc-TGA, congenital corrected transposition of the great arteries; Coarctation, coarctation of the aorta; Ebstein, Ebstein's anomaly; PAPVR/TAPVR, partial or total anomalous pulmonary venous return; Pul valve, pulmonary valve disease; SV, single ventricle physiology; TGA, Transposition of the Great Arteries; ToF, Tetralogy of Fallot; VSD, ventricular septal defect.

tachycardia and 32 patients (36%) had atrial fibrillation as the first presenting atrial arrhythmia. The cumulative rate of atrial arrhythmias was 21, 29, and 39% at 5, 10, and 15 years, respectively. Univariate predictors of atrial arrhythmias are depicted in Table 2. Atrial-based pacing, history of atrial arrhythmias, older age (≥ 18 years) at pacemaker implantation, sick sinus syndrome, complex CHD, and endocardial pacing system were identified as significant univariate predictors of atrial arrhythmias. Multivariate analysis, including all significant univariate predictors, demonstrated that only a history of atrial arrhythmias, older age (≥ 18 years) at pacemaker implantation, and complex CHD were independent predictors of atrial arrhythmias. Atrial-based pacing was not an independent predictor of sustained atrial arrhythmias during follow-up [hazard ratio (HR), 1.53; 95% confidence interval (CI), 0.91 - 2.56; $P = 0.1$] (Figure 2).

Table 2. Predictors of atrial arrhythmia in CHD patients receiving pacemaker therapy

Variable	Univariate analysis		Multivariate analysis	
	Hazard ratio (95% CI)	P value	Hazard ratio (95% CI)	P value
History of atrial arrhythmia	6.90 (4.40-10.8)	< 0.0001	5.55 (3.47-8.89)	< 0.0001
Older age (≥ 18 years) at implant	2.74 (1.71-4.40)	< 0.0001	2.29 (1.29-4.04)	0.005
Sick sinus syndrome	1.99 (1.32-3.01)	0.001	1.50 (0.96-2.36)	0.08
Atrial-based pacing	1.89 (1.19-3.01)	0.007	1.53 (0.91-2.56)	0.1
Complex CHD	1.67 (1.10-2.54)	0.02	1.57 (1.01-2.45)	0.04
Endocardial pacemaker	1.66 (1.06-2.62)	0.02	1.10 (0.65-1.86)	0.7
Female gender	0.71 (0.47-1.08)	0.1		

CHD, congenital heart disease.

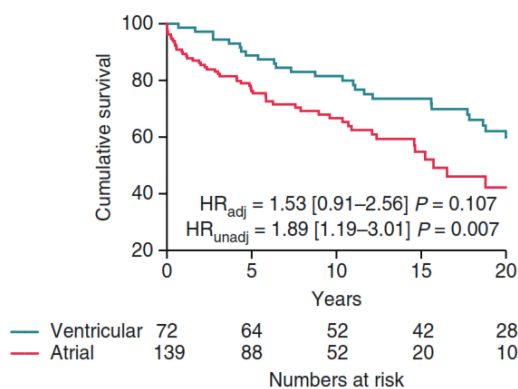


Figure 2. Freedom from atrial arrhythmias for ventricular pacing and atrial-based pacing in patients with CHD. Atrial, atrial-based pacing; HR_{adj} , adjusted hazard ratio, HR_{unadj} , unadjusted hazard ratio; ventricular, ventricular pacing.

Subgroup analysis

Subgroup analysis demonstrates that patients with single ventricle physiology had a high prevalence of previous atrial arrhythmias (50%) at pacemaker implantation

(Table 3). Interestingly, no patient with aortic valve disease was known with a history of atrial arrhythmia prior to implantation. During follow-up, patients with a single ventricle physiology were more prone to develop atrial arrhythmias compared with the other groups (Figure 3, Table 3).

Table 3. Overview of pacemaker details and atrial arrhythmias in selected CHD groups

Variable	Complete TGA ^a (n = 35)	Tetralogy of Fallot (n = 26)	Aortic valve disease (n = 26)	ASD secundum (n = 25)	Single ventricle physiology (n = 18)	P value
Clinical and pacemaker data						
Age at first implantation (years) ^b	18 (8-25)	28 (15-40)	34 (18-51)	27 (15-45)	24 (13-29)	
Male gender	69%	62%	73%	36%	44%	0.03
First implant < 18 years	49%	39%	23%	32%	33%	0.33
History of atrial arrhythmias	29%	23%	0%	28%	50%	0.004
Atrial-based pacing	54%	54%	77%	60%	88%	0.05
Epicardial leads	46%	12%	15%	28%	72%	0.07
Follow-up data						
5 year rate of atrial arrhythmias	20%	25%	0%	21%	51%	-
10 year rate of atrial arrhythmias	32%	30%	11%	27%	60%	-

TGA, transposition of the great arteries; ASD, atrial septal defect. ^a Atrial repair, ^b Expressed as median with IQR.

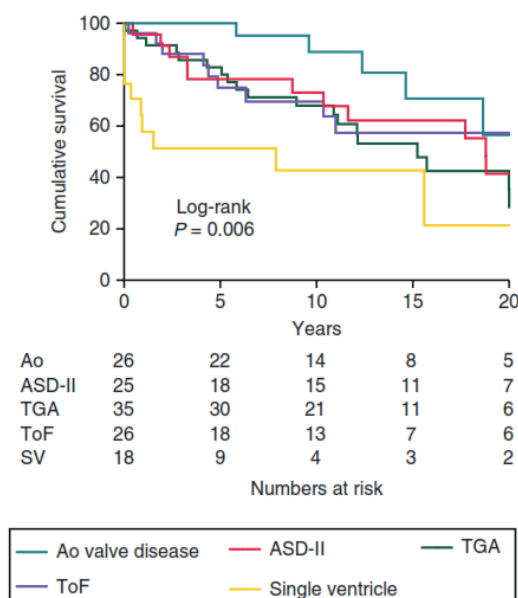


Figure 3. Freedom from atrial arrhythmias for ventricular pacing and atrial-based pacing in patients with CHD. Atrial, atrial-based pacing; HRadj, adjusted hazard ratio; HRunadj, unadjusted hazard ratio; ventricular, ventricular pacing.

Peri-procedural complications

Overall, the peri-procedural complication rate is comparable between patients with atrial-based pacing and those with ventricular pacing (Table 4). When looking at the different complications, there was a higher incidence of pocket infection in those with ventricular pacing when compared with those with atrial-based pacing (5.6 vs. 0%, $P = 0.01$).

Table 4. Peri-procedural complication rates for atrial-based and ventricular pacing

Complication	Total (n = 211)	Atrial-based (n = 139)	Ventricular (n = 72)	P value
Total number of patients	22 (10.4%)	11 (7.9%)	11 (15.3%)	0.1
Lead failure	9 (4.3%)	5 (3.6%)	4 (5.6%)	0.5
Bleeding	3 (1.4%)	3 (2.2%)	-	0.5
Pneumothorax	2 (0.9%)	2 (1.4%)	-	0.5
Pocket infection	4 (1.9%)	-	4 (5.6%)	0.01
Ventricular arrhythmias	2 (0.9%)	-	2 (2.8%)	0.1
Other	2 (0.9%)	1 (0.7%)	1 (1.4%)	1.0

DISCUSSION

In the general population without CHD, atrial-based pacing is beneficial in reducing the incidence of atrial fibrillation compared with ventricular pacing (5-10). The present multicentre study, however, demonstrates that the beneficial effects of atrial-based pacing cannot be extrapolated to the adult CHD population. After correction for important confounders, the incidence of atrial arrhythmias was not different between atrial-based pacing and ventricular pacing. These findings suggest that the mode of pacing does not play an important role in adults with CHD for the reduction of atrial arrhythmias. Patients with CHD are prone to rhythm and conduction disease, which is not surprising considering the underlying congenital cardiac defect, abnormal anatomy, longstanding haemodynamic alterations, and the consequences of surgical interventions. Atrial arrhythmias are a burden to the adult CHD population and are associated with increased morbidity and mortality (2-4). These arrhythmias may be difficult to treat pharmacologically and may require (a combination of) catheter ablation or atrial antitachycardia pacing (16, 17). The purpose of the present study was to explore whether the pacing mode may play a role in the prevention of atrial arrhythmias in CHD patients who had a bradycardia indication for permanent pacing. Loss of AV synchrony due to ventricular pacing may contribute to increased atrial arrhythmogenesis. A meta-analysis by Healey et al. (5), summarizing the data of five randomized trials in patients without CHD, demonstrated that atrial-based pacing reduced the incidence of atrial fibrillation (HR, 0.80; 95% CI, 0.72 - 0.89; $P < 0.001$) and stroke (HR, 0.81; 95% CI, 0.67 - 0.99, $P = 0.035$) compared with ventricular pacing.

Interestingly, our study cohort showed no beneficial effect of atrial-based pacing in preventing atrial arrhythmias. Unexpectedly, we found that atrial-based pacing was associated with an increased risk of atrial arrhythmias in the univariate analysis (HR, 1.89; 95% CI, 1.19 - 3.00, $P = 0.006$). This can be explained by the older age at pacemaker implantation of the cohort who received atrial-based pacing. In the multivariate analysis, the pacing mode was not a predictor of atrial arrhythmias. One previous single-centre study demonstrated that atrial-based pacing did not appear to be protective against subsequent atrial arrhythmias (13). The reason for this lack of beneficial effect of atrial-based pacing may be inherent to the increased vulnerability of the adult CHD population for atrial arrhythmias due to increased natriuretic peptides, altered loading conditions, and presence of surgical atrial scar (18, 19). The loss of AV synchrony induced by ventricular pacing may add little incremental arrhythmogenic risk in such patients, and therefore atrial-based pacing may not be as beneficial as in the general population. This is in agreement with results from the Mode Selection Trial (MOST) in Sinus-Node Dysfunction, where a significant reduction in atrial fibrillation with DDDR pacing when compared with ventricular pacing was observed solely in the subgroup of patients without a history of atrial fibrillation (9). These results support that pacing mode selection is less important with respect to later development of atrial fibrillation in patients who already are at high risk of developing atrial fibrillation. Another explanation for the lack of beneficial effect of atrial-based pacing may be related to the type of atrial arrhythmias in the CHD population. In the present study, the majority of patients with atrial arrhythmias during follow-up experienced intra-atrial reentry tachycardia. Approximately one-third of patients had atrial fibrillation. This ratio is in accordance with a previous study in adult CHD patients who underwent electrical cardioversion (20). Atrial-based pacing may be less beneficial for the prevention of intra-atrial reentrant tachycardia than atrial fibrillation. With regard to predictors for future arrhythmias after pacemaker implantation, Harris and coworkers identified a history of atrial arrhythmias as an independent predictor. In addition, we identified older age (≥ 18 years) at pacemaker implantation and complex CHD as independent predictors of atrial arrhythmias. In particular, patients with single ventricle physiology, mostly Fontan patients with an atriopulmonary connection, are at increased risk of developing atrial arrhythmias later in life (Figure 3). Previous electrophysiological mapping studies have shown that Fontan patients undergo progressive adverse atrial mechano-electrical remodelling with increasing age, rendering them more prone to atrial arrhythmias (19). It is important to stress that the primary aim of the current study was to investigate the role of pacing mode on the incidence of

atrial arrhythmias. This study does not evaluate the potential beneficial effects of atrial-based pacing, by maintaining AV synchrony, on haemodynamic parameters, risk of heart failure, and avoidance of symptoms related to pacemaker syndrome.

The current study demonstrated in a relative high proportion of patients who received ventricular pacing as the initial pacing mode (34%). Implantation of the pacemaker in an older era (before 1994) or at paediatric/adolescent age may explain this phenomenon. The beneficial effects of dual-chamber pacing became more appreciated from the early 1990's (7-9). However in the paediatric population, there is still some debate whether dual-chamber pacing is superior to ventricular pacing (21).

Finally, the rate of peri-procedural complication in the general population without CHD is nearly twice as high with atrial-based pacing compared with ventricular pacing (6.2 vs. 3.2%), primarily due to a significant increase in the rate of lead failure and infarction (5). Our study cohort did not confirm this difference in overall peri-procedural complication rate between patients with atrial-based pacing or ventricular pacing. However, CHD patients with ventricular pacing did demonstrate more pocket infections (5.6 vs. 0%, $P = 0.01$).

Study limitations

This study has limitations inherent to any retrospective study. The major limitation of the present study is the observational study design, which renders the data subject to selection bias. We tried to overcome this limitation by using a multivariate analysis including all potential confounders. Clearly, this approach cannot replace a randomized controlled trial design. Furthermore, despite its relative large size due to its multicentre nature, this study may be underpowered to demonstrate a potential benefit of atrial-based pacing. In addition, the heterogeneity of pacemaker settings limited our ability to draw conclusions with regard to desired pacemaker settings. Owing to the retrospective study design, we had incomplete echocardiographic data limiting our ability to correct for potential confounders such as atrial dilatation or significant atrioventricular regurgitation. Finally, the patient sample is drawn from an adult-based practice and hence skewed towards this age group. Therefore, the patients who died or were lost to follow-up before reaching adulthood are not addressed in this study. Considering the abovementioned limitations, the conclusions of the present study must be drawn with caution.

CONCLUSION

Compared with ventricular pacing, the use of atrial-based pacing was not associated with a lower incidence of atrial arrhythmias in adults with CHD. There is a high vulnerability for developing atrial arrhythmias, especially intra-atrial reentrant tachycardia, which is largely determined by older age, underlying atrial substrate, and prior atrial arrhythmias. Atrial-based pacing may be less beneficial for prevention of intra-atrial re-

entrant tachycardia than atrial fibrillation. To develop effective therapies for preventing atrial arrhythmias, future research should focus on understanding the pathophysiology of atrial arrhythmia in adults with CHD.

Conflict of interest: none declared.

REFERENCES

1. Walsh EP, Cecchin F. Arrhythmias in adult patients with congenital heart disease. *Circulation*. 2007;115(4):534-45.
2. Bouchardy J, Therrien J, Pilote L, Ionescu-Iltu R, Martucci G, Bottega N, et al. Atrial arrhythmias in adults with congenital heart disease. *Circulation*. 2009;120(17):1679-86.
3. Verheugt CL, Uiterwaal CS, van der Velde ET, Meijboom FJ, Pieper PG, van Dijk AP, et al. Mortality in adult congenital heart disease. *European heart journal*. 2010;31(10):1220-9.
4. Yap SC, Harris L, Chauhan VS, Oechslin EN, Silversides CK. Identifying high risk in adults with congenital heart disease and atrial arrhythmias. *The American journal of cardiology*. 2011;108(5):723-8.
5. Healey JS, Toff WD, Lamas GA, Andersen HR, Thorpe KE, Ellenbogen KA, et al. Cardiovascular outcomes with atrial-based pacing compared with ventricular pacing: meta-analysis of randomized trials, using individual patient data. *Circulation*. 2006;114(1):11-7.
6. Connolly SJ, Kerr CR, Gent M, Roberts RS, Yusuf S, Gillis AM, et al. Effects of physiologic pacing versus ventricular pacing on the risk of stroke and death due to cardiovascular causes. Canadian Trial of Physiologic Pacing Investigators. *The New England journal of medicine*. 2000;342(19):1385-91.
7. Andersen HR, Thuesen L, Bagger JP, Vesterlund T, Thomsen PE. Prospective randomised trial of atrial versus ventricular pacing in sick-sinus syndrome. *Lancet*. 1994;344(8936):1523-8.
8. Andersen HR, Nielsen JC, Thomsen PE, Thuesen L, Mortensen PT, Vesterlund T, et al. Long-term follow-up of patients from a randomised trial of atrial versus ventricular pacing for sick-sinus syndrome. *Lancet*. 1997;350(9086):1210-6.
9. Lamas GA, Lee KL, Sweeney MO, Silverman R, Leon A, Yee R, et al. Ventricular pacing or dual-chamber pacing for sinus-node dysfunction. *The New England journal of medicine*. 2002;346(24):1854-62.
10. Toff WD, Camm AJ, Skehan JD, United Kingdom P, Cardiovascular Events Trial I. Single-chamber versus dual-chamber pacing for high-grade atrioventricular block. *The New England journal of medicine*. 2005;353(2):145-55.
11. Horie H, Tsutamoto T, Ishimoto N, Minai K, Yokohama H, Nozawa M, et al. Plasma brain natriuretic peptide as a biochemical marker for atrioventricular sequence in patients with pacemakers. *Pacing and clinical electrophysiology : PACE*. 1999;22(2):282-90.
12. Taylor JA, Morillo CA, Eckberg DL, Ellenbogen KA. Higher sympathetic nerve activity during ventricular (VVI) than during dual-chamber (DDD) pacing. *Journal of the American College of Cardiology*. 1996;28(7):1753-8.
13. Walker F, Siu SC, Woods S, Cameron DA, Webb GD, Harris L. Long-term outcomes of cardiac pacing in adults with congenital heart disease. *Journal of the American College of Cardiology*. 2004;43(10):1894-901.
14. van der Velde ET, Vriend JW, Mannens MM, Uiterwaal CS, Brand R, Mulder BJ. CONCOR, an initiative towards a national registry and DNA-bank of patients with congenital heart disease in the Netherlands: rationale, design, and first results. *European journal of epidemiology*. 2005;20(6):549-57.
15. Warnes CA, Williams RG, Bashore TM, Child JS, Connolly HM, Dearani JA, et al. ACC/AHA 2008 guidelines for the management of adults with congenital heart disease: a report of the American College of Cardiology/American Heart Association Task Force on Practice Guidelines (Writing Committee to Develop Guidelines on the Management of Adults With Congenital Heart Disease). Developed in Collaboration With the American Society of Echocardiography, Heart Rhythm Society, International Society for Adult Congenital Heart Disease, Society for Cardiovascular An-

- giography and Interventions, and Society of Thoracic Surgeons. *Journal of the American College of Cardiology*. 2008;52(23):e143-263.
16. Stephenson EA, Casavant D, Tuzi J, Alexander ME, Law I, Serwer G, et al. Efficacy of atrial antitachycardia pacing using the Medtronic AT500 pacemaker in patients with congenital heart disease. *The American journal of cardiology*. 2003;92(7):871-6.
 17. Yap SC, Harris L, Silversides CK, Downar E, Chauhan VS. Outcome of intra-atrial re-entrant tachycardia catheter ablation in adults with congenital heart disease: negative impact of age and complex atrial surgery. *Journal of the American College of Cardiology*. 2010;56(19):1589-96.
 18. Bolger AP, Sharma R, Li W, Leenarts M, Kalra PR, Kemp M, et al. Neurohormonal activation and the chronic heart failure syndrome in adults with congenital heart disease. *Circulation*. 2002;106(1):92-9.
 19. Yap SC, Harris L, Downar E, Nanthakumar K, Silversides CK, Chauhan VS. Evolving electroanatomic substrate and intra-atrial reentrant tachycardia late after Fontan surgery. *Journal of cardiovascular electrophysiology*. 2012;23(4):339-45.
 20. Kirsh JA, Walsh EP, Triedman JK. Prevalence of and risk factors for atrial fibrillation and intra-atrial reentrant tachycardia among patients with congenital heart disease. *The American journal of cardiology*. 2002;90(3):338-40.
 21. Horenstein MS, Karpawich PP. Pacemaker syndrome in the young: do children need dual chamber as the initial pacing mode? *Pacing and clinical electrophysiology : PACE*. 2004;27(5):600-5.



Chapter 11

Complications of pacemaker therapy in adults with congenital heart disease: A multicenter study.

Opić P, **van Kranenburg M**, Yap S-C, van Dijk AP, Budts W, Vliegen HW, van Erven L, Can A, Sahin G, Theuns DAMJ, Witsenburg M, Roos-Hesselink JW.

Int J Cardiol. 2013;

ABSTRACT

Background - This study aims to investigate indications and complications of permanent cardiac pacing in adults with congenital heart disease (CHD).

Methods and results - Two-hundred and seventy-four CHD patients were identified who underwent permanent pacemaker implantation between 1972 and 2009. The indication for pacing was acquired sinus node or AV node conduction disease (63%), sinus node or AV node conduction disease after cardiac surgery (28%), and drug/arrhythmia-related indications (9%). Patients with complex CHD received a pacemaker at younger age (23 versus 31 years, $p < 0.0001$) and more often received an epicardial pacing system (51% versus 23%, $p < 0.0001$) compared to those with simple or moderate CHD. Twenty-nine patients (10.6%) had a periprocedural complication during the primary pacemaker implantation (general population: 5.2%). The most common acute complications were lead dysfunction (4.0%), bleeding (2.6%), pocket infection (1.5%) and pneumothorax (1.5%). During a median follow-up of 12 years, pacemaker-related complications requiring intervention occurred in 95 patients (34.6%). The most common late pacemaker-related complications included lead failure (24.8%), pacemaker dysfunction/early battery depletion (5.1%), pacemaker migration (4.7%) and erosion (4.7%). Pacemaker implantation at younger age (< 18 years) was an independent predictor of late pacemaker-related complication (adjusted hazard ratio 1.68, 95% confidence interval 1.07 to 2.63, $p = 0.023$).

Conclusions - The risk of periprocedural complications seems higher in the CHD population compared to the general population and more than one-third of CHD patients encountered a pacemaker-related complication during long-term follow-up. This risk increases for those who receive a pacemaker at younger age.

INTRODUCTION

The population of adult patients with congenital heart disease (CHD) is rapidly expanding due to advances in pediatric cardiology and cardiothoracic surgery over the past several decades (1, 2). However, this improved survival following congenital heart surgery is hampered by both structural and electrical late sequelae including atrio-ventricular (AV) block, sinus node dysfunction and atrial arrhythmias (3, 4). Many will require pacemaker therapy and are subject to lifelong need for reinterventions and follow-up (3). Pacemaker implantation in this population may be a challenge due to the complexity of the systemic venous anatomy, venous obstructions and/or residual intra-cardiac shunting (5, 6). Furthermore, pacemaker implantation at young age and the use of epicardial leads have been associated with a high incidence of lead failures during follow-up (6-10). Because of these issues, pacemaker therapy should be considered carefully in the patient with CHD. To improve patient management, knowledge regarding the indications and impact of pacemaker therapy is essential. Unfortunately, these data are scarce for the adult CHD population and large multi-center studies are lacking (5, 6). Furthermore, most CHD studies only focus on lead failure rate. The objective of the present multi-center study is to investigate the indications, periprocedural and late complications of permanent pacemaker therapy in adults with CHD.

METHODS

For the present retrospective study, all adults with CHD and a history of pacemaker implantation were identified from the participating centers using the nationwide CONgenital CORvitia (CONCOR) registry in The Netherlands and a Belgian tertiary care center adult CHD database (11). Patients with a primary electrical disease or cardiomyopathy were excluded from analysis. We also excluded patients with an implantable cardioverter defibrillator as we previously published our experience with this specific patient group (12). Crosscheck with the local pacemaker registries of the four participating tertiary centers revealed a total of 274 patients. The central medical Ethics Committee in The Netherlands and the local Belgian Ethics Board approved the protocol. The authors of this manuscript have certified that they comply with the Principles of Ethical Publishing in the International Journal of Cardiology. Data were collected from medical records and pacemaker databases. Baseline data prior to pacemaker implantation were registered from the patient records including, gender, congenital anatomic diagnosis, surgical procedures, and history of atrial arrhythmias. The complexity of the CHD diagnosis was defined as simple, moderate or complex according to the classification adopted at the American Heart Association Task Force on Adults with CHD (13). Detailed information

concerning the pacemaker implantation was recorded, including age at implantation, indication for pacemaker implantation, method of implant (endocardial/epicardial), pacing mode (AAI, VVI, DDD, or VDD), and periprocedural complications. Periprocedural pacemaker complications were defined as complications occurring in the first 30 days after initial pacemaker implantation. Follow-up data included late pacemaker complications (> 30 days of implantation), major clinical complications and pacemaker reinterventions. Major clinical complications included endocarditis (not pacing system-related), hospitalization for heart failure, stroke, heart transplantation, aborted sudden cardiac death, and death. Documented pacemaker complications were: bleeding (any swelling of the pocket with clinical suspicion of hematoma requiring intervention), pacing system-related endocarditis, erosion (skin penetration of the pacemaker requiring intervention), lead failure (leads repaired, repositioned, replaced, or abandoned due to fracture, insulation break, dislodgment, or abnormalities in pacing or sensing), pacemaker dysfunction/ early battery depletion (pacemaker malfunction requiring pacemaker replacement or early battery depletion necessitating replacement < 3 years post implant), pacemaker migration (requiring pacemaker repositioning), pneumothorax (absence of lung markings over the lung ipsilateral to the pacemaker pocket assessed from x-ray), pocket infection (superficial wound infection), and ventricular arrhythmias (related to lead manipulation). Normal elective replacement of a pacemaker (> 3 years post-implant) or pacemaker upgrade was not considered a pacemaker complication.

Statistical Methods

Continuous data are presented as mean \pm SD. In the case of skewed data, medians and interquartile ranges (IQR) were used. Categorical variables are represented by frequencies and percentages. Comparison of continuous variables between groups was made by unpaired Student's t-tests. In the case of a skewed distribution, the Mann-Whitney U test was used. When comparing frequencies, the chi-square test or Fisher's exact test was used, where applicable. Potential predictors of late pacemaker-related complications were identified by means of Cox regression models, and hazard ratios (HR) and 95% confidence intervals (95%CI) are reported. Variables with a $p < 0.10$ on univariable analysis were included in a multivariable model. Two-tailed probability values < 0.05 were considered statistically significant. Statistical analysis was performed using the statistical package R (64 bit) for Mac, version 2.14.2.

RESULTS

Patient characteristics, pacemaker indications, procedural details

The baseline characteristics of the 274 included patients with CHD are summarized in Table 1. Patients with complex CHD comprised 36% of the population, and were mainly patients with transposition of the great arteries (after atrial correction or congenitally corrected transposition) or single ventricle physiology (Fig. 1). The first implant for most patients occurred in adulthood (70%). Patients with complex CHD underwent primary pacemaker implantation at younger age compared to those with simple/moderate CHD (median age 23 versus 31 years, $p < 0.0001$). Furthermore, patients who received an epicardial pacing system were younger at implantation compared to those with an endocardial pacing system (median age 14 versus 31 years, $p < 0.0001$). The primary pacemaker devices were implanted between March 1972 and Jan 2009.

The major indication for pacemaker therapy was acquired sinus node or AV node conduction disease (63%), the majority of patients had undergone surgery years previously. Seventy-seven patients (28%) required pacing within 30 days after cardiac surgical repair or palliation. The remainder (9%) required pacing for drug-refractory atrial arrhythmias or drug-induced bradycardia. Patients with complex CHD more often received an epi-

Table 1. Baseline characteristics at first pacemaker implantation

Variable	Total (n = 274)	Simple / moderate CHD (n = 175)	Complex CHD (n = 99)	P value
Age at first implantation (years), median (IQR)	26 [15-39]	31 [18-44]	23 [12-32]	< 0.0001
First implant < 18 years	83 (30)	46 (26)	37 (37)	0.06
Male gender	152 (55)	92 (53)	60 (61)	0.20
History of atrial arrhythmias	103 (38)	63 (36)	40 (40)	0.52
Indication for pacemaker				
Acquired SSS	91 (33)	56 (32)	35 (35)	0.57
Acquired AV block	81 (30)	47 (27)	34 (34)	0.19
Surgical AV block	70 (26)	57 (33)	13 (13)	< 0.001
Drug refractory atrial arrhythmias or drug-related bradycardia	25 (9)	14 (8)	11 (11)	0.39
Surgical SSS	7 (3)	1 (1)	6 (6)	0.01
Initial pacing mode: physiologic pacing (DDD, AAI, VDD)	239 (65)	113 (65)	66 (67)	0.86
Implantation technique:				
Endocardial leads	184 (67)	135 (77)	49 (49)	< 0.0001
Epicardial leads	90 (33)	40 (23)	50 (51)	

Data are presented as n (%), unless stated otherwise, AV = atrioventricular; SSS = sick sinus syndrome.

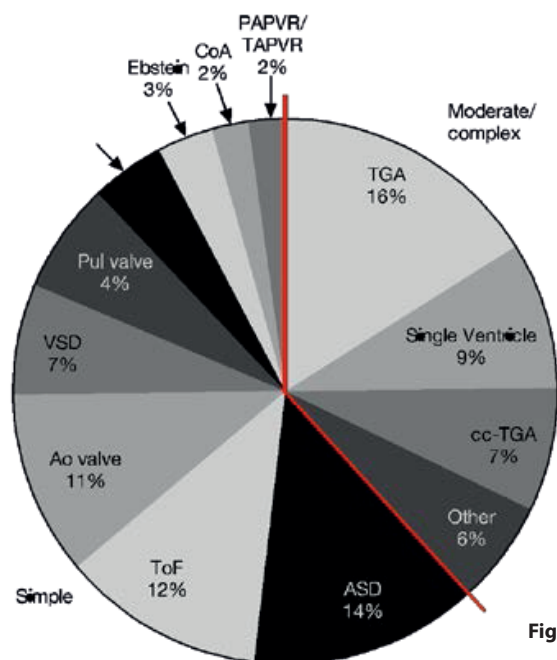


Figure 1.

cardiac pacing system compared to those with simple/moderate CHD (51% versus 23%, $p < 0.0001$). Reasons for implanting an epicardial system were small body size or young age ($n = 22$, 24%), complex systemic venous anatomy or venous access problems ($n = 20$, 22%), concomitant cardiac surgery ($n = 17$, 19%), right-sided mechanical AV valve ($n = 10$, 11%), intra-cardiac shunt ($n = 5$, 6%), endocarditis ($n = 2$, 2%), and unknown reason ($n = 14$, 16%). There were no differences in pacing mode between patients with complex and simple/moderate CHD. Table 2 provides an overview of pacemaker details in the five most common CHD groups. Patients with complete transposition of the great arteries usually required a pacemaker for acquired sick sinus dysfunction. In contrast, patients with aortic valve disease are more prone to surgical AV block. In addition, patients with single ventricle physiology are at high risk of atrial arrhythmias and a significant proportion requires a pacemaker related to treatment of atrial arrhythmias. Table 3 summarizes the initial mode of pacing and change in mode over time. The majority of patients (59%) received atrial-based/physiologic pacing (i.e., AAI, DDD, VDD) at baseline and during to atrial-based/physiologic pacing (i.e., VVI to DDD or VVI to AAI). The pacemaker was upgraded to an implantable cardioverter defibrillator in 20 patients (7%) during follow-up.

Periprocedural complications

Twenty-nine patients (10.6%) experienced one or more peri-procedural complications (< 30 days after implantation) during their first pacemaker implantation (Table 4). The

Table 2. overview of pacemaker details in the five most common CHD groups.

Variable	Complete TGA (n = 45)	Single ventricle physiology (n = 25)	Tetralogy of Fallot (n = 33)	Aortic valve disease (n = 30)	ASD secundum (n = 37)
Clinical					
Age at first implantation (years), median [IQR]	23 [10-27]	24 [15-30]	33 [17-41]	34 [22-50]	35 [18-52]
Follow-up duration (years), median [IQR]	15 [9-20]	8 [2-15]	13 [6-26]	10 [6-16]	12 [8-26]
Male gender	69%	52%	61%	73%	41%
History of atrial arrhythmias	44%	64%	39%	13%	51%
Indication for pacemaker					
Acquired SSS	60%	28%	48%	7%	43%
Acquired AV block	13%	36%	27%	30%	27%
Surgical AV block	7%	12%	18%	60%	16%
Drug-refractory atrial arrhythmias or drug induced bradycardia	11%	20%	6%	3%	14%
Surgical SSS	9%	-	-	-	-
Pacemaker details					
Physiologic pacing	53%	88%	58%	77%	62%
Epicardial leads	42%	76%	12%	17%	22%
Pacemaker complications					
Periprocedural complications	13%	12%	15%	-	8%
Late pacemaker-related complications	38%	20%	24%	23%	32%

Data are presented as percentages, unless stated otherwise, ASD = atrial septal defect; AV = atrioventricular; SSS= sick sinus syndrome; TGA = transposition of the great arteries, ASD = atrial septal defect.

Table 3. Mode of pacing at baseline and at most recent follow-up

Baseline	Follow-up	Number of patients (%)
AAI	AAI	16 (6%)
AAI	DDD	5 (2%)
VVI	VVI	55 (20%)
VVI	DDD	36 (13%)
VVI	AAI	4 (2%)
DDD	DDD	136 (50%)
DDD	VVI	15 (6%)
DDD	AAI	1 (0.4%)
VDD	VDD	3 (1%)
VDD	DDD	2 (0.7%)
VDD	VVi	1 (0.4%)

most common complication was lead failure requiring intervention (4.0%). Patients with complex CHD showed a trend towards more periprocedural complications compared to those with simple/moderate CHD (15% versus 8%, $p = 0.07$). There was a numerical decrease in the incidence of periprocedural complications when primary pacemaker implantations in a more contemporary cohort (1997-2009) were compared to an earlier cohort (1972-1996), however, this was not statistically significant (7.6% versus 13.4%, $p = 0.12$). Younger age (< 18 years) at implantation was not associated with a higher periprocedural complication rate (7.4% versus 11.9%, $p = 0.27$).

Late pacemaker-related complications

During a median follow-up period of 12 years (IQR 6-19 years) 95 patients (35%) experienced a late pacemaker-related complication (Table 5). The most common observed

Table 4. Periprocedural complications during first pacemaker implantation.

Complication	Total (n = 274)	Simple / Moderate CHD (n = 175)	Complex CHD (n = 99)	p-value	General population ^a
Total number of patients	29 (10.6)	14 (8.0)	15 (15.2)	0.07	5.2%
Early lead failure	11 (4.0)	5 (2.9)	6 (6.1)	0.21	2.3%
Bleeding	7 (2.6)	3 (1.7)	4 (4.0)	0.26	0.8%
Pneumothorax	4 (1.5)	2 (1.1)	2 (2.0)	0.62	0.5%
Pocket infection	4 (1.5)	2 (1.1)	2 (2.0)	0.62	0.1%
Ventricular arrhythmias	2 (0.7)	-	2 (2.0)	0.13	0.1%
Other	2 (0.7)	2 (1.1)	-	0.54	0.8%

Data are presented as n (%). CHD = congenital heart disease. ^a Modified from Nowak et al. [14].

complication was lead failure in 68 patients (25%). A large proportion of patients experienced an infection-related complication (pocket infection 4.4%, pacing system-related endocarditis 2.5%). The cumulative rate of late pacemaker-related complication was 8, 19, 28 and 41% at 1, 5, 10 and 15 years, respectively

Predictors of late pacemaker-related complications

Five variables were evaluated as possible predictors for late pacemaker-related complications: young age at implantation (< 18 years), complex CHD, epicardial leads, pacemaker implantation before 1997 and female gender. Only young age at implantation (< 18 years) was an independent predictor of late pacemaker-related complications (adjusted hazard ratio 1.68, 95% confidence interval 1.07 to 2.63, $p = 0.023$) (Table 6, Fig. 2).

Table 5. Late pacemaker –related complications

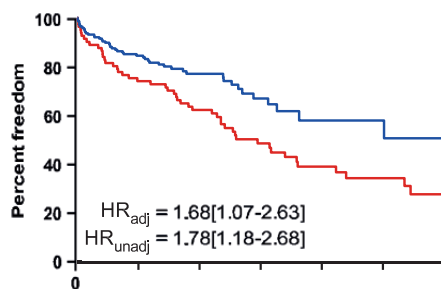
Variable	Total population (n = 274)
Duration of follow-up (years), median (IQR)	12 [6-19]
Total number of patients	95 (34.6)
Late lead failure	68 (24.8)
Pacemaker dysfunction/early battery depletion	14 (5.1)
Pacemaker migration	13 (4.7)
Erosion	13 (4.7)
Pocket infection	12 (4.4)
Pacing system-related endocarditis	7 (2.5)
Other	9 (3.3)

Data are presented as n (%), unless stated otherwise.

Table 6.

Variable	Univariate analysis	Multivariate analysis
	Hazard ratio [95% CI] and p-value	Hazard ratio [95% CI] and p-value
Young age (<18 years) at implantation	1.78 [1.18-2.68], 0.006	1.68 [1.07-2.63], 0.023
Complex CHD	0.94 [0.62-1.43], 0.78	-
Epicardial leads	1.43 [0.95-2.14], 0.09	0.84 [0.53-1.34], 0.52
Pacemaker implantation before 1997 ^a	1.30 [0.80-2.12], 0.29	-
Female gender	1.25 [0.83-1.86], 0.29	-

CHD = congenital heart disease. ^a compared to the period 1997-2009.

**Figure 2.** Pacemaker-related complication event-free survival in two age cohorts

Long-term outcome

During follow-up, a large proportion of patients was hospitalized for heart failure (n = 41, 15%) and ultimately four patients underwent heart transplantation (1.5%). Other clinical events were stroke (n = 13, 4.7%), aborted sudden cardiac death (n = 13, 4.7%) and endocarditis not related to the pacing system (n = 8, 2.9%). Twenty-three patients (8.4%) died during follow-up at a mean age of 46 ± 17 years. The cumulative rate of survival was 99, 96 and 92% at 5, 10 and 15 years, respectively.

DISCUSSION

Several anatomical and pathological issues render pacemaker implantation in patients with CHD more difficult compared to the general population [5,6]. Our study shows that the incidence of periprocedural complications in patients with CHD seems higher than in the general population (10.6% versus 5.2%)(14). Furthermore, more than one-third of our cohort (34.6%) experienced a late pacemaker-related complication during a median follow-up of 12 years. The most common late complication was lead failure necessitating intervention.

CHD patients are prone to rhythm and conduction disease, which is not surprising considering the underlying congenital cardiac defect, longstanding hemodynamic alterations, and the consequences of surgical interventions. Our study demonstrates that the indication for pacemaker therapy is associated with the underlying congenital anatomical diagnosis and the associated cardiac surgical procedures (Table 2). Sinus node dysfunction is a common late sequela in patients who underwent atrial surgery, while acquired AV conduction disorders are more common in those with displacement of the AV node outside the triangle of Koch. Furthermore, certain operations are associated with a high risk of AV block due to proximity of the AV conduction tissue. Besides conduction disorders, drug-refractory atrial arrhythmias are important late complications especially in Fontan patients palliated with an atriopulmonary connection (15).

Implantation of a pacemaker in a patient with CHD can be challenging. Our study population experienced more periprocedural complications (10.6%) compared to the general population. Using data from a large-scale German prospective pacemaker registry ($n = 17,826$, mean age 75 ± 10 years), the incidence of periprocedural complications after first pacemaker implantation was 5.2% in a non-CHD population (14). It is possible that the observed higher periprocedural complication rate in our cohort is related to the younger age of the study population and not to presence of congenital heart disease in itself. However, in our study population age was not associated with periprocedural complication rates.

Although the transvenous approach is the first choice, this approach may not be suitable for those with small body size, an intra-cardiac shunt, anatomic constraints (i.e. Fontan), a right-sided mechanical valve or absence of venous access. One-third of our study population received epicardial leads. This is in agreement with other large single-center studies in adults with CHD (Table 7)(5, 6). Interestingly, in our study the use of epicardial leads was not associated with a higher incidence of late pacemaker-related complications. This is in contrast to previous studies demonstrating a higher lead-failure rate in those with epicardial pacing systems (6-10). Previous studies have shown that the use of steroid-eluting epicardial leads renders the lead failure rate comparable to endocardial leads (10, 16). Data with regard to late pacemaker-related complications in adults with

Table 7. Comparison of studies of pacemaker therapy in adults with CHD

Variable	Walker 2004 [5]	Mcleod 2010 [6]	Opic 2012
Study design	Single-center, retrospective	Single-center, retrospective 1967-2005 (38 years)	Multi-center, retrospective 1972-2009 (37 years)
Time period	NA		
Number of patients	168	106	274
Male	47%	50%	55%
Complex CHD	40%	50%	36%
Indication for pacemaker:			
Acquired SSS	19%	40%	33%
Acquired AV block	27%	33%	30%
Surgical AV block	37%	15%	26%
Drug-refractory atrial arrhythmias or drug-induced bradycardia	9%	12%	9%
Surgical SSS	8%	0%	3%
Age at first implantation (years) ^a	28	37 ± 19	26 [15-39]
First implant < 18 years	33%	16%	30%
Epicardial leads	37%	33%	33%
Periprocedural complications during first implantation	NA	12% ^b	11%
Duration of follow-up (years)	11 ± 9	12 ± 14	26 [15-39]
Late pacemaker-related complications	NA	NA	35%
Lead failure during follow-up	27%	24% ^c	25%
Pocket infection	3.6%	4%	4.4%
Erosion	1.1%	NA	4.7%
Pacing system-related endocarditis	0.6%	NA	2.5%
Mortality	2.4%	20%	8.4%

NA = not available. ^a Data are presented as mean ± SD or median [IQR]. ^b Excluding failed or difficult placement. ^c Unit of analysis: number of leads.

CHD is scarce; most studies only report lead failures (5, 6). Our study demonstrates a high incidence of late pacemaker-related complications after primary device implantation. The overall cumulative 10-year rate of late pacemaker-related complications requiring intervention is 24%. Younger age at implantation (< 18 years) was independently associated with a higher risk of late pacemaker-related complications. This might be explained by the rapid body growth, more active lifestyle and more frequent traumatic events rendering these patients more prone to lead failure, pacemaker migration and erosion. Finally, protracted pacemaker procedures in patients with complex anatomy may render these patients more prone to both acute and late pacing-system-related infections. Our data shows that patients with complex CHD are younger when receiving their first pacemaker compared to those with simple/moderate CHD. The combination

of abovementioned factors may explain why younger patients experience more late pacemaker-related complications.

Study limitations

This study has limitations inherent to any retrospective study. The most important limitation is the potential for missing complications, which were not described in medical records. However, if we have underestimated the complication rate, this only strengthens our conclusion that the CHD population is at higher risk of periprocedural pacemaker complications compared to the general population. Furthermore, the comparison to other CHD studies may be hampered by differences in definitions of pacemaker-related complications (Table 7). The multi-center design limited our ability to collect information on certain risk factors, including pacing and sensing thresholds and lead impedances, the precise method of transvenous vascular access, or the precise types of fixation methods and materials used. The Patient sample is drawn from an adult-based practice and hence skewed towards this age group. Therefore, the patients who died or were lost to follow-up before reaching adulthood are not addressed in this study and this could introduce bias. Finally, although our study is the largest multicenter study in adults with CHD, some of our analyses may be underpowered. Therefore, the conclusions of the present study must be drawn with caution.

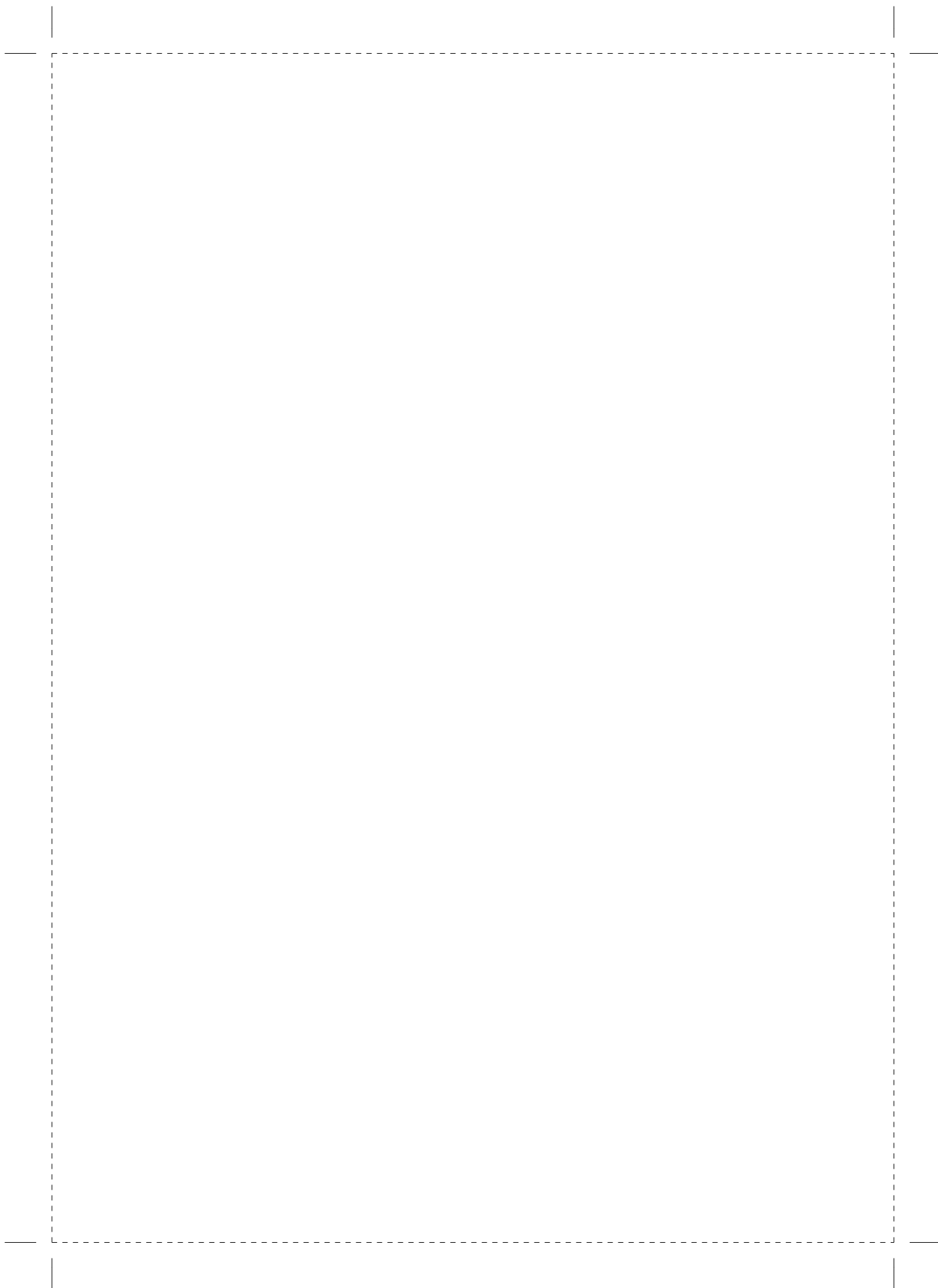
CONCLUSION

In this large multi-center study of adult patients with CHD receiving pacemaker therapy, we found a high incidence of periprocedural and late pacemaker-related complications. More than one third of patients will experience a late pacemaker-related complication during long-term follow-up. The most common late complication was lead failure. Age proved to be an independent predictor of late pacemaker-related complications, with a 68% increased relative risk in CHD patients younger than 18 years. Our data stress that meticulous follow-up is mandatory in this population to identify potential pacemaker complications, especially in the younger and active CHD population.

REFERENCES

1. Warnes CA. The adult with congenital heart disease: born to be bad? *Journal of the American College of Cardiology*. 2005;46(1):1-8.
2. Brickner ME, Hillis LD, Lange RA. Congenital heart disease in adults. First of two parts. *The New England journal of medicine*. 2000;342(4):256-63.
3. Yap SC, Harris L, Chauhan VS, Oechslin EN, Silversides CK. Identifying high risk in adults with congenital heart disease and atrial arrhythmias. *The American journal of cardiology*. 2011;108(5):723-8.
4. Verheugt CL, Uiterwaal CS, van der Velde ET, Meijboom FJ, Pieper PG, van Dijk AP, et al. Mortality in adult congenital heart disease. *European heart journal*. 2010;31(10):1220-9.
5. Walker F, Siu SC, Woods S, Cameron DA, Webb GD, Harris L. Long-term outcomes of cardiac pacing in adults with congenital heart disease. *Journal of the American College of Cardiology*. 2004;43(10):1894-901.
6. McLeod CJ, Attenhofer Jost CH, Warnes CA, Hodge D, 2nd, Hyberger L, Connolly HM, et al. Epicardial versus endocardial permanent pacing in adults with congenital heart disease. *Journal of interventional cardiac electrophysiology : an international journal of arrhythmias and pacing*. 2010;28(3):235-43.
7. Sachweh JS, Vazquez-Jimenez JF, Schondube FA, Daebritz SH, Dorge H, Muhler EG, et al. Twenty years experience with pediatric pacing: epicardial and transvenous stimulation. *European journal of cardio-thoracic surgery : official journal of the European Association for Cardio-thoracic Surgery*. 2000;17(4):455-61.
8. Fortescue EB, Berul CI, Cecchin F, Walsh EP, Friedman JK, Alexander ME. Patient, procedural, and hardware factors associated with pacemaker lead failures in pediatrics and congenital heart disease. *Heart rhythm : the official journal of the Heart Rhythm Society*. 2004;1(2):150-9.
9. Noiseux N, Khairy P, Fournier A, Vobecky SJ. Thirty years of experience with epicardial pacing in children. *Cardiology in the young*. 2004;14(5):512-9.
10. Silvetti MS, Drago F, Grutter G, De Santis A, Di Ciommo V, Rava L. Twenty years of paediatric cardiac pacing: 515 pacemakers and 480 leads implanted in 292 patients. *Europace : European pacing, arrhythmias, and cardiac electrophysiology : journal of the working groups on cardiac pacing, arrhythmias, and cardiac cellular electrophysiology of the European Society of Cardiology*. 2006;8(7):530-6.
11. van der Velde ET, Vriend JW, Mannens MM, Uiterwaal CS, Brand R, Mulder BJ. CONCOR, an initiative towards a national registry and DNA-bank of patients with congenital heart disease in the Netherlands: rationale, design, and first results. *European journal of epidemiology*. 2005;20(6):549-57.
12. Yap SC, Roos-Hesselink JW, Hoendermis ES, Budts W, Vliegen HW, Mulder BJ, et al. Outcome of implantable cardioverter defibrillators in adults with congenital heart disease: a multi-centre study. *European heart journal*. 2007;28(15):1854-61.
13. Warnes CA, Williams RG, Bashore TM, Child JS, Connolly HM, Dearani JA, et al. ACC/AHA 2008 guidelines for the management of adults with congenital heart disease: a report of the American College of Cardiology/American Heart Association Task Force on Practice Guidelines (Writing Committee to Develop Guidelines on the Management of Adults With Congenital Heart Disease). Developed in Collaboration With the American Society of Echocardiography, Heart Rhythm Society, International Society for Adult Congenital Heart Disease, Society for Cardiovascular Angiography and Interventions, and Society of Thoracic Surgeons. *Journal of the American College of Cardiology*. 2008;52(23):e143-263.

14. Nowak B, Misselwitz B, Expert committee 'Pacemaker IoQAH, Erdogan A, Funck R, Irnich W, et al. Do gender differences exist in pacemaker implantation?--results of an obligatory external quality control program. *Europace : European pacing, arrhythmias, and cardiac electrophysiology : journal of the working groups on cardiac pacing, arrhythmias, and cardiac cellular electrophysiology of the European Society of Cardiology*. 2010;12(2):210-5.
15. Stephenson EA, Lu M, Berul CI, Etheridge SP, Idriss SF, Margossian R, et al. Arrhythmias in a contemporary fontan cohort: prevalence and clinical associations in a multicenter cross-sectional study. *Journal of the American College of Cardiology*. 2010;56(11):890-6.
16. Fortescue EB, Berul CI, Cecchin F, Walsh EP, Friedman JK, Alexander ME. Comparison of modern steroid-eluting epicardial and thin transvenous pacemaker leads in pediatric and congenital heart disease patients. *Journal of interventional cardiac electrophysiology : an international journal of arrhythmias and pacing*. 2005;14(1):27-36.



PART 5

**SUMMARY,
GENERAL DISCUSSION
AND FUTURE PERSPECTIVES**

**SUMMARY, GENERAL DISCUSSION
AND FUTURE PERSPECTIVES**

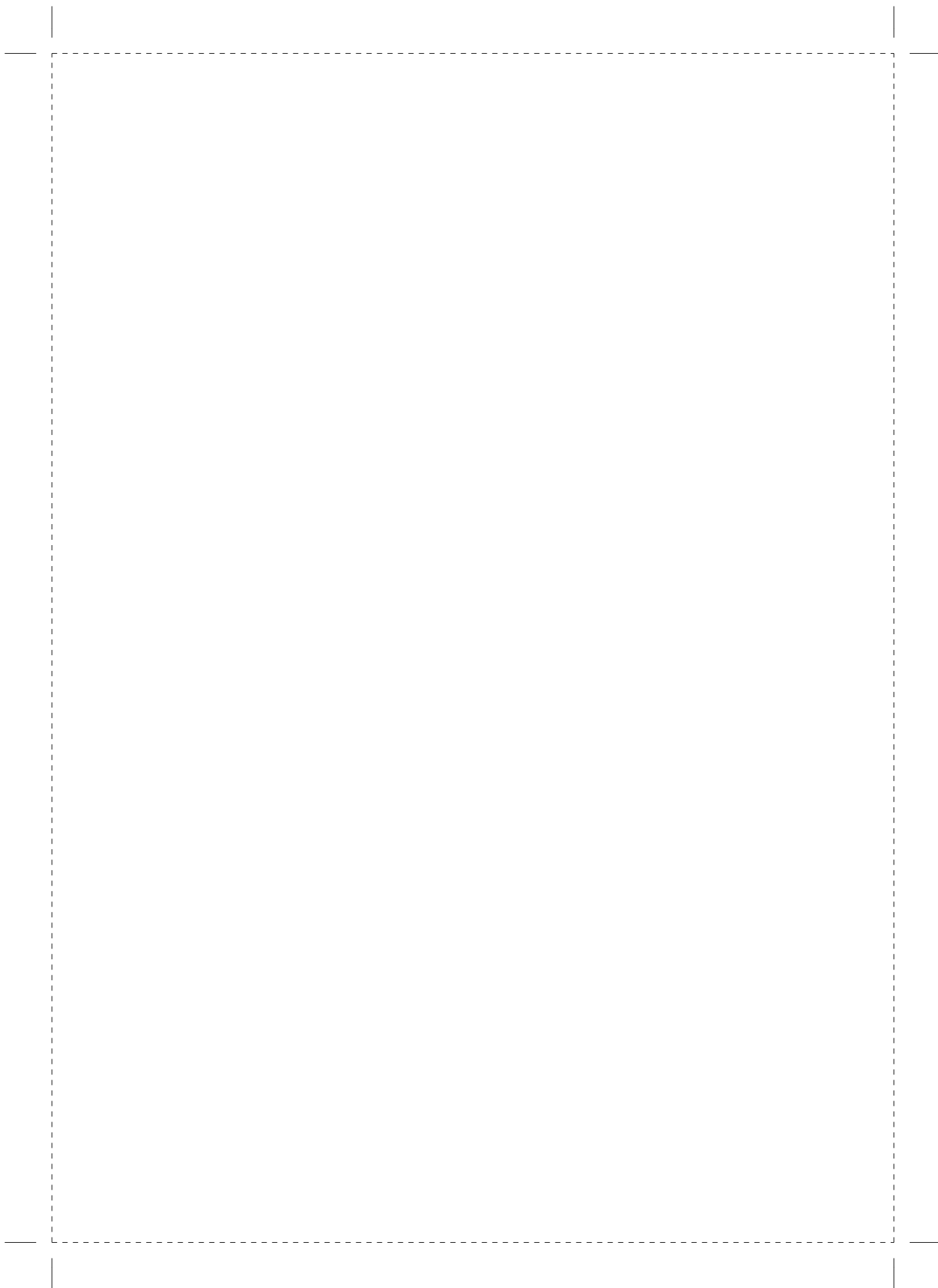
SAMENVATTING EN DISCUSSIE

M. van Kranenburg



Chapter 12

Summary, general discussion
and future perspectives



SUMMARY, GENERAL DISCUSSION AND FUTURE PERSPECTIVES

This thesis investigated the application of cardiac MRI in patients with IHD and CHD and evaluated novel non-invasive MRI techniques in both humans and in a porcine model. As you may notice, unfortunately we did not succeed in finishing our main objective to limit infarct size with bivalirudine. However, the results of this thesis could contribute to the application of MRI in IHD trials and establishing a diagnosis in patients with CHD. Magnetic resonance imaging is an excellent non-invasive imaging modality that depicts the infarct size, global left ventricular function and MO, as well as offers detailed and reproducible information of renal artery characteristics. In this thesis we used novel MRI techniques to measure the effect of novel treatment strategies and to predict prognosis in the clinical setting. In this general discussion we will address the results of our studies against the background of the published literature and its implications for clinical practice and further research.

VALIDATION OF MAGNETIC RESONANCE ANGIOGRAPHY AND CMR 4D FLOW IN PATIENTS WITH RESISTENT HYPERTENSION AND CONGENITAL HEART DISEASE

Magnetic resonance angiography (MRA) is a well-established modality for assessment of renal artery stenosis (1). In **chapter 2** we studied the application of MRA in patients with resistant hypertension in which renal sympathetic denervation, a potential treatment, was performed (2). The purpose of this study was to test the reproducibility of a novel MRA quantitative imaging tool to measure renal artery dimensions and to validate these measurements against invasive intravascular ultrasound (IVUS). Hypertension is a well-known risk factor for ischaemic and diastolic heart failure, and is therefore an attractive parameter to treat. The results might shed further light on the long-term safety of this experimental procedure in patients with resistant hypertension. Some early reports showed that there might be vascular damage induced by the catheters (3, 4). By postdenervation optical coherence tomography, an invasive method to image vessels inside the human body, dissection was seen in 14/50 arteries (32.6%). The percentage of frames with dissection was higher in balloon-based denervation catheters. Using MRA, we tested a non-invasive method to depict the renal arteries, to observe the short-term safety of renal denervation. We used a high resolution spoiled gradient-echo sequence with a high spatial resolution of 0.89 x 0.89 x 1.66 mm. Our study (5) demonstrated that with MRA, renal artery dimensions can be measured with good intraobserver and interobserver variability of less than 5%. The correlation of total lumen volume as measured with MRA against IVUS was excellent with an R-value (a measurement of correla-

tion) of 0.951. The technique required minimal user interaction. To our best knowledge, this is the first study validating MRA measurements with IVUS measurements. In **chapter 3** we describe the results of patients with resistant hypertension treated with renal sympathetic denervation. Besides the fact that initial promising, but non-controlled, studies on clinical efficacy in patients with therapy resistant hypertension were recently challenged by a negative randomised controlled trial, data on long-term safety have been mainly limited to the use of the first generation radiofrequency devices (6-8). In this study, quantitative MRA of patients treated with RDN revealed no significant change in renal artery dimensions up to 12 months follow-up. Over the past 10 years there has been intense research in the development of volumetric visualisation of intra and extra cardiac flow, so called CMR 4D (9). The acquisition offers, in a free breathing acquisition, information about blood flow and anatomical information. In **chapter 4**, we authors evaluated a cloud-based application package that combines volumetric data. Detection and grading of aortic valve regurgitation using CMR 4D flow imaging were evaluated against transthoracic echocardiography. The agreement between the two techniques was good with a kappa value of 0.73. The aortic regurgitation can be well visualised with excellent sensitivity and specificity. To our best knowledge this is the first report on the performance of a cloud-based software that applies eddy currents correction and direct, interactive flow visualisation of CMR 4D flow data in a single tool package by internet connection, with remote processing of transferred raw datasets on high performance workstations. This was a small, single centre study, and as a proof of concept we limited the analysis to the qualitative evaluation of aortic valve regurgitation.

CARDIAC MAGNETIC RESONANCE IMAGING IN ISCHEMIC HEART DISEASE TRIALS

In **chapters 5**, (11), we investigated whether proteins known to stimulate angiogenesis (VEGF), which should help to restore the delivery of oxygen to the heart and may help to reduce the amount of damage. VEGF was delivered by biodegradable microspheres. In 32 swine, the left circumflex artery was occluded for two hours followed by reperfusion. The microspheres appeared to be non-toxic. However no significant reduction in infarct size was noticed between the groups. VEGF165A therapy resulted in a dose dependent increase in microvascular density, but this did not translate into global or regional improvements of cardiac function. More than 50% of patients with heart failure present with heart failure with a preserved ejection fraction (HFpEF) (12, 13). Hospitalised patients with HFpEF have high mortality and rehospitalisation rates, and there is currently no effective treatment available for these patients (14). Common metabolic and cardiovascular risk factors appear to be critical in the development of HFpEF. In **chapter**

6 we tested whether swine exposed to common comorbidities, diabetes mellitus (DM) (induced by streptozotocin), hypercholesterolaemia (HC) (high fat diet) and hypertension (HT) (resulting from renal artery embolisation) are prone to developing HFpEF. In summary, the conclusion of this study was that the combination of three comorbidities leads to systemic inflammation, myocardial oxidative stress and coronary microvascular dysfunction, which may be associated with myocardial stiffening and diastolic dysfunction with a preserved ejection fraction. Paulus and Tschope (15) recently suggested that a systemic inflammatory state produced by cardiovascular comorbidities or risk factors is common in many heart failure patients including those with HFpEF (16, 17). The inflammatory state promotes coronary microvascular endothelial dysfunction, which is characterised by generation of reactive oxygen species and reduced nitric oxide bioavailability, leading to a cascade of signaling events that ultimately promote cardiac fibrosis and myocyte stiffness. It seems to be that multiple common comorbidities, including obesity, diabetes and hypertension, are strongly associated with HFpEF (18). Results in line with this hypothesis were faithfully produced in the present study.

Predicting the future after STEMI has been a subject of great interest since the introduction of MRI (19). Engineers, radiologists and cardiologists play a pivotal role in this challenging field (20). The enormous possibilities in pulse sequences might be disturbing for the end-user, and therefore specific, tailor-made study protocols are used (21, 22). A pPCI is the best available reperfusion strategy to open an occluded artery in patients with STEMI. Despite re-establishing epicardial flow, a failure of reperfusion of the myocardium may occur known as no-reflow due to MO (23). No-reflow occurs in up to 60% of STEMI patients (24). One potential problem is the heterogeneity of MO. Broadly speaking, there are three essential components for MO: (i) ischaemic injury; (ii) reperfusion injury; and (iii) atherothrombotic embolisation (25). Several studies suggest that MO is an important predictor of outcome, but these studies were hampered by a limited number of patients, evaluated a combined clinical endpoint, and were single centre studies. Furthermore, infarct size is intuitively an independent predictor of outcome, and there is conflicting evidence to support this (26) (19).

We performed a collaborative patient pooled analysis to evaluate the prognostic value of infarct size, MO and LVEF. We performed a meta-analysis to evaluate the hypotheses that MO and infarct size, expressed as a percentage of LV mass are independent predictors of major adverse cardiovascular events and cardiac death in patients with STEMI undergoing pPCI (27). The results of this study, as a consequence of collaboration between Dutch, German, French, Spanish, Norwegian, Austrian and U.S. sites, are described in **chapter 7-8**. The main findings - and important part of this thesis - of this study were that: 1) MO was present in > 50% of patients; 2) MO, IS%LV and LVEF were predictors for MACE, with value added to clinical risk factors; 3) MO was associated with cardiac death when adjusted for age and LVEF; and 4) IS%LV, adjusted for MO and LVEF was not an

independent predictor for MACE or cardiac death. The cause of the detrimental effect remains unknown. Baks et al. (28) demonstrated that the presence of MO in dysfunctional myocardial segments was associated with significant thinning of the myocardium compared with normal segments. Nijveldt et al. (29) demonstrated that a significant portion of patients with MO developed a significant increase in LV end-diastolic volume, with no improvement of LVEF. Both studies suggest that MO is involved in adverse ventricular remodeling of the heart after STEMI. Our finding that IS%LV is secondary to MO and LVEF is remarkable. It is important to realise that IS%LV is correlated with LVEF and MO. However, due to its univariate association with outcome (i.e. myocardial infarction, heart failure and cardiac death), its correlation with LVEF and its contribution to the model, as shown as an improvement in the c-index, suggest that IS%LV is an attractive option as an endpoint in IHD trials. Importantly, MO seems to be an important predictor of cardiac death, which might be a game changer, as the focus of current studies is on infarct size. As shown by Ito (30) patients with no-reflow more often had malignant arrhythmias, cardiac tamponade and early congestive heart failure compared with patients without no-reflow. In addition, according to a study previously performed by Ndrepepa et al., there is a clear relationship between infarct size and no-reflow. Infarct size, as estimated by single-photon emission computed tomography (SPECT), was larger in the no-reflow group (percentage of the LV affected: 15% versus 8%, $p < 0.001$) (31). Of the current variables, MO is still the best predictor and probably indicates which patients should be investigated further. The results are in line with the studies of de Waha (32), Eitel (33) and Stone et al. (34). Stone et al. performed a similar pooled patient-level analysis from 10 randomised pPCI trials (total of 2,632 patients) in which infarct size was assessed within one month after randomisation by either CMR imaging or technetium-99m sestamibi SPECT, with clinical follow-up for \geq six months. Infarct size measured by CMR or tc-99m sestamibi SPECT within one month after primary PCI was strongly associated with all-cause mortality and hospitalisation for HF within one year, even after adjustment for multiple clinical, angiographic and treatment parameters (35).

The findings of our study are important in the design of IHD trials for the evaluation of new treatment options. Secondly, although it is clear that CMR offers valuable information in infarct size characterisation, a compelling case for routine clinical use is lacking. In patients with a typical presentation of ACS, there is currently no role in the diagnostic work-up and patient triage (36). To complicate clinical matters further, as highlighted in the editorial of JACC Cardiovascular Imaging by Nathaniel Reichek dedicated to this study, MRI is costly and time consuming (37). Unfortunately we did not take myocardial salvage index and a hypointense infarct core into account in our regression analysis (38, 39). In **chapter 9**, the authors described in detail how to setup a trial to reduce infarct size in patients with STEMI. Postconditioning Rotterdam Trial tested the hypothesis that adding ischaemic postconditioning to routine thrombus aspiration could prevent MO.

In that study a strategy was used in which controlled, brief, intermittent episodes of re-occlusions in the first few minutes of reperfusion were determined to protect the myocardium from lethal reperfusion injury. Unfortunately that study was withdrawn. In this study, MRI was performed early (3-5 days) after STEMI and after three months using a 1.5 or 3 Tesla MRI scanner. In essence, this trial was set up to limit infarct size in patients with STEMI undergoing pPCI.

OUTCOME STUDIES IN CONGENITAL HEART DISEASE

Part 4 describes the application of MRI in patients with CHD. Magnetic resonance imaging provides excellent information for establishing the diagnosis and image-guided treatment of CHD. The enormous possibilities in imaging might be overwhelming. Therefore, a specific question has to be formulated by the referring physician for the radiologist and MRI technicians to tailor the protocol, as the different pulse sequences may provide overlapping information about cardiac anatomy and function. Preferably, data should be checked during or after examination, when the patient is still in the MRI bore. In **chapters 10-11** we aimed to investigate the indication and complications of permanent cardiac pacing in adults with CHD. In this large multicentre study, which included the department of cardiology of Erasmus Medical Center, Rotterdam, the Netherlands, Radboud University Nijmegen Medical Center, Nijmegen, the Netherlands, University Hospitals Leuven, Leuven, Belgium and Leiden University Medical Center, Leiden, the Netherlands, the authors retrospectively identified all adults with CHD and a history of pacemaker implantation using a nationwide CONgenital CORvitia (CONCOR) registry in the Netherlands and a Belgian tertiary care centre adult CHD database. In **chapter 10** we demonstrated that atrial-based pacing was not associated with a lower incidence of atrial arrhythmias (41). In **chapter 11**, our study showed that the incidence of per procedural complications in patients with CHD seems higher than in the general population (10.6% versus 5.2%), suggesting that placement of a pacemaker device might be challenging in this group of patients. Patients with complex CHD more often received an epicardial pacemaker system. Furthermore, more than one-third of our cohort (34.6%) experienced a late pacemaker-related complication during a median follow-up of 12 years. The most common late complication was lead failure necessitating intervention (42).

CONCLUSIONS

In this thesis we showed that cardiac MRI is an excellent tool for the evaluation of atherosclerotic and congenital cardiovascular disease. It is an excellent tool in predicting outcome after STEMI in patients undergoing pPCI. Microvascular obstruction and infarct size were predictors of adverse outcomes. Microvascular obstruction was an independent predictor for cardiac death in patients with STEMI. In patients with resistant hypertension, referred for renal denervation, the renal arteries can be accurately measured with high correlation with invasive measurements and in a reproducible manner. With emerging sequences, such as CMR 4D flow imaging, MRI is an attractive option for establishing a diagnosis and follow-up compared to echocardiography in patients with CHD. The incidence of per procedural complications in patients with CHD seems higher than in the general population suggesting that placement of a pacemaker device might be challenging in this group of patients.

FUTURE PERSPECTIVES

As experienced as a researcher, ambitious projects with highly valued objectives, like the promised bivalirudine CMR study and PORT study which were a main objective of this thesis, will not always take place. Project management and expectation management are essential to maintain good relationships with the stakeholders, like financial stakeholders. Mechanical reperfusion in acute myocardial infarction does not always result in desirable optimal myocardial perfusion (43). As studied in this thesis, the no-reflow phenomenon is an ominous sign beyond its association with infarct size. Prevention of so-called no-reflow is a crucial step in improving the prognosis of patients with STEMI (44). Several strategies including pharmacological and mechanical strategies, and perhaps a combination have been proposed, and despite negative studies (45-49), doubt and discord, the search for the holy grail to limit infarct size and reperfusion injury will continue (50). A better understanding of the no-reflow phenomenon and the visualisation by MRI should enable us to modify the disease process, resulting in a better outcome. Magnetic resonance imaging might play a pivotal role in these experimental studies as a surrogate endpoint, as nowadays the survival of patients with myocardial infarction is good with less than 5% mortality per year. The essential feature of a surrogate endpoint is its sensitivity. Clinical events are generally insensitive markers of disease activity because clinical events are generally rare, and therefore typically require large numbers of individuals to be followed for protracted periods. Surrogate endpoints are more sensitive markers of disease presence, severity or activity, are usually continuous variables, and therefore are 'common' and reduce the sample sizes required to have a certain power to detect

an effect of given clinical and statistical significance. These reductions in sample size can often be translated into reduced cost and duration of a trial compared with a study based on clinical endpoints or trials using less precise surrogates (51) (52). As noted earlier, project and people management are essential to finish these complex projects between multiple departments and stakeholders. Interesting developments are in the field of CHD with advances in 4D flow imaging and echocardiographic techniques such as speckle tracking echocardiography. With the use of speckle tracking, ventricular dysfunction may be detected (53). The application of MRI is increasing in the field of risk stratification in structural and acquired genetic heart disease such as hypertrophic cardiomyopathy, non-compaction cardiomyopathy and ARVC. Beyond the scope of this thesis, one might oversee things from an insurance company perspective, and therefore it is important to evaluate costs and downstream testing in the interesting field of CAD detection (54). Secondly, sudden out of hospital cardiac arrest is an important public health problem with survival rates of less than 10%. An interesting project created by Momont et al. is a collaboration between the Technical University of Delft and University Hospital Leuven to improve the outcome of patients with cardiac arrest due to ventricular fibrillation with a network of drones (55). Their objective is to improve current infrastructure to create a network of drones equipped with an onboard AED, capable of saving lives. This might increase the survival rate of patients with cardiac arrest from 8% to 80%. Furthermore text message alert systems and research into S-ICD's are an interesting development, this might result in a marked increase of survival chances in patients with cardiac arrest (56). We hope our efforts and results may eventually lead to improvement of the prognosis of patients with IHD and CHD.

REFERENCES:

1. Lao D, Parasher PS, Cho KC, Yeghiazarians Y. Atherosclerotic renal artery stenosis--diagnosis and treatment. *Mayo Clinic proceedings*. 2011;86(7):649-57.
2. Krum H, Schlaich M, Whitbourn R, Sobotka PA, Sadowski J, Bartus K, et al. Catheter-based renal sympathetic denervation for resistant hypertension: a multicentre safety and proof-of-principle cohort study. *Lancet*. 2009;373(9671):1275-81.
3. Karanasos A, Van Mieghem N, Bergmann MW, Hartman E, Ligthart J, van der Heide E, et al. Multimodality Intra-Arterial Imaging Assessment of the Vascular Trauma Induced by Balloon-Based and Nonballoon-Based Renal Denervation Systems. *Circulation Cardiovascular interventions*. 2015;8(7):e002474.
4. Karanasos A, Van Mieghem NM, Regar E, Daemen J. Serial imaging observations of vascular healing in a denervation-induced renal artery dissection. *European heart journal*. 2015;36(17):1040.
5. van Kranenburg M, Karanasos A, Chelu RG, van der Heide E, Ouhlous M, Nieman K, et al. Validation of renal artery dimensions measured by magnetic resonance angiography in patients referred for renal sympathetic denervation. *Academic radiology*. 2015;22(9):1106-14.
6. Bhatt DL, Kandzari DE, O'Neill WW, D'Agostino R, Flack JM, Katzen BT, et al. A controlled trial of renal denervation for resistant hypertension. *The New England journal of medicine*. 2014;370(15):1393-401.
7. Symplicity HTN1, Esler MD, Krum H, Sobotka PA, Schlaich MP, Schmieder RE, et al. Renal sympathetic denervation in patients with treatment-resistant hypertension (The Symplicity HTN-2 Trial): a randomised controlled trial. *Lancet*. 2010;376(9756):1903-9.
8. Krum H, Schlaich MP, Sobotka PA, Bohm M, Mahfoud F, Rocha-Singh K, et al. Percutaneous renal denervation in patients with treatment-resistant hypertension: final 3-year report of the Symplicity HTN-1 study. *Lancet*. 2014;383(9917):622-9.
9. Pelc NJ, Bernstein MA, Shimakawa A, Glover GH. Encoding strategies for three-direction phase-contrast MR imaging of flow. *Journal of magnetic resonance imaging : JMRI*. 1991;1(4):405-13.
10. Dyverfeldt P, Bissell M, Barker AJ, Bolger AF, Carlhall CJ, Ebbers T, et al. 4D flow cardiovascular magnetic resonance consensus statement. *Journal of cardiovascular magnetic resonance : official journal of the Society for Cardiovascular Magnetic Resonance*. 2015;17(1):72.
11. Madonna R, Van Laake LW, Davidson SM, Engel FB, Hausenloy DJ, Lecour S, et al. Position Paper of the European Society of Cardiology Working Group Cellular Biology of the Heart: cell-based therapies for myocardial repair and regeneration in ischemic heart disease and heart failure. *European heart journal*. 2016;37(23):1789-98.
12. Dickstein K, Cohen-Solal A, Filippatos G, McMurray JJ, Ponikowski P, Poole-Wilson PA, et al. ESC guidelines for the diagnosis and treatment of acute and chronic heart failure 2008: the Task Force for the diagnosis and treatment of acute and chronic heart failure 2008 of the European Society of Cardiology. Developed in collaboration with the Heart Failure Association of the ESC (HFA) and endorsed by the European Society of Intensive Care Medicine (ESICM). *European journal of heart failure*. 2008;10(10):933-89.
13. Borlaug BA, Jaber WA, Ommen SR, Lam CS, Redfield MM, Nishimura RA. Diastolic relaxation and compliance reserve during dynamic exercise in heart failure with preserved ejection fraction. *Heart*. 2011;97(12):964-9.
14. Ambrosy AP, Fonarow GC, Butler J, Chioncel O, Greene SJ, Vaduganathan M, et al. The global health and economic burden of hospitalizations for heart failure: lessons learned from hospitalized heart failure registries. *Journal of the American College of Cardiology*. 2014;63(12):1123-33.

15. Paulus WJ, Tschope C. A novel paradigm for heart failure with preserved ejection fraction: comorbidities drive myocardial dysfunction and remodeling through coronary microvascular endothelial inflammation. *Journal of the American College of Cardiology*. 2013;62(4):263-71.
16. Rauchhaus M, Doehner W, Francis DP, Davos C, Kemp M, Liebenthal C, et al. Plasma cytokine parameters and mortality in patients with chronic heart failure. *Circulation*. 2000;102(25):3060-7.
17. Deswal A, Petersen NJ, Feldman AM, Young JB, White BG, Mann DL. Cytokines and cytokine receptors in advanced heart failure: an analysis of the cytokine database from the Vesnarinone trial (VEST). *Circulation*. 2001;103(16):2055-9.
18. Alagiakrishnan K, Banach M, Jones LG, Datta S, Ahmed A, Aronow WS. Update on diastolic heart failure or heart failure with preserved ejection fraction in the older adults. *Annals of medicine*. 2013;45(1):37-50.
19. Wu KC, Zerhouni EA, Judd RM, Lugo-Olivieri CH, Barouch LA, Schulman SP, et al. Prognostic significance of microvascular obstruction by magnetic resonance imaging in patients with acute myocardial infarction. *Circulation*. 1998;97(8):765-72.
20. Rochitte CE, Lima JA, Bluemke DA, Reeder SB, McVeigh ER, Furuta T, et al. Magnitude and time course of microvascular obstruction and tissue injury after acute myocardial infarction. *Circulation*. 1998;98(10):1006-14.
21. Kim HW, Farzaneh-Far A, Kim RJ. Cardiovascular magnetic resonance in patients with myocardial infarction: current and emerging applications. *Journal of the American College of Cardiology*. 2009;55(1):1-16.
22. Katus HA, Giannitsis E. Who is David and who is Goliath? There is an urgent need to improve the reference standards for estimation of myocardial infarct size. *JACC Cardiovascular imaging*. 2011;4(5):534-6.
23. Bouleti C, Mewton N, Germain S. The no-reflow phenomenon: State of the art. *Archives of cardiovascular diseases*. 2015;108(12):661-74.
24. Rezkalla SH, Dharmashankar KC, Abdalrahman IB, Kloner RA. No-reflow phenomenon following percutaneous coronary intervention for acute myocardial infarction: incidence, outcome, and effect of pharmacologic therapy. *Journal of interventional cardiology*. 2010;23(5):429-36.
25. Kumbhani DJ, de Lemos JA. Finding an effective treatment for microvascular obstruction in STEMI: a road to perdition? *European heart journal*. 2016;37(24):1920-2.
26. Wu E, Ortiz JT, Tejedor P, Lee DC, Bucciarelli-Ducci C, Kansal P, et al. Infarct size by contrast enhanced cardiac magnetic resonance is a stronger predictor of outcomes than left ventricular ejection fraction or end-systolic volume index: prospective cohort study. *Heart*. 2008;94(6):730-6.
27. van Kranenburg M, Magro M, Thiele H, de Waha S, Eitel I, Cochet A, et al. Prognostic value of microvascular obstruction and infarct size, as measured by CMR in STEMI patients. *JACC Cardiovascular imaging*. 2014;7(9):930-9.
28. Baks T, van Geuns RJ, Biagini E, Wielopolski P, Mollet NR, Cademartiri F, et al. Effects of primary angioplasty for acute myocardial infarction on early and late infarct size and left ventricular wall characteristics. *Journal of the American College of Cardiology*. 2006;47(1):40-4.
29. Nijveldt R, Beek AM, Hirsch A, Stoel MG, Hofman MB, Umans VA, et al. Functional recovery after acute myocardial infarction: comparison between angiography, electrocardiography, and cardiovascular magnetic resonance measures of microvascular injury. *Journal of the American College of Cardiology*. 2008;52(3):181-9.
30. Ito H, Maruyama A, Iwakura K, Takiuchi S, Masuyama T, Hori M, et al. Clinical implications of the 'no reflow' phenomenon. A predictor of complications and left ventricular remodeling in reperfused anterior wall myocardial infarction. *Circulation*. 1996;93(2):223-8.

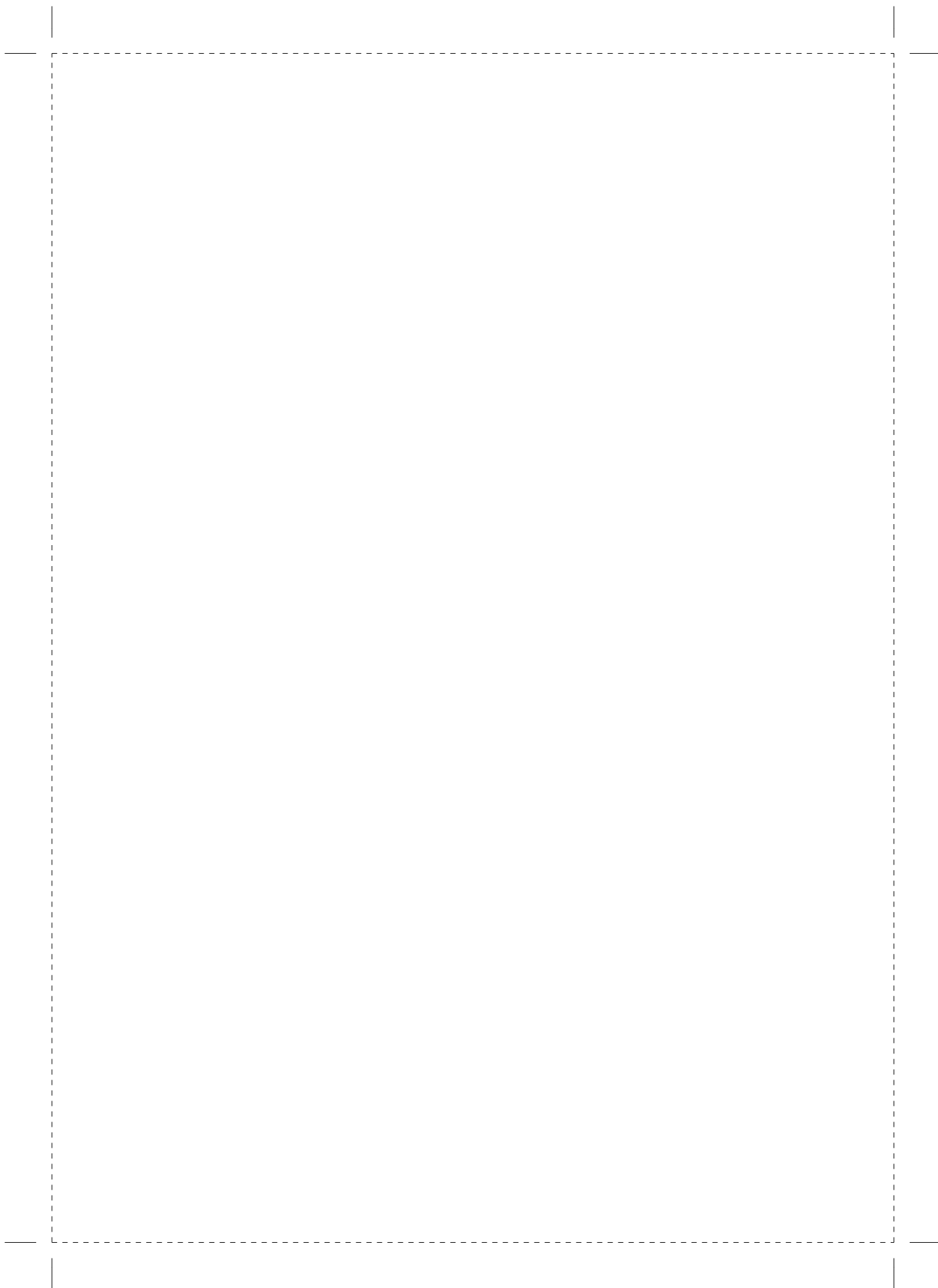
31. Ndrepepa G, Tiroch K, Fusaro M, Keta D, Seyfarth M, Byrne RA, et al. 5-year prognostic value of no-reflow phenomenon after percutaneous coronary intervention in patients with acute myocardial infarction. *Journal of the American College of Cardiology*. 2010;55(21):2383-9.
32. de Waha S, Desch S, Eitel I, Fuernau G, Zachrau J, Leuschner A, et al. Impact of early vs. late microvascular obstruction assessed by magnetic resonance imaging on long-term outcome after ST-elevation myocardial infarction: a comparison with traditional prognostic markers. *European heart journal*. 2010;31(21):2660-8.
33. Eitel I, de Waha S, Wohrle J, Fuernau G, Lurz P, Pauschinger M, et al. Comprehensive prognosis assessment by CMR imaging after ST-segment elevation myocardial infarction. *Journal of the American College of Cardiology*. 2014;64(12):1217-26.
34. Stone GW, Selker HP, Thiele H, Patel MR, Udelson JE, Ohman EM, et al. Relationship Between Infarct Size and Outcomes Following Primary PCI: Patient-Level Analysis From 10 Randomized Trials. *Journal of the American College of Cardiology*. 2016;67(14):1674-83.
35. Gibbons RJ, Araoz P. Does Infarct Size Matter? *Journal of the American College of Cardiology*. 2016;67(14):1684-6.
36. Bogaert J, Eitel I. Role of cardiovascular magnetic resonance in acute coronary syndrome. *Global cardiology science & practice*. 2015;2015(2):24.
37. Reichek N. Meta-analysis of MACE in MI: what's the MO? *JACC Cardiovascular imaging*. 2014;7(9):953-5.
38. Eitel I, Desch S, Fuernau G, Hildebrand L, Gutberlet M, Schuler G, et al. Prognostic significance and determinants of myocardial salvage assessed by cardiovascular magnetic resonance in acute re-perfused myocardial infarction. *Journal of the American College of Cardiology*. 2010;55(22):2470-9.
39. Eitel I, Gehrmlich D, Amer O, Wohrle J, Kerber S, Lauer B, et al. Prognostic relevance of papillary muscle infarction in reperfused infarction as visualized by cardiovascular magnetic resonance. *Circulation Cardiovascular imaging*. 2013;6(6):890-8.
40. Kuijpers JM, van der Bom T, van Riel AC, Meijboom FJ, van Dijk AP, Pieper PG, et al. Secundum atrial septal defect is associated with reduced survival in adult men. *European heart journal*. 2015;36(31):2079-86.
41. Opic P, Yap SC, Van Kranenburg M, Van Dijk AP, Budts W, Vliegen HW, et al. Atrial-based pacing has no benefit over ventricular pacing in preventing atrial arrhythmias in adults with congenital heart disease. *Europace : European pacing, arrhythmias, and cardiac electrophysiology : journal of the working groups on cardiac pacing, arrhythmias, and cardiac cellular electrophysiology of the European Society of Cardiology*. 2013;15(12):1757-62.
42. Opic P, van Kranenburg M, Yap SC, van Dijk AP, Budts W, Vliegen HW, et al. Complications of pacemaker therapy in adults with congenital heart disease: a multicenter study. *International journal of cardiology*. 2013;168(4):3212-6.
43. Magro M, Serruys PW. Acute coronary syndromes: No-reflow--an ominous sign of cardiac dysfunction. *Nature reviews Cardiology*. 2010;7(9):480-2.
44. Magro M, Springeling T, van Geuns RJ, Zijlstra F. Myocardial 'no-reflow' prevention. *Current vascular pharmacology*. 2013;11(2):263-77.
45. Jolly SS, Cairns JA, Yusuf S, Meeks B, Pogue J, Rokoss MJ, et al. Randomized trial of primary PCI with or without routine manual thrombectomy. *The New England journal of medicine*. 2015;372(15):1389-98.
46. Eitel I, Wohrle J, Suenkel H, Meissner J, Kerber S, Lauer B, et al. Intracoronary compared with intravenous bolus abciximab application during primary percutaneous coronary intervention in

- ST-segment elevation myocardial infarction: cardiac magnetic resonance substudy of the AIDA STEMI trial. *Journal of the American College of Cardiology*. 2013;61(13):1447-54.
47. Nazir SA, McCann GP, Greenwood JP, Kunadian V, Khan JN, Mahmoud IZ, et al. Strategies to attenuate micro-vascular obstruction during P-PCI: the randomized reperfusion facilitated by local adjunctive therapy in ST-elevation myocardial infarction trial. *European heart journal*. 2016;37(24):1910-9.
 48. Atar D, Petzelbauer P, Schwitter J, Huber K, Rensing B, Kasprzak JD, et al. Effect of intravenous FX06 as an adjunct to primary percutaneous coronary intervention for acute ST-segment elevation myocardial infarction results of the F.I.R.E. (Efficacy of FX06 in the Prevention of Myocardial Reperfusion Injury) trial. *Journal of the American College of Cardiology*. 2009;53(8):720-9.
 49. Atar D, Arheden H, Berdeaux A, Bonnet JL, Carlsson M, Clemmensen P, et al. Effect of intravenous TRO40303 as an adjunct to primary percutaneous coronary intervention for acute ST-elevation myocardial infarction: MITOCARE study results. *European heart journal*. 2015;36(2):112-9.
 50. Jackson N, Atar D, Borentain M, Breithardt G, van Eickels M, Endres M, et al. Improving clinical trials for cardiovascular diseases: a position paper from the Cardiovascular Round Table of the European Society of Cardiology. *European heart journal*. 2016;37(9):747-54.
 51. Pitcher A, Ashby D, Elliott P, Petersen SE. Cardiovascular MRI in clinical trials: expanded applications through novel surrogate endpoints. *Heart*. 2011;97(16):1286-92.
 52. Engblom H, Heiberg E, Erlinge D, Jensen SE, Nordrehaug JE, Dubois-Rande JL, et al. Sample Size in Clinical Cardioprotection Trials Using Myocardial Salvage Index, Infarct Size, or Biochemical Markers as Endpoint. *Journal of the American Heart Association*. 2016;4(3):e002708.
 53. Mondillo S, Galderisi M, Mele D, Cameli M, Lomoriello VS, Zaca V, et al. Speckle-tracking echocardiography: a new technique for assessing myocardial function. *Journal of ultrasound in medicine : official journal of the American Institute of Ultrasound in Medicine*. 2011;30(1):71-83.
 54. Lubbers M, Dedic A, Coenen A, Galema T, Akkerhuis J, Bruning T, et al. Calcium imaging and selective computed tomography angiography in comparison to functional testing for suspected coronary artery disease: the multicentre, randomized CRESCENT trial. *European heart journal*. 2016;37(15):1232-43.
 55. <http://www.tudelft.nl/actueel/laatste-nieuws/artikel/detail/ambulance-drone-tu-delft-vergroot-overlevingskansen-bij-hartstilstand-drastisch/>.
 56. Pijls RW, Nelemans PJ, Rahel BM, Gorgels AP. A text message alert system for trained volunteers improves out-of-hospital cardiac arrest survival. *Resuscitation*. 2016.



Chapter 13

Samenvatting en discussie



NEDERLANDSE SAMENVATTING

Studies in dit proefschrift omschrijven de toepassing van magnetische resonantie imaging (MRI) in patiënten met ischemische en aangeboren hartziekten. Nieuwe pulse sequenties werden toegepast in zowel patiënten als in experimentele modellen. De resultaten die beschreven zijn in dit proefschrift kunnen worden gebruikt in studies om het effect van nieuwe therapieën tijdens een acuut hart infarct te beoordelen. Verder kan een MRI scan worden gebruikt voor het stellen van een diagnose bij patiënten verdacht voor een aangeboren hartaandoening. MRI is een unieke niet-invasieve beeldvormende technologie waarmee de linker en rechter kamer functie kan worden bestudeerd. Het biedt gedetailleerde en reproduceerbare informatie om de grootte van een hartinfarct te meten. Helaas zijn we er niet in geslaagd om het hoofddoel; het beperken van infarct grootte met bivalirudine te bereiken. In de discussie worden de resultaten van de studies uitgezet tegen de reeds bestaande literatuur.

VALIDATIE EN METHODOLOGIE

Magnetische resonantie imaging is een gebruikelijk diagnosticum om nierslagader vernauwing te meten. In **hoofdstuk 2** hebben we MRI toegepast in patiënten met therapie resistente hypertensie; ofwel hoge bloeddruk. Renale denervatie is een experimentele behandeling en nieuwkomer om therapie resistente hypertensie te behandelen. Het doel van de studie was om de reproduceerbaarheid van de dikte van een nierslagader te meten, en om deze meting te valideren met een invasieve meting (Intravasculaire ultrasound - IVUS). In deze studie gebruikte we een MRI sequentie met een hoge spatiele resolutie. Voxel grootte was 0.89 x 0.89 x 1.66 mm. Onze studie toonde aan dat met MRI de dimensies van een nierslagader met goede reproduceerbaarheid gemeten kunnen worden. De software was eenvoudig te gebruiken. Voor zover onze kennis reikt, is dit de eerste studie die de MRI meting van de nierslagader met invasieve echotechnieken heeft vergeleken. In **hoofdstuk 3**, beschrijven we de resultaten van renale denervatie bij patiënten met therapie resistente hypertensie. Ondanks veelbelovende niet gerandomiseerde studies is er in 2014 een negatieve studie gepubliceerd. Data wat betreft veiligheid is echter schaars en howel er case reports van nier-arterie stenose na denervatie zijn gepubliceerd ontbreekt een kwanitatieve analyse in de wetenschappelijke literatuur. In dit hoofdstuk wordt de veiligheid van deze nieuwe behandeling beschreven. In de laatste tien jaar, is er veel onderzoek verricht naar het in beeld brengen van bloedstromen in het hart. In tien minuten tijd is het mogelijk om doorstroming van het bloed over de hartkleppen zichtbaar te maken. In **hoofdstuk 4**, evalueerde de auteurs een cloud-based applicatie om aorta-klep lekkage te meten. MRI

4D flow beelden en daaruit volgende gemeten variabelen werden gevalideerd ten opzichte van doppler echocardiografie. De metingen kwamen redelijk met elkaar overeen met een kappa waarde (een maat die correlatie meet) van 0.73. Aortaklep lekkage kan goed in beeld worden gebracht met een uitstekende sensitiviteit en specificiteit. Dit was een kleine studie, en als een proof of concept zijn de analyses beperkt gebleven tot aortaklep lekkage.

MRI SURROGAAT EINDPUNTEN IN STUDIES OM HARTINFARCT BEHANDELING TE OPTIMALISEREN

In **hoofdstuk 5**, hebben de auteurs de effecten van groeifactoren bestudeerd na een infarct in een experimenteel model. Er wordt aangenomen dat groeifactoren de wondheling gunstig beïnvloedt en daarmee de schade kan worden beperkt. Deze groeifactoren, vessel endothelial growth factor (VEGF), waren verpakt in kleine polymeerbolletjes. Deze bolletjes zijn via een catheter in een opgewekt infarct (linker kransslagader) bij varkens ingespoten. Dit is gedaan in totaal 32 varkens verdeeld over 3 groepen. Na een periode van 2 uur waarin een kransslagader werd afgesloten werden in 3 behandelgroepen (placebo, lage dosis VEGF en hoge dosis VEGF) deze bolletjes ingebracht. Na 1 en 5 weken werd infarct grootte en linker ventrikel functie beoordeeld. Verder zijn er met histologische technieken vaatdichtheden bekeken. Helaas verbeterde de linker ventrikel functie van de behandelde dieren niet, er werden verder geen significante verschillen gevonden in de grootte van het hartinfarct tussen de verschillende groepen. In **hoofdstuk 6** werd hartfalen onderzocht in een varkensmodel. Meer dan 50% van de patiënten met hartfalen heeft een behouden linker ventrikel ejectie fractie (HFpEF). Patiënten met HFpEF hebben een hoge mortaliteit en worden vaak opgenomen in een ziekenhuis. Op dit moment is er geen effectieve therapie voor deze groep patiënten. Waarschijnlijk ligt er een metabole aandoening of cardiale risicofactoren aan de aan-doening aan ten grondslag. In **hoofdstuk 6** werden varkens aan diabetes (geïnduceerd door streptozotocin), een hoog cholesterol en hypertensie (hoge bloeddruk) bloot gesteld en wilden we weten of ze daarmee HFpEF kunnen ontwikkelen. Concluderend zagen we dat de combinatie kan leiden tot verstijving van de linker ventrikel en ontstond er diastolische dysfunctie. Het voorspellen van prognose na een hartinfarct; een goede of slechte uitkomst na een hartinfarct is belangrijk onderwerp van onderzoek en discussie. Een van de doelen van dit proefschrift was om te beoordelen of met MRI de prognose na een hartinfarct kan worden voorspeld. We hebben een internationale meta-analyse opgezet om de prognostische waarde van infarct grootte, obstructie van de kleine bloedvaten in het infarct gebied en linker ventrikel ejectie fractie (een maat om de knijpkracht van de linker kamer te meten), te onderzoeken. Onze hypothese was,

dat infarct grootte een onafhankelijke voorspeller voor het optreden van hartfalen, een volgend hartinfarct en cardiale dood zou zijn in patiënten met een acuut hartinfarct. De resultaten van een internationale samenwerking van Nederlandse, Duitse, Franse, Spaanse, Noorse, Oostenrijkse en Amerikaanse onderzoekers worden beschreven in **hoofdstuk 7 en 8**. De belangrijkste resultaten worden opgesomd: 1) obstructie van de kleine bloedvaten in het infarct gebied komt in meer dan 50% van de patiënten met een hartinfarct voor; 2) obstructie van de kleine bloedvaten, de grootte van het infarct en linker ventrikel ejectie fractie zijn voorspellers voor het optreden van een volgend hartinfarct, hartfalen of zelfs overlijden; 3) obstructie van de kleine bloedvaten is geassocieerd met overlijden wanneer dat ook wordt gecorrigeerd voor leeftijd en linker ventrikel ejectie fractie; 4) Infarct grootte, gecorrigeerd voor obstructie van de kleine bloedvaten en linker ventrikel ejectie fractie was geen onafhankelijke voorspeller voor een slechte prognose. De oorzaak hiervan blijft speculatief. Baks et al. toonde aan dat de aanwezigheid van obstructie van de kleine bloedvaten in segmenten van de hartspier geassocieerd zijn met het dunner worden van deze segmenten. Nijveldt et al. toonde aan dat een significant deel van de patiënten met obstructie van de kleine bloedvaten dilatatie en afname van de linker ventrikel functie vertoonde. Beide studies toonden aan dat obstructie van de kleine bloedvaten geassocieerd is met negatieve remodelering van de linker ventrikel. Het is opmerkelijk om te zien dat de grootte van het infarct van secundair belang is. Men moet zich realiseren dat infarct grootte en obstructie van de kleine bloedvaten en linker ventrikel functie nauw met elkaar zijn verbonden. Een groot infarct is geassocieerd met obstructie van de kleine bloedvaten en een slechte linker ventrikel ejectie fractie. In lijn met de studie is een recent gepubliceerde meta-analyse van Stone et al. Op een vergelijkbare manier werden 10 individuele studies samen gevoegd. In deze studie werd ook een SPECT scan gebruikt om infarct grootte te bestuderen. De conclusie van deze studie was, dat infarct grootte een onafhankelijke voorspeller was voor het optreden van hartfalen en overlijden na een hartinfarct. De resultaten zijn relevant voor het opzetten van nieuwe studies. Routine gebruik van een MRI na infarct is echter op het moment een brug te ver. Op dit moment is er nog geen plaats in de diagnostische work-up van patiënten met een acuut coronair syndroom. In **hoofdstuk 9** beschrijven de auteurs in detail hoe je een onderzoek kan opzetten om infarct grootte te beperken in patiënten met een hartinfarct. PORT (Post-conditioning Rotterdam Trial) testte de hypothese dat een catheterballon welke een aantal maal werd opgeblazen tijdens een dotterbehandeling, de infarct grootte zou kunnen beperken. Helaas werd deze studie teruggetrokken.

STUDIES IN PATIENTEN MET AANGEBOREN HARTZIEKTEN

MRI is een uitstekend diagnosticum om een aangeboren hartaandoening vast te stellen en om de behandeling te optimaliseren. De mogelijkheden van MRI kunnen overweldigend zijn, daarom moet er een specifieke vraag gesteld worden door de verwijzend specialist aan de radioloog en de laboranten om het juiste protocol in gebruik te nemen, aangezien verschillende puls sequenties overlappende informatie kunnen bevatten. Bij voorkeur moet de data worden gecheckt wanneer de patiënt in de MRI scanner bevindt. In **hoofdstuk 10 en 11** onderzochten we indicaties en complicaties van pacemaker therapie bij patiënten met een aangeboren hartaandoening. In deze grote multicenter studie, deelnemers: Erasmus MC, Rotterdam, Radboud Universiteit Nijmegen, Leiden Universitair Medisch Centrum en Universiteit ziekenhuis Leven, onderzochten de auteurs retrospectief naar complicaties. In **hoofdstuk 10** demonstreerden we dat een atriaal gepaced systeem niet geassocieerd is met met een lage incidentie van ritmestoornissen. In **hoofdstuk 11** toonden we aan dat het per-procedurele complicatie cijfer van pacemaker implantaties hoger lag in vergelijking met de 'algemene patiënten populatie' (10.6% versus 5.2%). Dit suggereert dat het lastige procedure is bij patiënten met een aangeboren hartaandoening. Patiënten met een aangeboren complexe hartaandoening kregen vaker een epicardiaal (op het hart geplaatste leads) lead systeem, via een thoracotomie. Ongeveer een derde van de populatie ervaarde een pacemaker gerelateerde complicatie gedurende een mediaan follow-up van twaalf jaar. Een bekende late complicatie was lead-falen, welke een indicatie was tot interventie.

CONCLUSIES

In dit proefschrift hebben we aangetoond dat met een cardiale MRI een prognose kan worden gegeven na een hartinfarct en na een dotterbehandeling. Obstructie van de kleine bloedvaten en de grootte van het hartinfarct waren voorspellers voor een slechte uitkomst. Verder was obstructie van de kleine bloedvaten een onafhankelijke voorspeller voor overlijden in patiënten met een hartinfarct. In patiënten met therapie resistente hypertensie, verwezen voor renale denervatie, kan MRI uitstekend de grootte van de niervaten beoordelen. Dit kan met hoge accuraatheid en met hoge reproduceerbaarheid in vergelijking met IVUS. Met nieuwe MRI pulse sequenties in aantocht, is MRI een aantrekkelijke manier in de diagnostische work-up bij een vermoeden van een aangeboren hartaandoening. Het optreden van per-procedurele complicaties in patiënten met een aangeboren hartaandoening was hoger dan in de "algemene populatie", wat suggereert dat het een uitdagende ingreep is.

TOEKOMSTPERSPECTIEF

Een dotterbehandeling tijdens een hartinfarct leid niet altijd tot een optimale doorbloeding van de hartspier. Gezien het onderzoek in dit proefschrift is het zogenoemde no-reflow fenomeen een prognostisch ongunstig teken. Preventie van dit fenomeen is een cruciale stap om de prognose van een hartinfarct positief te beïnvloeden. Verschillende strategieën worden geopperd, zowel mechanisch als medicamenteus, om dit te behandelen. Verder zou er onderzoek gedaan kunnen worden naar het succesvol opvolgen van leefstijl adviezen zoals roken, gezien dat het naast longkanker ook hart en vaatziekten kan veroorzaken. Met MRI kan uitstekend obstructie van de kleine bloedvaten in beeld worden gebracht en waarschijnlijk gaat MRI een belangrijke rol spelen in experimentele studies. Interessante ontwikkelingen zijn er in de diagnostiek van aangeboren hartaandoeningen in de vorm van speckle tracking echocardiografie en 4D flow MRI. Mogelijk kan er met speckle tracking hartfalen eerder worden gedetecteerd. Ook neemt de toepassing van MRI toe in het veld van structurele en/of verworven genetische hartafwijkingen zoals hypertrofische cardiomyopathie, non-compaction cardiomyopathie, gedilateerde cardiomyopathie en ARVC in de risicostratificatie en behandeling. Buiten beschouwing van dit proefschrift, blijft het interessant om te kijken vanuit een verzekeringsoogpunt. Gezien de toename van gezondheidskosten voor de samenleving, denk alleen al aan atriumfibrilleren en ischemiedetectie, is onderzoek naar kosten-effectiviteit van behandelingen en 'down-stream testen' wellicht noodzakelijk. Het optreden van een hartstilstand is een belangrijk maatschappelijk probleem met een overlevingskans van ongeveer 10% wanneer een hartstilstand buiten het ziekenhuis optreedt. Een boeiend project van Moment en collega's is het inzetten van drones met AED's om de uitkomst te verbeteren. Verder is een tekst message alert systeem en onderzoek naar subcutane ICD's een kans om de prognose te verbeteren. Project management is essentieel om deze complexe projecten tussen meerdere afdelingen en belanghebbende succesvol af te sluiten. We hopen dat met onze inspanning uiteindelijk de diagnostiek, prognose en levenskwaliteit van patiënten met ischemische en congenitale aandoeningen zal verbeteren.

APPENDIX

ACKNOWLEDGEMENTS / DANKWOORD

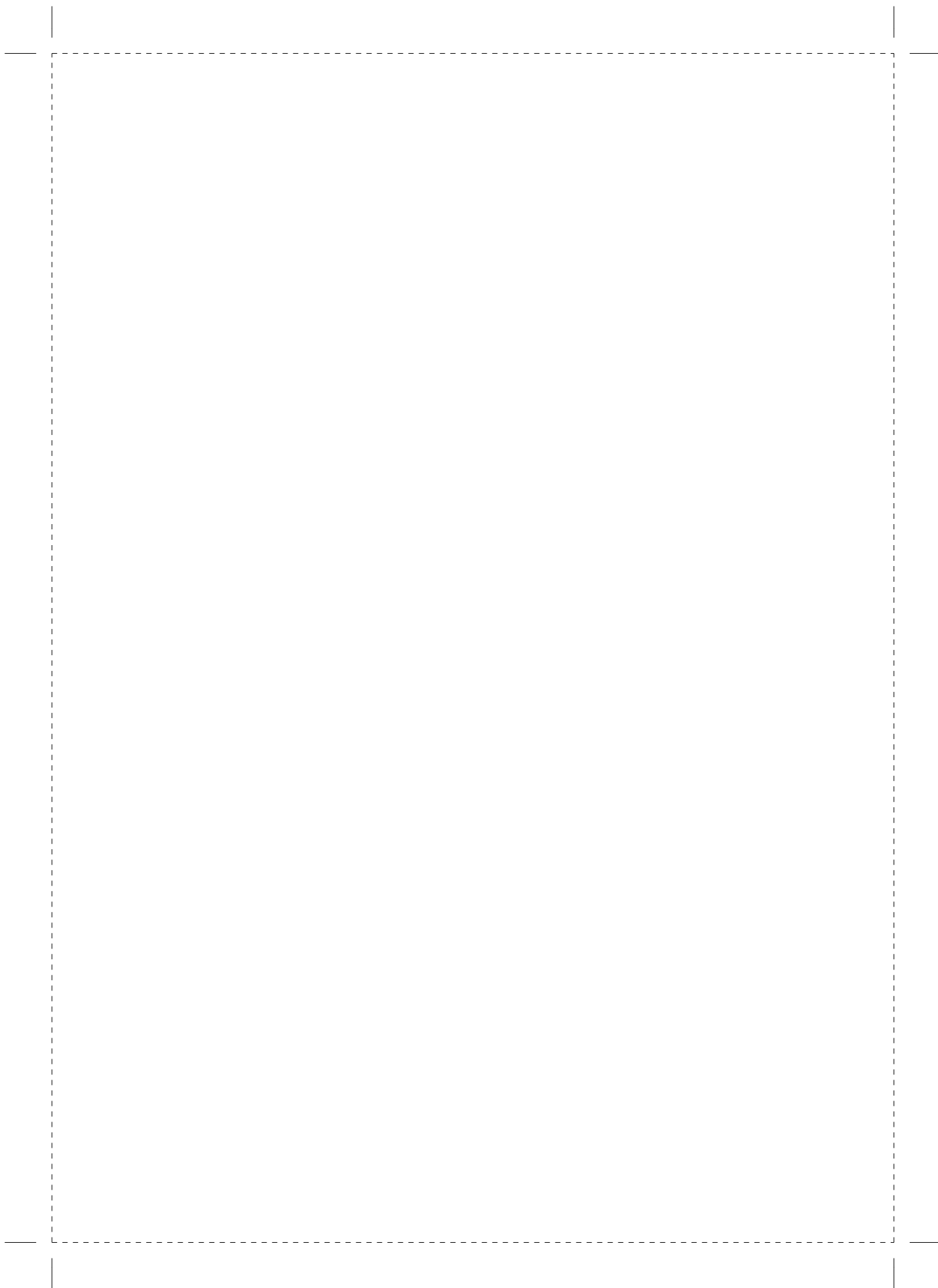
PHD PORTFOLIO SUMMARY

LIST OF PUBLICATIONS / ABSTRACTS

CURRICULUM VITAE

ABBREVIATIONS

M. van Kranenburg



ACKNOWLEDGEMENTS / DANKWOORD

Dit proefschrift kon niet tot stand komen zonder de hulp van vele mensen. Als je iets niet alleen doet, is het schrijven van een proefschrift. Graag wil ik hierbij iedereen bedanken die een bijdrage heeft geleverd, waaronder alle patiënten die hebben deel genomen aan wetenschappelijk onderzoek en die de moeite hebben genomen om een MRI scan te ondergaan. Het dankwoord is ook een stukje geschiedschrijving, en zoals dat met geschiedschrijving gaat, is niet alles op papier de waarheid, aldus Jacky Kennedy en Ockhams Razor.

Mijn excuses voor diegene die ik vergeet te noemen.

STICHTING DIRA

Dhr. Moerman, Zonder u zou dit proefschrift niet zijn geschreven. Dit soort wetenschap kan niet achter een bureau of door een commissie worden uitgevoerd. De motiverende gesprekken en het gegeven vertrouwen, toen het u beloofde bivalirudine (obstructie van de kleine bloedvaten) project, dat niet van de grond is gekomen voor dit proefschrift, zal ik niet vergeten. Daarvoor in de plaats zijn andere MRI studies gekomen.

Ik heb u leren kennen als een ondernemer. Om Richard Branson te citeren: Ondernemers beschikken over de dynamiek om iets nieuws te beginnen, om de wereld op een andere manier dan anderen te bekijken. Ze scheppen kansen die anderen niet perse zien en hebben de moed het erop te wagen. Dank voor uw persoonlijke vertrouwen in het thoraxcentrum, Rotterdam. Hartelijk dank voor de financiële steun en het eindeloze vertrouwen. Ik vond het een voorrecht u te mogen ontmoeten.

Dhr. van 't Zelfde en dhr. Olmer. Dank voor de gesprekken om MRI onderzoek na een hartinfarct te verrichten en om deze methode bij aangeboren hartaandoeningen naar een volgend niveau te brengen. De bedrijfskundige input was inspirerend.

Prof. dr. R.J.M. van Geuns, beste Robert-Jan, je onderzoekslijn begon in de cardiale beeldvorming door middel van MRI richtte zich in eerste instantie op beeldvorming van de hartspier en kransslagaderen. Inmiddels bent u professor in de interventiecardiologie. Ik dank je voor de mogelijkheden die je hebt geboden, de vele uren die besteed zijn aan onderzoek, en je tips in de patiënt pooled analysis.

Prof. dr. F. Zijlstra, Het was een eer om op uw afdeling in het Thoraxcentrum in het Erasmus MC in Rotterdam te mogen werken. Dank voor de mogelijkheden op uw afdeling en uw steun.

Prof. dr. G.P. Krestin, U was voorzitter van de Europese Radiologie Vereniging (ESR) tijdens dit traject. De afdeling radiologie is plezierig en warm. Bovendien voorzien van de

nieuwste beeldvormende technologie. Mede is het daardoor een geweldige omgeving voor het uitvoeren van onderzoek. Dit proefschrift was gezien de verrichte MRI-scans zonder uw afdeling niet mogelijk. Verder heb ik kennis gemaakt met de research commissie. De commissie is een belangrijk middel om pijnpunten gedurende het verrichten van onderzoek bloot te leggen; een potentiële kans voor de cardiologie afdeling. Ik voelde me thuis op uw afdeling.

Prof. dr. J.W. Roos-Hesselink, beste Jolien, dank u voor de onvoorwaardelijke steun tijdens het promotie-traject, woorden schieten hierbij tekort. Ik begon de onderzoeksperiode op uw afdeling tijdens mijn studie geneeskunde en daarmee staat u aan het begin van mijn carrière. Dank ook voor de fijne gesprekken en vele uren begeleiding op persoonlijk vlak in crisis-tijden met daarbij het geduld, adviezen en het vertrouwen. Je hebt me door dit traject heen gesleept en je interventies en gesprekken met de sponsors waren onmisbaar.

Prof.dr. H.J. Lamb, Prof.ir. H. Reiber, Prof.dr. N. van Royen, dank voor het plaatsnemen in de promotiecommissie.

Prof. H. Thiele, from Leipzig University, Germany, many thanks for your contribution and evaluation of our manuscript during the international patient pooled analysis, discussed as first during the conference EuroCMR 2012 in Vienna. I regard your research as exemplary, and is frequently published in the high-impact scientific journals i.e. European Heart Journal and the Journal of American College of Cardiology. You inspired me.

Prof. dr. D. Atar, dear Dan, as skillfull as Thor Heyerdahl during his Kon-Tiki expedition, many thanks for your collaboration during der patient pooled analysis. "placebo-group" data from the FX06-trial, published in the JACC, was an excellent contribution. I am greatly in debted to this dedicated cardiologist. **Dr. I. Eitel, dr. S. de Waha, dr. A. Cochet, prof. dr. Y. Cottin, prof. dr. P. Buser, dr. E. Wu, dr. D. Lee, prof. dr. V. Bodi, dr. G. Klug, prof. dr. B. Metzler, dr. R. Delewi, prof. dr. P. Bernhardt, prof. dr. W. Rottbauer**, many thanks for your enthusiasm and contribution during der patient pooled analysis. **Prof. dr. ir. E. Boersma**, hartelijk dank voor de "time-dependent c-statistics". **Dr. M. Magro**, one of the first projects during this thesis brought me to a passionate cardiologist. Beste Michael, voor vragen vloog je over vanuit Malta, inmiddels ben je gepromoveerd met een indrukwekkend dik proefschrift! What a great sigh of relief and satisfaction when the paper was published!

Andre Uitterdijk, Richard, Felix, dr. H. van Beusekom, het proefdieronderzoek was interessant, en de T1 mapping was uitdagend en overigens geflopt en misschien een grote bel in de cardiale imaging. De varkens met een infarct, mede gescand door **Tirza Springeling**, hebben een extra dimensie gegeven aan dit proefschrift en geresulteerd

in drie prachtige publicaties en een bookchapter! **Prof. dr. D.J. Duncker**, tijdens de studie geneeskunde inspireerde u me voor de cardiologie gedurende de "Frank-Starling-curves" colleges in het eerstejaar. Dank voor uw bijdrage met het MEDIA, diastolisch hartfalen project, in dit proefschrift aldus beschreven.

Dr. V. de Beer, Dr. O. Sorop, Dr. I. Heinonen, beste Vincent en Oana, proefdieronderzoek was intensief, maar het zweten resulteerde in een mooie publicatie.

Dr. J. Daemen, beste **Joost**, je doorzettingsvermogen om complexe multi-disciplinaire studies op het gebied van renale denervatie op te zetten is indrukwekkend. **Dr. O.C. Manintveld**, beste **Olivier**, dank voor de ondersteuning en het invullen van het co-promotor schap. **beste Tuncay Yetgin**, dank voor jullie support en tips. **Gyula Kotek, Mika Vogel, Piotr Wielopolski** who invented physics, but still it remains difficult to explain it to a PhD student. I enjoyed your stay in the MRI-cockpit. **Henk Smit, Ruben Pellicer, Dirk Poot, Wyke Huizinga, Wiro Niessen Gavin Houston**, brilliant engineers from Erasmus MC, thanks for your support to understand to get things done at Erasmus MC. **Prof. Dr. A. van der Lugt**, dank voor het gebruik maken van het proefpersonen-METC-protocol. **Ron van Domburg**, dank voor statistische ondersteuning. **Dr. M. Witsenburg, Dr. J.A.A.E. Cuypers, Dr. A.E. van den Bosch, Dr. S.C. Yap**, dank voor jullie hulp en tips in de LOPAC en 4D flow artikelen, verder jullie ondersteuning in prille begin van de carrière! **Timo Baks**, je hebt me in je vrije tijd geleerd om een cardiale MRI in een patiënt met een STEMI te maken. **Dr. M. Michels**, beste **Michelle**, Dank voor de ketenzorg.

Dr. S.W.M. Kirschbaum, beste **Sharon**. Dank voor de altijd prettige samenwerking en het vertrouwen toen je me in contact bracht met je co-promotor voor de sollicitatie voor een promotie-plek.

Bob van Buuren, Greg Ogrodnick, Circle Cardiovascular Imaging, Calgary, dank voor de samenwerking met de T1 mapping. **Karel van den Hengel, Jean-Paul Aben, Pie Medical Imaging, Maastricht**, dank voor de samenwerking in het beoordelen van de MRI scans.

Speciale dank gaat uit naar naar de cardiale beeldvorming groep, onderzoekers van CA207a en de congenitale cardiologie groep, arts-assistenten, arts-onderzoekers en MRI laboranten.

Dr. K. Nieman, beste **Koen**. Van oudsher lijkt er een scheiding te zijn binnen de cardiale imaging groep, door super-specialisatie, tussen de MRI-groep en de CT-groep, waarbij de CT-groep wat betreft aantal promovendi de overhand heeft. Dank je voor het kunnen meegenieten van de vruchten van de succesvolle CT-groep in de afgelopen jaren. Ik geniet van je onderwijs, dank voor je ondersteuning en succes in de VS. Je vertrek is een aderlating voor de cardiale imaging groep.

Dr. M. Ouhlous, beste **Mohamed**, de rust zelve. Dank voor de altijd prettige samenwerking, ik heb veel van je geleerd gedurende de MRI besprekingen.

Dr. A. Moelker, beste Adriaan, dank voor je hulp met MRI protocollen voor de renale denervatie.

Dr. R. Budde, beste **Ricardo**, succes tijdens het PET-CT onderzoek.

Alexia Rossi, **Anoeshka Dharampal**, **Lisan Neefjes**, **Gert-Jan Richter ten Kate**, het was erg prettig om met een nuchtere Rotterdammer te werken **Admir Dedic**, dank voor de adviezen **Marisa Lubbers**, succes met de CT-studies en het afronden van je promotie **Raluca Gabriela Saru Chelu**, het was fijn met iemand te sparren in de "MRI-groep" **Adriaan Coenen**, succes met de 4D flow en CT studies **Philip Linsen**; inmiddels al beroemder dan papa Linsen te Breda, **Laurens Swart and international research fellows**, **Atsushi Kono (Japan)**, **Akira Kurata (Japan)**, **Kevin Wanambiro Were (Kenya)**, habari dactari za asabuhi?

Andrea, **Chiara**, **Michela**, **Sara (Italy)**. Dank voor jullie support, succes met het afronden van de studies. Het was een voorrecht om bij jullie op de kamer te schrijven.

Petra Opic, **Titia Ruys**, **Jannet Eindhoven**, **John Younge**, **Denise van der Linde**, **Myrthe Menting**, binnenkort repetitie van de Olmo house band? **Vivan Baggen**, **Iris van Hagen**, **Allard van den Hoven**

Antonios Karanasos, **Nienke van Ditzhuijzen**, **Marijn Hol**, **Jors van der Sijde**, **Cor-dula Felix**, **Hannah van Velzen**, **Pieter Vriesendorp**, **Stijn van den Oord**, **Jin Ming Cheng** **Jonathan Lipton**, **Marius Szymanski**.

MRI en CT technici / planners.

Sylvia, **Sita**, **Hanneke**, **Erna**, **Anja**, **Teun** dank voor de samenwerking. Bedankt voor de tallozen keren dat ik even tussendoor kon scannen. Bedankt voor alle praktische zaken en hun flexibiliteit die als onderzoeker broodnodig zijn.

Mart Rentmeester, **Jeroen van IJperen** de heren achter de schermen.

Ton Everaers

Alle collega's van de cardiologie, cardiothoracale chirurgie en radiologie afdeling van het Amphia ziekenhuis te Breda wil ik graag bedanken voor de samenwerking en hun flexibiliteit. In het bijzonder:

dr. R.P. Wielenga, afdelingshoofd van een professionele en sterk geoutilleerde afdeling, voor zijn continue enthousiasme en optimisme, dank voor uw steun

dr. J. Schaap, **dr. S.G. Molhoek**

dr. H.J. Houtgraaf, **dr. D. Segers**, **drs. K. Urgel**, chefs de clinique

dr. E. Sanders, **dr. D. Haans**, **dr. M.M. Krouwels**, **dr. M.F.A.M Sturm**, radiologen, bedankt voor het betrekken in de ischemie detectie met adenosine stress MRI. Hartelijk dank.

Collega's van de cardiothoracale chirurgie.

Drs. D. Meester, beste Daan, cardio thoracaal chirurg, bedankt voor het kunnen afronden van mijn proefschrift. Dank voor de mogelijkheden op jullie afdeling om me verder te ontwikkelen als arts.

Sanne, Leonieke, Joel, Tom, Elmer, Jitte, Wiebe, toch cardiologie kant op? **Alicia, Brulot en den Exter, Josephine, amies, oud-dispuutsgenootjes**, ik hoop jullie iets vaker te zien! **Ilia en Annemijn**, van trouwe bondgenoot in het EMC naar goede vriend, het sparren over onderzoek, de gezellige weekendjes en relativerende woorden in Friesland, Gent en Berlijn, werden zeer gewaardeerd! Veel plezier in jullie nieuwe huis in Utrecht. **Beste Luc**, van al mijn vrienden ken ik jou het langst, ik leerde je kennen tijdens de geschiedenislessen op het Camphusianum. De vakanties waren een welkome afwisseling tijdens het schrijven. Thanks PADI. **Maarten van Eck**, als "Comissaris Oude Bal tijdens het COB-diner van het oudste en meest illustere dispuut N.I.R.E.A.", nodigde je me uit bij het begin van de studie geneeskunde aan de Erasmus Universiteit om in je studentenhuus 1 4 B aan de Treubstraat te komen wonen. Herinneringen worden afgewisseld met vele nieuwe in de maak. **Paul Lankhorst**, oud-huisgenoot, dispuutsgenoot, en inmiddels paranimf en heb ik de grote eer om een van je getuige te zijn op je huwelijk! Wat kunnen we lachen, en ik ga er van uit dat het na het afronden van dit proefschrift weer het geval is! **Frederik de Pont**, dispuutsgenoot, oud-huisgenoot en inmiddels paranimf. Je hebt me door het promotie-traject gesleept, dankjewel! Op jou kon ik terugvallen indien de nood het hoogst was en dat is een fijne gedachte. Geflankeerd door deze heren heb ik er alle vertrouwen in de verdediging te voltooien.

Graag wil ik mijn familie bedanken.

Het schrijven van een dankwoord is in zekere zin een verkapte excuusbrief. Tot snel!

Graag wil ik mijn broers en zus bedanken.

Jan Willem, broer, je verhuisde met **Eva** naar Londen in 2014. Op een schitterende dag zijn jullie getrouwd in Amsterdam en inmiddels zijn jullie ouders geworden van een prachtige dochter, **Sofie van Kranenburg**. Broer, ik ben al de fijne weekendjes in Amsterdam aan het missen. Tot snel in de Maasstad!

Maike, zusje, als meisje opgegroeid tussen de mannen. In september 2016 ben je getrouwd met **Robbert**. Je bent afgestudeerd aan de Universiteit van Utrecht in de farmacie en je bent in opleiding tot ziekenhuisapotheker. Veel plezier met Robbert in Leusden.

Wouter, broertje, inmiddels ben je afgestudeerd aan de Erasmus Universiteit Rotterdam en ben je bedrijfskundige bij ABN AMRO. Veel plezier met **Minerva**. Jij blijft toch wel in Rotterdam!

Graag wil ik mijn ouders bedanken.

Aat Jan en Janneke van Kranenburg, jullie zorgden in Rhoon, Giessen en Sleeuwijk voor een warme en stabiele omgeving om op te groeien. De eindeloze mogelijkheden die jullie bieden, gericht op de kinderen, zijn zelden vanzelfsprekend. Erg belangrijk waren jullie in dit traject, te vergelijken met topsport en vallen en opstaan. Ik bof met zo'n fijne familie.

Pa, **Aat Jan**, Bedankt voor de wekelijkse gesprekken om me bij te sturen, om me voor te bereiden voor een gesprek met de sponsor en voor het uitwisselen van ideeën. Verder voor het delen van je ervaringen in het bedrijfsleven bij toonaangevende bedrijven en overheid in Nederland.

Ma, **Janneke**, zonder jou, was het maar niks geworden. Je praktische en sociale vaardigheden, je perfectionisme en doorzettingsvermogen zijn eigenschappen die dit proefschrift hebben gemaakt! Ik ben je veel dankbaar.

PHD PORTFOLIO SUMMARY

Summary of PhD training and teaching activities

Name PhD student: drs. M. van Kranenburg	PhD period: november 2011 - juni 2015
Erasmus MC Department: Cardiologie en Radiologie	Promotors: prof.dr. G.P. Krestin, prof.dr. R.J.M. van Geuns
Research School: COEUR	Co-Promotor: dr. O.C. Manintveld
	Supervisor: prof. dr. J.W. Roos-Hesselink

1. PhD training

	Year	Workload Hours/ECTS
General academic skills		
Basiscursus Regelgeving en Organisatie voor Klinisch onderzoekers (BROK), Erasmus MC, Rotterdam, the Netherlands	12-16 November, 2012	1.5 ECTS
Biomedical English Writing and Communication, Erasmus MC, Rotterdam, the Netherlands	February – April, 2014	3.0 ECTS
Research skills		
Biostatistical Methods I, CC02: Basic principles, Netherlands Institute for Health Sciences, Erasmus MC, Rotterdam, the Netherlands	24 September – 19 October, 2012	5.7 ECTS
In-depth courses (e.g. Research school, Medical Training)		
Pathophysiology of ischemic heart disease, COEUR, Erasmus MC, Rotterdam, the Netherlands	9-10 February, 2012	1.5 ECTS
Cardiovascular Imaging and Diagnostics, COEUR, Erasmus MC, Rotterdam, the Netherlands	10-11 January, 2013	1.5 ECTS
Congenital Heart Disease and the Left side: An introduction to Congenital Heart Disease, COEUR, Erasmus MC, Rotterdam, the Netherlands	25-26 April, 2013	1.5 ECTS
Cardiovascular Medicine	12-13 December, 2013	1.5 ECTS
Presentations		
ACC, San Francisco, California, U.S.A. oral presentation:	9 March, 2013	0.4 ECTS
Abstract: Prognostic Value of Microvascular Obstruction and Infarct Size Measured by Cardiac Magnetic Resonance in Patients with ST-Segment Elevation Myocardial Infarction: a Meta-Analysis of Individual Patient Data, JACC March 12, 2013, Volume 61, Issue 10.	28 March, 2014	0.4 ECTS
ACC, Washington, U.S.A. poster presentation:		
Abstract: Prognostic Significance of Microvascular Obstruction and Infarct Size Measured by Cardiovascular Magnetic Resonance for the Assessment of Left Ventricular Remodeling in Patients with ST-Segment Elevation Myocardial Infarction: Insight from a Pooled Analysis of Individual Patient Data, JACC 2014;63.		
International conferences		
EuroCMR, 10th International Congress on Cardiovascular Magnetic Resonance, ESC Working Group, Vienna, Austria	17-19 May, 2012	0.9 ECTS
62 nd Annual Scientific Session, American College of Cardiology, San Francisco, U.S.A.	9-11 March, 2013	0.9 ECTS

ESC Congress 2013, Amsterdam, the Netherlands	3 September, 2013	0.4 ECTS
63 Annual Scientific Session, American College of Cardiology, Washington, U.S.A.	29-31 March, 2014	0.9 ECTS
ESC Congress 2015, London, U.K.	29 August – 2 September, 2015	1.5 ECTS

Seminars and workshops

Research Seminar focus on Aging COEUR.	2 March, 2012	0.5 ECTS
Annual COEUR PhD-day.	9 March, 2012	0.4 ECTS
Seminar: Do we need to improve our techniques for diagnosing functional coronary artery disease?	4 October, 2013	0.4 ECTS
Non-invasive Imaging of Myocardial Ischemia COEUR	17 January, 2014	0.4 ECTS
New imaging strategies for the detection of atherosclerosis, COEUR, Erasmus MC, Rotterdam, the Netherlands	10 October, 2014	0.2 ECTS
Aortapathologie, te nauw of te wijd, Erasmus MC, Rotterdam, the Netherlands	23 April, 2015	0.4 ECTS

Didactic skills

Tutor, Desiderius School	2012	1.5 ECTS
COEUR, 2 nd grade Medical Students, education cardiac MRI	2012, 2013	
Supervising 2 nd year medical students in writing a systematic review, Erasmus MC, Rotterdam the Netherlands.	2012	
Supervising 2 nd year medical students in writing a systematic review, Erasmus MC, Rotterdam the Netherlands.	2013	

Other**2. Teaching activities**

-	Year	Workload Hours/ECTS
---	-------------	----------------------------

Lecturing

Oral presentation, pathophysiology of ischemic heart disease, COEUR, Rotterdam, the Netherlands	May 1-2, 2014	0.4 ECTS
Staflunch, prognostic value of microvascular obstruction and infarct size measured by cardiac magnetic resonance in patients with ST-segment elevation myocardial infarction: meta-analysis of individual patient data	2013	0.4 ECTS
Staflunch, renal sympathetic denervation, non-invasive imaging	2014	0.4 ECTS

Supervising practicals and excursions**Supervising Master's theses**

Total	30.5
--------------	------

ECTS = European Credit Transfer System; 1 ECTS is equivalent to 28 hours of study.

Attendance at internal meetings and at conferences as well as both internal and external presentations may qualify for ECTS points. The Research Office has more info. Erasmus MC requires 30 ECTS at the time of the defense. Requirements for certification by an 'Onderzoekschool' can differ from the Erasmus MC requirement.

LIST OF PUBLICATIONS / ABSTRACTS

(1-10)

1. **van Kranenburg M**, Karanasos A, Chelu RG, van der Heide E, Ouhlous M, Nieman K, et al. Validation of renal artery dimensions measured by magnetic resonance angiography in patients referred for renal sympathetic denervation. *Academic radiology*. 2015;22(9):1106-14.
2. Chelu RG, van den Bosch AE, **van Kranenburg M**, Hsiao A, van den Hoven AT, Ouhlous M, et al. Qualitative grading of aortic regurgitation: a pilot study comparing CMR 4D flow and echocardiography. *The international journal of cardiovascular imaging*. 2016;32(2):301-7.
3. Huizinga W, Poot DH, Guyader JM, Klaassen R, Coolen BF, **van Kranenburg M**, et al. PCA-based groupwise image registration for quantitative MRI. *Medical image analysis*. 2016;29:65-78.
4. Uitterdijk A, Springeling T, **van Kranenburg M**, van Duin RW, Krabbendam-Peters I, Gorsse-Bakker C, et al. VEGF165A microsphere therapy for myocardial infarction suppresses acute cytokine release and increases microvascular density but does not improve cardiac function. *American journal of physiology Heart and circulatory physiology*. 2015;309(3):H396-406.
5. **van Kranenburg M**, Magro M, Thiele H, de Waha S, Eitel I, Cochet A, et al. Prognostic value of microvascular obstruction and infarct size, as measured by CMR in STEMI patients. *JACC Cardiovascular imaging*. 2014;7(9):930-9.
6. Yetgin T, **van Kranenburg M**, Ten Cate T, Duncker DJ, de Boer MJ, Diletti R, et al. Ischemic postconditioning after routine thrombus aspiration during primary percutaneous coronary intervention: Rationale and design of the POstconditioning Rotterdam trial. *Catheterization and cardiovascular interventions : official journal of the Society for Cardiac Angiography & Interventions*. 2015.
7. Opic P, Yap SC, **Van Kranenburg M**, Van Dijk AP, Budts W, Vliegen HW, et al. Atrial-based pacing has no benefit over ventricular pacing in preventing atrial arrhythmias in adults with congenital heart disease. *Europace : European pacing, arrhythmias, and cardiac electrophysiology : journal of the working groups on cardiac pacing, arrhythmias, and cardiac cellular electrophysiology of the European Society of Cardiology*. 2013;15(12):1757-62.
8. Opic P, **van Kranenburg M**, Yap SC, van Dijk AP, Budts W, Vliegen HW, et al. Complications of pacemaker therapy in adults with congenital heart disease: a multicenter study. *International journal of cardiology*. 2013;168(4):3212-6.
9. Serial quantitative magnetic resonance angiography follow-up of renal artery dimensions following treatment by four different renal denervation systems, van

- Zandvoort L, **van Kranenburg M**, Karanasos A, van Mieghem N, Ouhlous M, van Geuns RJM, van Domburg R., Daemen J, EuroIntervention. 2017 Jan 3; 12(13)
10. Cload-processed 4D CMR flow imaging for pulmonary flow quantification. Chelu R.G., Wanambiro K.W., Hsiao A., Swart L.E., Voogd T. van den Hoven A.T. **van Kranenburg M**, Coenen A, Boccalini S, Wielopolski PA, Vogel MW, Krestin GP, Vasanawala SS, Budde RP, Roos-Hesselink JW, Nieman K. Eur J Radiol. 2016 Oct;85(10):1849-56. doi: 10.1016/j.ejrad.2016.07.018.

BOOKCHAPTER

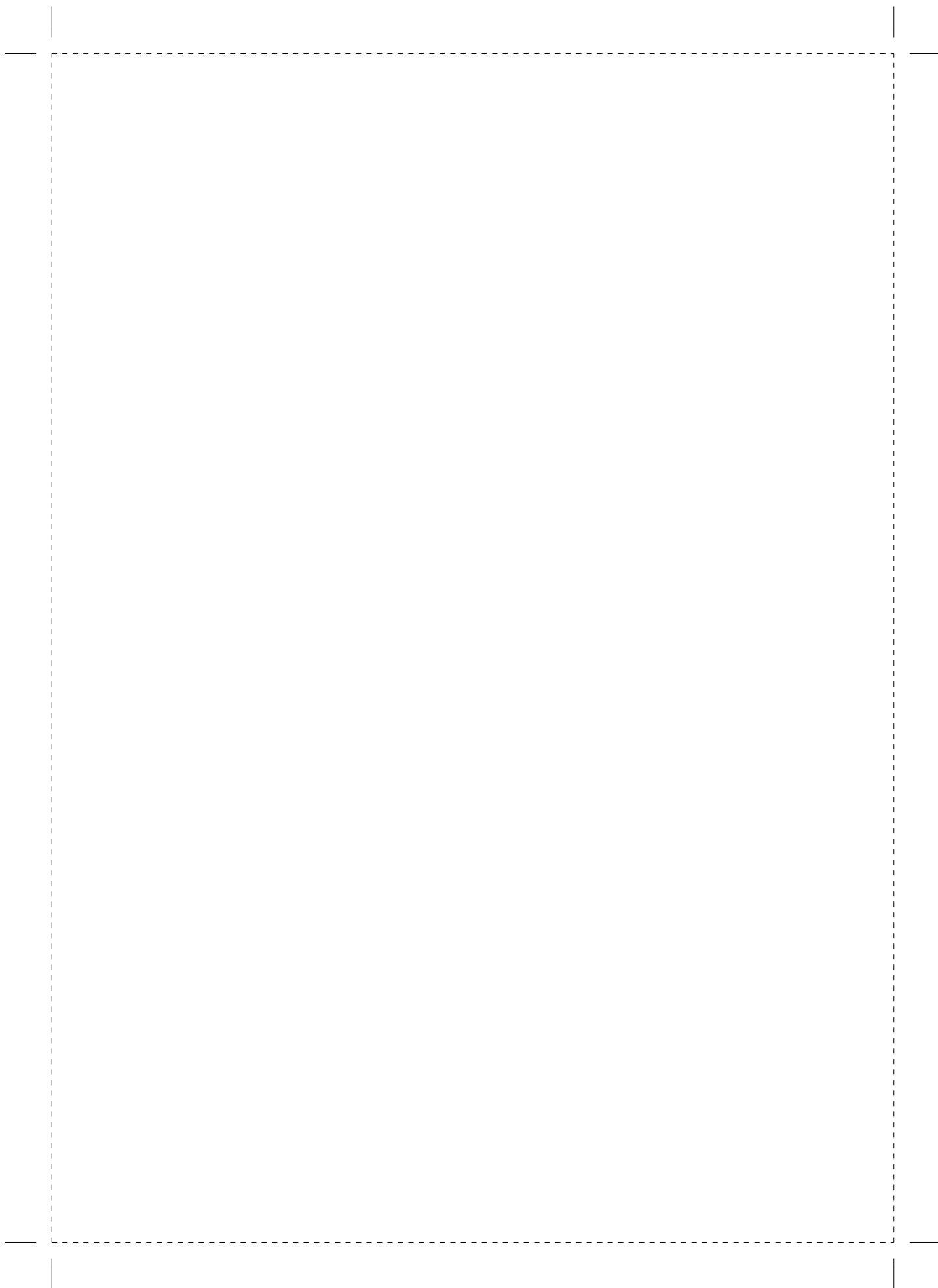
1. Non-rigid Groupwise Image Registration for Motion Compensation in Quantitative MRI. Huizinga W, Poot DHJ, Guyader J, Smit H, **Kranenburg M Van**, Geuns RM Van, Uitterdijk A, van Beusekom HMM, Coolen BF, Leemans A, Niessen W.J, Klein S. Non-rigid Groupwise Image Registration for Motion Compensation in Quantitative MRI. :184–93.

SUBMITTED

1. *Groupwise multimodal image registration based on total correlation.* Guyader J, Huizinga W, Fortunatia V, Poot D.H.J., **van Kranenburg M**, Veenland J.F., Paulides M.M., Niessen W.J., Klein S. submitted
2. *Multiple common co-morbidities produce left ventricular diastolic dysfunction associated with coronary microvascular dysfunction, cardiac oxidative stress and myocardial stiffening.* O. Sorop, I. Heinonen, **M. van Kranenburg**, V.J. de Beer, Y. Octavia, R.W.B. van Duin, K. Stam, R.J. van Geuns, A.H. van den Meiracker, A.H. Danser, W.J. Paulus, J. van der Velden, D. Merkus and D.J. Duncker, submitted
3. *Predictors of right and left ventricular function and dilatation in patients with atrial septal defects after surgical correction.* **Matthijs van Kranenburg**, Myrthe Menting, Judith Cuypers, Annemien van den Bosch, Petra Opic, Mohamed Ouhlous, Ad Bogers, Maarten Witsenburg, Wim Helbing, Folkert Meijboom, Jolien Roos-Hesselink. submitted
4. *Prognostic significance of microvascular obstruction and infarct size measured by cardiovascular magnetic resonance for the prediction of adverse left ventricular remodelling in patients with ST-segment elevation myocardial infarction: insight from a pooled analysis of individual patient data* **M. van Kranenburg**, O.C. Manintveld, T. Yetgin, V. Bodi, D. Atar, P. Buser, E. Wu, D. Lee, P. Bernhardt, W. Rottbauer, A.C. van Rossum, E. Boersma, G. Krestin, F. Zijlstra, R.J.M. van Geuns. Submitted

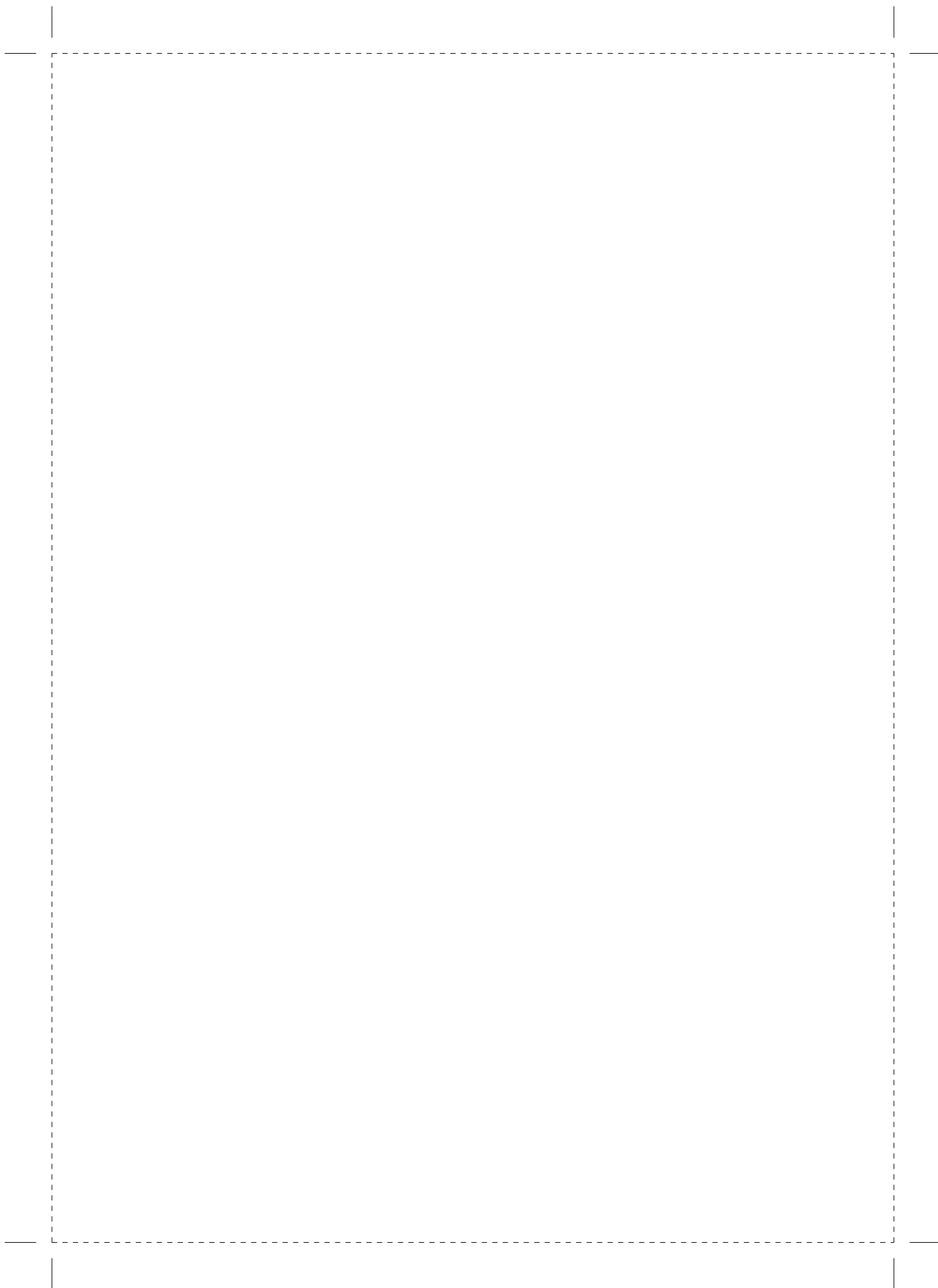
ABSTRACTS

1. **M. van Kranenburg**, Michael Magro, Suzanne de Waha, Holger Thiele, Vicente Bodi Peris, Alexandre Cochet, Gert Klug, Edwin Wu, Dan Atar, Peter Bernhardt, Ronak Delewi, Eric Boersma, Felix Zijlstra, Robert-Jan van Geuns. Prognostic Value of Microvascular Obstruction and Infarct Size Measured by Cardiac Magnetic Resonance in Patients with ST-Segment Elevation Myocardial Infarction: a Meta-Analysis of Individual Patient Data. At the ACC.13, 62nd Annual Scientific Session & Expo, San Francisco, U.S.A., date. (Oral Presentation)
2. **M. van Kranenburg**, Tuncay Yetgin, Olivier Manintveld, Dan Atar, Peter Buser, Edwin Wu, Daniel Lee, Vicente Bodi Peris, Peter Bernhardt, Wolfgang Rottbauer, Ronak Delewi, Eric Boersma, Gabriel Krestin, Felix Zijlstra, Robert-Jan van Geuns. Prognostic Significance of Microvascular Obstruction and Infarct Size Measured by Cardiovascular Magnetic Resonance for the Assessment of Left Ventricular Remodeling in Patients with ST-Segment Elevation Myocardial Infarction: Insight from a Pooled Analysis of Individual Patient Data. At the ACC.14, 63rd Annual Scientific Session & Expo, Washington, U.S.A., date. (Poster)



CURRICULUM VITAE

Matthijs van Kranenburg was born on the 2nd of April, 1986 in Rhoon, Albrandswaard the Netherlands. After graduating from secondary school in 2004 (Nature & Health, Gymnasium Camphusianum, Gorinchem), he started his medicine study at the Erasmus University in Rotterdam, Erasmus MC, in 2005 after studying civil engineering, at the TU Delft. During his medical study he visited the Moi Teaching and Referral Hospital, Eldoret, Kenya, as part of an elective internship surgery and internal medicine. His interest in cardiology was raised during his master thesis about pacemaker complications in patients with congenital heart disease under supervision of prof. dr. J.W. Roos-Hesselink at the department of cardiology, Erasmus MC, Rotterdam and his elective internship in cardiology under supervision of dr. R. van Mechelen (Sint Franciscus Gasthuis, Rotterdam) in 2011. In 2011 he graduated from medical school and began to work as a research fellow under supervision of prof. dr. R.J.M. van Geuns, prof. dr. F. Zijlstra and prof. J.W. Roos-Hesselink at the department of cardiology in collaboration with the department of radiology prof. dr. G.P. Krestin, Erasmus MC, Thoraxcenter in Rotterdam, the Netherlands. Research was focused on the application of magnetic resonance imaging in patients with ischemic and congenital heart disease. Research was funded by DIRA - Moerman, Olmer, van 't Zelfde. In July 2015 he started as a resident not in training at the department of cardiology under supervision of dr. R.P. Wielenga, Amphia Ziekenhuis, Breda. He was involved in detection of myocardial ischemia as measured by cardiac magnetic resonance imaging. Furthermore in June 2016 till January 2017 he was employed at the department of cardiothoracic surgery at the Amphia Ziekenhuis Breda under supervision of drs. D.J. Meester. Currently he is working at Dunes holding B.V.



ABBREVIATIONS

Part 1: PREFACE

Chapter 1: Introduction

ACS	=	acute coronary syndrome
CMR	=	cardiac magnetic resonance
CT	=	computed tomography
STEMI	=	ST-elevation myocardial infarction
pPCI	=	primary percutaneous coronary intervention
MO	=	microvascular obstruction
IS%LV	=	infarct size expressed as percentage of left ventricle
LVEF	=	left ventricular ejection fraction
ECG	=	electrocardiogram
IHD	=	ischemic heart disease
CAD	=	coronary artery disease
GUCH	=	grown up population with congenital heart disease
RDN	=	renal denervation
MRA	=	magnetic resonance angiography
MACE	=	major adverse cardiovascular events
CHD	=	congenital heart disease
VSD	=	ventricular septal defect
ASD	=	atrial septal defect
TOF	=	tetralogy of fallot
CoA	=	coarctation of aorta
TGA	=	transposition of the great arteries
GRE	=	gradient echo

Part 2: VALIDATION OF MAGNETIC RESONANCE ANGIOGRAPHY AND CMR 4D FLOW IN PATIENTS WITH RESISTENT HYPERTENSION AND CONGENITAL HEART DISEASE

Chapter 2: Validation of renal artery dimensions measured by magnetic resonance angiography in patients referred for renal sympathetic denervation.

RDN	=	renal sympathetic denervation
CTA	=	computed tomography angiography
MRA	=	magnetic resonance angiography
IVUS	=	intravascular ultrasound
3D	=	three-dimensional
TOF	=	time of flight
POC	=	polygon of confluence

SD	=	standard deviation
OCT	=	optical coherence tomography
RAS	=	renal artery stenosis
2D	=	two dimensional

Chapter 3: Serial quantitative magnetic resonance angiography follow-up of renal artery dimensions following treatment by four different renal denervation systems.

MRA	=	magnetic resonance angiography
RDN	=	percutaneous renal sympathetic denervation
CTA	=	computed tomography angiography
MRI	=	magnetic resonance imaging
IVUS	=	intravascular ultrasound
OCT	=	optical coherence tomography

Chapter 4: Qualitative grading of aortic regurgitation: a pilot study comparing CMR 4D flow and echocardiography.

CMR	=	cardiac magnetic resonance
4D	=	four dimensional
CMP	=	cardiomyopathy

Part 3: CARDIAC MAGNETIC RESONANCE IMAGING IN ISCHEMIC HEART DISEASE TRIALS

ANIMAL STUDIES

Chapter 5: VEGF165A microsphere therapy for myocardial infarction suppresses acute cytokine release and increases microvascular density but does not improve cardiac function.

AMI	=	acute myocardial infarction
PEG-PBT	=	polyethylene-glycol/polybutylene terephthalate
MSP	=	microsphere
TTC	=	tirphenyltetrazolium chloride
LCx	=	left circumflex coronary artery
DE-MRI	=	delayed enhancement MRI
MSPA	=	MSP treated area

Chapter 6: Multiple common co-morbidities produce left ventricular diastolic dysfunction associated with coronary microvascular dysfunction, cardiac oxidative stress and myocardial stiffening.

HFpEF	=	heart failure with preserved ejection fraction
HT	=	hypertension

HC	=	hypercholesterolemia
DM	=	diabetes mellitus
LV	=	left ventricular
MAP	=	mean aortic pressure
PAP	=	pulmonary artery pressure
PCWP	=	pulmonary capillary wedge pressure
CO	=	cardiac output
EDPVR	=	end-diastolic pressure volume relation
ESPVR	=	end-systolic pressure volume relation
IR-SPGR	=	inversion recovery spoiled gradient echo
LDL	=	low-density lipoprotein
HDL	=	high-density lipoprotein (HDL)
ASAT	=	aspartate aminotransferase (ASAT)
ROS	=	reactive oxygen species
NO	=	nitric oxide
NOS	=	nitric oxide synthase

HUMAN STUDIES

Chapter 7 and 8: Prognostic value of microvascular obstruction and infarct size, as measured by CMR in STEMI patients.

STEMI	=	ST-segment elevation myocardial infarction
pPCI	=	primary percutaneous coronary intervention
MO	=	microvascular obstruction
CE-CMR	=	contrast-enhanced cardiac magnetic resonance
LVEF	=	left ventricular ejection fraction
MACE	=	major adverse cardiovascular events
LV	=	left ventricular
IS%LV	=	infarct size expressed as left ventricular mass
TIMI	=	thrombolysis in myocardial infarction
CMR	=	cardiac magnetic resonance
IQR	=	interquartile range
HR	=	hazard ratio
aHR	=	adjusted hazard ratio
CI	=	confidence interval
AMI	=	acute myocardial infarction
ICD	=	implantable cardioverter defibrillator
NSTEMI	=	non ST-elevation myocardial infarction
IS	=	infarct size
BMI	=	body mass index

CABG	=	coronary artery bypass graft
CK	=	creatinine kinase
CV	=	cardiovascular
LAD	=	left anterior descending
LCA	=	left circumflex artery
LVEDV	=	left ventricular end-diastolic volume
LVESV	=	left ventricular end-systolic volume
MI	=	myocardial infarction
PCI	=	percutaneous coronary intervention
RCA	=	right coronary artery
CE-CMR	=	contrast-enhanced cardiac magnetic resonance

Chapter 9: Ischemic postconditioning after routine thrombus aspiration during primary percutaneous coronary intervention: rationale and design of the POstconditioning Rotterdam Trial.

IPOC	=	ischemic postconditioning
TA	=	thrombus aspiration
PORT	=	Postconditioning Rotterdam Trial
IRA	=	infarct related artery
MVO	=	microvascular obstruction
CK-MB	=	creatinine kinase myocardial bound
AAR	=	area at risk
FFR	=	fractional flow reserve
IMR	=	index microcirculatory resistance

Part 4: OUTCOME STUDIES IN CONGENITAL HEART DISEASE

Chapter 10: Atrial-based pacing has no benefit over ventricular pacing in preventing atrial arrhythmias in adults with congenital heart disease.

CHD	=	congenital heart disease
Ao valve	=	aortic valve
ASD	=	atrial septal defect
AVSD	=	atrioventricular septal defect
cc-TGA	=	congenitally corrected transposition of the great arteries
Ebstein	=	ebstein anomaly
PAPVR/TAPVR	=	partial anomalous pulmonary venous return, total anomalous pulmonary venous return
Pul Valve	=	pulmonary valve
SV	=	single ventricle
TGA	=	transposition of the great arteries

ToF	=	tetralogy of fallot
VSD	=	ventricular septal defect

Chapter 11: Complications of pacemaker therapy in adults with congenital heart disease:

A multicenter study.

CHD	=	congenital heart disease
AV	=	atrialventricular
IQR	=	interquartile range
ASD	=	atrial septal defect
SSS	=	sick sinus syndrome
TGA	=	transposition of the great arteries
Ao valve	=	aortic valve
AVSD	=	atrioventricular septal defect
cc-TGA	=	congenitally corrected transposition of the great arteries
CoA	=	coarctation aortae
Ebstein	=	Ebsteins anomaly
PAPVR/TAPVR	=	partial anomalous pulmonary venous return, total anomalous pulmonary venous return
Pul valve	=	pulmonary valve
Single ventricle	=	single ventricle physiology (fontan)
ToF	=	tetralogy of Fallot
VSD	=	ventricular septal defect

